

NX

NASA CR-165621



(NASA-CR-165621) LOW-THRUST ISP SENSITIVITY
STUDY Final Report (Aerojet Liquid Rocket
Co.) 265 p HC A12/MF A01 CSCI 21H

N82-22309

Unclassified
GS/20 09711

LOW-THRUST ISP SENSITIVITY STUDY

by

L. Schoenman

AEROJET LIQUID ROCKET COMPANY

Prepared For:

NATIONAL AERONAUTICS AND SPACE ADMINISTRATION

NASA/Lewis Research Center

Contract NAS 3-22665

A. Pavli, Project Manager



1. Report No.	2. Government Accession No.	3. Recipient's Catalog No.	
4. Title and Subtitle Low-Thrust Isp Sensitivity Study		5. Report Date 12 April 1982	
7. Author(s) L. Schoenman		6. Performing Organization Code	
9. Performing Organization Name and Address Aerojet Liquid Rocket Company P.O. Box 13222 Sacramento, CA 95813		8. Performing Organization Report No.	
12. Sponsoring Agency Name and Address National Aeronautics and Space Administration NASA/Lewis Research Center 21000 Brookpark Rd. Cleveland, Ohio 44135		10. Work Unit No.	
15. Supplementary Notes Project Manager - A. Pavli NASA/Lewis Research Center 21000 Brookpark Rd. Cleveland, Ohio 44135		11. Contract or Grant No. NAS 3-22665	
16. Abstract This report presents a comparison of the cooling requirements and attainable specific impulse performance of engines in the 445 to 4448N (100 to 1000 lbF) thrust class utilizing LOX/RP-1, LOX/Hydrogen and LOX/Methane propellants. The unique design requirements for the regenerative cooling of low-thrust engines operating at high pressures (up to 6894 kPa [1000 psia]) are explored analytically by comparing single cooling with the fuel and the oxidizer, and dual cooling with both the fuel and the oxidizer. The effects of coolant channel geometry, chamber length, and contraction ratio on the ability to provide proper cooling are evaluated, as is the resulting specific impulse. The results show that larger contraction ratios and smaller channels are highly desirable for certain propellant combinations.		13. Type of Report and Period Covered Contractor Report, Final	
17. Key Words (Suggested by Author(s)) Rocket Engines Orbit Transfer Vehicle Propulsion LOX/Hydrogen, LOX/RP-1, and LOX/Methane Cooling - Cooling Requirements - Specific Impulse - Thrust Class		18. Distribution Statement Unclassified	
19. Security Classification (of this report)	20. Security Classification (of this page)	21. No. of Pages	22. Price*
Unclassified	Unclassified	251	

PRECEDING PAGE BLANK NOT FILMED

FOREWORD

This final report, submitted per the requirements of Contract NAS 3-22665, documents the results of an analytical study undertaken to relate the attainable specific impulse (I_{sp}) for LOX/RP-1, LOX/hydrogen, and LOX/methane propellants to the various cooling concepts applicable to low-thrust, long-life liquid rocket engines. The sensitivity of I_{sp} to mixture ratio (MR), thrust (F), chamber pressure (Pc), and cooling method for each propellant combination is presented in this report.

The NASA-Lewis project manager for this program was Mr. Al Pavli. The ALRC program manager was Mr. J. W. Salmon, and the project engineer was Mr. L. Schoenman. Other key ALRC personnel assigned to the program were Gregg Meagher, Performance Analysis, and W. R. Thompson, Heat Transfer. Consultants were Dr. R. L. Ewen, J. I. Ito, J. Mellish, J. L. Pieper, and R. E. Walker.

TABLE OF CONTENTS

	<u>Page</u>
I. Introduction	1
A. Application and Requirements for Low-Thrust Engines	1
B. Objectives of the Present Study	1
C. Program Organization	3
D. Results of Previous Studies	4
E. Final Report Organization	6
II. Summary	7
A. Analytical Approach	7
B. Cooling Concept Selections and Engine Cycle Considerations	7
1. Cooling Concept	7
2. Applicable Engine Cycles	9
C. Cooling Concept Selection, Isp Sensitivity, Conclusions, and Recommendations	10
1. General Conclusions <u>Applicable to All Propellant Systems</u>	10
2. LOX/RP-1	15
3. LOX/Hydrogen	17
4. LOX/Methane	17
5. Effect of Added Enthalpy	21
D. Conclusions and Recommendations for Future Work	25
1. General	25
2. LOX/RP-1	25
3. LOX/LH ₂	25
4. LOX/LCH ₄	26
III. Results of Parametric Studies for LOX/RP-1	27
A. Summary	27
B. Thermal Design	27
1. Scope and Analytical Basis	27
2. Analysis Methodology	29

TABLE OF CONTENTS (cont.)

	<u>Page</u>
3. Single-Propellant Regenerative Cooling Results (Fuel or Oxygen)	31
4. Dual-Propellant Regenerative Cooling Results (Fuel and Oxygen)	53
5. Thermal Conclusions for LOX/RP-1 Cooling	59
6. Additional Remarks Pertaining to Chamber Gas-Side Wall Thickness and Channel Geometry at Low Thrust	63
C. Performance Sensitivity	65
1. Performance Model	81
2. Attainable Isp for RP-1-Regenerative Cooling	82
3. Attainable Isp for Oxygen-Regenerative Cooling	85
4. Attainable Isp for Dual-Propellant Regenerative Cooling	88
5. Performance Summary for LOX/RP-1	90
IV. Results of Parametric Studies for LOX/Hydrogen	91
A. Summary	91
B. Thermal Design	91
1. Scope and Analytical Basis	91
2. Analysis Methodology	92
3. Hydrogen Regenerative Cooling Results	93
4. Effect of Added Enthalpy	101
5. Thermal Conclusions for Hydrogen Cooling	101
C. Performance Sensitivity	106
1. Performance Model	106
2. Attainable Isp for NBP LOX/Hydrogen	107
3. Effect of Added Enthalpy	111
4. Performance Conclusions for LOX/Hydrogen	113
V. Results of Parametric Studies for LOX/Methane	115
A. Summary	115
B. Thermal Design	115
1. Scope and Analytical Basis	115

TABLE OF CONTENTS (cont.)

	<u>Page</u>
2. Analysis Methodology	115
3. Single-Propellant Regenerative Cooling Results (Fuel or Oxygen)	128
4. Dual-Propellant Regenerative Cooling and Coating Applicability	131
5. Thermal Conclusions for NBP LO ₂ /LCH ₄	133
C. Performance Sensitivity	134
1. Performance Model	134
2. Attainable Isp for NBP LOX/LCH ₄	134
3. Performance Conclusions for LOX/Methane	141
References	143
Appendix A - Simplified Thermal Model	145
Appendix B - Simplified Performance Model	181
Appendix C - Performance Data Tabulations	227

PRECEDING PAGE BLANK NOT FILMED

LIST OF TABLES

TABLE NO.	Page
I Primary Independent Variables	2
II Added Enthalpy Results (Propellants: LOX/LH ₂)	23
III Effect of Enthalpy Addition to Propellant(s) for LOX/Hydrogen System	24
IV Selected Parameters Characterizing Engine Regenerative Cooling with RP-1 (Single-Regen)	32
V Selected Parameters Characterizing Engine Regenerative Cooling with Oxygen (Single-Regen)	34
VI Table Nomenclature	36
VII Selected Parameters Characterizing Engine Regenerative Cooling (Dual-Regen)	56
VIII Parametric Data and Results	69
IX Max. Performance Single-Regen Cooling	80
X Thermal Liner Influence on Performance	86
XI Performance Comparison Between Oxygen-Regenerative and Dual-Regenerative Cooling	89
XII Selected Parameters Characterizing Engine Regenerative Cooling with NBP Hydrogen with LO ₂ /LH ₂ Propellants (Single-Regen)	94
XIII Effect of Enthalpy Addition to LO ₂ /LH ₂ Propellants on One-Dimensional Equilibrium Parameters	104
XIV Effect of Enthalpy Addition to Propellant(s) for LO ₂ /Hydrogen System	105
XV LOX/LH ₂ Parametric Data and Results, Fuel-Regen Cases	108
XVI Added Enthalpy Results for LOX/LH ₂ Propellants	114
XVII Selected Parameters Characterizing Engine Regenerative Cooling with NBP Oxygen with LO ₂ /LCH ₄ Propellants (Single-Regen)	116
XVIII Selected Parameters Characterizing Engine Regenerative Cooling with NBP Oxygen with LO ₂ /LCH ₂ Propellants (Single-Regen)	118
XIX Comparison of Selected Parameters for Single-Regen (Fuel) and Dual-Regen (Oxygen-Fuel Series) Chamber Cooling	132

LIST OF TABLES (cont.)

<u>Table No.</u>		<u>Page</u>
XX	LOX/LCH ₄ Results for Fuel-Regen-Cooled Cases	135
XXI	LOX/LCH ₄ Results for Oxygen-Regen-Cooled Cases	137
XXII	LOX/LCH ₄ Results for Dual-Regen Cooling	138

LIST OF FIGURES

<u>Figure No.</u>		<u>Page</u>
1	Cooling Concepts Selection	8
2	Attainable Isp vs Propellant, F, P_c , MR, and Cooling Concept	13
3	Volumetric Impulse Comparison for LOX/RP-1, LCH ₄ , and LH ₂ Fuels	14
4	Range of Applicability for LOX and RP-1 Regenerative Cooling	16
5	Ranges in Minimum Channel Size as a Function of Chamber Pressure and Thrust, LO ₂ /LH ₂ at MR = 6	18
6	Range of Applicability for LOX and LCH ₄ Regenerative Cooling	19
7	Minimum Coolant Channel Widths Required for Regenerative Cooling with LOX/LCH ₄ Propellants at MR = 3.5	20
8	Attainable Specific Impulse for LOX/LH ₂ with Propellant Preheating by External Energy Sources	22
9	Coolant Pressure Drop for LOX, RP-1, and Dual-Regenerative Cooling Concepts, F = 4448N (1000 lbF)	37
10	Coolant Pressure Drop for LOX, RP-1, and Dual-Regenerative Cooling Concepts, F = 1779N (400 lbF)	38
11	Coolant Pressure Drop for LOX, RP-1, and Dual-Regenerative Cooling Concepts, F = 445N (100 lbF)	39
12	Coolant Discharge Temperature for LOX, RP-1, and Dual-Regenerative Cooling Concepts, F = 4448N (1000 lbF)	40
13	Coolant Discharge Temperature for LOX, RP-1, and Dual-Regenerative Cooling Concepts, F = 1779N (400 lbF)	41
14	Coolant Discharge Temperature for LOX, RP-1, and Dual-Regenerative Cooling Concepts, F = 445N (100 lbF)	42
15	Maximum Chamber L' for LOX, RP-1, and Dual-Regenerative Cooling Concepts, F = 4448N (1000 lbF)	43
16	Maximum Chamber L' for LOX, RP-1, and Dual-Regenerative Cooling Concepts, F = 1779N (400 lbF)	44
17	Maximum Chamber L' for LOX, RP-1, and Dual-Regenerative Cooling Concepts, F = 445N (100 lbF)	45
18	Minimum Coolant Channel Width Required for LOX, RP-1, and Dual-Regenerative Cooling Concepts, F = 4448N (1000 lbF)	46

LIST OF FIGURES (cont.)

<u>Figure No.</u>		<u>Page</u>
19	Minimum Coolant Channel Width Required for LOX, RP-1, and Dual-Regenerative Cooling Concepts, $F = 1779\text{N}$ (400 lbF)	47
20	Minimum Coolant Channel Width Required for LOX, RP-1, and Dual-Regenerative Cooling Concepts, $F = 445\text{N}$ (100 lbF)	48
21	$\text{LO}_2/\text{RP-1}$ Minimum Required Channel Width for RP-1 Regenerative Cooling as a Function of Mixture Ratio and Thrust	51
22	$\text{LO}_2/\text{RP-1}$ Minimum Required Channel Width for Oxygen Regenerative Cooling as a Function of Mixture Ratio and Thrust	52
23	Sensitivity of Required Minimum Coolant Channel Width to Chamber Pressure, Mixture Ratio, and Thrust for Oxygen Regenerative Cooling of $\text{LO}_2/\text{RP-1}$ Engines	54
24	Sensitivity of Required Minimum Coolant Channel Width to Chamber Pressure, Mixture Ratio and Thrust for RP-1 Regenerative Cooling of $\text{LO}_2/\text{RP-1}$ Engines	55
25	$\text{LO}_2/\text{RP-1}$ Regenerative Cooling Analysis Matrix, $F = 4448\text{N}$ (1000 lbF)	60
26	$\text{LO}_2/\text{RP-1}$ Regenerative Cooling Analysis Matrix, $F = 1779\text{N}$ (400 lbF)	61
27	$\text{LO}_2/\text{RP-1}$ Regenerative Cooling Analysis Matrix, $F = 445\text{N}$ (100 lbF)	62
28	Thrust/Chamber Pressure/Mixture Ratio Operating Limits for Regenerative Cooling Concepts for $\text{LO}_2/\text{RP-1}$ Engines	64
29	Design Requirements for Low-Thrust, High-Pc Regeneratively Cooled Chambers	66
30	Wall Thickness as a Function of Chamber Pressure and Thrust for a Constant Wall Temperature Drop	67
31	RP-1 Regeneratively Cooled Chamber Channel Land Size Sensitivity	68
32	Delivered Performance Versus Mixture Ratio for 445N (100 lbF)	73
33	Delivered Performance Versus Mixture Ratio for 1779N (400 lbF)	73
34	Delivered Performance Versus Mixture Ratio for 4448N (1000 lbF)	73
35	Delivered Performance Versus Thrust for 689 kPa (100 psia) Chamber Pressure	74

LIST OF FIGURES (cont.)

<u>Figure No.</u>		<u>Page</u>
36	Delivered Performance Versus Thrust for 2758 kPa (400 psia) Chamber Pressure	75
37	Delivered Performance Versus Thrust for 6894 kPa (1000 psia) Chamber Pressure	76
38	Delivered Performance Versus Chamber Pressure for 445N (100 lb Thrust)	77
39	Delivered Performance Versus Chamber Pressure for 1279N (400 lb Thrust)	78
40	Delivered Performance Versus Chamber Pressure for 4448N (1000 lb Thrust)	79
41	Performance Mathematical Modeling (Loss Accounting)	83
42	Guidelines from Preliminary Investigations	84
43	Energy Release Efficiency Sensitivity	87
44	Coolant Pressure Drop for NBP Hydrogen Cooling Concepts, $F = 4448N$ (1000 lbF)	96
45	Coolant Pressure Drop for NBP Hydrogen Cooling Concepts, $F = 1779N$ (400 lbF)	96
46	Coolant Pressure Drop for NBP Hydrogen Cooling Concepts, $F = 445N$ (100 lbF)	96
47	Coolant Discharge Temperature for NBP Hydrogen Cooling Concepts, $F = 4448N$ (1000 lbF)	97
48	Coolant Discharge Temperature for NBP Hydrogen Cooling Concepts, $F = 1779N$ (400 lbF)	97
49	Coolant Discharge Temperature for NBP Hydrogen Cooling Concepts, $F = 445N$ (100 lbF)	97
50	Minimum Chamber L' for NBP Hydrogen Cooling Concepts, $F = 4448N$ (1000 lbF)	98
51	Minimum Chamber L' for NBP Hydrogen Cooling Concepts, $F = 1779N$ (400 lbF)	98
52	Minimum Chamber L' for NBP Hydrogen Cooling Concepts $F = 445N$ (100 lbF)	98
53	Minimum Coolant Channel Width Required for NBP Hydrogen Cooling Concepts, $F = 4448N$ (1000 lbF)	99
54	Minimum Coolant Channel Width Required for NBP Hydrogen Cooling Concepts, $F = 1779N$ (400 lbF)	99

LIST OF FIGURES (cont.)

<u>Figure No.</u>		<u>Page</u>
55	Minimum Coolant Channel Width Required for NBP Hydrogen Cooling Concepts, $F = 445\text{N}$ (100 lbF)	99
56	Minimum Channel Width vs Thrust for Constant Chamber Pressures, O_2/H_2 at $\text{MR} = 6$	102
57	Ranges in Minimum Channel Size as a Function of Chamber Pressure and Thrust, O_2/H_2 at $\text{MR} = 6$	103
58	Predicted Performance for LOX/LH ₂ as a Function of Mixture Ratio for 4448, 1779, and 445N (1000, 400, and 100 lbF)	109
59	LOX/LH ₂ Delivered Performance vs Chamber Pressure for 4448N (1000 lbF)	110
60	LOX/LH ₂ Delivered Performance vs Chamber Pressure for 1779N (400 lbF)	110
61	LOX/LH ₂ Delivered Performance vs Chamber Pressure for 445N (100 lbF)	110
62	LOX/LH ₂ Delivered Performance vs Thrust for 6894 kPa (1000 psia) Chamber Pressure	112
63	LOX/LH ₂ Delivered Performance vs Thrust for 2758 kPa (400 psia) Chamber Pressure	112
64	LOX/LH ₂ Delivered Performance vs Thrust for 689 kPa (100 psia) Chamber Pressure	112
65	Coolant Pressure Drop for NBP Methane and Oxygen Cooling vs Mixture Ratio, $F = 4448\text{N}$ (1000 lbF)	119
66	Coolant Pressure Drop for NBP Methane and Oxygen Cooling vs Mixture Ratio, $F = 1779\text{N}$ (400 lbF)	119
67	Coolant Pressure Drop for NBP Methane and Oxygen Cooling vs Mixture Ratio, $F = 445\text{N}$ (100 lbF)	119
68	Coolant Pressure Drop for NBP Methane and Oxygen Cooling, $F = 4448\text{N}$ (1000 lbF)	120
69	Coolant Pressure Drop for NBP Methane and Oxygen Cooling, $F = 1779\text{N}$ (400 lbF)	120
70	Coolant Pressure Drop for NBP Methane and Oxygen Cooling, $F = 445\text{N}$ (100 lbF)	120
71	Coolant Discharge Temperature for NBP Methane and Oxygen Cooling, $F = 4448\text{N}$ (1000 lbF)	121

LIST OF FIGURES (cont.)

<u>Figure No.</u>		<u>Page</u>
72	Coolant Discharge Temperature for NBP Methane and Oxygen Cooling, $F = 1779\text{N}$ (400 1bF)	121
73	Coolant Discharge Temperature for NBP Methane and Oxygen Cooling, $F = 445\text{N}$ (100 1bF)	121
74	Chamber L' for NBP Methane and Oxygen, $F = 4448\text{N}$ (1000 1bF)	122
75	Chamber L' for NBP Methane and Oxygen, $F = 1779\text{N}$ (400 1bF)	122
76	Chamber L' for NBP Methane and Oxygen, $F = 445\text{N}$ (100 1bF)	122
77	Coolant Channel Width Required for NBP Methane and Oxygen Cooling, $F = 4448\text{N}$ (1000 1bF)	123
78	Coolant Channel Width Required for NBP Methane and Oxygen Cooling, $F = 1779\text{N}$ (400 1bF)	123
79	Coolant Channel Width Required for NBP Methane and Oxygen Cooling, $F = 445\text{N}$ (100 1bF)	123
80	LO_2/LCH_4 Regenerative Cooling Analysis Matrix, $F = 4448\text{N}$ (1000 1bF)	124
81	LO_2/LCH_4 Regenerative Cooling Analysis Matrix, $F = 1779\text{N}$ (400 1bF)	125
82	LO_2/LCH_4 Regenerative Cooling Analysis Matrix, $F = 445\text{N}$ (100 1bF)	126
83	Thrust/Chamber Pressure/Mixture Ratio Operating Limits for Regenerative Cooling Concepts for LO_2/LCH_4 Engines	127
84	Predicted LOX/LCH_4 Performance as a Function of Mixture Ratio for 4448, 1779, and 445N (1000, 400 and 100 1bF)	136
85	Delivered Performance vs Chamber Pressure for 445N (100 1bF)	140
86	Delivered Performance vs Chamber Pressure for 1779N (400 1bF)	140
87	Delivered Performance vs Chamber Pressure for 4448N (1000 1bF)	140

PRECEDING PAGE BLANK NOT FILMED

ACRONYMS/NOMENCLATURE

MR	=	Mixture Ratio
F	=	Thrust
Pc	=	Chamber Pressure
STS	=	Space Transportation System
OTV	=	Orbit Transfer Vehicle
LEO	=	Low Earth Orbit
GEO	=	Geosynchronous Equatorial Orbit
NBP	=	Normal Boiling Point.
ERE	=	Energy Release Efficiency.
NEL	=	Number of Injection Elements

I. INTRODUCTION

A. APPLICATIONS AND REQUIREMENTS FOR LOW-THRUST ENGINES

The development of an economical space transportation system (STS) requires the generation of an orbit transfer vehicle (OTV) capable of moving space shuttle payloads to more distant orbits and beyond. A number of studies have forecast an appreciable number of these payloads to be large space structures which would be launched to low earth-orbit (LEO) in a stowed condition aboard the space shuttle. These structures would be assembled near the shuttle and subsequently transferred to geosynchronous equatorial orbit (GEO), by way of a high-energy space propulsion system. One or more low-thrust engines would be required for this mission in order to avoid high inertial loading which could cause damage to the assembled payload. To date, the technology base for this class of cryogenic chemical rocket engines, capable of providing very high performance while operating for periods up to 50 hours, is virtually nonexistent. Since present plans project that a single engine will be employed for this mission, it is essential that it possess both high reliability and high performance.

To determine optimum vehicle configurations required to transport large space structures from low earth-orbit to geosynchronous earth-orbit, the interaction of the following three basic inputs is required:

1. A description of the attainable specific impulse (I_{sp}) as a function of engine parameters such as propellants, thrust level, chamber pressure, mixture ratio, cooling method, and nozzle expansion area ratio.
2. The vehicle mass fraction as a function of the same configuration variables.
3. The mission requirements in terms of thrust level, burn duration, number of burns, and ΔV for the range of payloads considered.

B. OBJECTIVES OF THE PRESENT STUDY

The objective of this program was to furnish the data for the first input noted above: namely, to describe the attainable I_{sp} as a function of the primary engine design variables. This was to be done by accounting for cooling losses, kinetic losses, boundary layer losses, and combustion inefficiencies over the range of interest of the six primary independent variables listed in Table I. However, the optimization of these six variables to obtain maximum I_{sp} was not the purpose of this work as the ultimate optimum vehicle design may occur at other than maximum specific impulse due to mass fraction, mission requirement conditions such as stage length

TABLE I

PRIMARY INDEPENDENT VARIABLES

Variable	Selected Values for Specific Program Tasks			
	Task I	Task II	Task III	Task IV
1. P_c , kPa (psi)	276-5515 (40-800)	689-5515 (100-800)	689-5515 (100-800)	689-6894 (100-1000)
2. F , N (lbF)	667-3114 (150-700)	445-3558 (100-800)	445-3558 (100-800)	445-4448 (100-1000)
3. O/F	2,4	2,4	1-6	1-5
4. Propellant	$RP-1/L0_2$	$RP-1/L0_2$	$RP-1/L0_2$	H_2/O_2
5. Propellant Temperature -				
Fuel	289°K (60°F)	289°K (60°F)	289°K (60°F)	20-922°K (36-1660°F) (160°R)
Oxidizer	89°K (160°R)	89°K (160°R)	89°K (160°R)	89-922°K (160-1660°F) (160°R)
6. Expansion Area Ratio	100	10-1000	400	400
				400

I, B, Objectives of the Present Study (cont.)

and volume, etc. Propellant temperature as a variable was also investigated in order to evaluate if improved performance could be attained by adding enthalpy to the propellants from "free" sources (e.g., waste heat or solar heat).

The analysis addressed the thrust chamber and nozzle only. The designs evaluated were configurations suitable for long-duration, multiple-burn missions.

C. PROGRAM ORGANIZATION

The technical effort consisted of the following four tasks:

Task I - Preliminary Survey and Qualification of Simplified Procedure

The Task I activities consisted of developing the simplified analytical techniques used in the program to conduct the broad range of required parametric analyses. These analytical models included both thermal design and performance analyses and were calibrated against more detailed analytical procedures and experimental data where available. The LOX/RP-1 propellant combination was specified for the Task I activities and encompassed the range of primary independent variables listed in Table I.

Task II - Survey of Expansion Area Ratio and Mixture Ratio Effects

This task considered the sensitivity of Isp to the indicated Table I variables, and the influence of the candidate chamber cooling concepts on area ratio and MR selections.

Task III - Detailed Survey of the Sensitivity of Isp

This task required a full exploration of the domain described in Table I by using the simplified calculational procedures developed in Task I and a singular area ratio selected in Task II. A minimum of two cooling concepts for each operating point was included.

Task IV - Survey of Alternate Propellants and Propellant Enthalpy

This task extended the results of the LOX/RP-1 propellants to LOX/hydrogen and LOX/methane, as indicated in Table I. In addition, an evaluation was made of the potential for attaining improved performance by adding enthalpy to the propellant from free sources such as waste heat and solar heat.

I. Introduction (cont.)

D. RESULTS OF PREVIOUS STUDIES

Related cooling studies conducted on previous contracts (NAS 3-21940 and NAS 3-21941) examined the applicability of the fuel regenerative cooling and fuel film-cooling to rocket engines in the 445 to 13,444N (100 to 3000 lbF) thrust range operating at chamber pressures from 138 to 6894 kPa (20 to 1000 psia). All engines utilized LO₂ oxidizer; the fuels included hydrogen (LH₂), methane (LCH₄), and RP-1. These studies were restricted to considering limited ranges for propellant temperatures, coolant pressures, velocities, and coking limits and were also constrained in terms of fabrication methods and dimensional limits. These criteria are described in the following table.

- 90% Bell Nozzles
- Fuel to be Used for Cooling
- Coolant Inlet Temperature:
 - LH₂ = 21°K (37.8°R)
 - RP-1 = 298°K (537°R)
 - LCH₄ = 112°K (201°R)
- Regenerative-Coolant Discharge or Film Coolant Inlet:
 - Liquid = 1.176 Times Chamber Pressure (Minimum)
 - Gas = 1.087 Times Chamber Pressure (Minimum)
- Maximum Coolant Velocity (Regenerative):
 - Liquid = 61 m/sec (200 ft/sec)
 - Gas = Mach 0.3
- Possible Benefit of Carbon Deposition on Hot Gas-Side Wall was Neglected
- Coking Limit:
 - RP-1 = 561°K (1010°R)
 - LCH₄ = 978°K (1760°R)

I, D, Results of Previous Studies (cont.)

- Dimensional Limits:

Tubular Construction

Minimum Wall Thickness = 0.025 cm (0.010 in.)

Nontubular Construction

Minimum Slot Width = 0.076 cm (0.03 in.)

Maximum Slot Depth/Width = 4 to 1

Minimum Web Thickness = 0.076 cm (0.03 in.)

Minimum Wall Thickness = 0.064 cm (0.025 in.)

The results obtained from the previous studies disclosed that the regenerative cooling and film-cooling concepts were only applicable over a limited range of operating conditions, as summarized below:

- Regenerative cooling with RP-1 was not feasible at any combination of thrust and chamber pressure because the walls exceeded the coking temperature limit and the bulk temperature rise was excessive.
- Regenerative cooling with methane was feasible only at high thrust and supercritical pressures.
- Regenerative cooling with hydrogen was feasible except at low thrust/high chamber pressure and high thrust/low chamber pressure conditions and when the coolant is near the critical pressure and temperature.
- Film cooling was feasible only at higher thrusts and lower chamber pressures. Hydrogen-cooled and methane-cooled units were found to have a broader operating range than RP-1-cooled designs.

The limitations of the regeneratively cooled and film-cooled concepts were due to the operating criteria imposed which required that

- Only fuel be used as a coolant.
- Channel sizes meet certain minimum dimensional criteria and be limited to the current state-of-the-art fabrication configurations.

I, D, Results of Previous Studies (cont.)

- ° Neither high temperature coatings nor soot effects be considered.
- ° Combined cooling concepts not be considered.
- ° A cooling concept be rejected if the associated performance decrement exceeded 10%.

In addition, combustion chamber lengths and contraction ratios were extrapolated from a data base for much higher-thrust engines. These extrapolations produced long chamber lengths and low contraction ratios and did not consider the particular cooling needs of low-thrust applications. The long chamber lengths and low contraction ratios resulted in excessive heat input to the regenerative coolant.

The minimum cooling channel width restrictions prevented optimization of the coolant channel surface for maximum regenerative cooling effectiveness. This produced high coolant pressure losses and, in some cases, excessive performance loss when less efficient processes, such as film cooling, became necessary because regenerative cooling was identified as non-feasible.

E. FINAL REPORT

This final report consists of five main sections and three appendices. Following the Introduction, Section I, and Summary, Section II, detailed thermal and Isp sensitivity results are presented for each of the three propellant combinations considered in this program: for LOX/RP-1 in Section III, LOX/hydrogen in Section IV, and LOX/methane in Section V.

Appendices A and B define the results of the Task I and II simplified model development, the model calibration, the MR and chamber geometry sensitivities, the element injector type and element quantity, and the chamber nozzle area ratio to be used for the Task III and IV analyses.

Appendix C provides the performance parametric data tabulations employed in the graphical displays of the other sections.

II. SUMMARY

A. ANALYTICAL APPROACH

This program produced performance predictions for different families of low-thrust orbit transfer engines. Tasks I and II of the program were devoted to preparing and calibrating the simplified thermal design and performance computer models which were employed in subsequent tasks.

The calculation of attainable specific impulse values for liquid propellant rocket engines requires that kinetic, boundary layer, energy release, divergence, and cooling losses be subtracted from a theoretical performance for each particular operating condition. These losses relate to the engine operating condition and are directly associated with the specific cooling concept being employed. The selection of a different cooling concept could alter both the performance and design margin at any operating point.

The generation of performance values for engines operating over a broad range of conditions and with different fuels required identification of the cooling systems applicable at each condition. The candidate cooling concepts were screened to keep the total quantity of engine operating points to be studied manageable. Selection of a single "optimum" concept was deemed undesirable as it would have prevented an evaluation of engine performance sensitivity to cooling concept selection.

The screening of various cooling concept candidates was based upon the concept's applicability at a particular operating condition and the performance loss attributable to its use. Other factors included the associated interface values, the concept's development status, and the vulnerabilities of each concept at its particular operating condition. The preliminary screening effort required semi-qualitative judgments used in combination with parametric analyses which examined performance, the performance decrement with coolant mass addition, propellant total heat capacity and maximum flux values, and the effect of thrust chamber surface area and wall temperatures on total heat rejected and maximum heat flux. The resultant selections were subsequently analyzed in greater detail to obtain quantitative performance data for the various engine configurations and cooling concepts as applied to different operating conditions. The extent of the independent variables considered for each propellant combination is defined in Table I.

B. COOLING CONCEPT SELECTIONS AND ENGINE CYCLE CONSIDERATIONS

1. Cooling Concept

The program logic applied to explore the cooling concept capabilities is illustrated in Figure 1. Conventional single-mode cooling

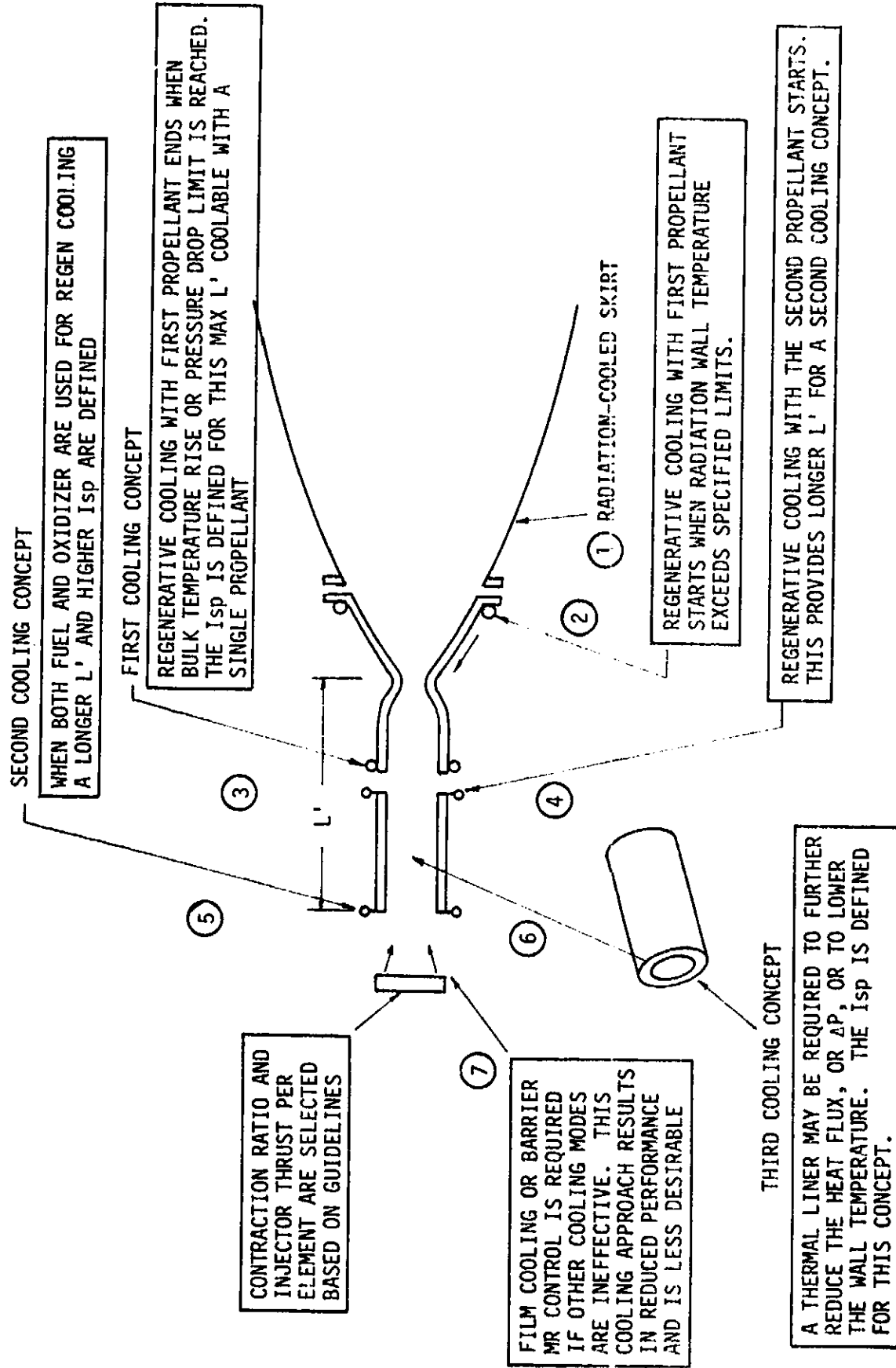


Figure 1. Cooling Concepts Selection

II, B, Cooling Concept Selections and Engine Cycle Considerations (cont.)

concepts having the highest performance potential, such as radiation cooling and/or regenerative cooling with one propellant, were considered first. These were followed by a) regenerative cooling with the other propellant, b) regenerative cooling with both propellants (dual-regen), c) the addition of thermal barriers in the cylindrical chamber to reduce chamber regenerative heat loads, or d) the reduction of chamber lengths, at the expense of performance, to attain the same cooling objective. Lower-performing configurations which require mass addition cooling were identified as applicable only after the limits of the higher-performing concepts had been reached.

2. Applicable Engine Cycles

Applicable engine cycles included both pressure-fed and pump-fed systems. The pump-fed engines can utilize a gas generator, an expander cycle, or staged-combustion cycles to provide power to drive the pumps. The pumps can also be driven by electric motors powered by batteries, solar cells, or fuel cells. Reference 1 indicates that the pressure-fed and electric motor-driven pump-fed systems are less desirable because of the excessive weight of the propellant pressurizing system. The expander cycle and a modified expander cycle utilizing a direct drive for one propellant and an alternator and electric motor for the second were the lowest-weight approaches. The latter cycle is defined as the turboalternator expander cycle. As the expander cycle becomes power-balance-limited at higher pressures and thrust levels, staged-combustion cycles become more attractive.

The present thermal analyses were based on the assumption that the coolant jacket discharge pressures for LOX, LH₂, or LCH₄ cooling are above the critical pressure (thus eliminating the concern for two-phase coolant flow) and that the coolant expands through a preburner or turbine prior to being delivered to the injector. Two-phase flow (bulk boiling) does not constitute a cycle limitation for the RP-1 coolant since coking is known to result at temperatures below its boiling temperature at the pressures of interest. Both the expander cycles and staged combustion cycles are compatible with the cooling design assumption in almost all cases, except at the very highest chamber pressure where the expander cycle may fail to power-balance. The inlet and discharge pressures of the chamber coolant jacket were based upon a power-balanced expander cycle where practical. All propellants, with the exception of RP-1, were assumed to be suitable turbine-drive fluids. The following upper temperature limits were placed on the expander-cycle turbine drive gas, based on chamber material limitations:

Oxygen	394°K (250°F)
Methane	450°K (350°F)
Hydrogen	450°K (350°F)

The thrust chambers were not optimized to provide the above temperatures if the chamber coolant discharge temperatures were less than the above values.

II. B, Cooling Concept Selections and Engine Cycle Considerations (cont.)

With these temperature limitations, power-balanced expander cycles were possible up to the following chamber pressures:

LOX/RP-1, LOX cooling	3792 kPa (550 psia) at MR = 2; 4826 kPa (700 psia) at MR = 4
LOX/LH ₂ , hydrogen cooling	4481 kPa (650 psia) at MR = 6
LOX/LCH ₄ , LOX cooling Methane cooling	4826 kPa (700 psia) at MR = 3.5 3447 kPa (500 psia) at MR = 3.5

C. COOLING CONCEPT SELECTION, ISP SENSITIVITY, CONCLUSIONS, AND RECOMMENDATIONS

This section presents the conclusions generally applicable to all propellant combinations. This is followed by more specific conclusions applicable to the individual propellant combinations. The section concludes with recommendations for the experimental activities which are required to verify or calibrate the analytical efforts of this program. The figures employed in this summary section are composites of all data and identify overall trends and differences between propellant systems. The same information is provided in expanded graphical and tabular format in the subsequent sections and appendices of this report.

1. General Conclusions Applicable to All Propellant Systems

Maximum specific impulse is attainable in systems employing regenerative cooling with oxidizer, fuel, or both propellants. The applicability of regenerative cooling can be extended to low-thrust, high-pressure pump-fed engines although it requires some departure from the practices which have evolved from the design of larger engines and/or have become industry guidelines or standards. These departures include:

- ° The use of larger-than-normal chamber contraction ratios.
- ° The use of copper chamber wall configurations having narrower and deeper slotted cooling channels.
- ° The use of both propellants for cooling.

a. Geometric Considerations

Low-thrust, high-pressure engines designed with conventional chamber contraction ratios of 2 to 6 result in very small chamber diameters; in many cases less than 1.27cm (0.5 in.). This small diameter does not provide the space required for a high-performing, multi-element injector and a center-mounted ignition source. Multi-element, fine-pattern injectors are required for maximum combustion efficiency within the limited-length, propellant-cooled combustion chamber.

II, C, Cooling Concept Selection, Isp Sensitivity, Conclusions, and Recommendations (cont.)

The need for an injector design containing a minimum of two rows of elements and a central igniter port was identified. This injector requires a minimum diameter of approximately 3.8 cm (1.5 in.). When this packaging requirement is applied to the low-thrust, high-pressure design points, it can result in chamber contraction ratios of up to ≈ 40 .

b. Coolant Selection

The use of regenerative cooling for LOX/RP-1 and LOX/methane engines is limited by the total heat load and the maximum local heat flux. Large contraction ratios reduce both total heat load and local flux in the chamber region and relieve the cooling problems that occur with RP-1 and methane fuels. This cooling solution drives the chamber geometry to "non-standard" configurations which offer both improved performance and improved cooling margin. The problems of handling high total heat load and high local heat flux were not encountered with fuel regeneratively cooled LOX/LH₂ systems.

The small quantity of propellant available for cooling at low thrust, combined with the need for high cooling velocities at high pressure, results in the need for very small cooling channels. In order to maximize the coolant surface area, these slots should be narrow and deep rather than rectangular or shallow and wide as is common in larger engines. Significant gains in regenerative cooling capability can be attained when channels smaller than the 0.076-cm. (0.030-in.) minimum-standard values are utilized for the design analyses.

Supercritical oxygen was found to be the preferred coolant in two of the three propellant systems considered. The fuel was preferred over the oxidizer only in the LOX/hydrogen system.

Oxidizer cooling was found to be superior to RP-1 cooling because the oxidizer flow is three times that of the fuel at the optimum performance mixture ratio and because cooling with oxygen avoids the coking problem experienced with RP-1. Supercritical oxygen cooling was also preferred for the LOX/methane system due to its higher mass flowrate (the LOX flow being 3 to 4 times that of the methane).

Significant performance advantages were predicted in the methane and RP-1 systems when both propellants are used as coolants. Using both LOX and RP-1 or LOX and LCH₄ as coolants resulted in longer coolable chamber lengths as well as preheating of both propellants prior to injection. The combination of preheated propellants and greater chamber length yielded higher performance. There was no significant performance

II, C, Cooling Concept Selection, Isp Sensitivity, Conclusions, and Recommendations (cont.)

benefit predicted for using both propellants as coolants in the LOX/LH₂ system as the hydrogen cooling capacity was adequate even at oxidizer/fuel (O/F) weight flow ratios up to 8.

c. Attainable Isp

Figure 2 provides a composite plot of attainable Isp for the three propellant systems considered. This plot includes the highest and lowest values of thrust, P_c, and mixture ratio. Each data point on the performance summary figure has a defined cooled chamber configuration, including channel size, chamber length, and coolant pressure loss, which is compatible with the stress, life, and material limits for the proposed application. The symbols in the figure represent the chamber pressure and cooling media. Solid symbols define fuel cooling whereas open symbols are for oxygen cooling and half solid/half open symbols are for dual-propellant regenerative cooling. The dual-cooling design points provided higher performance. This was especially significant for the low-thrust RP-1 propellant systems where a 4% improvement in specific impulse was predicted over an oxygen-only cooling approach. When operating at a mixture ratio of 3.0, the dual-regen configuration provided 14% higher efficiency than the best RP-1-cooled design which was cooling-limited to a maximum mixture ratio of 2.

The superiority of the hydrogen/oxygen system as measured by the standard Isp (force/unit mass/sec) criteria for a weight-limited system is obvious from Figure 2. However, when a propellant selection is based on the volume-limited Space Shuttle cargo bay, the ranking of propellant system desirability in terms of Isp times density is reversed, as shown in Figure 3. The transport of O₂/H₂ as H₂O and its subsequent conversion to propellant in space could result in this combination being optimum in both the Isp and volumetric efficiency categories.

The data provided in this report have been designed to allow the members of the technical community charged with packaging payloads in the shuttle bay the choice of propellants and mixture ratios which best meet the weight and volume capabilities.

d. Applicability of Cooling Approaches

The following paragraphs and figures identify the applicability of various cooling approaches for each of the propellant combinations over the thrust, P_c, and MR operating ranges of this survey. The level of technology advancements required for cooling can be measured by 1) the symbols which indicate which of the propellants is best-suited for cooling and/or if both propellants are required, and 2) the minimum size of the cooling channel which must be fabricated in order to provide proper cooling.

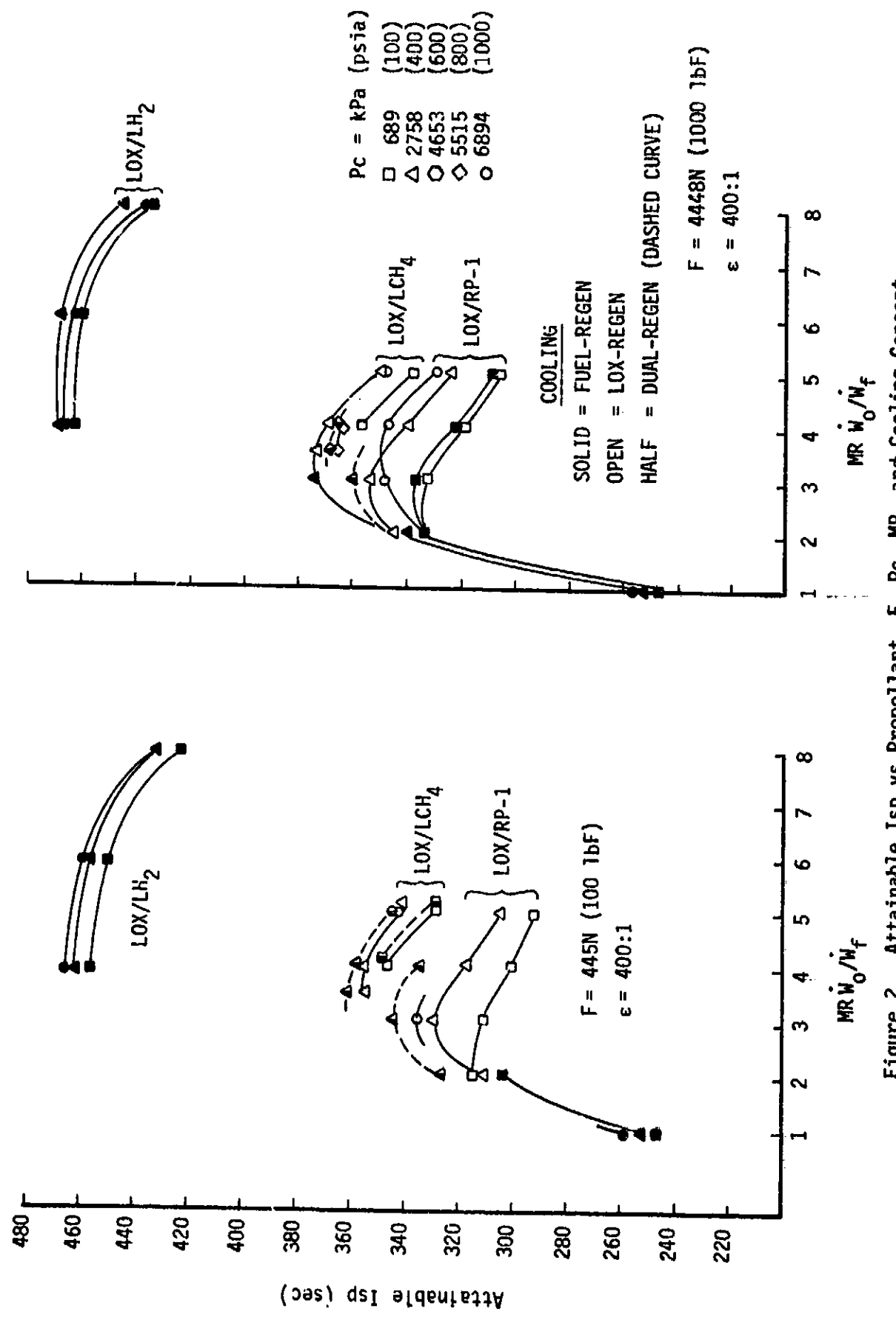


Figure 2. Attainable Isp vs Propellant, F , P_c , MR , and Cooling Concept

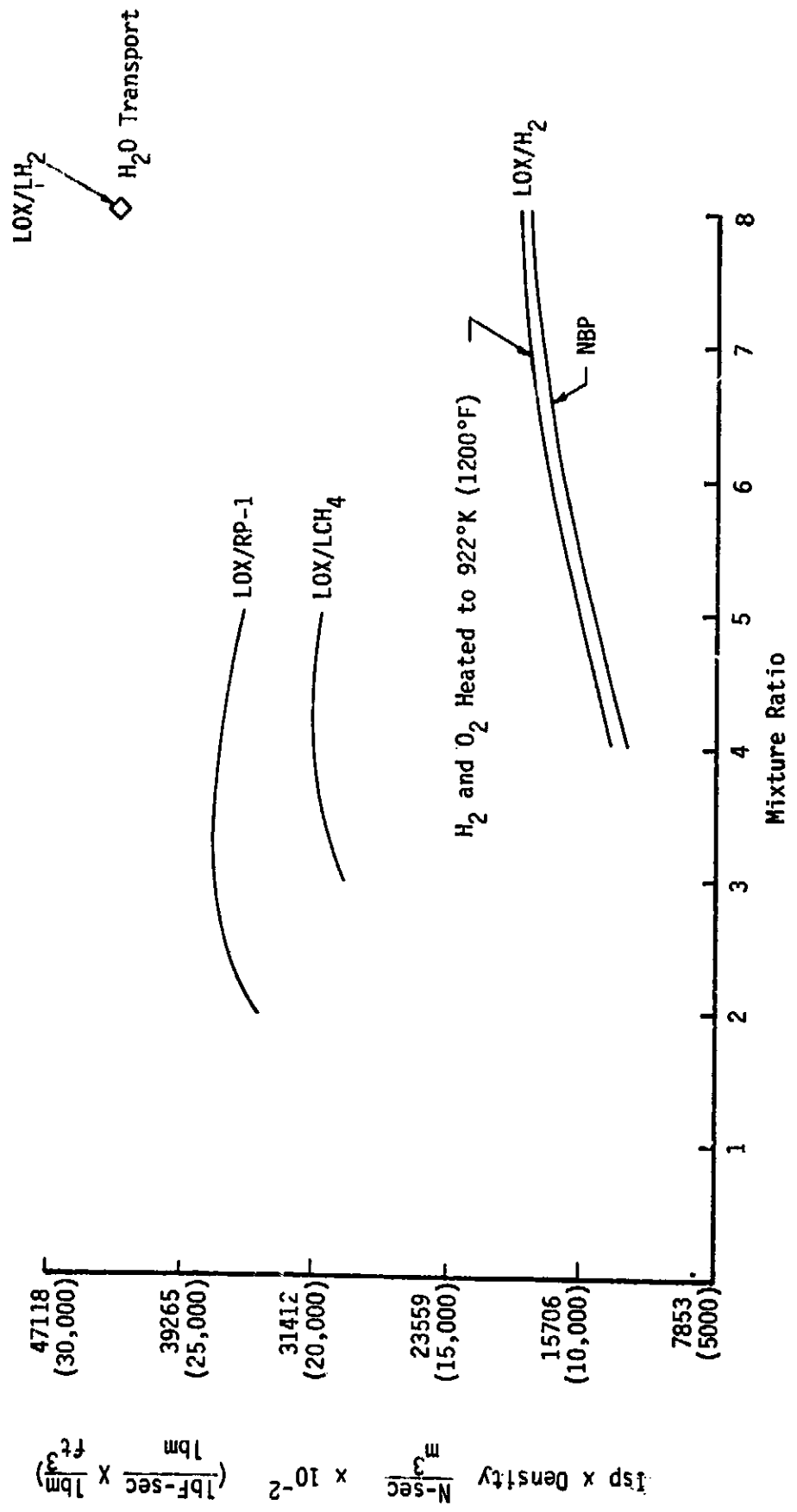


Figure 3. Volumetric Impulse Comparison for LOX/RP-1, LCH₄, and LH₂ Fuels

II, C, Cooling Concept Selection, Isp Sensitivity, Conclusions, and Recommendations (cont.)

2. LOX/RP-1

The cooling results for the LOX/RP-1 system are presented in Figure 4. This figure defines the cooling concept and channel size as a function of mixture ratio at three levels of thrust. The figure shows that RP-1 is suitable for cooling only at pressures <1379 kPa (200 psi) at the higher thrust levels. In order to operate at the optimum mixture ratio of ≈ 3 , the chamber length must be reduced from the optimum performance value. The required coolant channel sizes for RP-1 cooling are as small as 0.013 cm (0.005 in.).

In contrast, cooling with supercritical oxygen allows cooling at pressures to 4136 kPa (600 psi) at 445N (100 lbF) and to 6894 kPa (1000 psia) at 4448N (1000 lbF). Small channel sizes are also required for the oxygen, though not as small as those for the fuel, and oxidizer cooling does not present the concern for carbon fouling of the channels observed with fuel cooling.

Dual-propellant cooling provides for a higher operating pressure range at thrust levels of 445 and 1779N (100 and 400 lbF), respectively. In the dual-propellant cooling system, the oxygen is used to cool the chamber and throat while the RP-1 is employed as a coolant for the higher area ratios in the nozzle where the heat flux is low and the channel sizes are much larger. Dual-propellant cooling does not significantly influence the minimum-channel size for the oxidizer.

At fuel-rich mixture ratios (below ≈ 1.5), RP-1 is more suitable for cooling than oxygen because it results in slightly larger channels; however, the performance is very poor in this region. If larger channels are desired, it would be better to consider oxidizer-rich higher mixture ratios where both the Isp performance and the Isp density parameters are more favorable.

Figure 4 indicates that, except at very high and very low mixture ratios, regenerative LOX/RP-1 cooling is not possible when 0.076-cm (0.030-in.) channel widths are specified to be the minimum practical coolant channel size. These results are consistent with those of previous studies (Ref. 1). If the minimum practical coolant channel width is specified to be 0.025 cm (0.010 in.), oxygen cooling becomes possible over a large portion of the P_c/MR box at thrust levels of 4448N (1000 lbF) and 1779N (400 lbF). Oxygen cooling at 445N (100 lbF) requires channels of 0.013 cm (0.005 in.) or smaller.

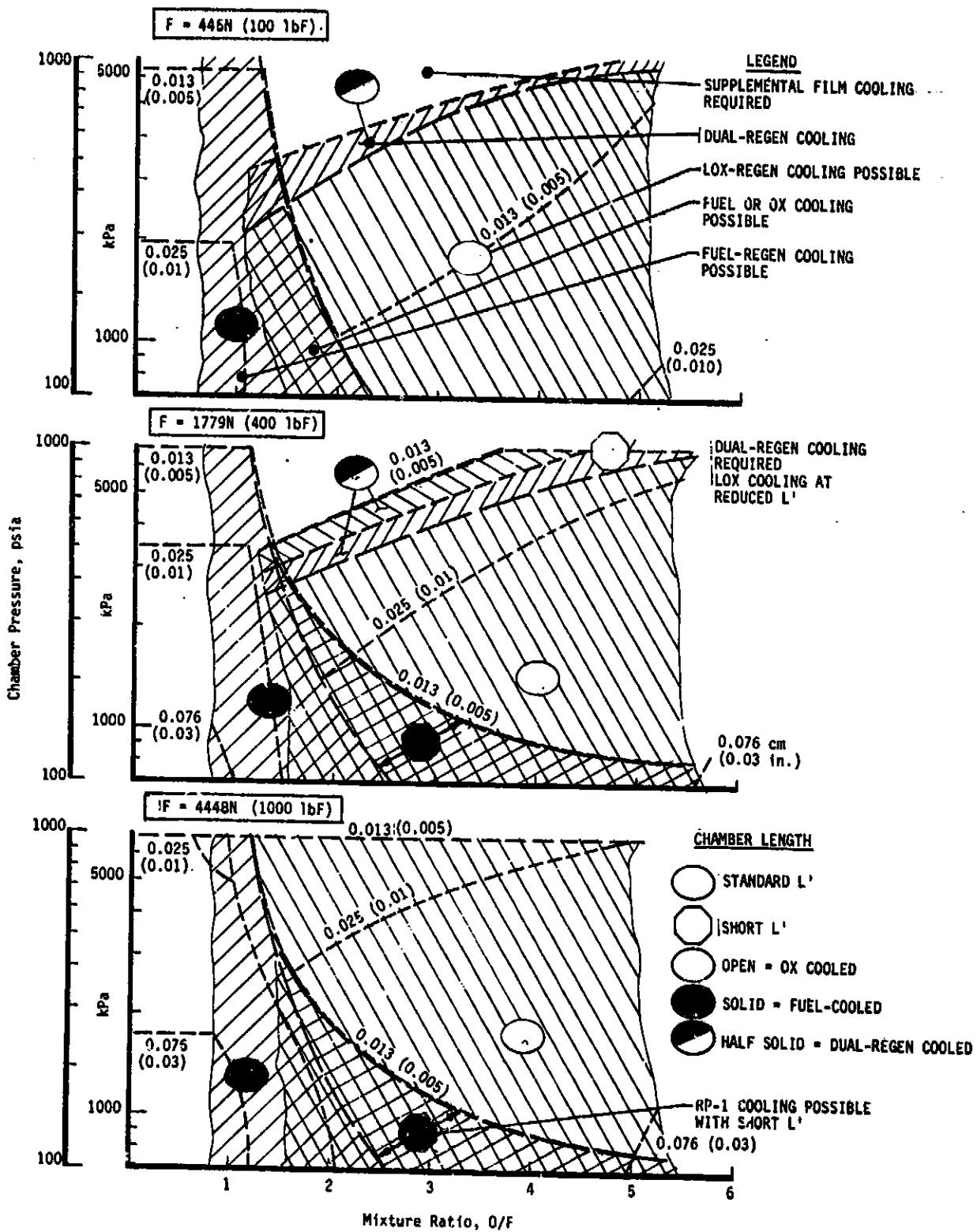


Figure 4. Range of Applicability for LOX and RP-1 Regenerative Cooling

II, C, Cooling Concept Selection, Isp Sensitivity, Conclusions, and Recommendations (cont.)

3. LOX/Hydrogen

With hydrogen as the coolant, no cooling limitations were encountered at mixture ratios between 4 and 8 and at chamber pressures up to 6894 kPa (1000 psia); consequently, the use of oxygen as a coolant was not considered. The minimum coolant channel widths required to provide proper cooling are displayed in Figure 5. As can be seen, the most difficult region to cool, that of high pressure and low thrust, requires cooling channel widths between 0.025 and 0.05 cm (0.010 and 0.020 in.). The maximum channel depth-to-width ratio employed was 4. Although the channel widths become slightly smaller at higher mixture ratios, this was not found to significantly alter the conclusions regarding cooling feasibility.

4. LOX/Methane

In the LOX/methane system, both propellants were found to be almost equally suited for cooling, with only a slight advantage for oxygen at the optimum performance mixture ratio of 3.5. (See Figure 6) At higher pressures and lower thrust, neither propellant, acting alone, provided sufficient heat removal capability to allow the required cooled chamber length to be attained at reasonable coolant pressure drop. The use of dual-propellant regenerative cooling, however, provided sufficient heat removal capability to overcome this limitation. The design limitations with dual-regenerative cooling are based strictly on the minimum-coolant channel size which can be fabricated and operated without plugging. The use of dual-regenerative cooling has only a minor effect on the minimum channel size as the latter is controlled by the cooling mass velocities required to maintain chamber wall temperature in the high heat-flux region and is not strongly influenced by rises in bulk temperature in the single-pass counterflow designs considered for this study.

The minimum channel widths required to regeneratively cool zirconium copper (Zr-Cu) chambers operating at an engine MR of 3.5 are shown in Figure 7. In general, cooling with fuel is noted to result in larger channel sizes. However, the fuel cooling system becomes limited by bulk temperature rise as pressure increases; thus oxidizer must be employed for cooling at higher pressure even though the channels are smaller. As can be noted in the figure, there are certain thrust/chamber pressure regions where exceptions to this general conclusion exist, thus each case must be examined individually.

The ability to provide propellant regenerative cooling at low thrust and high pressure is again dictated by the minimum size of the coolant channel. Dimensions down to 0.013 cm (0.005 in.) will be required

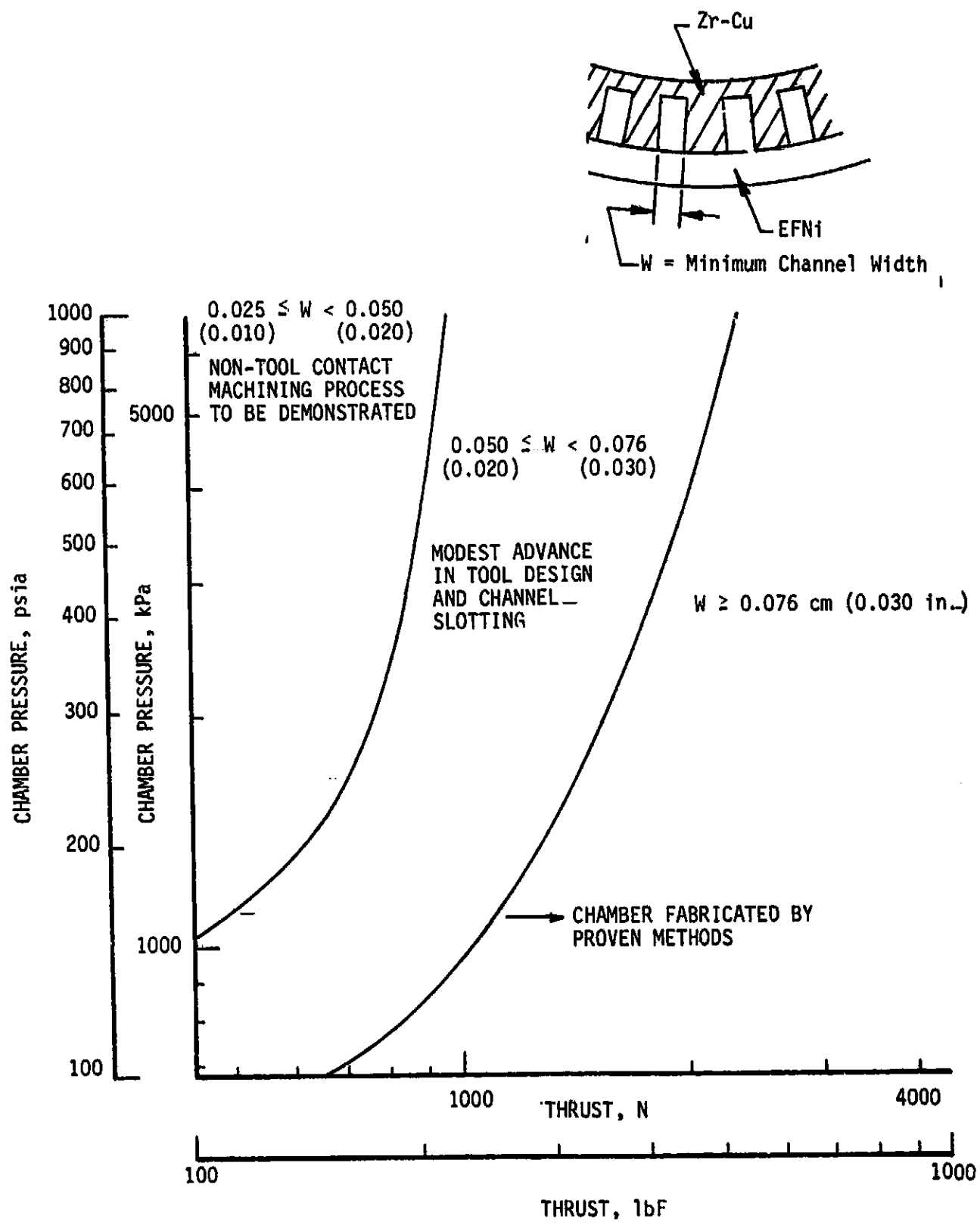


Figure 5. Ranges in Minimum Channel Size as a Function of Chamber Pressure and Thrust, LO_2/LH_2 at MR = 6

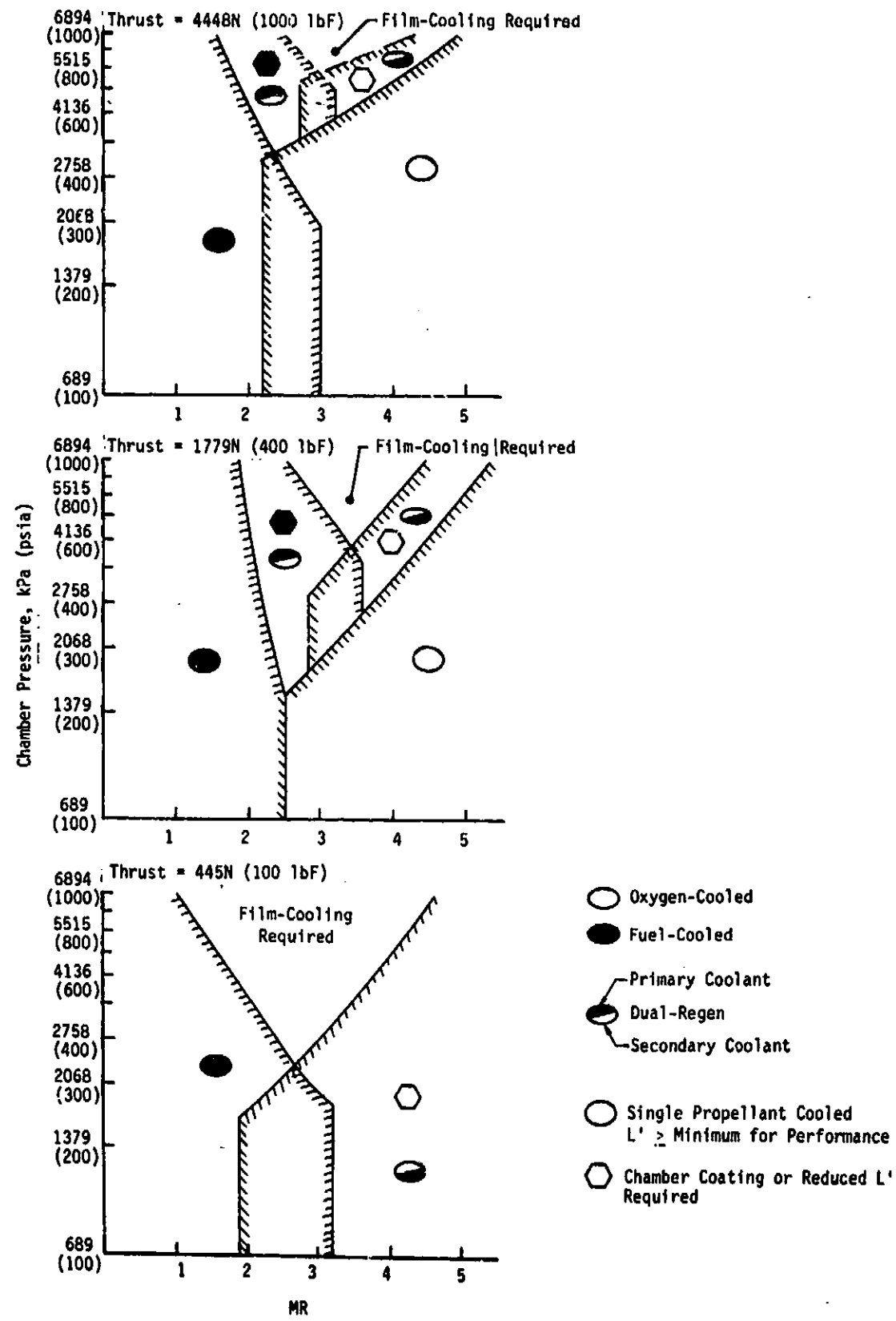


Figure 6. Range of Applicability for LOX and LCH_4 Regenerative Cooling

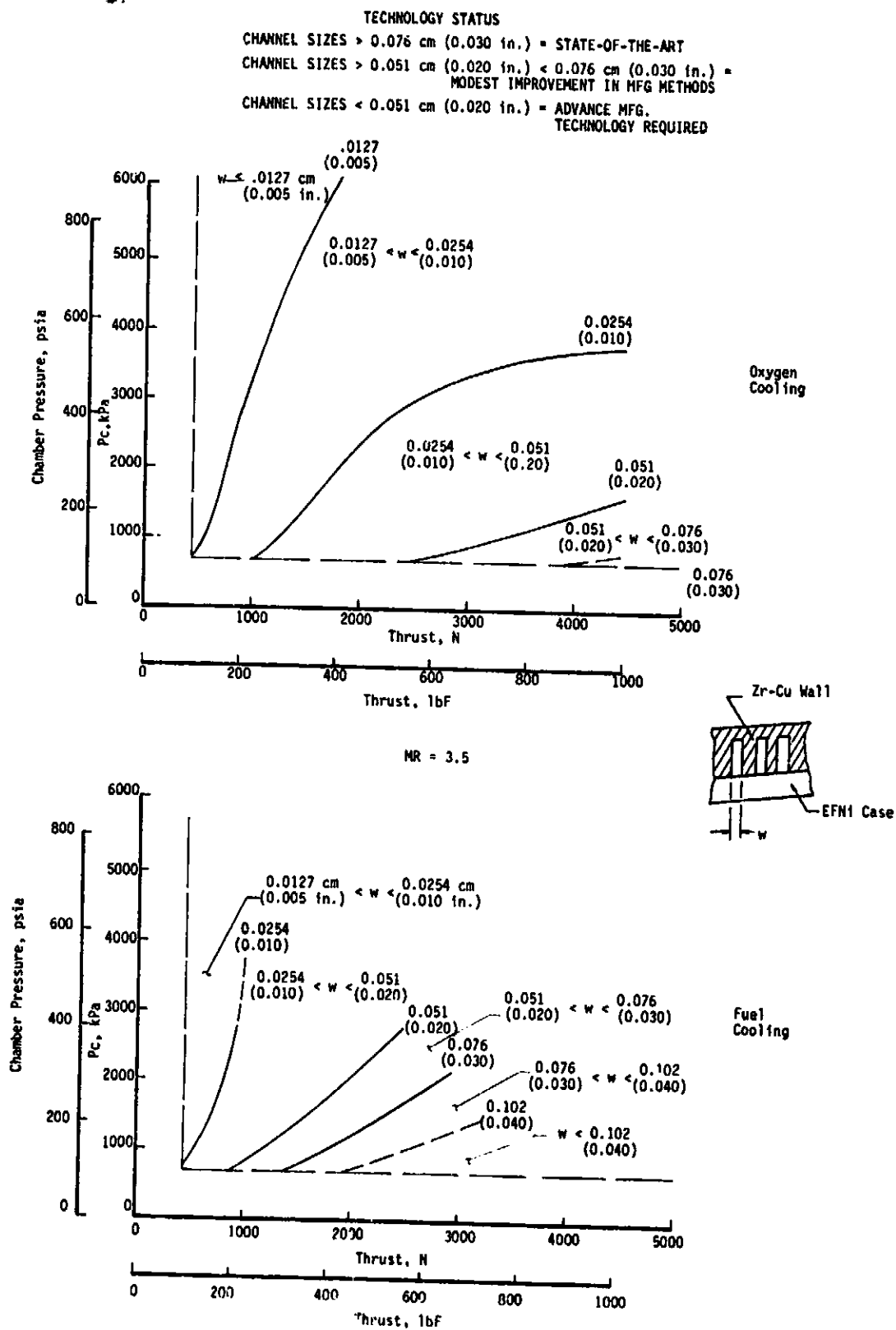


Figure 7. Minimum Coolant Channel Widths Required for Regenerative Cooling with LOX/LCH₄ Propellants at MR = 3.5

II, C, Cooling Concept Selection, Isp Sensitivity, Conclusions, and Recommendations (cont.)

for low thrust and high pressure. The specification of a 0.076-cm (0.030-in.) wide channel, as shown in Reference 1, limits cooling to the use of fuel only, and then only at high-thrust and low-pressure conditions.

5. Effect of Added Enthalpy

The LOX/hydrogen propellant system was examined to determine the potential improvements in specific impulse which could result if either the fuel or the oxidizer or both propellants were heated to 922°K (1200°F) prior to injection. The performance study was conducted at 1779N (400 lbF) thrust and a chamber pressure of 2758 kPa (400 psia) for mixture ratios ranging from 2.0 to 8.0. It was assumed that the hydrogen from the tank would be employed to cool the chamber and that the discharge coolant would then be externally heated to 922°K (1200°F). The increase in heat flux and the reduction in coolant flow due to the effect of the higher propellant energy were accounted for in subsequent chamber cooling analyses.

Figure 8 shows that the most significant gain in Isp occurs at low mixture ratio. Specific impulse improvements of up to 10% over normal boiling point (NBP) optimum MR values are attainable by heating both propellants and reducing the MR to ≈ 2 . The Isp values for 12 respective cases are shown in Table II.

Cooling analyses for cases involving heated hydrogen and heating of both propellants were completed for selected P_c and thrust conditions [2758 kPa and 1779N (400 psia and 400 lbF), respectively] at a mixture ratio of 4. These results were then compared to data where both propellants were supplied to the engine at NBP energy levels. The effect of the higher combustion temperature and lower coolant flowrate (due to higher performance) was found to produce slightly more adverse, but manageable, cooling channel configurations. Table III provides a cooling comparison for the three cases. The table shows a small increase in cooling pressure drop for the heated propellant cases. It should be noted that the size of the cooling channel must be made smaller in order to accommodate the 27% higher maximum flux for the added enthalpy cases. Representative cooling channel dimensions are as follows:

<u>Case</u>	<u>Channel Depth, cm (in.)</u>	<u>Channel Width, cm (in.)</u>
1 NPB H ₂ and O ₂	0.376 (0.148)	0.094 (0.037)
2 922°K (1200°F) H ₂ and NBP O ₂	0.252 (0.099)	0.064 (0.025)
3 922°K (1200°F) H ₂ and O ₂	0.249 (0.098)	0.061 (0.024)

$F = 1779N$ (400 lbF)
 $P_c = 2758 \text{ kPa}$ (400 psia)

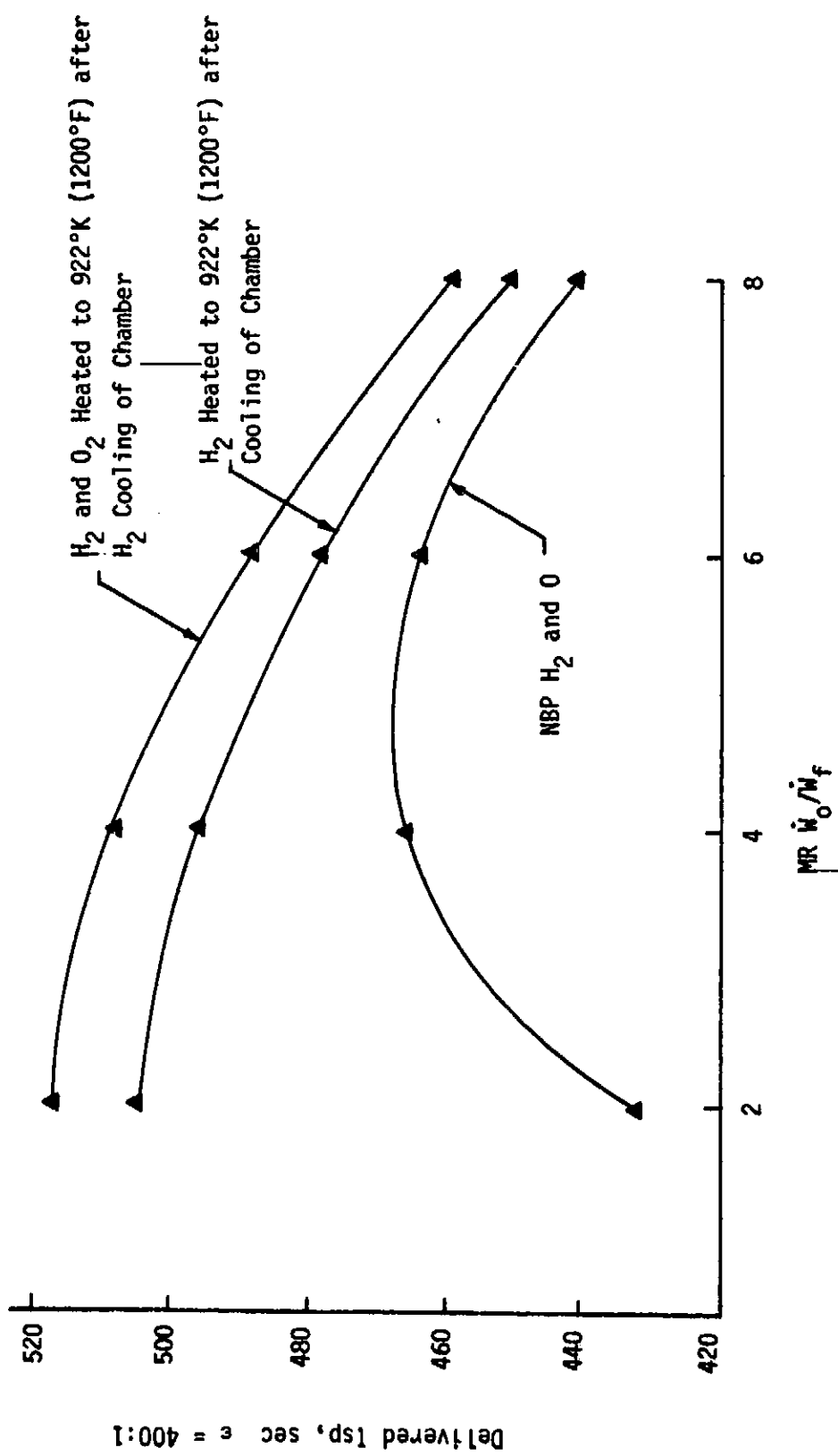


Figure 8. Attainable Specific Impulse for LOX/LH₂ with Propellant Preheating by External Energy Sources

TABLE II
ADDED ENTHALPY RESULTS (PROPELLANTS: LOX/LH₂)

P_c = 2758 kPa (400 psia) F = 1779 N (400 lbF) ε = 400:1

Case MR	NBP		Hot H ₂ , NBP Ox		Hot H ₂ and Hot O ₂		
	Isp _R	ΔT _F °K (°R)	Isp _{H₁}	% ΔIsp	ΔT _{OX} °K (°R)	Isp _{H₂}	% ΔIsp
2	433.8	778 (1400)	505.5	16.5	832 (1497)	518.1	19.4
4	466.4	721 (1296.9)	496.9	6.5	832 (1497)	508.4	9.0
6	464.9	641 (1153.5)	479.9	3.2	832 (1497)	489.3	5.2
8	441.6	623 (1121.9)	451.6	2.3	832 (1497)	459.9	4.1

where

Isp_R = Reference case NBP

Isp_{H₁} = Only hydrogen is heated by "free" source

ΔT_F = Temperature rise by "free" source

Isp_{H₂} = Both hydrogen and oxygen are heated

ΔT_{OX} = Temperature rise from tank condition

NBP = Normal boiling point

TABLE III
EFFECT OF ENTHALPY ADDITION TO PROPELLANT(S)
FOR LOX/HYDROGEN SYSTEM

PROPELLANTS	O ₂ /H ₂	O ₂ /H ₂	O ₂ /H ₂
NOMINAL P _c /F	400/400	400/400	400/400
CASE No.	1	2	3
	H ₂ O ₂ NBP	H ₂ @ 922 °K (1200 °F) O ₂ @ NBP	H ₂ O ₂ @ (1200 °F)
Thrust, N (lbf)	1779 (400)	1779 (400)	1779 (400)
P _c , kPa (psia)	2758 (400)	2758 (400)	2758 (400)
Throat Radius, cm (in.)	1.052 (0.414)	1.029 (0.405)	1.024 (0.403)
Contraction Ratio	8.00	8.00	8.00
MR	4	4	4
W _{ox} , kg/sec (lbm/sec)	0.323 (0.712)	0.287 (0.6318)	0.279 (0.6158)
W _f , kg/sec (lbm/sec)	0.081 (0.178)	0.072 (0.1579)	0.070 (0.1539)
ΔP _{cj} , kPa (psi)	7.58 (1.1)	17.92 (2.6)	19.30 (2.8)
P _{cj-in} , kpa (psia)	3894 (564.8)	3894 (564.8)	3894 (564.8)
P _{cj-out} , kPa (psia)	3886 (563.7)	3876 (562.2)	3874 (562.0)
T _{cj-in} , °K (°F)	23 (-418.0)	23 (-418.0)	23 (-418.0)
T _{cj-out} , °K (°F)	202 (-96.9)	250 (-9.6)	264 (14.6)
Regen c	11.32	7.28	8.21
h _g , max, kw/m ² °K (Btu/in. ² -sec °F)	6.854 (0.00233)	7.442 (0.00253)	7.354 (0.00250)
h _l , max, kw/m ² °K (Btu/in. ² -sec °F)	8.237 (0.00280)	10.149 (0.00345)	10.560 (0.00359)
Q/A _g max, kw/m ² (Btu/in. ² -sec)	14447 (8.84)	18320 (11.21)	18679 (11.43)
Q/A _l max, kw/m ² (Btu/in. ² -sec)	4952 (3.03)	5965 (3.65)	6079 (3.72)
Q _{total} , kw (Btu/sec)	232.3 (220.3)	261.9 (248.4)	269.6 (255.7)
T _r , °K (°F)	2924 (4803.3)	3275 (5425.3)	3352 (5573.3)
Wall Thickness, cm (in.)	.762 (0.3)	.762 (0.3)	.762 (0.3)
V _{cj-max} , m/sec (ft/sec)	24.5 (80.3)	32.9 (107.8)	35.1 (115.3)
M _{cj-max}	0.039	0.051	0.054
No. Channels	72	89	89
Min. Channel Depth, cm (in.)	0.142 (0.056)	0.124 (0.049)	0.137 (0.054)
Limiting Criterion	T _{wg}	T _{wg}	T _{wg}
Cooling Channel Geometry			
Depth/Width @ Max Flux Point, cm (in.)	0.376/0.094 (0.148/0.037)	0.251/.064 (0.099/0.025)	0.249/0.061 (0.098/0.024)
Depth/Width @ Max Bulk Temperature, cm (in.)	0.815/0.203 (0.321/0.080)	0.610/0.155 (0.240/0.061)	0.582/0.147 (0.229/0.058)

LEGEND

W _{ox}	= Total Weight Flow Oxygen	T _{wl}	= Liquid-Side Wall Temperature
W _f	= Total Weight Flow Fuel	h _g	= Gas-Side Heat Transfer Coefficient
W _{cj}	= Coolant Weight Flow	h _l	= Liquid-Side Heat Transfer Coefficient
ΔP _{cj}	= Cooling Jacket Inlet Pressure Drop	Q/A _g	= Gas-Side Heat Flux
P _{cj}	= Cooling Jacket Inlet Pressure	Q/A _l	= Liquid-Side Heat Flux
ΔT _{cj}	= Cooling Jacket Temperature Rise	T _r	= Recovery Temperature
T _{cj}	= Cooling Jacket Inlet Temperature	V _{cj}	= Maximum Coolant Jacket Velocity
W _{fcc}	= Fuel Film-Cooling Weight Flow	M _{cj-max}	= Maximum Coolant Jacket Mach Number
T _{wg}	= Gas-Side Wall Temperature		

II. Summary (cont.)

D. CONCLUSIONS AND RECOMMENDATIONS FOR FUTURE WORK

1. General

° The applicability of regenerative cooling can be extended to lower-thrust engines when larger chamber contraction ratios and smaller channels are employed.

° The use of larger contraction ratios lowers the total chamber heat load and local chamber flux. Larger contraction ratios allow more injector elements to be utilized, and this yields higher performance for a given chamber length. Lower total heat loads allow increased combustion chamber length and increased Isp.

° The contraction ratios used in low-thrust designs (8:40) are larger than normally employed, and experimental verification of the heat flux profiles and vaporization/mixing efficiency should be experimentally verified.

° The fabrication limits of smaller cooling channels should be identified for several candidate processes; also, data on channel surface roughness and manufacturing tolerances should be obtained.

2. LOX/RP-1

° Supercritical oxygen should be employed as the primary coolant for LOX/RP-1 engines operating at high chamber pressures. RP-1 cooling is suitable only at low pressures and thrust levels above 1779N (400 lbF).

° Performance advantages are attainable when both propellants are used as coolants.

° The maximum Isp for fuel cooling, oxidizer cooling, and dual-regenerative cooling is 341, 354, and 359 sec, respectively, at 4448N (1000 lbF) thrust, and 303, 334, and 345 sec, respectively, at 445N (100 lbF) thrust.

3. LOX/LH₂

° Hydrogen cooling is adequate for the entire F, P_c, and MR box of interest [(445-4448N [100-1000 lbF], 689-6894 kPa (100-1000 psf), and 4 to 8]. Cooling channel widths of 0.025 and 0.051 cm (0.010 and 0.020 in.) are required for low-thrust, high-pressure operations.

II, D, Conclusions and Recommendations for Future Work (cont.)

° When using NPB propellants for an area ratio of 400:1, the maximum attainable Isp for hydrogen cooling is 468 seconds. This occurs at the following conditions: $P_c = 2758 \text{ kPa}$ (400 psi), $F = 4448\text{N}$ (1000 lbF), and $MR = 4$. Further improvements are possible if injector element density guidelines are adjusted to a finer pattern (more than $0.93 \text{ elements/cm}^2$ (6 elements/in.²) of face surface). A perfect injector ERE = 100% would provide an Isp of 472 seconds.

° Isp values of 490 to 510 sec are attainable with hydrogen and oxygen if the propellants are heated to 922°K (1200°F) by an external source. Liquid hydrogen regenerative cooling prior to heating the propellant is recommended.

4. LOX/LCH₄

Either supercritical fuel or oxidizer can be employed as a regenerative coolant at higher thrust and at pressures below $\approx 2068 \text{ kPa}$ (300 psi). Oxidizer cooling allows operation at lower thrust and more optimum MR (≈ 3.5) at chamber pressures up to 2758 kPa (400 psi).

° Dual-propellant cooling allows operation to ≈ 4136 (600 psi) at a thrust of 1779N (400 lbF) and to 5515 kPa (800 psi) at 4448N (1000 lbF). Oxygen should be used as the primary coolant in the high-flux throat region, and fuel should be used as the coolant in the large contraction ratio chamber region to extend the chamber length and improve performance.

° Chamber pressures greater than $\approx 3447 \text{ kPa}$ (500 psi) do not provide any significant performance advantage and make cooling more difficult.

° The maximum Isp at 4448N (1000 lbF) thrust is 375 seconds. Fuel cooling, oxidizer cooling, or dual-propellant cooling provide approximately the same performance at the high-thrust level. At 445N (100 lbF) thrust, the maximum Isp is 356 sec for oxidizer-regenerative cooling and 360 sec for dual-regenerative cooling. Fuel cooling at the low-thrust condition was not recommended.

III. RESULTS OF METRIC STUDIES FOR LOX/RP-1

A. SUMMARY

The objective of the Task III analyses was to determine the extent of applicability of regenerative cooling concepts for LOX/RP-1 engines over a thrust range of 445 to 4448N (100 to 1000 lbF), a chamber pressure range of 689 to 6894 kPa (100 to 1000 psia), and a mixture ratio range of 1 to 5. Using the simplified thermal model developed in Task II, these studies minimized the design and cooling constraints imposed on earlier studies. In this study, either or both propellants could be utilized as coolants, and no restriction was placed on minimum channel size.

The results showed that cooling with RP-1 is limited to high-thrust, low-pressure, and low mixture ratio operating ranges. Cooling with oxygen allows higher chamber pressures and lower thrusts to be attained. If both the RP-1 and oxygen are used as coolants, an even broader operating range becomes feasible. A limited high-pressure, low-thrust region was identified where additional (film) cooling would be required. In general, the Task III analyses showed significant cooling advantages for channels whose widths are less and whose channel aspect ratios are greater than fabricable with conventional machining.

B. THERMAL DESIGN

1. Scope and Analytical Basis

The simplified thermal design model developed in Task II requires (a) preliminary performance parametric data to estimate weight flows and throat size, (b) engine and cooling channel design constraining guidelines, and (c) thermochemical data characterizing gas-side flow and thermal parameters. This model and the preliminary analyses performed in Task II for the LOX/RP-1 system at mixture ratios of 2 and 4 provided the methodology for the rapid investigation of design parameter variations.

The study envelope for Task III was as follows:

Propellants - LOX and RP-1

Thrust, F - $445 \text{ N} (100 \text{ lbF}) \leq F \leq 4448 \text{ N} (1000 \text{ lbF})$

Chamber Pressure, P_c - $689 \text{ kPa} (100 \text{ psia}) \leq P_c \leq 6894 \text{ kPa} (1000 \text{ psia})$

Mixture Ratio, O/F - $1 \leq x_{MR} \leq 5$

Chamber Material - Zirconium-Copper Alloy

No benefit was assumed for possible gas-side heat flux reduction due to carbon deposition.

III, B, Thermal Design (cont.)

a. Performance Parameters

Parametric specific impulse and thrust coefficient (C_F) data at the selected expansion ratio ($\epsilon = 400:1$) were generated as a function of F , P_c , and MR , then input directly to the SCALEF thermal design program. These data were used to determine the propellant flowrates and throat sizes. Engine L' values were estimated from these preliminary performance data as functions of thrust and chamber pressure for energy release efficiencies (ERE's) greater than 95%.

b. Design Guidelines

Although limiting design constraints were to be kept to a minimum by the philosophy of the study, practical considerations dictated certain assumptions to assess the feasibility of specific designs. These included:

- Coolant Pressure Drop
 LO_2 and RP-1 $\Delta P \leq 1724 \text{ kPa} (250 \text{ psi})$
- Maximum Bulk Temperature
 LO_2 $T_b \leq 394^\circ\text{K} (250^\circ\text{F})$
 $RP-1$ $T_b \leq 450^\circ\text{K} (350^\circ\text{F})$
- Maximum Gas-Side Wall Temperature
 LO_2 and RP-1 $T_{wg} \leq 811^\circ\text{K} (1000^\circ\text{F})$
- Maximum Coolant-Side Wall Temperature
 LO_2 $T_w \leq 589^\circ\text{K} (600^\circ\text{F})$
 $RP-1$ $T_w \leq 561^\circ\text{K} (550^\circ\text{F})$

The pressure drop limitation was based on power-balance considerations for typical engine cycles. The coolant bulk temperature limits and coolant-side wall temperature limits were based on oxygen-copper ($O_2\text{-Cu}$) reaction rates for oxygen and on incipient coking for RP-1. The gas-side wall temperature was limited by strength and cycle life to meet an engine firing duration of a typical mission (20 cycles and up to 50 hours).

III, B, Thermal Design (cont.)

c. Thermochemical and Gas Dynamic Parameters

The TRAN 72 and Rao nozzle design programs were utilized to generate gas-side parameters and nondimensional engine geometry for the ranges of thrust, P_c , and MR studied. The minimum engine contraction ratio was selected to be 8:1. This was based on test experience and a sensitivity analysis (Appendix A) which had shown undesirable high mixing and vaporization losses, high chamber heat fluxes, and high total heat loads at lower contraction ratios. The minimum chamber radius of 1.91 cm (0.75 in.) was chosen to allow for an igniter and two rows of injection elements. This resulted in contraction ratios up to 40:1 at low thrust and high chamber pressure.

The gas thermal transport properties, C_p/C_v ratio, and Prandtl number were found to be primarily functions of mixture ratio only, while chamber temperature, thrust coefficient, and specific impulse were functions of both P_c and mixture ratio.

2. Analysis Methodology

The parametric cooling analyses for LOX/RP-1 propellants were performed in accordance with the following logic:

a. Three values of thrust - 4448, 1779, and 445N (1000, 400, and 100 lbF) - were analyzed sequentially in that order.

b. Analysis for "single-regen" cooling was performed first for fuel cooling and then for oxidizer cooling. Single-regen cooling is defined as using one propellant only as coolant, and cooling the chamber from the radiation-cooled attachment area ratio (or from an area ratio of 6:1 if the attach point ratio is less than 6:1) to the injector in a single-pass counterflow configuration.

c. Single-regen fuel cooling was considered first, starting at $MR = 1$, for each of three chamber pressures [689, 2758, and 6894 kPa (100, 400, and 1000 psia)].

For each chamber pressure, the mixture ratio was successively increased to 2, 3, 4, and 5 until fuel-cooling became limited either by bulk temperature rise (reduced L') or by excessive coolant pressure drop. In a number of cases, computer solutions could not be achieved because of numerical difficulties resulting from fluid property variations,

III, B, Thermal Design (cont.)

high-pressure gradients or because channel widths of less than 0.005 cm (0.002 in.) were required.

d. Single-regen oxidizer cooling was then studied in the same fashion, starting with an MR of 5 and successively reducing the mixture ratio to an MR value of 2.

Where the bulk temperature rise in the engine barrel section was excessive, it led to a decrease in coolant density and a rapid increase in pressure drop as chamber length increased. This resulted in a termination of L' below the minimum dictated by performance criteria. When these conditions were encountered, calculations were performed to include a low-conductivity liner in the cylindrical section only. The thermal resistance of this liner was standardized at a t/k value of

$$1765 \left(\frac{m^2 \text{ } ^\circ K}{M_w} \right) [600 \left(\frac{\text{in.}^2 \text{ sec } ^\circ F}{\text{Btu}} \right)]$$

The addition of the liner increased the maximum gas-side temperature from 811°K (1000°F), set for copper, to a range between 1089° and 1644°K (1500° and 2500°F).

e. Dual-regen cooling, with or without a liner, was analyzed when cooling with a single propellant could not be achieved within the constraints imposed by the thermal design criteria. In this mode, RP-1 cooling was considered from the radiation skirt attachment point area ratio to an expansion area ratio of 6:1. This was selected as a practical point from a fabrication and cooling standpoint as it was not reasonable to make this transition in the high-flux throat area. Oxygen cooling was then analyzed from $\epsilon = 6:1$ to the injector plane.

Normally, two significant design cooling problems are encountered: first, that posed by the locally high heat-flux region near the throat, and, secondly, the high total heat gain region in the cylindrical section. The latter is characterized by low flux over a large surface. The dual-regen concept attacks both problems because the use of RP-1 cooling in the skirt allows colder oxygen to be available for throat as well as for chamber cooling.

f. These analyses provided the chamber L' and propellant temperatures to the injector required for the performance analyses for each F, P_c , MR, and cooling concept combination.

III, B, Thermal Design (cont.)

3. Single-Propellant Regenerative Cooling Results (Fuel or Oxygen)

Selected input data and calculated results for cooling with RP-1 and oxygen are presented in Tables IV and V, respectively. The table nomenclature is given in Table VI. The more significant results are displayed graphically in Figures 9 through 20.

a. Coolant Pressure Drop

Cooling channel pressure drops for both RP-1 and oxygen as single-regen coolants are shown in Figures 9 through 11 as a function of mixture ratio for thrusts of 4448, 1779, and 445N (1000, 400, and 100 lbF), respectively. Chamber pressures of 689, 2758, and 6894 kPa (100, 400, and 1000 psia) are shown at all thrust levels for both coolants, while data at additional P_c values are displayed for $F = 445N$ (100 lbF) with oxygen as the coolant.

A key design parameter is the area ratio at which the regenerative cooling ends and the radiation-cooled skirt begins. At a mixture ratio of 1, the engine can be completely radiation-cooled or regeneratively cooled at all thrust levels and P_c 's. If the allowable radiation-cooling temperature is reduced from the allowable 1589°K (2400°F) (coated columbium) to 1311°K (1900°F), regenerative cooling is required. Acceptable coolant jacket pressure drops at all chamber pressures are possible at $MR=1$. With increasing MR , ΔP values 1) increase but remain acceptable at the $F = 4448N$ (1000 lbF) level for $P_c = 689$ kPa (100 psia), 2) become marginal up to $MR = 3$ for $F = 1779N$ (400 lbF), and 3) are unacceptable at $F = 445N$ (100 lbF). Consequently, fuel-regenerative cooling is practical at the following F , P_c , and MR combinations:

$MR = 1$ All F 's, 445-4448N (100-1000 lbF) and P_c 's, 689-6894 kPa (100-1000 psia)

$MR = 2-5$ $F = 4448N$ (1000 lbF); $P_c = 689$ kPa (100 psia)

$MR = 2,3$ $F = 1779N$ (400 lbF); $P_c = 689$ kPa (100 psia)

When oxygen is the coolant at mixture ratios from 2 through 5, channel pressure drops are acceptable at all P_c 's at $F = 4448N$ (1000 lbF). Note, however, that a reduced chamber L' (Table V) is required with $MR = 2$ and 3 at a P_c of 6894 kPa (1000 psia). At a thrust of 1779N (400 lbF), oxygen cooling is feasible for P_c 's of 689 and 2758 kPa (100 and 400 psia). At $P_c = 6894$ kPa (1000 psia) and $MR = 5$, an acceptable pressure drop is approached for single-regen cooling only with a channel depth/width ratio

TABLE IV
 SELECTED PARAMETERS CHARACTERIZING ENG
 COOLING WITH RP-1
 (Single Regen)

Code	MR	F	Pc	Coolant	P _{in}	P _{in} /Pc	t _{wall}	CR	T _c	C _F	Isp*	Channel Dimensions			
												--	N	kPa	--
1-1-1/F	1	445	689	F	1379	2.00	0.76	8.00	1424	1.948	-251.2	8.	0.076/0.610	0.076/0.180	14.40
1-1-4/F		2758		F	6205	2.25	0.76	13.96	1488	1.975	257.5	8.	0.0460/0.3673	0.0460/0.135	10.46
1-1-10/F		6894		F	9652	1.40	0.25	34.79	1551	1.969	259.5	8.	0.0170/0.1369	0.0358/0.236	10.41
1-4-1/F		1779	689	F	1379	2.00	0.76	8.00	1424	1.915	250.9	8.	0.1793/1.435	0.1798/0.297	19.79
1-4-4/F		2758		F	6205	2.25	0.76	8.00	1488	1.936	257.2	8.	0.0330/0.218	0.0640/0.472	14.40
1-4-10/F		6894		F	9652	1.40	0.25	8.58	1551	1.942	260.4	8.	0.211/0.147	0.0406/0.325	14.55
1-10-1/F		4448	689	F	1379	2.00	0.76	8.00	1424	1.892	250.2	8.	1.977/1.262	0.2146/1.697	24.41
1-10-4/F		2758		F	6205	2.25	0.76	8.00	1488	1.903	255.7	8.	0.0498/0.335	0.1026/0.798	17.78
1-10-10/F		6894		F	9652	1.40	0.25	8.00	1551	1.907	259.0	8.	0.0315/0.226	0.0640/0.450	17.78
2-1-1/F	2	445	689	F	1379	2.00	0.76	8.00	3139	1.768	310.6	8.	0.9974/0.058	0.0114/0.091	4.06
2-4-1/F		1779	689	F	1379	2.00	0.76	8.00	3139	1.822	324.8	8.	0.0168/0.135	0.0236/0.191	10.77
2-4-4/F		2758		F	6205	2.25	0.76	8.00	3266	1.875	333.3	8.	0.0099/0.079	0.0119/0.097	6.05
2-10-1/F		4448	689	F	1379	2.00	0.25	8.00	3139	1.844	330.0	8.	0.0318/0.254	0.0414/0.333	20.07
2-10-4/F		2758		F	6205	2.25	0.76	8.00	3266	1.899	341.7	8.	0.0132/0.107	0.0185/0.150	7.92
3-4-1/F	3	1779	689	F	1379	2.00	0.76	8.00	3358	1.903	321.4	8.	0.0130/0.104	0.0206/----	7.42
3-10-1/F		4448	689	F	1379	2.00	0.25	8.00	3358	1.956	330.0	8.	0.0249/0.201	0.0323/0.257	17.30
4-4-1/F	4	1779	689	F	1379	2.00	0.76	8.00	3306	1.954	311.4	8.	0.0117/0.086	0.0168/0.135	6.22
4-10-1/F		4448	689	F	1379	2.00	0.25	8.00	3306	1.968	317.5	8.	0.0226/0.180	0.0292/0.234	12.22
5-4-1/F	5	1779	689	F	1379	2.00	0.76	8.00	3221	1.969	300.2	8.	0.0109/0.086	0.0132/0.107	7.42
5-10-1/F		4448	689	F	1379	2.00	0.25	8.00	3221	1.978	305.0	8.	0.0211/0.168	0.0300/0.236	11.10

FOLDOUT FRAME

TABLE IV
**CHARACTERIZING ENGINE REGENERATIVE
COOLING WITH RP-1
(Single Regen)**

SI Units												
Barrel w/d	L'	r _t	r _{ch}	e _A	ΔP	T _{b,in}	T _{b,out}	ΔT _b	h _{g,max}	Q _{g,max}	Q _{c,max}	No. of Channels
cm	cm	cm	cm		kPa	°K	°K	°K	kw/m ² °K x 10 ⁻³	kw/m ²	kw/m ²	
0.076/0.180	14.40	1.026	2.903	6.00	11.0	289	362	73	1714	1471	752	-
0.0460/0.135	10.46	0.511	1.905	6.00	72.4	289	372	83	5030	4412	1993	80
0.0358/0.236	10.41	0.323	1.905	6.67*	717	289	392	103	16679	14935	6945	73
0.1798/0.297	19.79	2.070	5.857	6.00	6.2	289	334	45	1533	1291	719	45
0.0640/0.472	14.40	1.029	2.913	6.00	62.0	289	359	70	10502	8431	1781	73
0.0406/0.325	14.55	0.650	1.905	8.17*	902	289	390	101	24180	20850	6928	117
0.2146/1.697	24.41	3.294	9.319	6.00	0.69	289	326	36	1683	1373	310	67
0.1026/0.798	17.78	1.643	4.646	6.00	43.4	289	342	53	9501	7631	1585	115
0.0640/0.450	17.78	1.039	2.936	7.31*	506	289	366	77	21797	18939	5311	134
0.0114/0.091	4.06	1.080	3.040	6.00	1062	289	450	161	1868	4690	2059	85
0.0236/0.191	10.77	2.123	6.005	6.00	232	289	450	161	1462	3693	1209	163
0.0119/0.097	6.05	1.046	2.959	8.61	3114	289	450	161	4324	11062	5016	226
0.0414/0.333	20.07	3.338	9.439	6.00	104.8	289	456	166	---	2990	637	155
0.0185/0.150	7.92	1.643	4.651	11.56	3334	289	456	161	5618	13971	4705	237
0.0206/-----	7.42	2.062	5.834	6.00	412	289	451	162	1385	3807	1471	197
0.0323/0.257	17.30	3.241	9.164	6.00	112.4	289	450	161	1100	3056	981	232
0.0168/0.135	6.22	2.050	5.799	6.00	483	289	468	179	1327	3562	147	248
0.0292/0.234	12.22	3.231	9.136	6.00	121.3	289	450	161	1050	2876	981	235
0.0132/0.107	7.42	2.042	5.776	6.00	533	289	478	189	1291	3366	1454	254
0.0300/0.236	11.10	3.223	9.114	6.00	126.8	289	456	167	1024	2712	981	237
												259

*TWRAD = 1311°K (otherwise 1786°K)

FOLDOUT FRAMES

TABLE IV (Cont.)

**SELECTED PARAMETERS CHARACTERIZING
COOLING WITH RP
(Single Regen)**

Code	MR	F	P _c psia	Coolant	P _{in} psia	P _{in} /P _c	t _{wall} in.	CR	T _c °R	C _F	Isp*	Channel Dimensions				
												Aspect Ratio	d/w	w/d in./in.	Barrel w/d in./in.	L' in.
1-1-1/F	1	100	100	F	200	2.00	.3	8.00	2564	1.948	251.2	8.	.030/.240	.030/.071	5.67	.
1-1-4/F		400	400	F	900	2.25	.3	13.96	2680	1.975	257.5	8.	.0181/.1446	.0181/.053	4.12	.
1-1-10/F		1000	1000	F	1400	1.40	.1	34.79	2791	1.989	259.5	8.	.0067/.0539	.0141/.093	4.17	.
1-4-1/F		400	100	F	200	2.00	.3	8.00	2564	1.915	250.9	8.	.0706/.565	.0708/.117	7.79	.
1-4-4/F		400	400	F	900	2.25	.3	8.00	2680	1.936	257.2	8.	.0130/.086	.0252/.186	5.67	.
1-4-10/F		1000	1000	F	1400	1.40	.1	8.58	2791	1.942	260.4	8.	.0083/.058	.0160/.128	5.73	.
1-10-1/F		1000	100	F	200	2.00	.3	8.00	2564	1.892	250.2	8.	.0621/.497	.0845/.668	9.61	1.
1-10-4/F		400	400	F	900	2.25	.3	8.00	2680	1.903	255.7	8.	.0194/.132	.0404/.314	7.00	.
1-10-10/F		1000	1000	F	1400	1.40	.1	8.00	2791	1.907	259.0	8.	.0124/.089	.0252/.177	7.08	.
2-1-1/F	2	100	100	F	200	2.00	.3	8.00	5651	1.768	310.6	8.	.0029/.023	.0045/.036	1.60	.
2-4-1/F		400	100	F	200	2.00	.3	8.00	5651	1.822	324.8	8.	.0066/.053	.0093/.075	4.24	.
2-4-4/F		400	400	F	900	2.25	.3	8.00	5878	1.875	333.3	8.	.0039/.031	.0047/.038	2.38	.
2-10-1/F		1000	100	F	200	2.00	.1	8.00	5651	1.844	330.0	8.	.0125/.100	.0163/.131	7.90	1.
2-10-4/F		400	400	F	900	2.25	.3	8.00	5878	1.899	341.7	8.	.0052/.042	.0073/.059	3.12	.
3-4-1/F	3	400	100	F	200	2.00	.3	8.00	6044	1.930	321.4	8.	.0051/.041	.0081/—	2.92	.
3-10-1/F		1000	100	F	200	2.00	.1	8.00	6044	1.956	330.0	8.	.0098/.079	.0127/.101	5.63	1.
4-4-1/F	4	400	100	F	200	2.00	.3	8.00	5950	1.954	311.4	8.	.0046/.037	.0066/.053	2.45	.
4-10-1/F		1000	100	F	200	2.00	.1	8.00	5950	1.968	317.5	8.	.0089/.071	.0115/.092	4.81	1.
5-4-1/F	5	400	100	F	200	2.00	.3	8.00	5797	1.969	300.2	8.	.0043/.034	.0052/.042	2.92	.
5-10-1/F		1000	100	F	200	2.00	.1	8.00	5797	1.978	305.0	8.	.0083/.066	.0118/.093	4.37	1.

*Estimated For Thermal Design

EOLDOUT FRAME

TABLE IV (Cont.)

**PARAMETERS CHARACTERIZING ENGINE REGENERATIVE
COOLING WITH RP-1
(Single Regen)**

English Units

Dimensions											No. of channels		
Barrel w/d in./in.	L in.	r _t in.	r _{ch} in.	Code	ε _A	ΔP psi	T _{b,in} °F	T _{b,out} °F	ΔT _b °F	hg,max Btu/in. ² sec °F x 10 ⁻³			
.030/.071	5.67	.404	1.143	1-1-1/F	6.00	1.6	60.3	191.3	131.0	.592	.90	.46	80
.0181/.053	4.12	.201	.750	1-1-4/F	6.00	10.5	60.3	210.0	149.7	1.710	2.70	1.22	73
.0141/.093	4.17	.127	.750	1-1-10/F	6.67*	104.	60.3	245.1	184.8	5.670	9.14	4.23	45
.0708/.117	7.79	.815	2.306	1-4-1/F	6.00	.9	60.3	141.3	81.0	.521	.78	.44	73
.0252/.186	5.67	.405	1.147	1-4-4/F	6.00	9.0	60.3	185.7	125.4	3.57	5.16	1.09	117
.0160/.128	5.73	.256	.750	1-4-10/F	8.17*	130.9	60.3	242.6	182.3	8.22	12.76	4.24	67
.0845/.668	9.61	1.297	3.668	1-10-1/F	6.00	.1	60.3	125.9	65.6	.572	.84	.19	115
.0404/.314	7.00	.647	1.829	1-10-4/F	6.00	6.3	60.3	155.6	95.3	3.23	4.67	.97	134
.0252/.177	7.08	.409	1.156	1-10-10/F	7.31*	73.4	60.3	199.4	139.1	7.41	11.59	3.25	85
.0045/.036	1.60	.424	1.200	2-1-1/F	6.00	154.	60.3	350.7	290.4	.635	2.87	1.26	163
.0093/.075	4.24	.836	2.364	2-4-1/F	6.00	33.6	60.3	350.7	290.4	.497	2.26	.74	226
.0047/.038	2.38	.412	1.165	2-4-4/F	8.61	451.7	60.3	350.0	289.7	1.42	6.77	3.07	156
.0163/.131	7.90	1.314	3.716	2-10-1/F	6.00	15.2	60.3	360.0	299.7	—	1.83	.39	237
.0073/.059	3.12	.647	1.831	2-10-4/F	11.56	483.6	60.3	350.2	289.9	1.91	-8.55	2.88	197
.0081/—	2.92	.812	2.297	3-4-1/F	6.00	59.7	60.3	351.9	291.6	.471	2.33	.90	232
.0127/.101	5.63	1.276	3.608	3-10-1/F	6.00	16.3	60.3	350.4	290.1	.374	1.87	.60	248
.0068/.053	2.45	.807	2.283	4-4-1/F	6.00	70.0	60.3	381.7	321.4	.451—	2.18	.90	235
.0115/.092	4.81	1.272	3.597	4-10-1/F	6.00	17.6	60.3	350.3	290.0	.357	1.76	.60	254
.0052/.042	2.92	.804	2.274	5-4-1/F	6.00	77.3	60.3	400.8	340.5	.439	2.06	.89	237
.0118/.093	4.37	1.269	3.588	5-10-1/F	6.00	18.4	60.3	360.1	299.8	.348	1.66	.60	259

* TWRAD = 2360°R (otherwise 3215°R)

2
FOLDOUT FRAME

TABLE V

TABLE V
SELECTED PARAMETERS CHARACTERIZING ENGINE REGEN
(Single Regen)

Code	MR	F	Pc	Coolant	P _{in} /Pc	t _{wall} (n,t,b)*	CR	T _c °K	C _F	lsp sec	Aspect Ratio d/w**	Channel Dimensions					
												Throat w/d	Barrel w/d	L'	r _t cm	r _{ch} cm	
2-1-1/0	2	445	689	0	6205	9.00	0.76	8.00	3139	1.768	310.6	8.	0.0152/0.122	0.0300/0.102	14.40	1.080	3.040
2-1-4/0			2758	0	6205	2.25	0.76	13.10	3266	1.853	315.5	20.	0.0079/0.155	0.0155/0.307	7.24	0.526	1.905
2-4-1/0		1779	689	0	1379	2.00	0.76	8.00	3139	1.822	324.8	8.	0.0272/0.218	0.0884/0.706	19.79	2.123	6.005
2-4-4/0			2758	0	6205	2.25	0.76	8.00	3266	1.875	333.3	8.	0.0257/0.206	0.0353/0.231	14.44	1.046	2.957
2-10-1/0		4448	689	0	1379	2.00	0.76	8.00	3139	1.844	330.0	8.	0.0531/0.424	0.1453/1.163	24.41	3.338	9.439
2-10-4/0			2758	0	6205	2.25	0.76	8.00	3266	1.899	341.7	8.	0.0358/0.287	0.0599/--	17.78	1.643	4.651
2-10-10/0			6894	0	9652	1.40	.0635	8.00	3327	1.871	332.9	20.	0.0185/0.549	0.0325/0.480	12.32	1.046	2.961
3-1-1/0	3	445	689	0	6205	9.00	0.76	8.00	3358	1.944	305.5	8.	0.0183/0.0356	0.0356/0.1911	44	1.029	2.909
3-1-4/0			2758	0	6205	2.25	0.76,1.02,1.02	14.39	3562	2.036	320.1	20.	0.0081/0.165	0.0254/0.196	10.16	0.503	1.905
3-1-5/0			3447	0	6791	1.97	0.76,1.02,1.02	16.70	3602	2.056	322.3	20.	0.0076/0.152	0.0244/0.168	10.16	0.447	1.826
3-1-6/0			4136	0	7370	1.78	0.76,1.02,1.02	20.00	3634	2.073	324.0	20.	0.0066/0.132	0.0239/0.155	10.16	4.06	1.816
3-1-7/0			4826	0	7928	1.64	0.76,1.02,1.02	23.40	3659	2.085	325.3	20.	0.0056/0.112	0.0249/0.091	10.16	0.375	1.814
3-4-1/0		1779	689	0	1379	2.00	0.76	8.00	3556	1.930	321.4	8.	0.0315/0.251	0.1024/0.798	19.79	2.062	5.834
3-4-4/0			2758	0	6205	2.25	0.76	8.00	3562	2.061	340.1	8.	0.0274/0.218	0.0391/0.277	14.44	.998	2.824
3-10-1/0		4448	689	0	1379	2.00	0.76	8.00	3556	1.956	330.0	8.	0.0610/0.488	0.1641/1.313	24.41	3.241	9.164
3-10-4/0			2758	0	6205	2.25	0.76	8.00	3562	2.066	348.4	8.	0.0434/0.348	0.0655/0.523	17.78	1.577	4.458
3-10-10/0			6894	0	9652	1.40	0.0635	8.00	3703	2.090	344.9	20.	0.0193/0.59	0.0343/0.325	12.88	0.991	2.804
4-1-1/0	4	445	689	0	6205	9.00	0.76	8.00	3306	1.935	297.2	8.	0.0224/0.178	0.0437/0.315	13.49	1.031	2.913
4-1-4/0			2758	0	6205	2.25	0.76	14.54	3578	2.056	306.8	8.	0.0117/0.094	0.0434/0.127	10.46	0.500	1.905
4-1-5/0			3447	0	6205	1.80	0.76,1.02,1.02	16.70	3550	2.073	309.2	20.	0.0091/0.180	0.0290/0.345	10.16	0.445	1.819
4-1-6/0			4136	0	6205	1.50	0.76,1.02,1.02	20.00	3575	2.084	311.2	20.	0.0084/0.165	0.0284/0.338	10.16	0.406	1.814
4-1-8/0			5515	0	8514	1.54	0.76,1.02,1.02	26.70	3609	2.095	313.9	20.	0.0071/0.142	0.0267/0.318	10.16	0.351	1.808
4-1-9/0			6205	0	9086	1.46	0.76,1.02,1.02	30.00	3622	2.097	314.7	20.	0.0061/0.124	0.0272/0.279	10.16	0.330	1.806
4-4-1/0	4	1779	689	0	1379	2.00	0.76	8.00	3306	1.954	311.4	8.	0.0379/0.302	0.1186/0.947	19.79	2.050	5.799
4-4-4/0			2758	0	6205	2.25	0.76	8.00	3578	2.069	326.4	8.	0.0333/0.267	0.0465/0.373	14.44	0.996	2.817
4-4-10/0			6894	0	9657	1.400	0.0635	9.32	3634	2.109	323.9	20.	0.0168/0.338	0.0279/0.203	3.07	0.625	1.905
4-10-1/0		4448	689	0	1379	2.00	0.76	8.00	3306	1.968	317.5	8.	0.0726/0.579	0.1864/1.491	24.41	3.23	9.136
4-10-4/0			2758	0	6205	2.25	0.76	8.00	3578	2.076	335.3	8.	0.0513/0.411	0.0749/0.566	17.78	1.572	4.448
4-10-10/0			6894	0	9652	1.40	0.0635	8.00	3634	2.106	336.2	20.	0.0211/0.422	0.0417/0.483	16.54	0.988	2.794
5-1-1/0	5	445	689	0	6205	9.00	0.76	8.00	3221	1.963	288.9	8.	0.0267/0.213	0.0500/0.366	14.44	1.024	2.893
5-1-3/0			2068	0	6205	3.00	0.76	10.94	3350	2.064	293.4	8.	0.0152/0.127	0.0330/0.244	11.10	0.577	1.905
5-1-4/0			2758	0	6205	2.25	0.76	14.77	3396	2.090	295.0	8.	0.0142/0.114	0.0375/0.221	10.46	0.495	1.905
5-1-10/0			6894	0	9652	1.40	0.0635	37.54	3514	2.124	299.6	20.	0.0107/0.213	0.0272/0.061	2.36	0.310	1.905
5-4-1/0		1779	689	0	1379	2.00	0.76	8.00	3221	1.969	300.2	8.	0.0412/0.353	0.1316/1.052	19.79	2.042	5.776
5-4-4/0			2758	0	6205	2.25	0.76	8.00	3396	2.085	312.3	8.	0.0396/0.318	0.0538/0.376	14.44	0.993	2.807
5-4-10/0			6894	0	9652	1.40	0.0635	9.40	3514	2.127	305.9	20.	0.0198/0.396	0.0318/0.127	3.07	0.622	1.905
5-10-1/0		4448	689	0	1379	2.00	0.76	8.00	3221	1.978	305.0	8.	0.0826/0.660	0.207/1.656	24.41	3.223	9.114
5-10-4/0			2758	0	6205	2.25	0.76	8.00	3396	2.084	320.9	8.	0.0599/0.480	0.0851/0.462	17.78	1.569	4.465
5-10-10/0			6894	0	9652	1.40	0.0635	8.00	3514	2.112	318.8	20.	0.0272/0.541	0.0472/0.886	17.98	0.985	2.789

*n - nozzle
t - throat
b - barrel

**When two numbers are given, the first refers to throat d/w, while the second to barrel d/w

TABLE V

ENRIZING ENGINE REGENERATIVE COOLING WITH OXYGEN
(Single Regen)

Metric Units

L'	r _t	r _{ch}	ϵ_A	ΔP	T _{b,in}	T _{b,out}	ΔT _b	h _{g,max}	Q _{g,max}	Q _{c,max}	No. of Channels	Liner t/k
cm	cm	cm	-	kPa	°K	°K	°K	kw/m ²	kw/m ²	kw/m ²		in. ² sec°F/Btu
0.102	14.40	1.080	3.040	0.03	207	94.5	428	334	1868	4723	1177	-
0.307	7.24	0.526	1.905	14.04	824	91.5	385	290	6207	15,754	2288	147
0.706	19.79	2.123	6.005	6.00	174	90.7	365	274	1462	3661	833	-
0.231	14.44	1.046	2.957	0.61	869	94.5	352	258	4324	11,080	4412	200
0.163	24.41	3.338	9.439	6.00	64	90.7	277	186	1165	2991	964	128
0.17	17.78	1.643	4.651	11.56	385	94.5	283	188	5618	14,773	3628	-
0.480	12.32	1.046	2.961	41.63	1595	97.1	333	236	18,032	47,228	7991	152
0.191	14.44	1.029	2.909	6.00	105	94.5	365	271	1788	4903	1046	85
0.196	10.16	0.503	1.905	18.05	454	94.5	390	295	6060	16,947	1977	-
0.168	10.16	0.447	1.826	23.39	659	94.9	389	294	7295	20,395	2566	-
0.155	10.16	4.06	1.816	29.08	1038	95.4	389	293	8442	24,039	3154	-
0.091	10.16	0.375	1.814	33.74	2225	95.8	426	330	9560	27,585	4086	-
0.798	19.79	2.062	5.834	6.00	86	90.7	321	230	1385	3775	735	-
0.277	14.44	.998	2.824	10.86	684	94.5	318	224	4206	11,979	3889	187
0.313	24.41	3.241	9.164	6.00	71	90.7	246	155	1100	3072	948	-
0.523	17.78	1.577	4.458	12.80	319	94.5	244	149	4412	13,204	3775	202
0.325	12.88	0.991	2.804	52.63	1717	97.1	330	233	17,061	51,265	8220	137
0.315	13.49	1.031	2.913	6.00	57	94.5	280	185	1677	4527	866	-
0.127	10.46	0.500	1.905	16.72	946	94.5	395	301	5824	16,113	3677	131
0.345	10.16	0.445	1.819	21.66	331	97.1	341	244	6972	19,251	2026	-
0.338	10.16	0.406	1.814	26.87	498	97.1	363	266	8031	22,241	2190	-
0.318	10.16	0.351	1.808	36.10	833	96.2	334	238	10,060	28,517	3432	-
0.279	10.16	0.330	1.806	41.02	1790	96.6	344	248	11,031	31,572	4396	-
0.947	19.79	2.050	5.799	6.00	94	90.7	278	187	1327	3546	1030	-
0.373	14.44	0.996	2.817	10.15	412	94.5	258	163	4030	11,325	3285	174
0.203	3.07	0.625	1.905	44.94	3655	97.1	174	77	12,619	39,940	7141	-
1.491	24.41	3.23	9.136	6.00	51	90.7	214	124	1050	2860	817	-
0.566	17.78	1.572	4.448	12.27	187	94.5	206	111	4442	13,025	3105	184
0.483	16.54	0.988	2.794	48.76	1726	97.1	320	223	16,061	49,222	7321	128
0.366	14.44	1.024	2.893	6.00	35.8	94.5	251	157	1615	4233	719	-
0.244	11.10	0.577	1.905	10.23	300	91.8	303	211	4529	11,979	2304	125
0.221	10.46	0.495	1.905	14.74	424	94.5	315	221	5735	15,247	3023	-
0.061	2.36	0.310	1.905	40.70	266	97.1	172	74	11,882	34,334	7926	106
1.052	19.79	2.042	5.776	6.00	64.8	90.7	245	154	1291	3350	899	-
0.376	14.44	0.993	2.807	8.92	255	94.5	214	119	3971	10,688	2680	164
0.127	3.07	0.622	1.905	43.58	1679	97.1	301	70	13,735	41,394	6341	-
0.656	24.41	3.223	9.114	6.00	30.3	90.7	191	100	1024	2713	670	-
0.462	17.78	1.569	4.465	11.21	110	94.5	182	88	4588	12,828	2484	107
0.886	17.98	0.985	2.789	44.53	783	97.1	279	182	15,647	45,643	5867	119
												73

FOLDOUT FRAME 2

TABLE V (Cont.)

SELECTED PARAMETERS CHARACTERIZING ENGINE REG
(Single Regen)

Code	MR	F	Pc	Coolant	P _{in}	P _{in} /Pc	t _{wall} in. (n,t,b)*	CR	T _c °R	C _F	Isp sec	Aspect Ratio d/w**	Channel Dimensions				
													Throat w/d	Barrel w/d	L' in.	r _t in.	r _{ch} in.
2-1-1/0	2	100	100	0	900	9.00	.3	8.00	5651	1.768	310.6	8.	.0060/.048	.0118/.040	5.67	.424	1.200
2-1-4/0		400	0	900	2.25		.3	13.10	5878	1.853	315.5	20.	.0031/.061	.0061/.121	2.85	.207	.750
2-4-1/0		400	100	0	200	2.00	.3	8.00	5651	1.822	324.8	8.	.0107/.086	.0348/.278	7.79	.836	2.364
2-4-4/0		400	0	900	2.25		.3	8.00	5878	1.875	333.3	8.	.0101/.081	.0139/.091	5.67	.412	1.164
2-10-1/0		1000	100	0	200	2.00	.3	8.00	5651	1.844	330.0	8.	.0209/.167	.0572/.458	9.61	1.314	3.716
2-10-4/0		400	0	900	2.25		.3	8.00	5878	1.899	341.7	8.	.0141/.113	.0236/---	7.00	.647	1.831
2-10-10/0		1000	0	1400	1.40	.025		8.00	5998	1.871	332.9	20.,30.	.0073/.216	.0128/.189	4.85	.412	1.167
3-1-1/0	3	100	100	0	900	9.00	.3	8.00	6044	1.944	305.5	8.	.0072/.014	.0140/.075	5.67	.405	1.145
3-1-4/0		400	0	900	2.25		.3,.4,.4	14.39	6411	2.036	320.1	20.	.0032/.065	.0100/.077	4.00	.198	.750
3-1-5/0		500	0	985	1.97		.3,.4,.4	16.70	6483	2.056	322.3	20.	.0030/.060	.0096/.066	4.00	.176	.719
3-1-6/0		600	0	1069	1.78		.3,.4,.4	20.00	6541	2.073	324.0	20.	.0026/.052	.0094/.061	4.00	.160	.715
3-1-7/0		700	0	1150	1.64		.3,.4,.4	23.40	6587	2.085	325.3	20.	.0022/.044	.0098/.036	4.00	.148	.714
3-4-1/0		400	100	0	200	2.00	.3	8.00	6044	1.930	321.4	8.	.0124/.099	.0403/.314	7.79	.812	2.297
3-4-4/0		400	0	900	2.25		.3	8.00	6411	2.061	340.1	8.	.0108/.086	.0154/.109	5.67	.393	1.112
3-10-1/0		1000	100	0	200	2.00	.3	8.00	6044	1.956	330.0	8.	.0240/.192	.0646/.517	9.61	1.276	3.608
3-10-4/0		400	0	900	2.25		.3	8.00	6411	2.066	348.4	8.	.0171/.137	.0258/.206	7.00	.621	1.755
3-10-10/0		1000	0	1400	1.40	.025		8.00	6665	2.090	344.9	20.,30.	.0076/.228	.0135/.128	5.07	.390	1.104
4-1-1/0	4	100	100	0	900	9.00	.3	8.00	5950	1.935	297.2	8.	.0088/.070	.0172/.124	5.31	.406	1.147
4-1-4/0		400	0	900	2.25		.3	14.54	6332	2.056	306.8	8.	.0046/.037	.0107/.050	4.12	.197	.750
4-1-5/0		500	0	900	1.80		.3,.4,.4	16.70	6390	2.073	309.2	20.	.0036/.071	.0114/.136	4.00	.175	.716
4-1-6/0		600	0	900	1.50		.3,.4,.4	20.00	6435	2.084	311.2	20.	.0033/.065	.0112/.133	4.00	.160	.714
4-1-8/0		800	0	1235	1.54		.3,.4,.4	26.70	6497	2.095	313.9	20.	.0028/.056	.0105/.125	4.00	.138	.712
4-1-9/0		900	0	1318	1.46		.3,.4,.4	30.00	6520	2.097	314.7	20.	.0024/.049	.0107/.110	4.00	.130	.711
4-4-1/0	4	400	100	0	200	2.00	.3	8.00	5950	1.954	311.4	8.	.0149/.119	.0467/.373	7.79	.807	2.283
4-4-4/0		400	0	900	2.25		.3	8.00	6332	2.069	326.4	8.	.0131/.105	.0183/.47	5.67	.392	1.109
4-4-10/0		1000	0	1400	1.400	.025		9.32	6541	2.109	323.9	20.	.0056/.133	.0110/.088	1.21	.246	.750
4-10-1/0		1000	100	0	200	2.00	.3	8.00	5950	1.968	317.5	8.	.0286/.228	.0734/.587	9.61	1.272	3.597
4-10-4/0		400	0	900	2.25		.3	8.00	6332	2.076	335.3	8.	.0202/.162	.0295/.219	7.00	.619	1.751
4-10-10/0		1000	0	1400	1.40	.025		8.00	6541	2.106	336.2	20.	.0083/.166	.0164/.190	6.51	.389	1.100
5-1-1/0	5	100	100	0	900	9.00	.3	8.00	5797	1.963	288.9	8.	.0105/.084	.0197/.144	5.67	.403	1.139
5-1-3/0		300	0	900	3.00		.3	10.94	6030	2.064	293.4	8.	.0063/.050	.0130/.096	4.37	.227	.750
5-1-4/0		400	0	900	2.25		.3	14.77	6112	2.090	295.0	8.	.0056/.045	.0128/.087	4.12	.195	.750
5-1-10/0		1000	0	1400	1.40	.025		37.54	6325	2.124	299.6	20.	.0078/.156	.0125/.05	.93	.122	.750
5-4-1/0		400	100	0	200	2.00	.3	8.00	5797	1.969	300.2	8.	.0174/.139	.0518/.414	7.79	.804	2.274
5-4-4/0		400	0	900	2.25		.3	8.00	6112	2.085	312.3	8.	.0156/.125	.0212/.148	5.67	.391	1.105
5-4-10/0		1000	0	1400	1.40	.025		9.40	6325	2.127	305.9	20.	.0078/.156	.0125/.05	1.21	.245	.750
5-10-1/0	000	100	0	200	2.00	.3	8.00	5797	1.978	305.0	8.	.0325/.260	.0815/.652	9.61	1.269	3.588	
5-10-4/0		400	0	900	2.25		.3	8.00	6112	2.084	320.9	8.	.0236/.189	.0335/.182	7.00	.618	1.748
5-10-10/0		1000	0	1400	1.40	.025		8.00	6325	2.112	318.8	20.	.0107/.213	.0186/.349	7.08	.388	1.098

*n - nozzle
t - throat
b - barrel

**When two numbers are given, the first refers to throat d/w, while the second to barrel d/w

LOADOUT FRAME

TABLE V (Cont.)

HEATING ENGINE REGENERATIVE COOLING WITH OXYGEN
(Single Regen)

English Units

	L'	r _t in.	r _{ch} in.	t _A °F	ΔP psi	T _b , in °F	T _b , out °F	ΔT _b °F	hg _{max} Btu/in. ² / sec°F x 10 ⁻³	g _{max} Btu/in. ² / sec	Q _{c,max} Btu/in. ² / sec	No. of Channels	Liner t/k in. ² sec°F/Btu	
Q40	5.67	.424	1.200	6.00	30.0	-289.9	310.6	600.5	.635	2.89	.72	147	-	
121	2.85	.207	.750	14.04	119.5	-289.9	232.7	522.6	2.11	9.64	1.40	114	-	
278	7.79	.836	2.364	6.00	25.3	-296.7	196.7	493.4	.497	2.24	.51	200	-	
Q91	5.67	.412	1.164	8.61	126.1	-289.9	174.7	464.6	1.47	-	6.78	2.70	128	-
458	9.61	1.314	3.716	6.00	9.3	-296.7	37.7	334.4	.396	1.83	.59	221	-	
-	7.00	.647	1.831	11.56	55.9	-289.9	48.7	338.6	1.91	9.04	2.22	152	-	
189	4.85	.412	1.167	41.63	231.3	-285.3	140.2	425.5	6.13	28.90	4.89	85	-	
Q75	5.67	.405	1.145	6.00	15.2	-289.9	197.3	487.2	.608	3.00	.64	138	-	
Q77	4.00	.198	.750	18.05	65.8	-289.9	241.3	531.2	2.06	10.37	1.21	133	600.	
Q66	4.00	.176	.719	23.39	95.6	-289.1	240.3	529.4	2.48	12.48	1.57	129	600.	
Q61	4.00	1.60	.715	29.08	150.6	-288.3	239.8	528.1	2.87	14.71	1.93	127	600.	
Q36	4.00	.148	.714	33.74	322.8	-287.6	306.8	594.4	3.25	16.88	2.50	126	600.	
314	7.79	.812	2.297	6.00	12.5	-296.7	117.0	413.7	.471	2.31	.45	187	-	
109	5.67	.393	1.112	10.86	99.2	-289.9	112.8	402.7	1.43	7.33	2.38	122	-	
517	9.61	1.276	3.608	6.00	10.3	-296.7	-17.5	279.2	.374	1.88	.58	202	-	
206	7.00	.621	1.755	12.80	46.3	-289.9	-21.0	268.9	1.50	8.08	2.31	137	-	
128	5.07	.390	1.104	52.63	249.0	-285.3	133.9	419.2	5.80	31.37	5.03	80	-	
124	5.31	.406	1.147	6.00	8.3	-289.9	44.0	333.9	.570	2.77	.53	131	-	
Q50	4.12	.197	.750	16.72	137.1	-289.9	251.6	541.5	1.98	9.86	2.25	105	-	
136	4.00	.175	.716	21.66	48.0	-285.3	154.2	439.5	2.37	11.78	1.24	126	600.	
133	4.00	.160	.714	26.87	72.2	-285.3	194.2	479.5	2.73	13.61	1.43	124	600.	
125	4.00	.138	.712	36.10	120.9	-286.8	141.8	428.6	3.42	17.45	2.10	122	600.	
110	4.00	.130	.711	41.02	259.7	-286.1	159.8	445.9	3.75	19.32	2.69	121	600.	
373	7.79	.807	2.283	6.00	13.6	-296.7	39.9	336.6	.451	2.17	.53	174	-	
47	5.67	.392	1.109	10.15	59.8	-289.9	3.8	293.7	1.37	6.93	2.01	114	-	
Q88	1.21	.246	.750	44.94	530.2	-285.3	-146.1	139.2	4.29	24.44	4.37	54	-	
587	9.61	1.272	3.597	6.00	7.4	-296.7	-74.3	222.4	.307	1.75	.50	184	-	
219	7.00	.619	1.751	12.27	27.1	-289.9	-90.1	199.8	1.51	7.97	1.90	128	-	
190	6.51	.389	1.100	48.76	250.3	-285.3	116.2	401.5	5.45	30.12	4.48	78	-	
144	5.67	.403	1.139	6.00	5.2	-289.9	-7.7	282.2	.549	2.59	.44	125	-	
Q96	4.37	.227	.750	10.23	43.5	-294.7	84.8	379.4	1.54	7.33	1.41	106	-	
Q87	4.12	.195	.750	14.74	61.5	-289.9	107.8	397.7	1.95	9.33	1.85	102	-	
Q5	.93	.122	.750	40.70	386.0	-285.3	-151.3	134.0	4.04	21.01	4.85	32	-	
414	7.79	.804	2.274	6.00	9.4	-296.7	-19.5	277.2	.439	2.05	.55	164	-	
148	5.67	.391	1.105	8.92	37.0	-289.9	-75.6	214.3	1.35	6.54	1.64	107	-	
Q5	1.21	.245	.750	43.58	243.5	-285.3	-158.6	126.7	4.67	25.33	3.88	52	-	
652	9.61	1.269	3.588	6.00	4.4	-296.7	-116.2	180.5	.348	1.66	.41	171	-	
182	7.00	.618	1.748	11.21	15.9	-289.9	-131.5	158.5	1.56	7.85	1.52	119	-	
349	7.08	.388	1.098	44.53	113.6	-285.3	41.6	326.9	5.32	27.93	3.59	73	-	

2

FOLDOUT FRAME

TABLE VI
TABLE NOMENCLATURE

<u>Code</u>	Designator for basic analysis parameters X-Y-Z/C where X = MR Y = F (last two zeros deleted) Z = Pc (last two zeros deleted) C = Coolant (F = fuel, O = oxidizer)
MR	TCA mixture ratio with no film cooling
F	Engine thrust, N (lbF)
Pc	Chamber pressure, kPa (psia)
Coolant	Regenerative coolant, where F = RP-1 O = O ₂
P _{in}	Coolant inlet pressure, kPa (psia)
P _{in} /Pc	Ratio of coolant inlet pressure to chamber pressure
t _{wall}	Gas-side wall thickness, cm (in.)
CR	Contraction ratio, chamber flow area/throat flow area
T _c	Chamber combustion temperature, °K (°R) (TRAN 72)
C _f	Thrust coefficient
Isp	Specific impulse, sec (vacuum, delivered)
d/w	Channel depth-to-width ratio
L'	Engine L', cm (in.)
r _t	Throat radius, cm (in.)
r _{ch}	Chamber radius (to metal), cm (in.) Liner considered to have no thickness.
ε _A	Attachment area ratio for radiation-cooled nozzle. Based on wall temperature of 1311°K (1900°F) for MR = 1 and 1786°K (2755°F) for other values of MR
ΔP	Calculated pressure drop for a multistation analysis, kPa (psi)
T _b , in	Coolant temperature at channel inlet, °K (°F)
T _b , out	Coolant temperature at coolant outlet (injector or discharge manifold), °K (°F)
ΔT _b	Coolant temperature rise, °K (°F)
hg, max	Maximum gas-side heat transfer coefficient, kw/m ² °K (Btu/in. ² sec °F)
Q _g , max	Maximum gas-side heat flux, kw/m ² (Btu/in. ² sec)
Q _c , max	Maximum coolant-side heat flux, kw/m ² (Btu/in. ² sec)
Throat w/d	Channel width/channel depth at throat, cm/cm (in./in.)
Barrel w/d	Channel width/channel depth in cylindrical section, cm/cm (in./in.)
No. of Channels	Number of coolant channels (single-pass, up-flow)

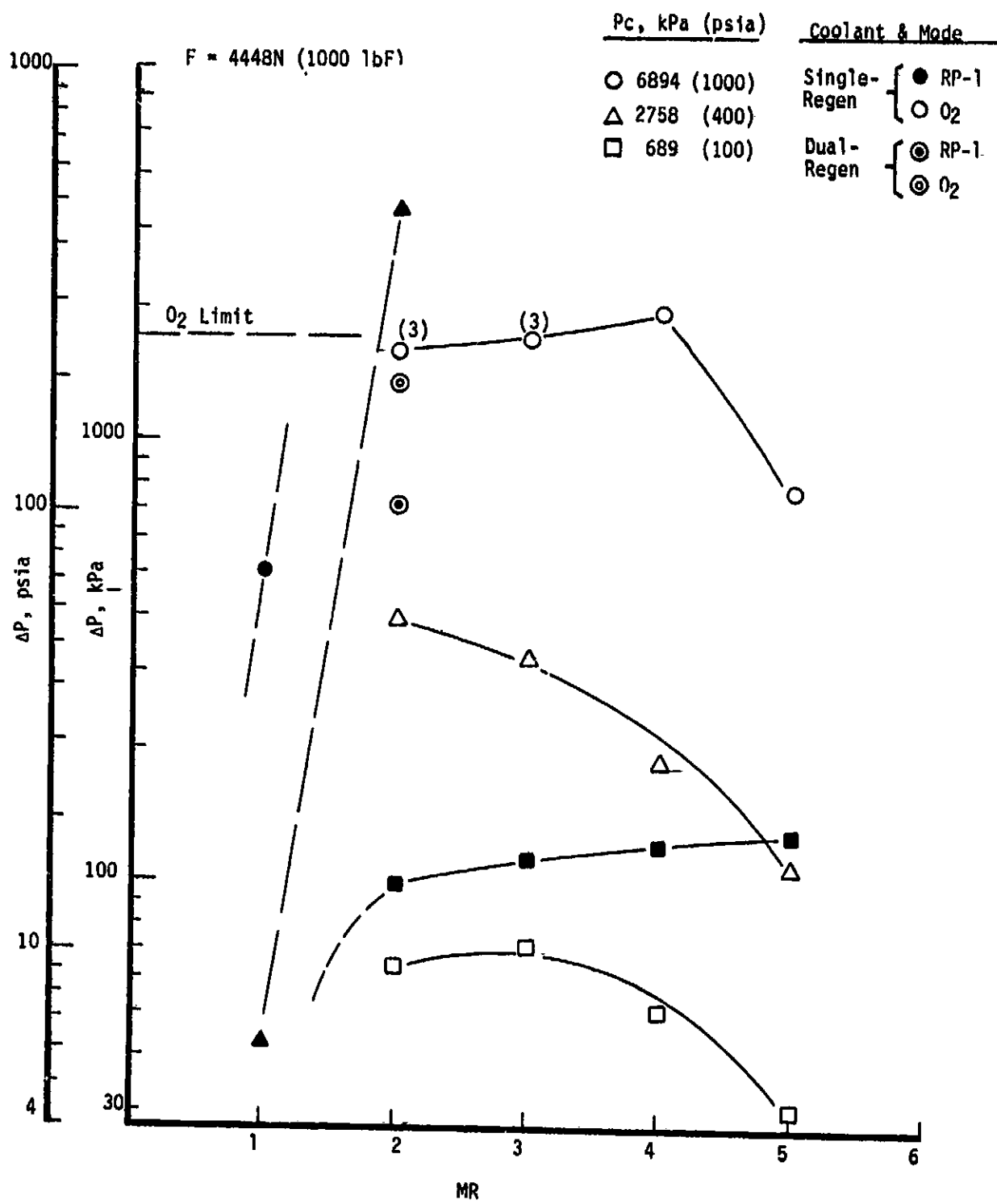


Figure 9. Coolant Pressure Drop for LOX, RP-1, and Dual-Regenerative Cooling Concepts, $F = 4448N$ (1000 lbF)

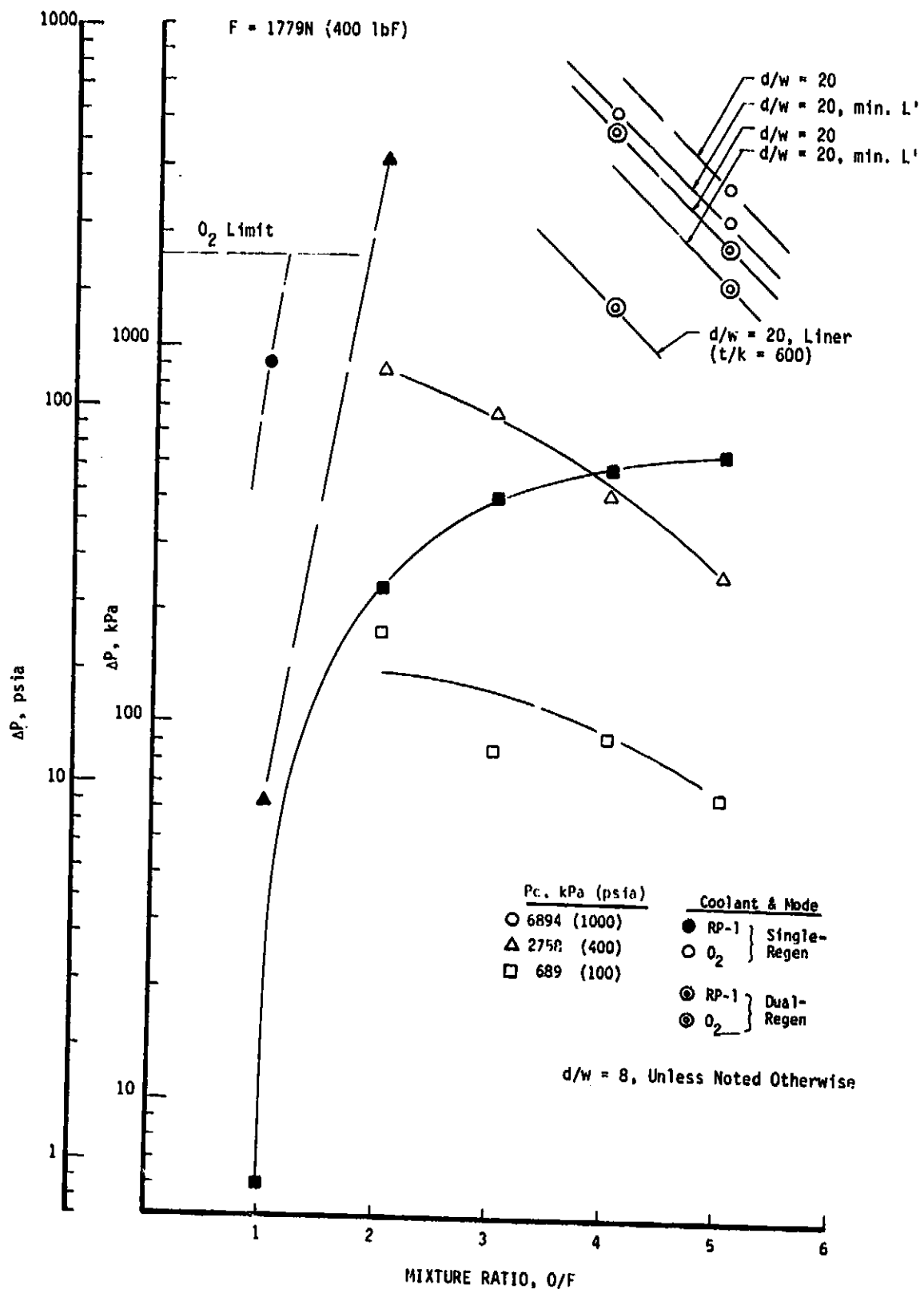


Figure 10. Coolant Pressure Drop for LOX, RP-1, and Dual-Regenerative Cooling Concepts, $F = 1779\text{N}$ (400 lbF)

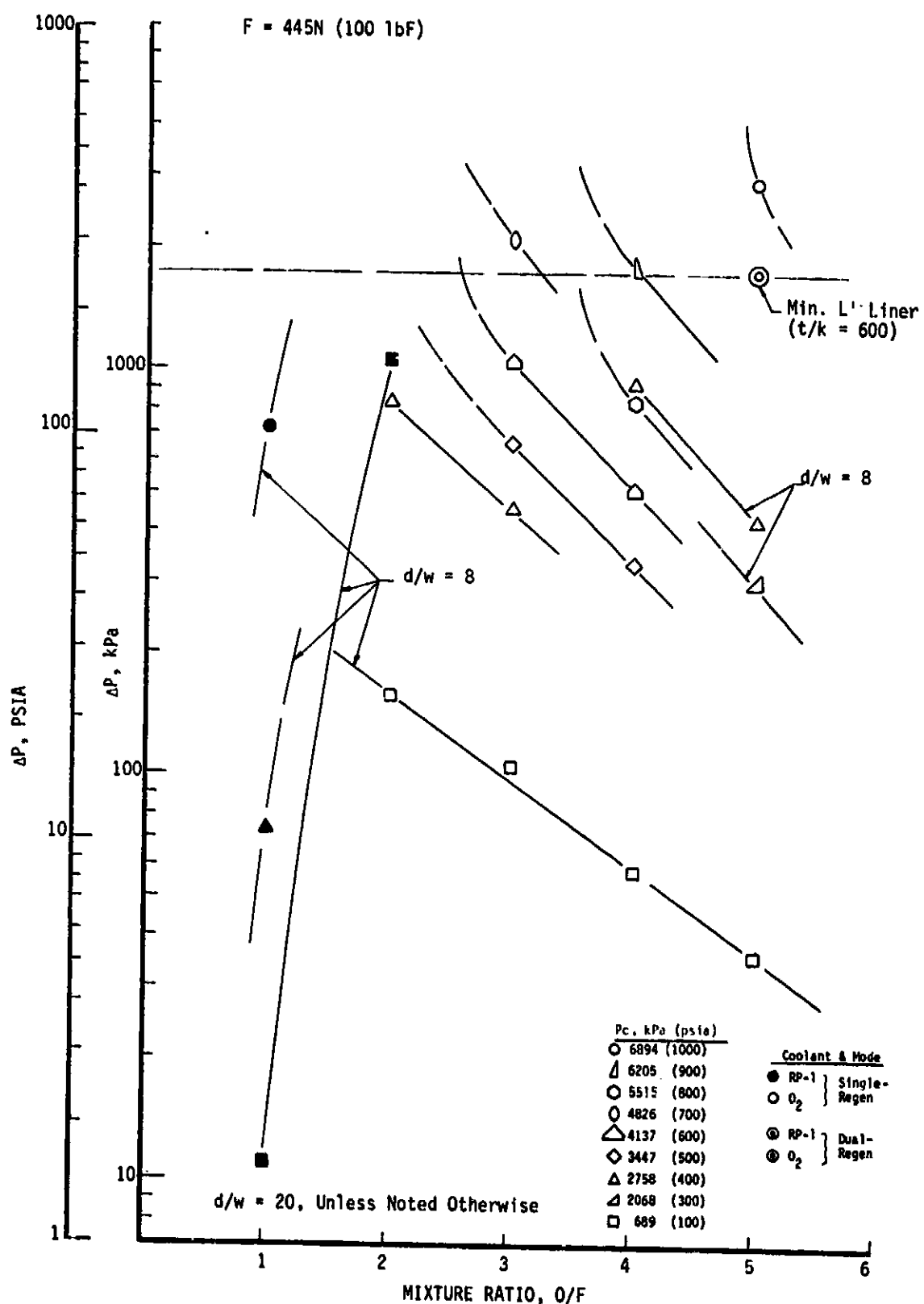


Figure 11. Coolant Pressure Drop for LOX, RP-1, and Dual-Regenerative Cooling Concepts, $F = 445\text{N} (100 \text{lbF})$

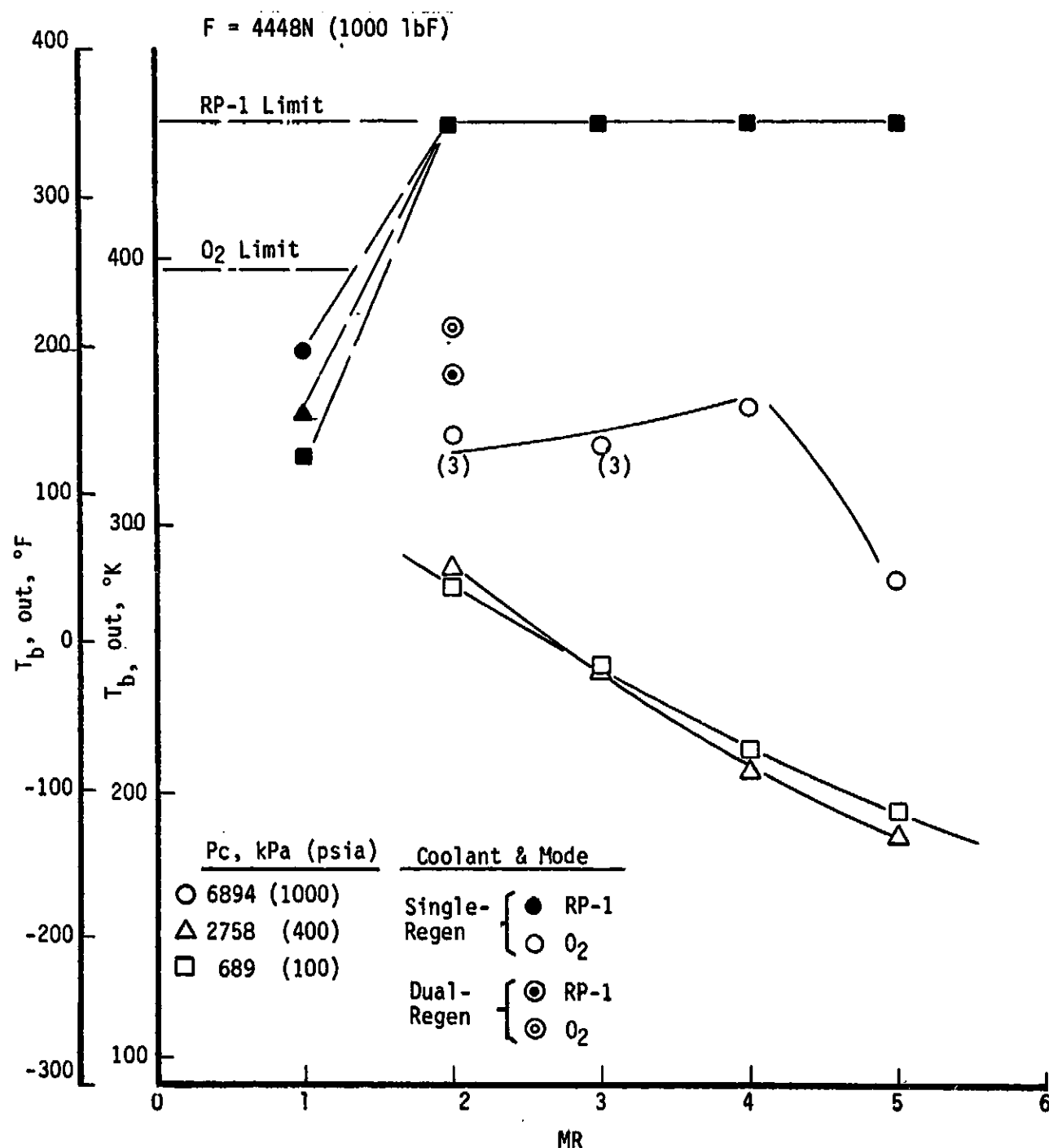


Figure 12. Coolant Discharge Temperature for LOX, RP-1, and Dual-Regenerative Cooling Concepts, $F = 4448\text{N} (1000 \text{lbf})$

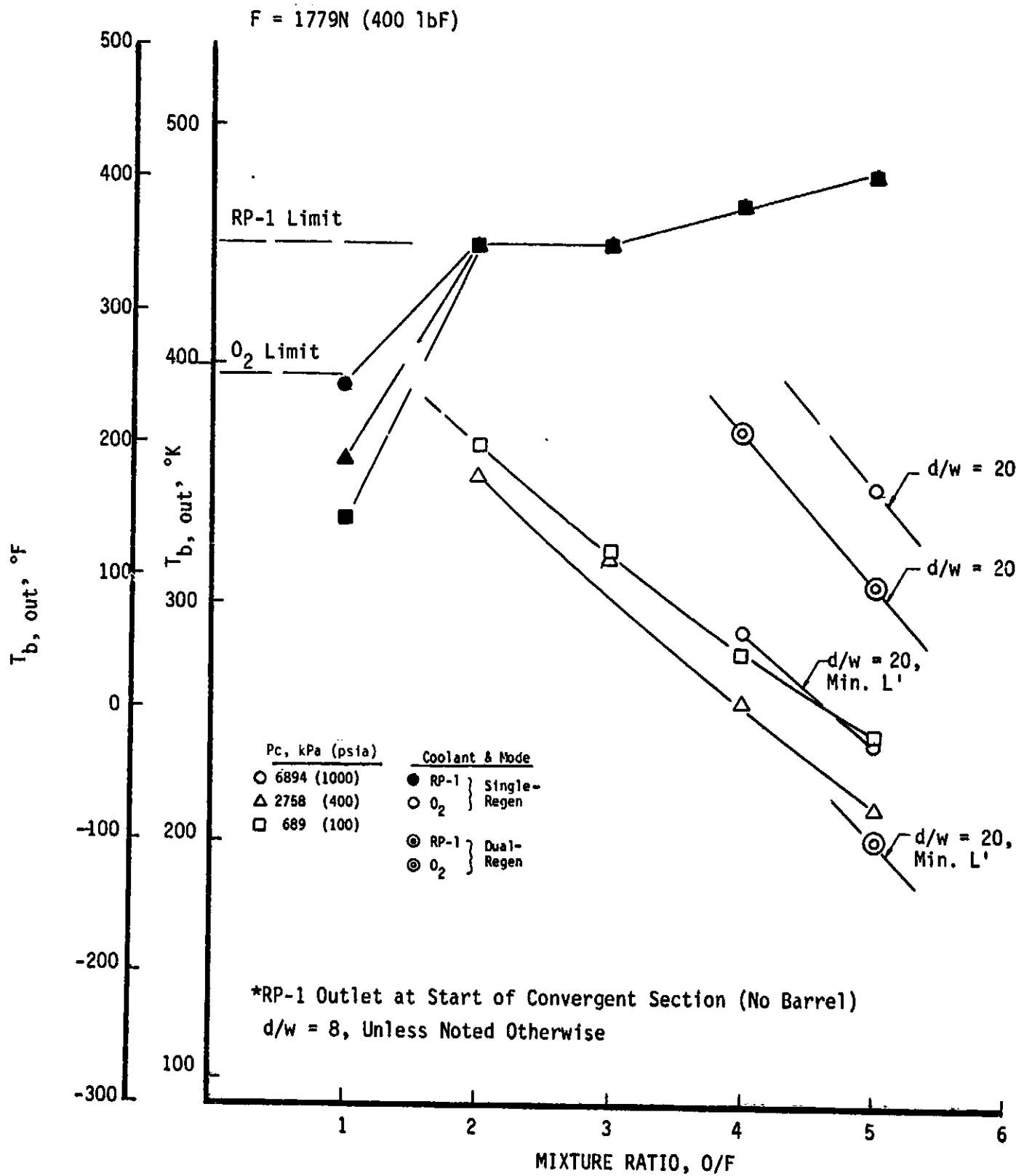


Figure 13. Coolant Discharge Temperature for LOX, RP-1, and Dual-Regenerative Cooling Concepts, $F = 1779N$ (400 lbF)

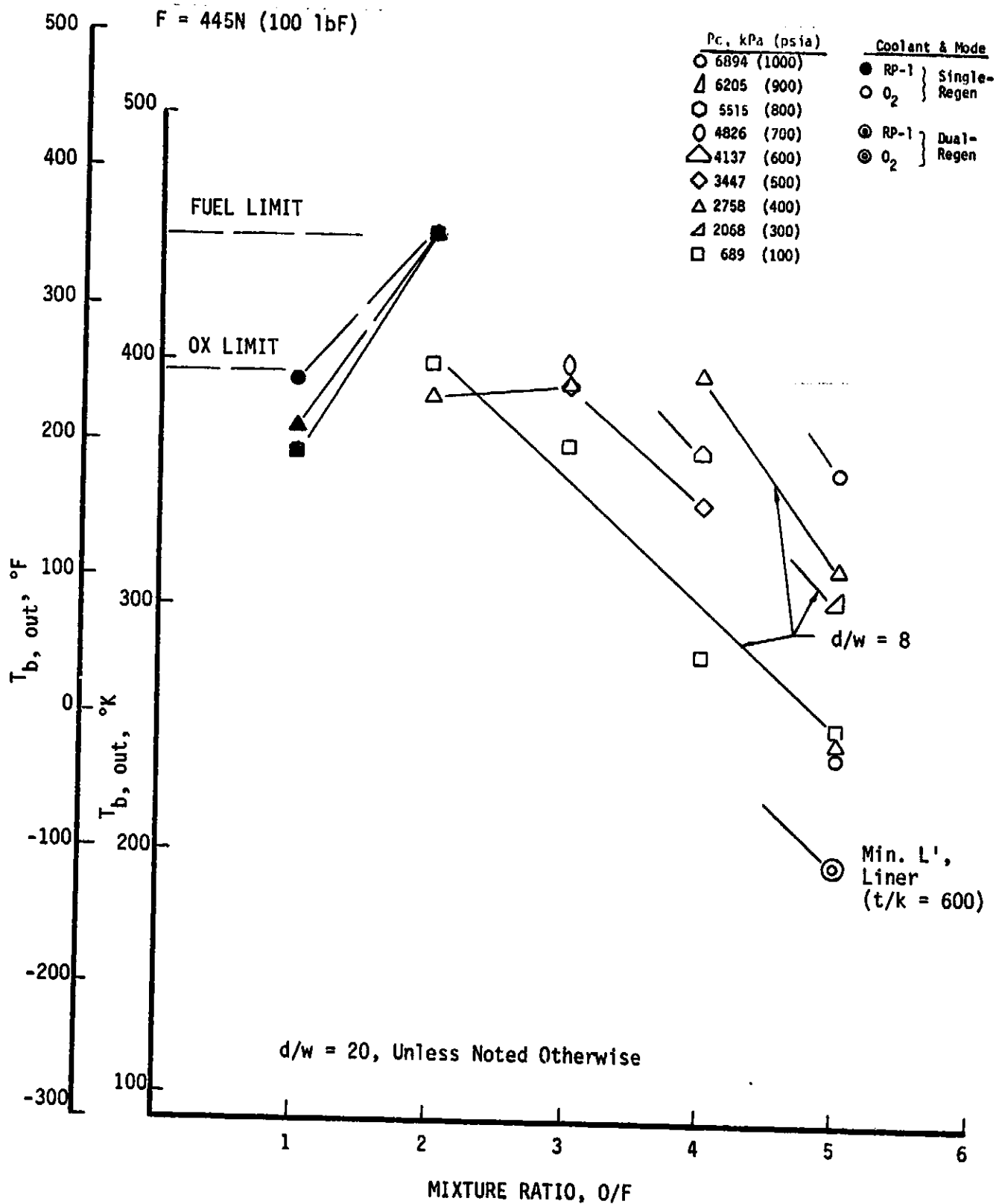


Figure 14. Coolant Discharge Temperature for LOX, RP-1, and Dual-Regenerative Cooling Concepts, $F = 445\text{N} (100 \text{lbf})$

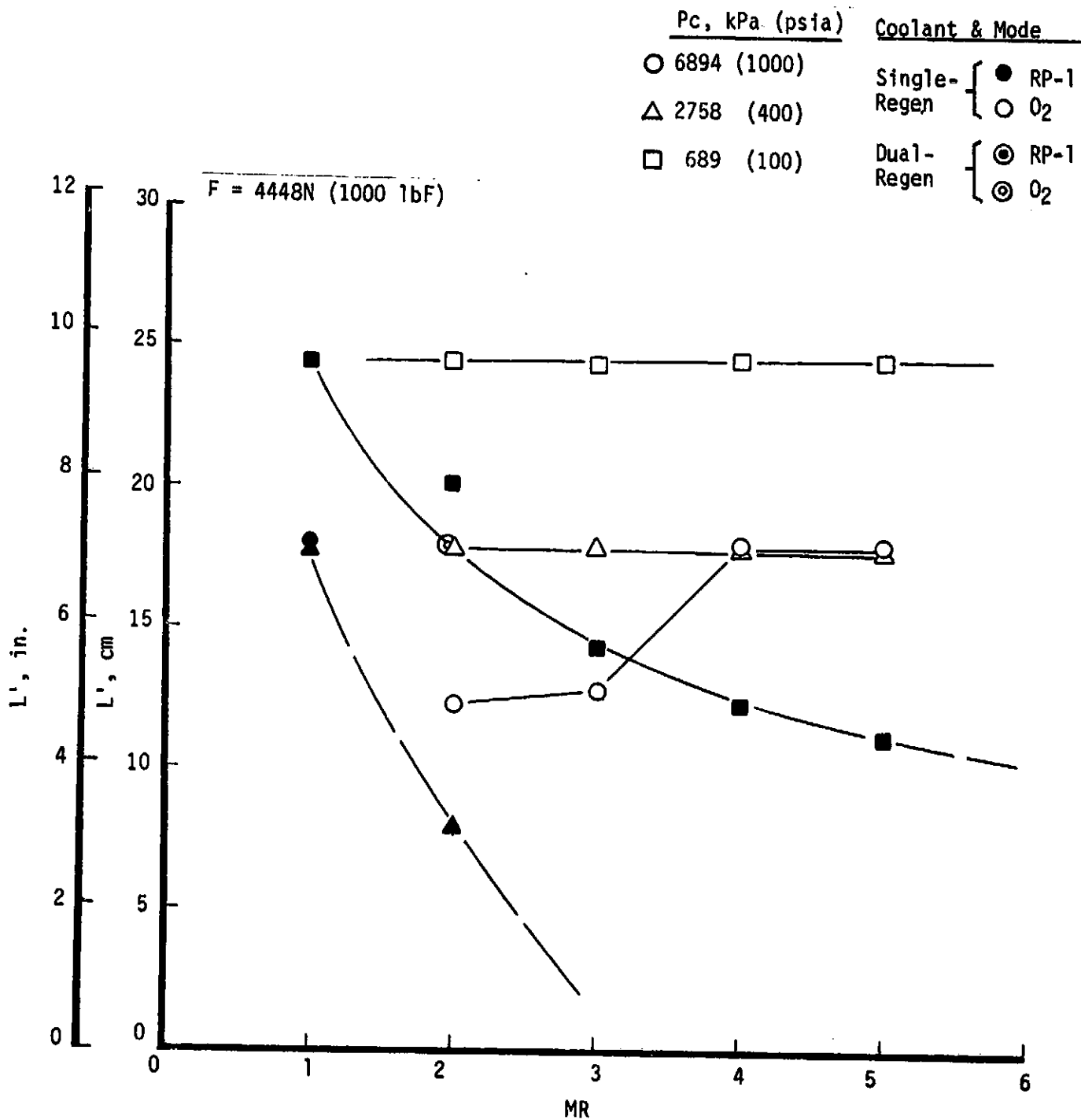


Figure 15. Maximum Chamber L' for LOX, RP-1, and Dual-Regenerative Cooling Concepts, $F = 4448N \text{ (1000 lbF)}$

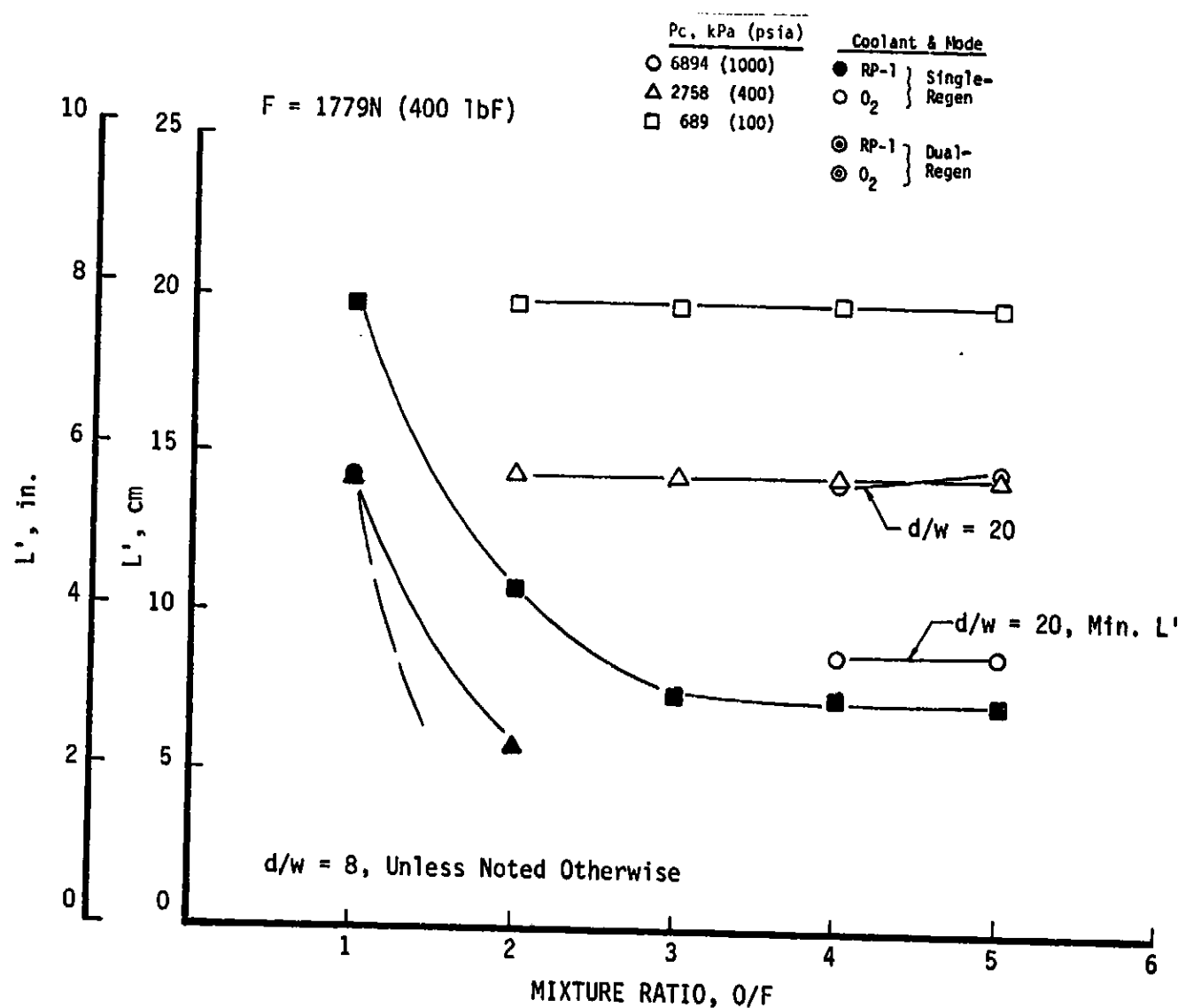


Figure 16. Maximum Chamber L' for LOX, RP-1, and Dual-Regenerative Cooling Concepts, $F = 1779\text{N}$ (400 lbF)

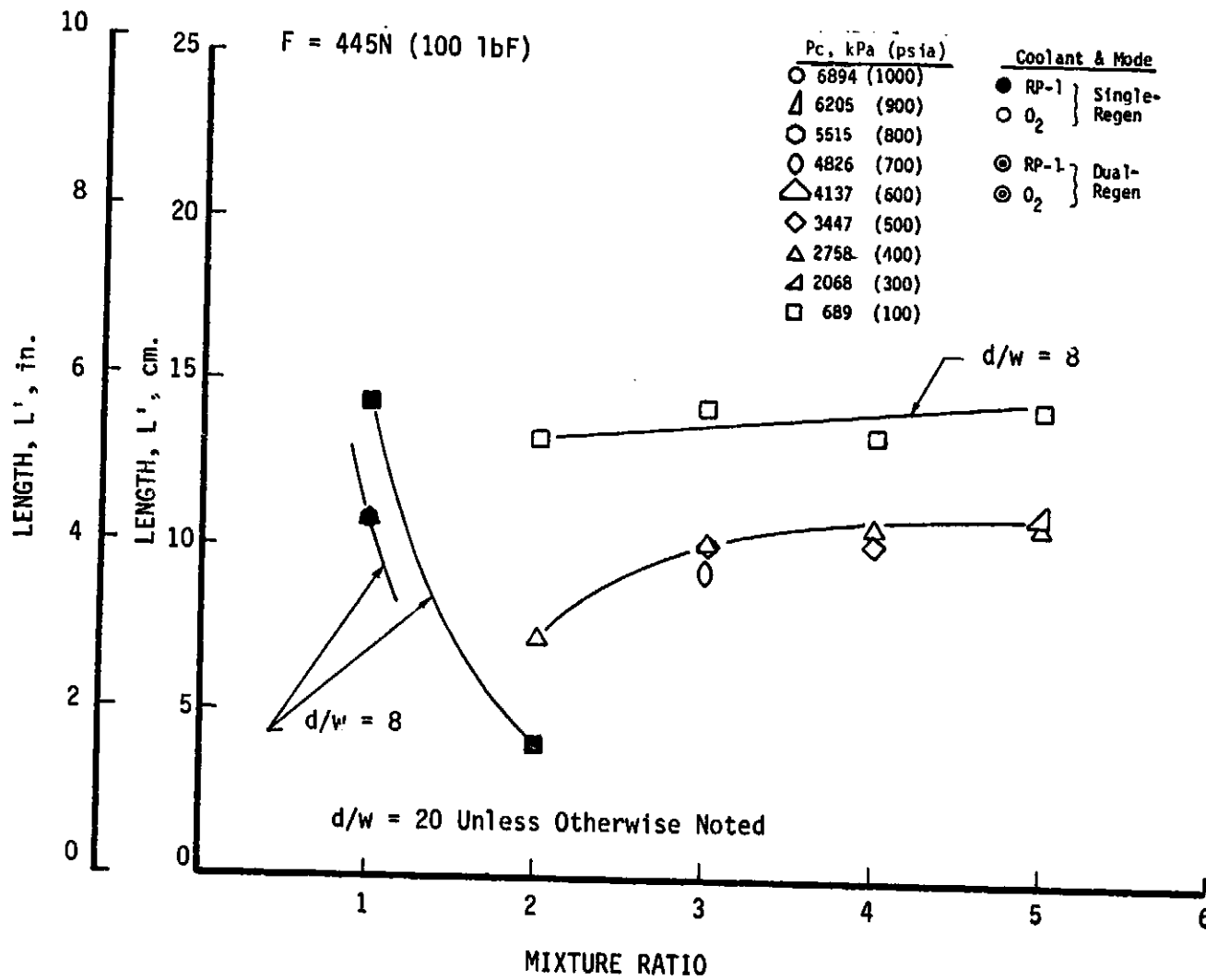


Figure 17. Maximum Chamber L' for LOX, RP-1, and Dual-Regenerative Cooling Concepts, $F = 445N$ (100 lbF)

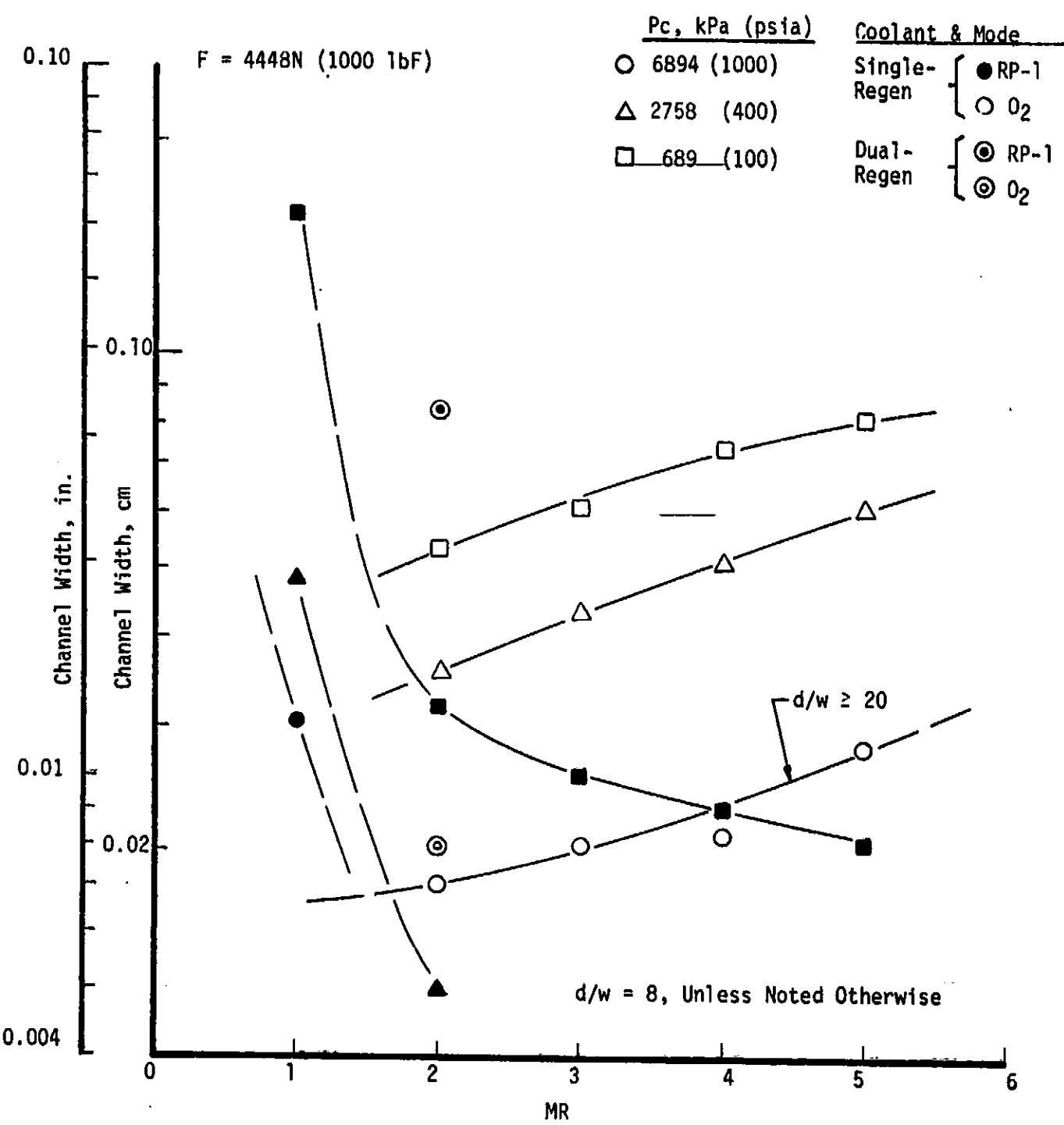


Figure 18. Minimum Coolant Channel Width Required for LOX, RP-1, and Dual-Regenerative Cooling Concepts, $F = 4448\text{N} (1000 \text{lbF})$

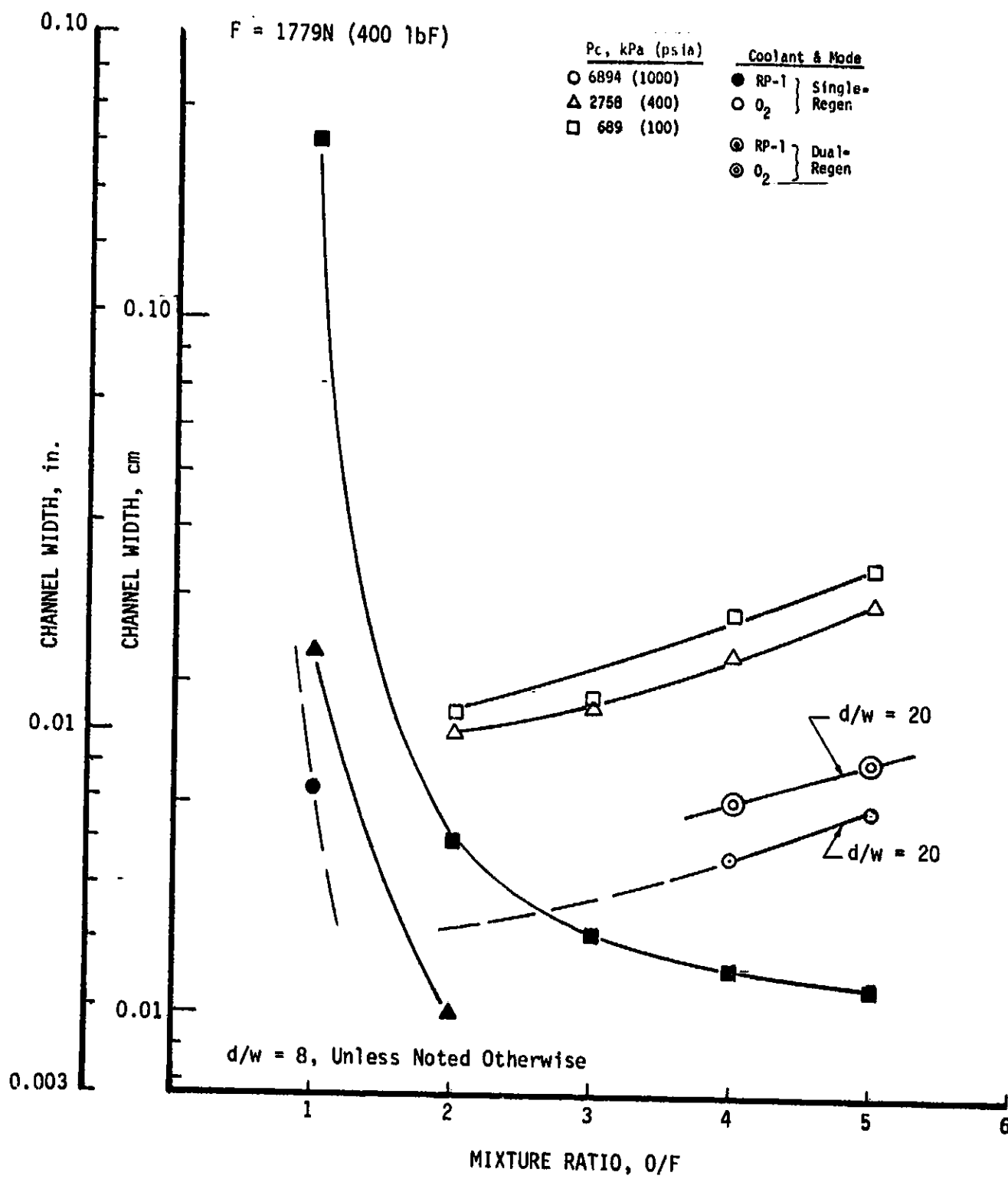


Figure 19. Minimum Coolant Channel Width Required for LOX, RP-1, and Dual-Regenerative Cooling Concepts, $F = 1779\text{N}$ (400 lbf)

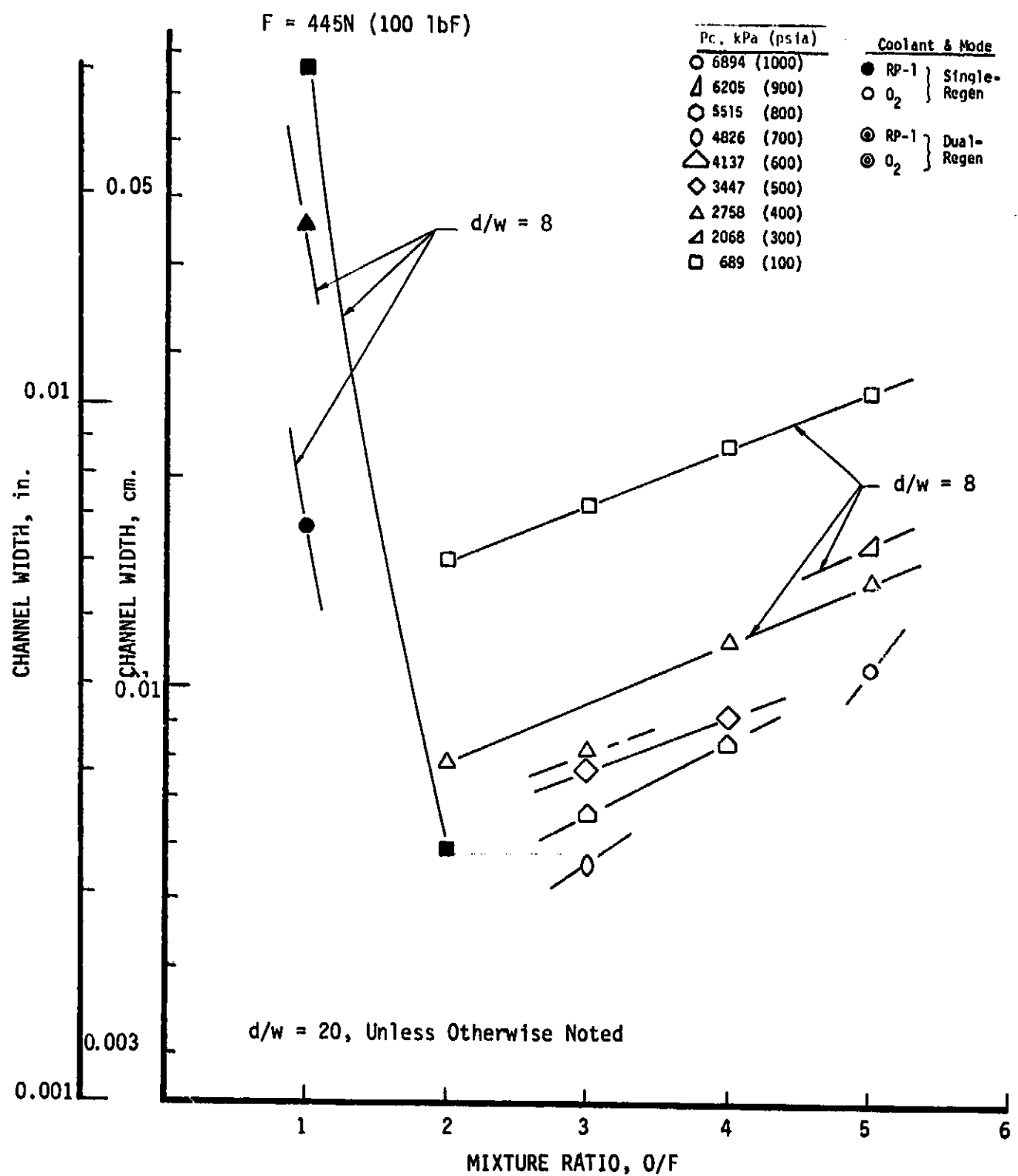


Figure 20. Minimum Coolant Channel Width Required for LOX, RP-1, and Dual-Regenerative Cooling Concepts, $F = 445N$ (100 lbF)

LII, B, Thermal Design (cont.)

of 20 and a reduced chamber L' ; also, it is necessary to resort to dual-regen cooling (oxygen inlet at $\epsilon = 6:1$) to achieve a pressure drop less than the ΔP limit criterion. Single-regen cooling with oxygen is not practical at mixture ratios below 5 at high operating pressures in the mid- and low-thrust range.

The excessive pressure drop problem is compounded at $F = 445N$ (100 lbF). The pressure drops are acceptable only for the MR range studied for $P_c = 689$ kPa (100 psia). Additional analyses at intermediate chamber pressures were made to assist in determining data trends. The decreased pressure drop associated with higher aspect ratio channels is illustrated by the data for $d/w = 8$ and 20 at $P_c = 2758$ kPa (400 psia). Thus, the additional P_c 's evaluated at MR's of 3 and 4 were characterized by the larger coolant channel aspect ratio. Although these analyses are limited, it appears that single-regen cooling with oxygen at the 445N (100 lbF) thrust level is possible at P_c 's up to about 4619 kPa (670 psia) at MR = 4, and at P_c 's of perhaps 3447 to 4136 kPa (500 to 600 psia) at MR = 2. Several data points suggest that the pressure drop curve is linear at the higher MR's but curves upward at MR's below about 3.

b. Coolant Discharge Temperature

The temperature of the coolant leaving the coolant jacket is displayed in Figures 12 through 14. For oxygen, the outlet temperature is below the limiting temperature for most design points except at the 445N (100 lbF) thrust level. The temperature limit is a complex function of MR, P_c , and channel aspect ratio. This parameter is a direct input to the performance sensitivity analysis.

The fuel outlet temperature is below the limiting value only at MR = 1. At higher MR's, it becomes the controlling parameter in determining chamber L' . Note that for $F = 1779N$ (400 lbF) at MR's of 4 and 5, the temperature shown exceeds the stated coking limit. This is the result of the limit being reached within the convergent section; consequently, if the desired contraction ratio is to be achieved (albeit with a zero-length cylindrical section), an increased outlet temperature is necessary.

c. Chamber L'

Trends in chamber L' as a function of MR and P_c are shown in Figures 15 through 17 for thrusts of 4448, 1779, and 445N (1000, 400, and 100 lbF). With RP-1 as the coolant, the L' values decrease with increasing mixture ratio at all thrust levels. Decreasing thrust also results in lower L' values for the same P_c and MR. Bulk temperature rise limitations result in reduced L' values as the coolant flowrate decreases with increasing mixture ratio.

III, B, Thermal Design (cont.)

With oxygen cooling, however, L' values are essentially independent of MR except at $F = 4448N$ (1000 lbF) and $P_c = 6894\text{ kPa}$ (1000 psia) where the bulk temperature rise limits L' at MR's of 2 and 3. Chamber L' decreases with decreasing thrust and increasing P_c up to a P_c of 2758 kPa (400 psia).

d. Channel Width

The results of an earlier analytical study (reported in Ref. 1 through 3) with LOX/RP-1, LOX/LCH₄, and LOX/LH₂ as coolants had shown that RP-1 could not be used to cool engines in this thrust and P_c range if conventional channel dimensions were used. Current fabrication technology limits milled channels to a width of 0.083 cm (0.0325 in.) with a maximum aspect ratio (depth/width) of 5.

As shown in Figures 18, 19, and 20, the analyses reported herein substantiate these earlier findings. Only for RP-1 at MR = 1 and at the lowest thrust and chamber pressure [445N (100 lbF) and 689 kPa (100 psia), respectively] does the predicted channel width of 0.076 cm (0.030 in.) approach the conventional minimum width of 0.083 cm (0.0325 in.). Increasing P_c or MR requires decreasing channel width for cooling; the smallest channel width for which a design solution was achieved was 0.058 cm (0.023 in.) for $F = 445N$ (100 lbF), $P_c = 689\text{ kPa}$ (100 psia), and MR = 2 (see Figure 20).

The maximum channel width calculated for oxygen was 0.081 cm (0.032 in.) at $F = 4448N$ (1000 lbF), $P_c = 689\text{ kPa}$ (100 psia), and MR = 5 (see Figure 18). A minimum value of 0.006 cm (0.0022 in.) was calculated for $F = 445N$ (100 lbF), $P_c = 4826\text{ kPa}$ (700 psia), and MR = 3. Channel width decreases with decreasing thrust and mixture ratio and increasing chamber pressure.

Channel width as a function of P_c for curves of constant thrust for each coolant at each mixture ratio are cross-plotted in Figures 21 and 22. Channel width is a sensitive function of P_c for RP-1 at MR = 1. The data indicate less sensitivity of channel width to both MR and P_c at higher mixture ratios.

The broader feasibility range for oxygen cooling, as shown in Figure 22, indicates a similar but somewhat lower sensitivity of channel width to P_c at all mixture ratios. The minimum channel width decreases with decreasing MR (i.e., decreasing oxygen flowrate) and increasing P_c .

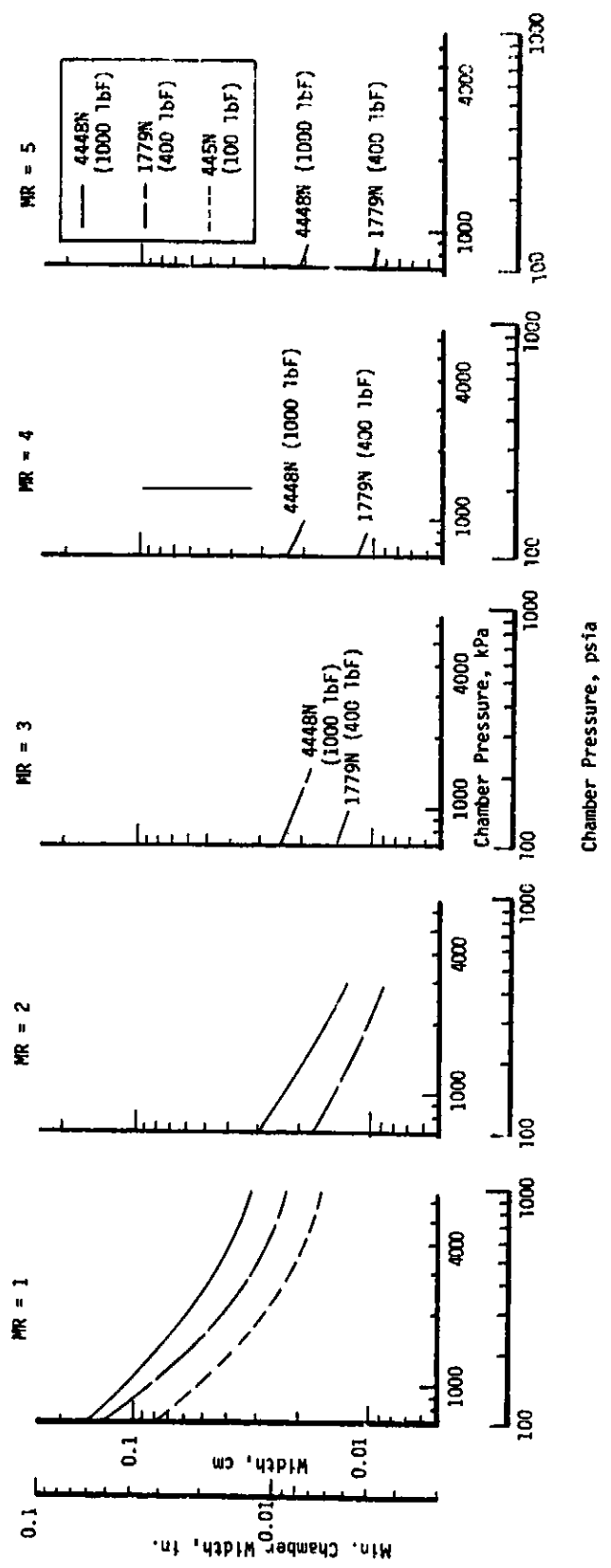


Figure 21. 102/RP-1 Minimum Required Channel Width for RP-1 Regenerative Cooling as a Function of Mixture Ratio and Thrust

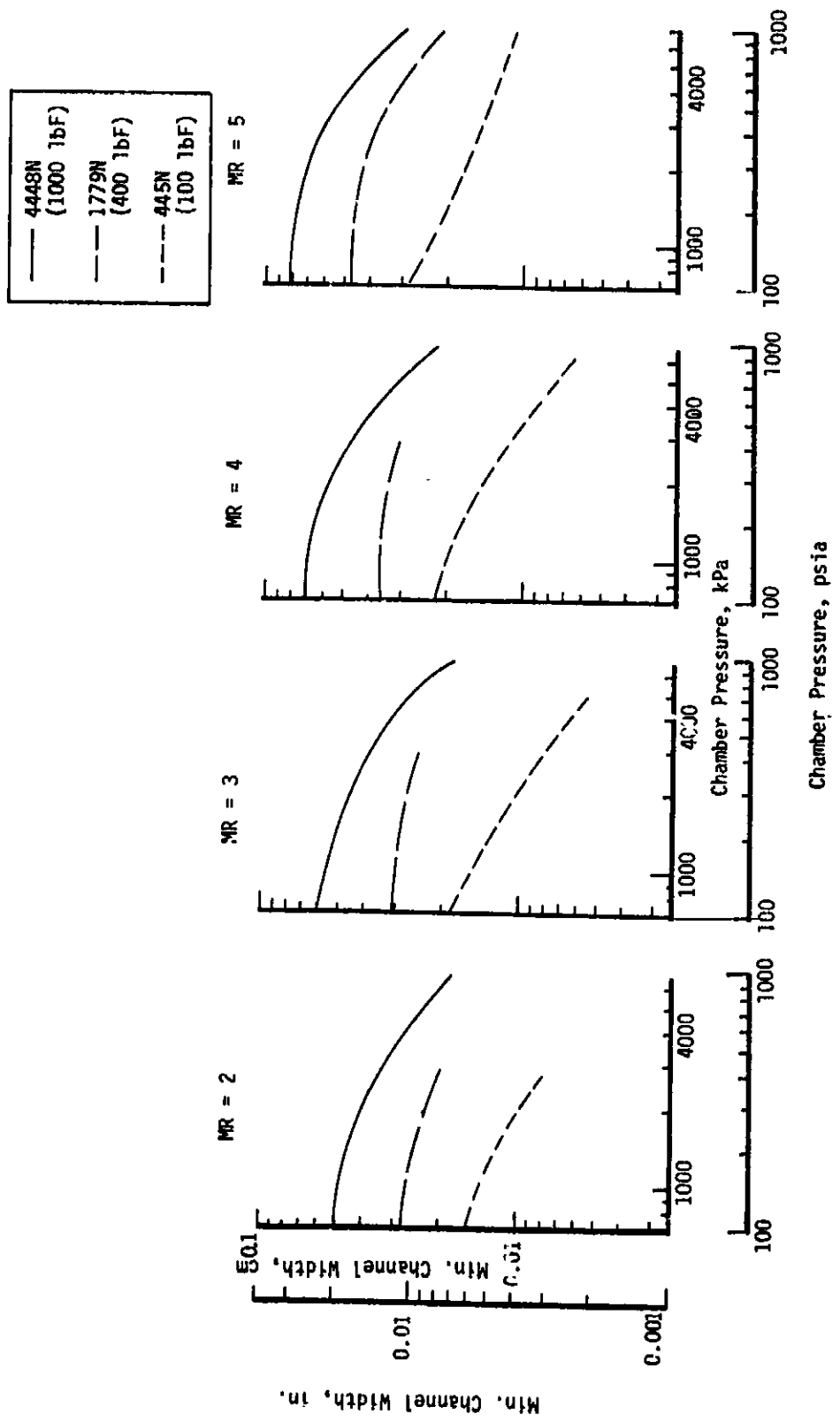


Figure 22. L₀₂/RP-1 Minimum Required Channel Width for Oxygen Regenerative Cooling as a Function of Mixture Ratio and Thrust

III, B, Thermal Design (cont.)

A graphic illustration of the relationship of fabrication technology to the regenerative cooling capabilities of oxygen is shown in Figure 23. The upper panel depicts the approximate operating limitations for a conventional channel width of 0.076 cm (0.030 in.). Only at MR = 5 does any cooling capability exist, and this only at the maximum thrust and at low P_c .

Design feasibility is greatly enhanced if the channel minimum width limit is reduced to 0.025 cm (0.010 in.), assumed achievable with a relatively modest investment in technology development. At MR = 5, operation at a thrust of 4448N (1000 lbf) is practical at all chamber pressures. At 1779N (400 lbf), the upper P_c limit is about 5515 kPa (800 psia), while a thrust of 445N (100 lbf) can be obtained at P_c 's near 689 kPa (100 psia). As the mixture ratio is reduced, the operating map becomes more restricted but still encompasses a broad range at the lowest MR.

For a minimum channel width of 0.013 cm (0.005 in.), considered the lowest constraint on size based on filtration limitations, the operating map covers most of the study range. The minimum thrust designs become progressively less feasible with decreasing mixture ratio. The obvious limitation for this expanded capability map is the increased difficulty anticipated in fabricating reproducible channels to this dimension.

The equivalent illustration for RP-1 coolant channels is given in Figure 24. Increased cooling capability is predicted as minimum channel width is successively decreased from 0.076 to 0.025 to 0.013 cm (0.030 to 0.010 to 0.005 in.). However, this improvement is limited to MR = 1, with only limited capability shown at higher mixture ratios for the 0.013-cm (0.005-in.) minimum channel width.

4. Dual-Propellant Regenerative Cooling Results (Fuel and Oxygen)

Selected input data and calculated results for dual-regenerative cooling are presented in Table VII. RP-1 cools the nozzle from the radiation attach point area ratio to $\epsilon = 6:1$, assumed to be a practical location for manifolding. Oxygen serves as the coolant from this point to the discharge manifold at the injector.

Of the six dual-regen cases studied, three analyses included both RP-1 and oxygen in terms of all system parameters (ΔP , channel width, discharge temperature, etc.). For the remaining cases, a complete analysis was performed only for the oxygen-cooled section which sustains both the maximum heat flux near the throat and the greatest total heat load in

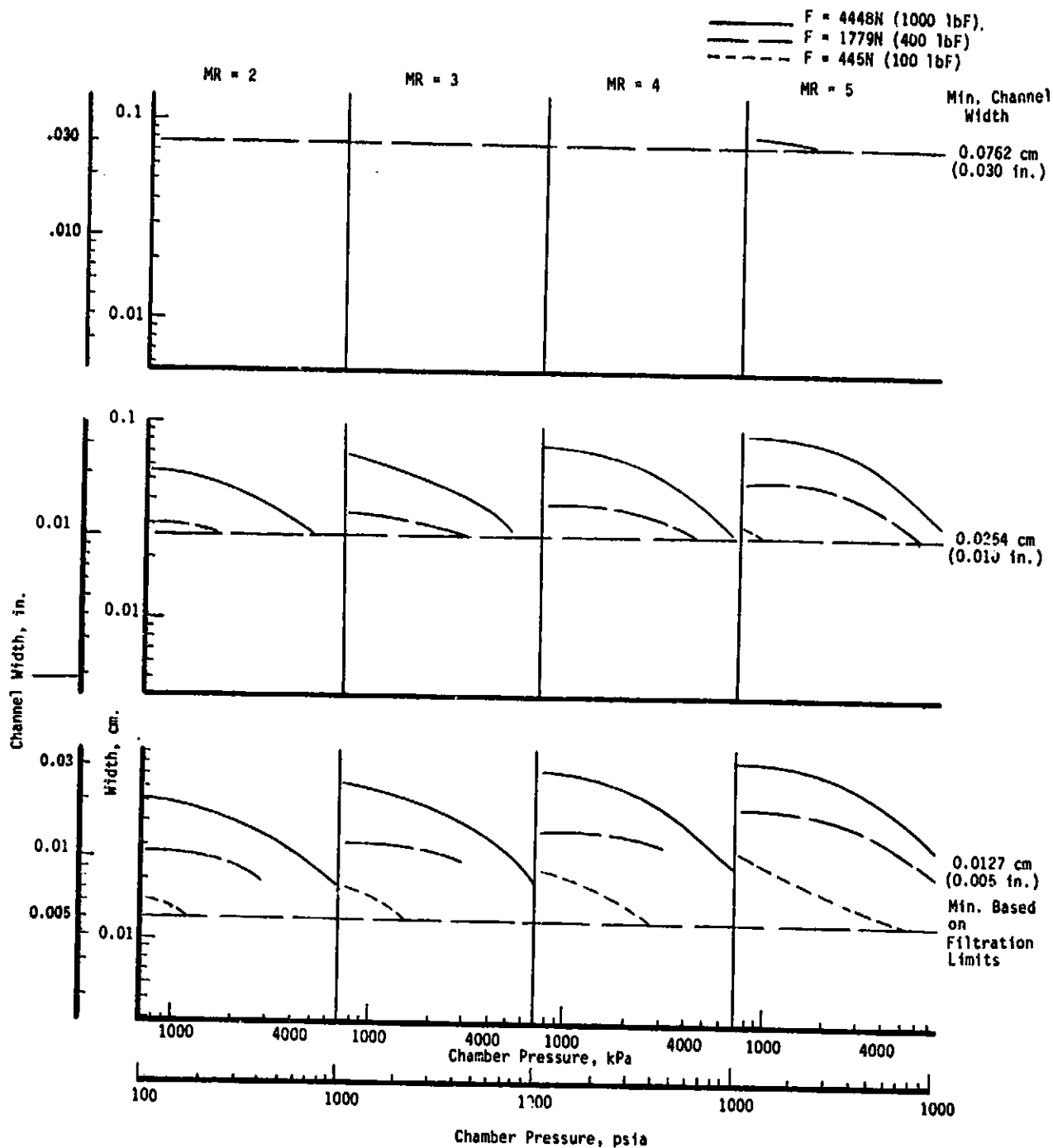


Figure 23. Sensitivity of Required Minimum Coolant Channel Width to Chamber Pressure, Mixture Ratio, and Thrust for Oxygen Regenerative Cooling of LO₂/RP-1 Engines

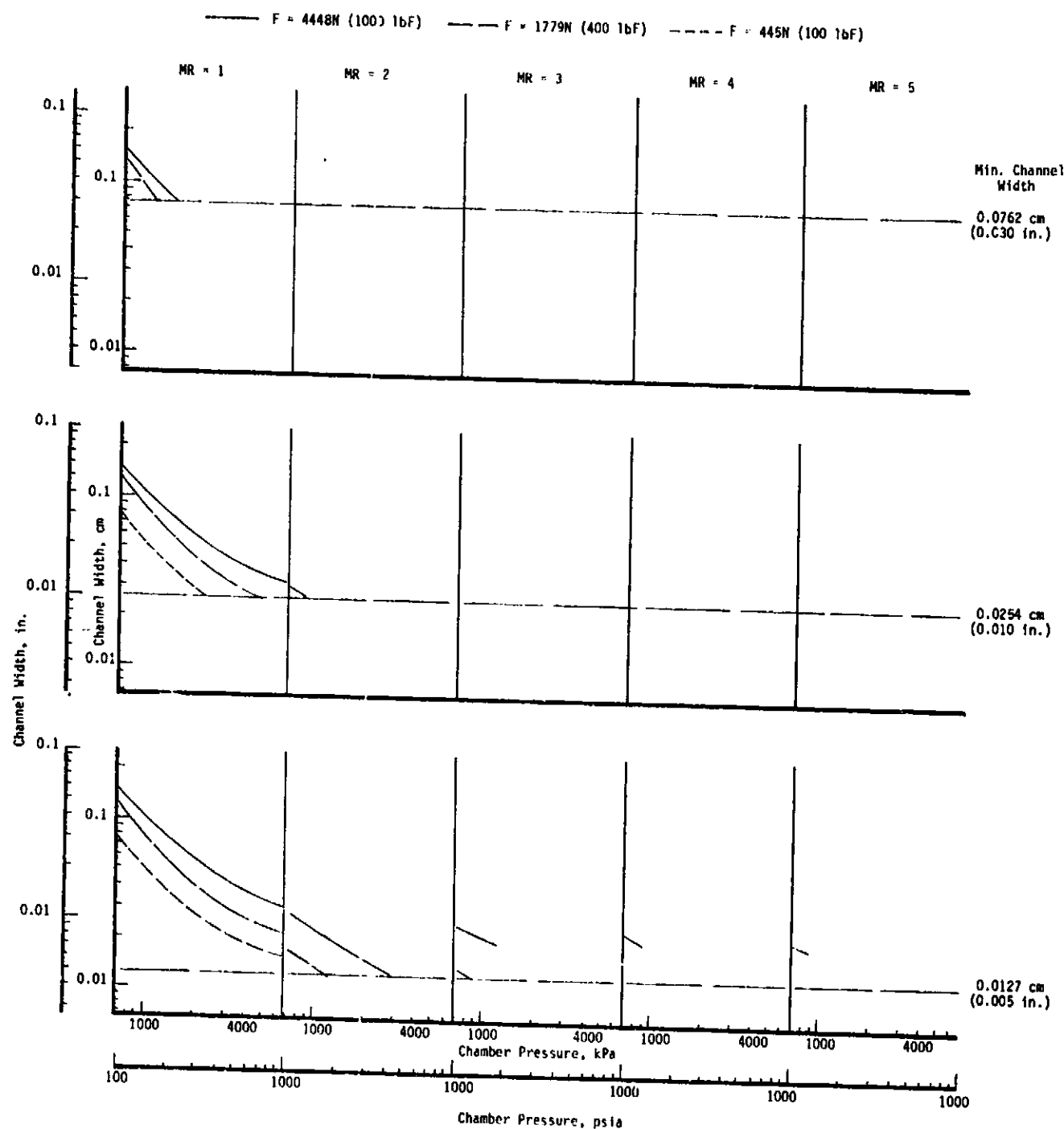


Figure 24. Sensitivity of Required Minimum Coolant Channel Width to Chamber Pressure, Mixture Ratio and Thrust for RP-1 Regenerative Cooling of $\text{LO}_2/\text{RP-1}$ Engines

TABLE VII

**SELECTED PARAMETERS CHARACTERIZING
REGENERATIVE COOLING
(Dual Regen)**

Code	MR	F	Pc kPa	Coolant	P _{in} kPa	P _{in} /Pc	t _{wall} cm (n, t, b)*	CR	T _c °K	C _F	Isp sec	Channel Dimensions			
												Throat w/d cm/cm	Barrel w/d cm/cm	L' cm	
2-1-4/F0	2	445	2758	F	6205 0	2.25 2.25	0.76 0.76	- 13.10	3266 3266	1.853 1.853	315.5 315.5	- 20	0.0081/0.163	0.0152/0.163	8.05
2-1-5/F0			3447	F	6791 0	1.97 1.97	0.76 0.76	- 16.75	3282 3282	1.862 1.862	315.7 315.7	- 20	0.0079/0.157	0.0155/0.157	8.66
2-10-10/F0		4448	6894	F	9652 0	1.40 1.40	0.0635 0.0635	- 8.00	3327 3327	1.871 1.871	332.9 332.9	8. 20., 30.	0.0201/0.602	0.0284/0.526	17.92
4-4-10/F0	4	1779	6894	F	9652 0	1.40 1.40	0.0635 0.0635	- 9.32	3634 3634	2.109 2.109	323.9 323.9	- 20.	0.0203/0.406	0.0229/0.483	14.55
5-1-10/F0	5	445	6894	F	9652 0	1.40 1.40	0.0635 0.0635	- 37.54	3514 3514	2.124 2.124	299.6 299.6	- 20.	0.0202/0.203	0.0254/0.485	6.48
5-4-10/F0		1779	6894	F	9652 0	1.40 1.40	0.0635 0.0635	- 9.40	3514 3514	2.127 2.127	305.9 305.9	- 20.	0.0229/0.462	0.0305/0.617	12.14

*n - nozzle
t - throat
b - barrel

**When two numbers are given, the first refers to throat d/w,
while the second to barrel d/w.

TABLE VII

METERS CHARACTERIZING ENGINE -
GENERATIVE COOLING
(Dual Regen)

SI Units

Barrel w/d cm/cm	L' cm	r _t cm	r _{ch} cm	A	ΔP kPa	T _b , in °K	T _b , out °K	→T _b °K	h _q , max kw/m ² °K sec × 10 ⁻³	Q _g , max kw/m ² sec	Q _c , max kw/m ² sec	No. of Channels	Liner t/k in ² sec °F/Btu
52/0.163	8.05	0.526 0.526	1.905 1.905	14.04 6.00	603	289 94.5	307 396	273 558	6207	15705	2173	113	-
55/0.157	8.66	0.470 0.470	1.923 1.923	17.74 6.00	673	289 94.5	311 397	278 558	7383	18646	2533	108	-
84/0.526	17.98	1.046 1.046	2.961 2.961	41.63 6.00	710 1358	289 97.1	356 373	322 532	2539 18032	6292 48307	5377 4903	83 84	-
29/0.483	14.55	0.625 0.625	1.905 1.905	6.00	1302	97.1	240	399	12619	39465	5622	52	600
54/0.485	6.48	0.310 0.310	1.905 1.905	6.00	1730	97.1	195	354	11884	35625	8710	32	600
05/0.617	12.14	0.622	1.905	6.00	1702	97.1	257	416	13737	40822	5050	50	-

2
FOLDOUT FRAME

ORIGINAL PAGE IS
OF POOR QUALITY

TABLE VII (Cont.)
SELECTED PARAMETERS CHARACTERIZING ENGINE
REGENERATIVE COOLING
(DUAL REGEN)

Code	MR	F	ρ_c lb/ft ³	Coolant ρ_{in} psia	P_{in}/P_c	t_{wall} in. (n, t, b)*	CR	T_c °R	C_F	Isp sec	Channel Dimensions		
											Aspect Ratio d/w**	Throat w/d	Barrel w/d
2-1-4/F0	2	100	400	F	900	2.25	.3	13.10	5378	1.853	315.5	—	—
2-1-5/F0	500	F	985	1.97	900	2.25	.3	—	5878	1.853	315.5	20	0.0032/0.064
2-10-10/F0	1000	1000	F	1400	1.40	0.025	.3	16.75	5908	1.862	315.7	—	—
4-4-10/F0	4	400	1000	F	1400	1.40	0.025	8.00	5988	1.871	332.9	8.	0.0061/0.162
5-1-10/F0	5	100	1000	F	1400	1.40	0.025	—	5988	1.871	332.9	20, 30	0.0079/0.237
5-4-10/F0	400	1000	F	1400	1.40	0.025	9.32	6541	2.109	323.9	—	—	0.0112/0.207
				0	1400	1.40	0.025	—	6541	2.109	323.9	20,	0.009/0.160
				0	1400	1.40	0.025	37.54	6325	2.124	299.6	—	—
				0	1400	1.40	0.025	—	6325	2.124	299.6	20,	0.004/0.060
				0	1400	1.40	0.025	9.40	6325	2.127	305.9	20,	0.009/0.152
				0	1400	1.40	0.025	—	6325	2.127	305.9	0.012/0.243	—

*n = nozzle
t = throat
b = barrel

**When two numbers are given, the first refers to throat d/w,
while the second to barrel d/w.

TABLE VII (Cont.)
**SELECTED PARAMETERS CHARACTERIZING ENGINE
 REGENERATIVE COOLING
 (Dual Regen)**

Code	ϵ_A	ΔP psi	T_b , in $^{\circ}$ F	T_b , out $^{\circ}$ F	ΔT_b $^{\circ}$ F	h_g, max Btu/in. ² $\text{sec}^0 F$ $\times 10^{-3}$	Q_c, max Btu/in. ² sec	No. of Channels	Liner t/k
2-1-4/FO	14.04	—	60.3	91.9	31.6	—	—	—	—
	6.00	87.5	-289.9	253.6	543.5	2.11	9.61	1.33	113
2-1-5/FO	17.74	—	60.3	100.6	40.3	—	—	—	—
	6.00	97.6	-289.9	255.3	545.2	2.51	11.41	1.55	108
2-10-10/FO	41.63	103	60.3	180.0	119.7	.863	3.85	3.29	83
	6.00	197	-285.3	212.0	497.3	6.13	29.56	3.00	84
4-4-10/FO	—	188.9	—	—	—	—	—	—	—
	6.00	—	-285.3	-27.4	257.9	4.29	24.15	3.44	52
5-1-10/FO	—	250.9	—	—	—	—	—	—	—
	6.00	—	-285.3	-108.5	176.8	4.04	21.80	5.33	32
5-4-10/FO	—	246.9	—	—	—	—	—	—	600
	6.00	—	-285.3	3.1	288.4	4.67	24.98	3.09	50

III. B, Thermal Design (cont.)

the barrel. An energy balance was sufficient to determine the RP-1 discharge temperature.

The results of the dual-regen analyses are included in Figures 9 through 20. Typical results are displayed for Case Code 2-10-10/F0 [MR = 2, F = 4448N (1000 lbF), P_c = 6894 kPa (1000 psia)]. If the data from the single-regen oxygen cooling are compared with the oxygen portion of the dual-regen system, the following results are obtained. With the dual-cooling, the oxygen ΔP (Figure 9) is decreased from 1595 to 1358 kPa (231.3 to 197 psia); L' (Figure 15) is significantly increased from 12.32 to 17.98 cm (4.85 to 7.08 in.); as a result of the increased L' which can be cooled, the outlet temperature (Figure 17) is increased from 333 to 373°K (140.2 to 212°F); and minimum channel width (Figure 18) is increased from 0.0185 to 0.0201 cm (0.0073 to 0.0079 in.). In addition, the temperature of the RP-1 to the injector is increased from 289 to 356°K (60 to 180°F), improving atomization and vaporization. These results should be reflected in an increased Isp and in decreased pump power requirements.

5. Thermal Conclusions for LOX/RP-1 Cooling

The primary conclusion to be drawn from this analytical study is that the narrow, high aspect ratio Zr-Cu cooling channels have far more favorable cooling capabilities than those achievable with current conventional channel designs for engines of relatively low thrust and chamber pressure. At thrust levels between 445 and 4448N (100 and 1000 lbF), chamber pressures from 689 to 6894 kPa (100 to 1000 psia), and mixture ratios from 1 through 5, the fuel RP-1 has been demonstrated to have some cooling capability (though limited) on the F-Pc-MR operating map. In contrast, use of oxygen as a coolant provides a much broader range of parameters. For the LOX/RP-1 propellant combination, regenerative cooling (RP-1, LO_2 , or RP-1 and LO_2) has been shown to be adequate at pressures below 3447 kPa (500 psia). Thermal liners become necessary in some F-Pc-MR ranges above 3447 kPa (500 psia) and at low thrust. For the remaining regions on the lower-thrust Pc-MR maps, cooling augmentation such as film cooling is needed.

The analysis matrices for the three thrust levels studied are given in Figures 25, 26, and 27. The design points are coded to indicate results, and boundary lines have been sketched to show the approximate extent of cooling concept applicability. Regions are defined by the design point codes.

The data of Figure 25 at $F = 4448N$ (1000 lbF) for single-regen RP-1 indicate a low MR region where regen cooling is practical. An extension to higher MR's at low P_c 's is possible at reduced L' values. Since the L' reduction is a result of the fuel cooling becoming bulk-temperature-

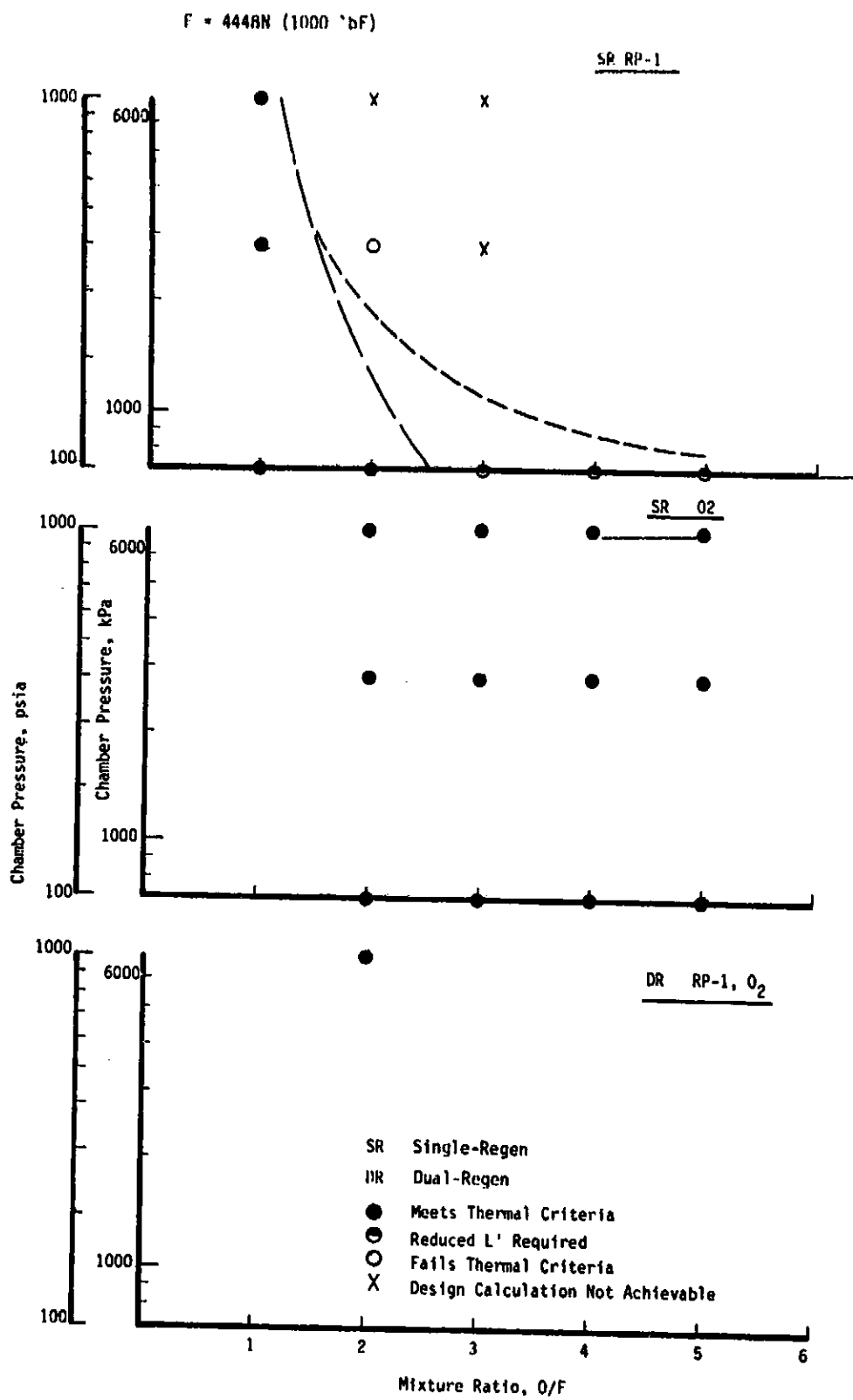


Figure 25. LO₂/RP-1 Regenerative Cooling Analysis Matrix,
 $F = 4448N$ (1000 lbF)

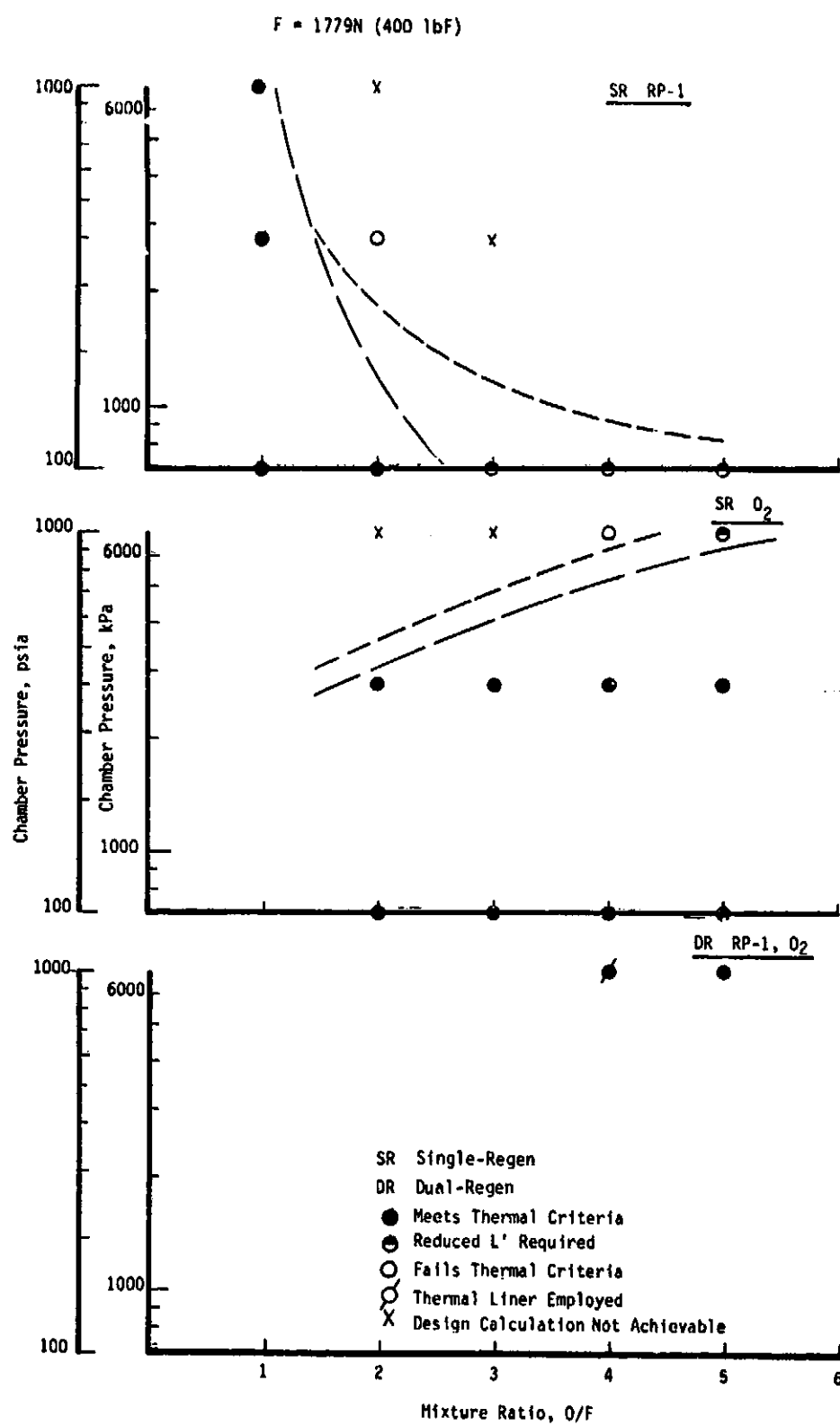


Figure 26. LO₂/RP-1 Regenerative Cooling Analysis Matrix,
 $F = 1779N$ (400 lbF)

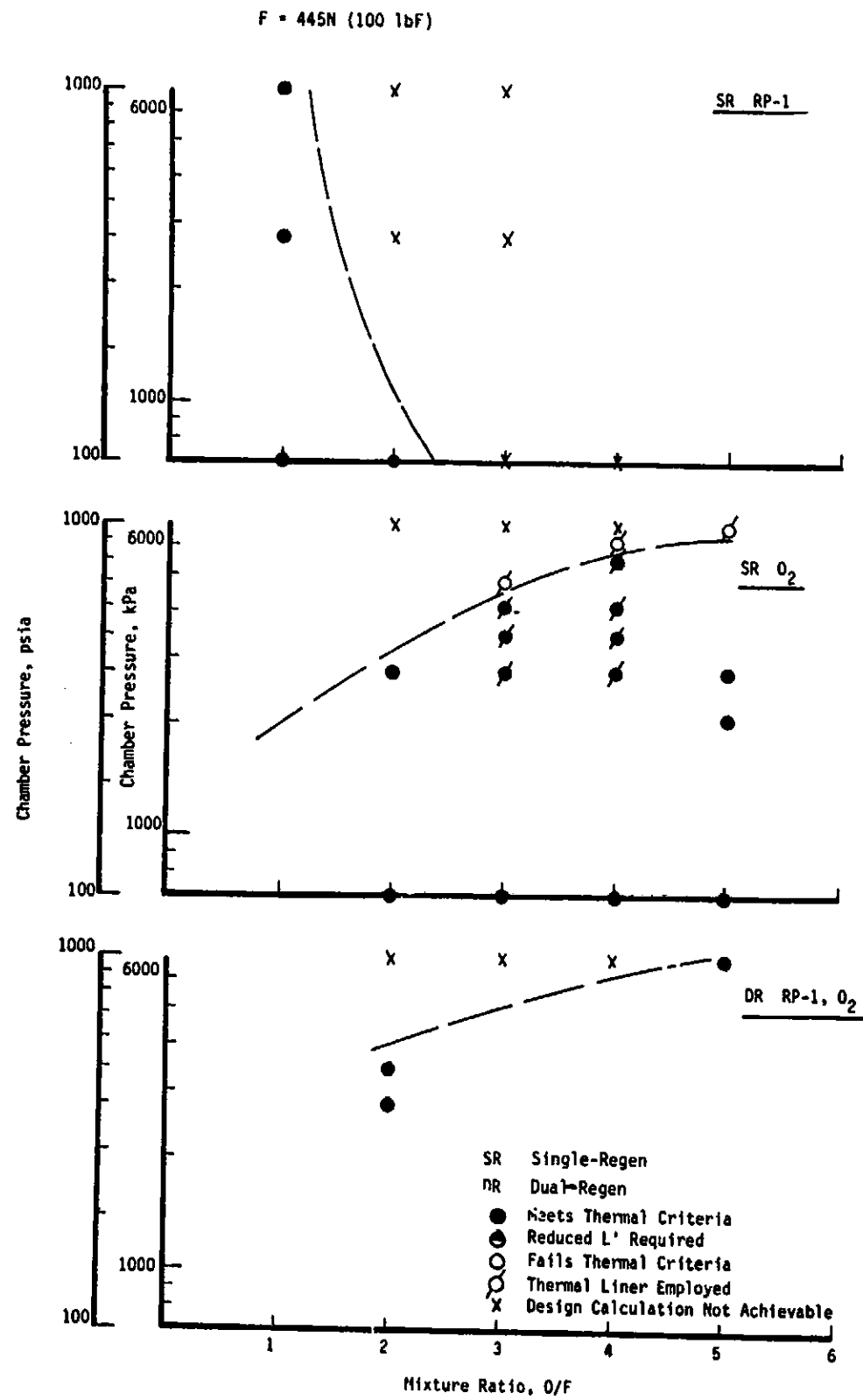


Figure 27. LO₂/RP-1 Regenerative Cooling Analysis Matrix,
 $F = 445N$ (100 lbf)

III, B, Thermal Design (cont.)

limited, a thermal liner in the barrel can be used to lengthen L' for a part of this region. However, a zero or negative cylindrical section length was determined for some points, obviating any liner usage.

Oxygen as a single-regen coolant can be satisfactorily used over the entire P_c -MR map at $F = 4448N$ (1000 lbF). Dual-regen cooling is applicable to reduce oxygen pressure drop and to raise the RP-1 temperature to the injector.

At 1779N (400 lbF), the single-regen RP-1 results, shown in Figure 26, are similar to those of Figure 25 for $F = 4448N$ (1000 lbF). Oxygen single-regen cooling is adequate at all MR's at P_c 's of 400 and below, but is marginal at 6894 kPa (1000 psia) at $MR = 5$ and inadequate at 6894 kPa (1000 psia) at $MR = 4$. However, dual-regen cooling achieves cooling feasibility for these points. Cooling capability could not be demonstrated at lower MR's at high P_c 's.

The trends initiated in Figure 26 at 1779N (400 lbF) are intensified at $F = 4448N$ (100 lbF), as shown in Figure 27. The feasible single-regen RP-1 region is somewhat smaller, as is the single-regen oxygen cooling region. As before, the use of dual-regen cooling increases the P_c level for which cooling can be achieved.

Design calculations at the points indicated by an "X" were not achievable due to numerical problems where very large pressure or temperature gradients were computed or where channel widths below 0.005 cm (0.002 in.) were required. For these points, calculational failure is equivalent to concept failure as no design feasibility exists.

In summation, the net results of the Task III study are shown in Figure 28 which provides F - P_c -MR operating maps delineating cooling concept areas. Some form of regenerative cooling is shown to be applicable over most of the study range; however, cooling augmentation is required over a limited region.

6. Additional Remarks Pertaining to Chamber Gas-Side Wall Thickness and Channel Geometry at Low Thrust

The preliminary Task III studies had shown a significant improvement in heat-flux transformation at low P_c 's with increasing wall thickness. These analyses considered a gas-side wall thickness of 0.76 cm (0.3 in.) at P_c 's through 2758 kPa (400 psia). At the higher gas-side flux levels associated with high P_c operation, the wall thickness was generally reduced to as low as 0.064 cm (0.025 in.) for these smaller engines.

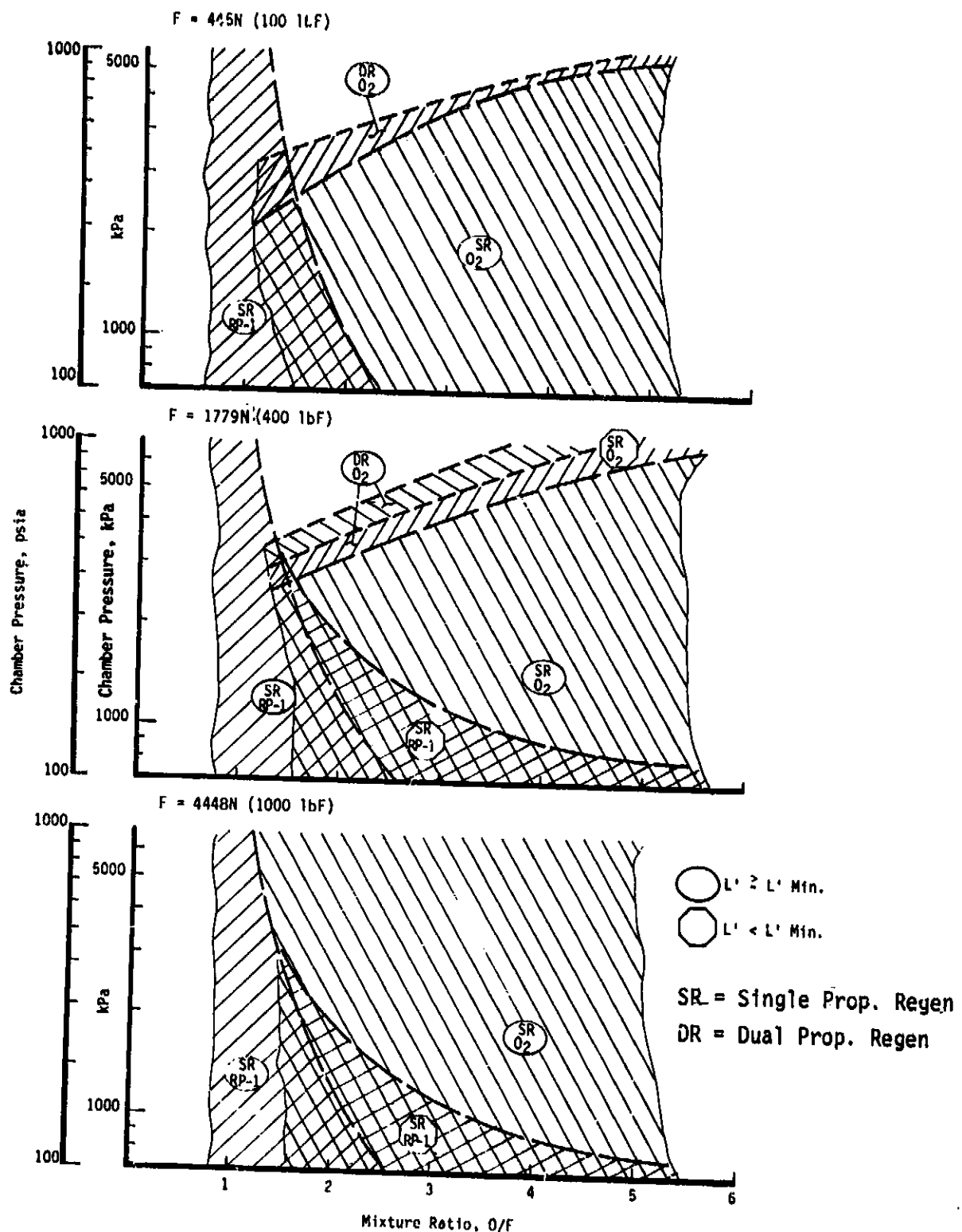


Figure 28. Thrust/Chamber Pressure/Mixture Ratio Operating Limits for Regenerative Cooling Concepts for I.O₂/RP-1 Engines

III, B, Thermal Design (cont.)

The effect of increasing wall thickness is illustrated in Figure 29. Figure 30 (for the throat of an LO₂/RP-1 thruster operating at a mixture ratio of 2.0) shows the wall thickness required to maintain a 222°K (400°F) temperature differential across the wall as a function of P_c while maintaining a maximum surface temperature of 811°K (1000°F). Curves are given for various thrust levels. For practical considerations, these curves cannot be used directly, but they do provide rough guidelines for estimating wall thicknesses required for this study.

In general, a channel aspect ratio (depth/width) of 8:1 was utilized at the lower P_c's where flux levels were lower and transformation requirements were less, thus reducing the demand on fabrication technology. At the higher P_c values and where pressure drops were unacceptable, an aspect ratio of 20:1 was normally considered. The criteria used to select the minimum land size of 0.064 cm (0.025 in.) are shown in Figure 31.

C.- PERFORMANCE SENSITIVITY

A parametric performance analysis was conducted to determine the delivered performance of engines using oxidizer, fuel, and oxidizer + fuel (dual-propellant) regenerative cooling.

The parametric operating points investigated are as follows:

Thrust (F), N (lbF)	445, 1779, 4448 (100, 400, 1000)
Chamber Pressure (P _c), kPa (psia)	689, 2758, 6894 (100, 400, 1000)
Mixture Ratio (MR)	1, 2, 3, 4, 5

The propellants were LOX/RP-1, and the area expansion ratio was fixed at 400:1 for all cases. Attainable combustion chamber lengths (L'), based on cooling limits, propellant temperatures, and contraction ratios (ϵ_c), were predetermined from thermal analyses. The chamber length and contraction ratio data and the results of the parametric performance analyses are listed in Table VIII. Figures 32 to 40 are cross-plots showing the influence of mixture ratio, thrust, and chamber pressure on predicted Isp. The peak performance and cooling schemes for various F/P_c combinations are identified in Table IX. The data contained in Figures 32, 33, and 34 show the delivered specific impulse as a function of mixture ratio cooling scheme and chamber pressure for thrust levels of 445, 1779, 4448N (100, 400, and 1000 lbF), respectively. These data show the following:

- With LOX/RP-1, performance of all cooling concepts decreases rapidly below a mixture ratio of 2.0.

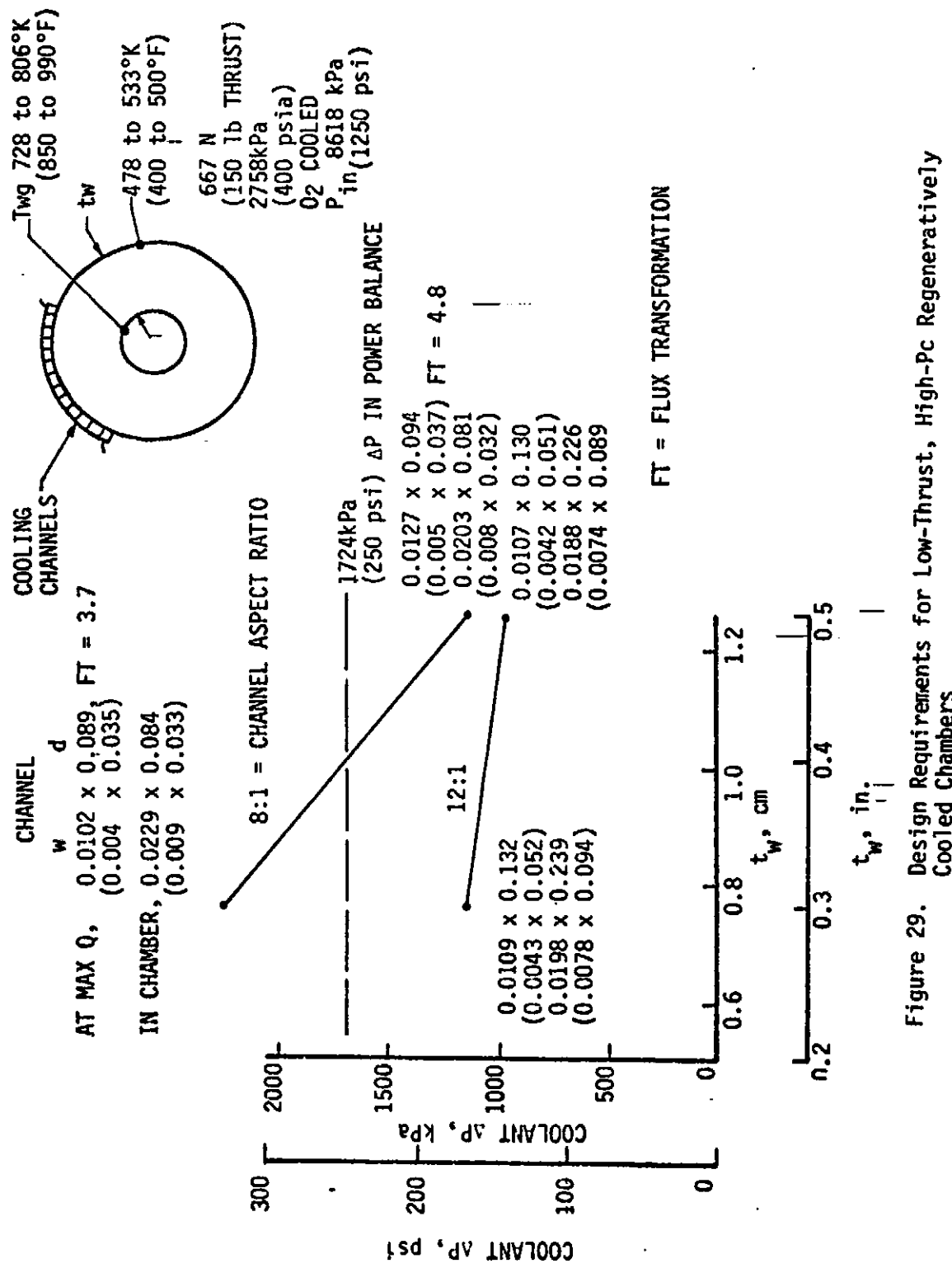


Figure 29. Design Requirements for Low-Thrust, High-Pc Regeneratively Cooled Chambers

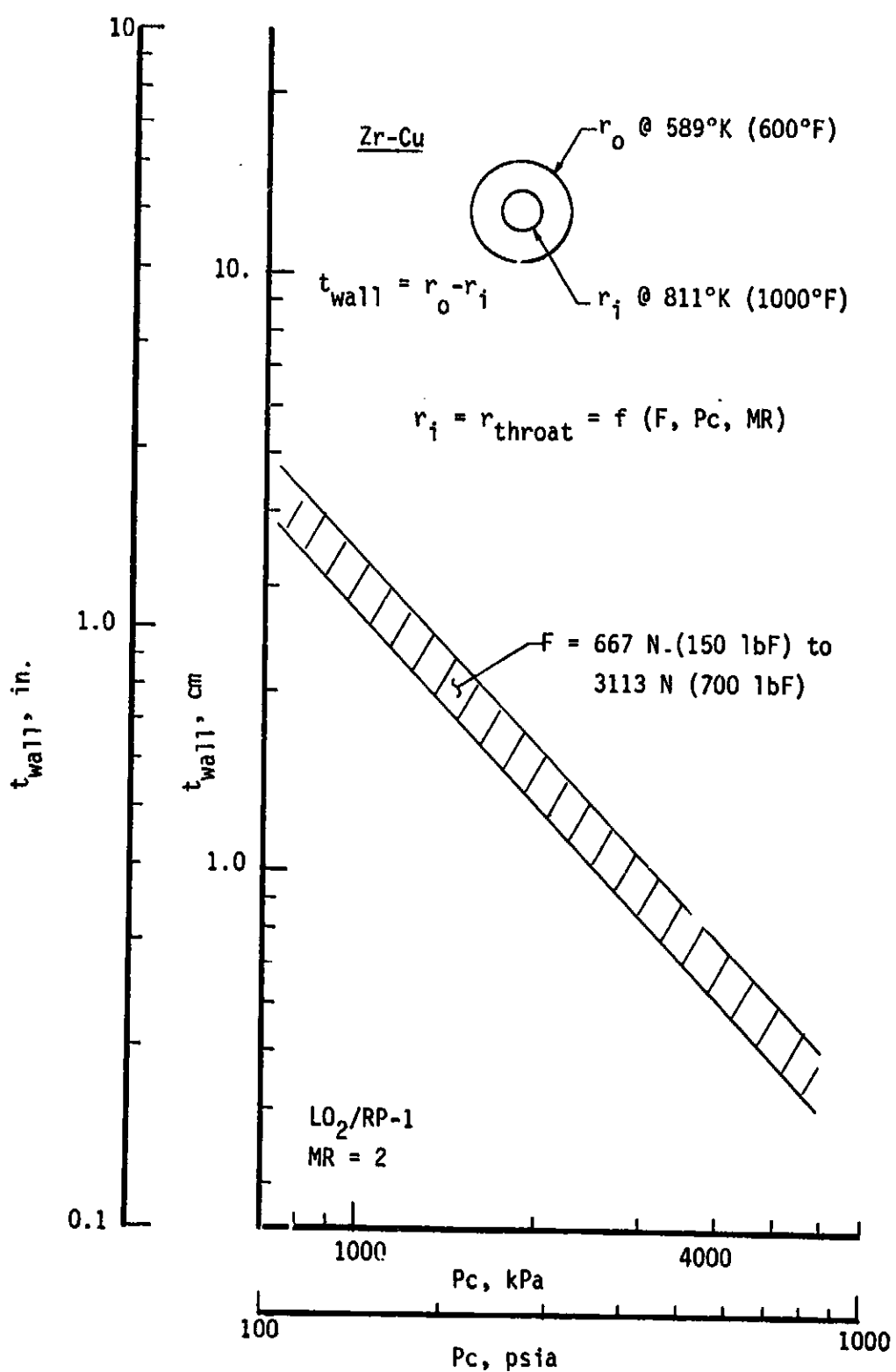


Figure 30. Wall Thickness as a Function of Chamber Pressure and Thrust for a Constant Wall Temperature Drop

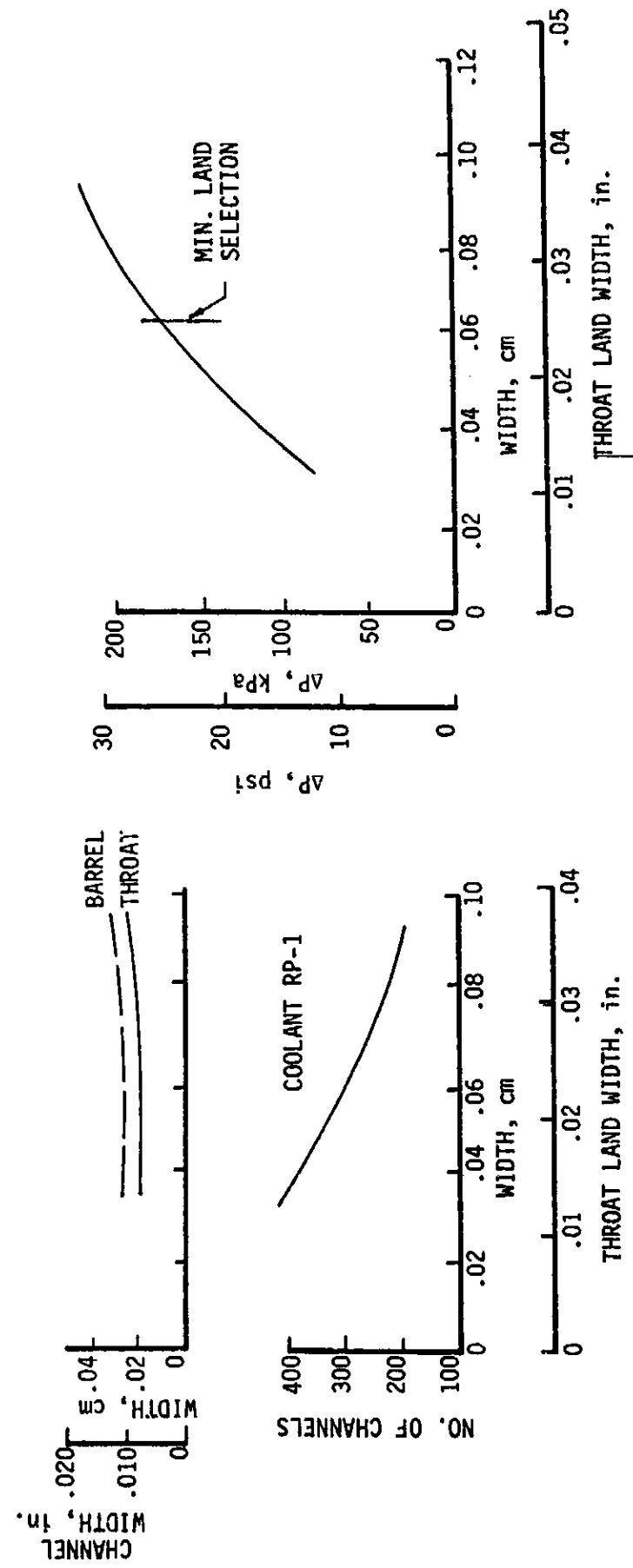
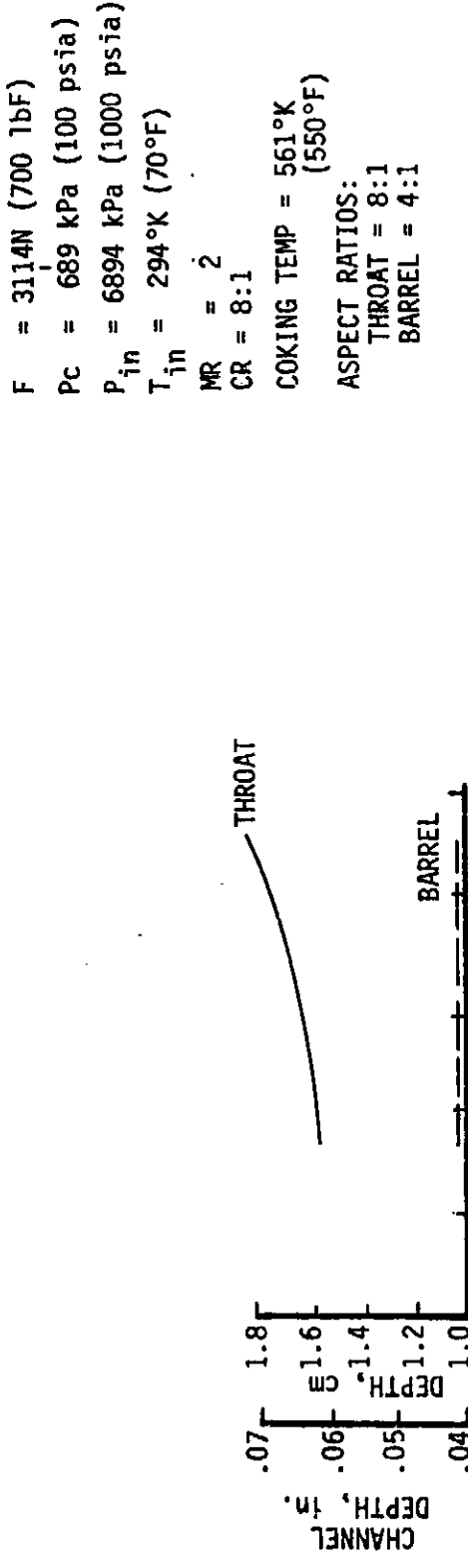


Figure 31. RP-1 Regeneratively Cooled Chamber Channel Land Size Sensitivity

TABLE VIII
PARAMETRIC DATA AND RESULTS

Page 1 of 2
Metric Units

F N Pc kPa	L' cm	Oxygen Regen Cooling				RP-1 Regen Cooling								
		T _{ox} °K	T _F °K	ε _C	NEL	ERe (%)	Isp sec	L'	cm	T _{ox} °K	T _F °K	ε _C	NEL	
445	6894	1	-	-	-	-	-	10.59	94	392	34.8	18	98.0	258.8
	-	2	-	-	-	-	-	-	-	-	-	-	-	-
	4653	3	9.53	396	289	22.7	7	90.7	335.6	-	-	-	-	-
	6205	4	10.16	344	289	30.0	7	92.9	330.5	-	-	-	-	-
	-	5	-	-	-	-	-	-	-	-	-	-	-	-
2758	1	-	-	-	-	-	-	10.46	94	372	14.0	36	97.5	253.5
	2	7.85	385	289	13.1	7	92.3	311.2	-	-	-	-	-	-
	3	10.16	389	289	14.4	7	90.8	329.5	-	-	-	-	-	-
	4	10.46	396	289	14.5	7	91.6	316.9	-	-	-	-	-	-
	5	10.46	316	289	14.8	7	91.2	304.3	-	-	-	-	-	-
689	1	-	-	-	-	-	-	14.40	94	362	8.0	22	97.4	247.4
	2	13.34	398	289	8.0	24	98.1	314.5	4.06	94	451	8.0	24	95.6
	3	14.40	365	289	8.0	22	91.4	311.5	-	-	-	-	-	-
	4	13.49	280	289	8.0	21	94.3	301.0	-	-	-	-	-	-
	5	14.38	251	289	8.0	21	95.1	293.0	-	-	-	-	-	-
1779	6894	1	-	-	-	-	-	14.66	94	391	8.50	7	99.0	259.9
	2758	1	-	-	-	-	-	14.40	94	359	8.0	22	98.1	254.8
	2	14.40	353	289	8.0	22	98.6	338.9	6.05	94	450	8.0	22	97.9
	3	14.40	318	289	8.0	20	94.6	345.8	-	-	-	-	-	-
	4	14.40	258	289	8.0	20	95.5	333.1	-	-	-	-	-	-
689	1	-	-	-	-	-	-	19.79	94	334	8.0	101	97.9	247.9
	2	19.79	365	289	8.0	102	99.2	327.2	10.77	94	451	8.0	101	99.7
	3	19.79	321	289	8.0	96	96.7	326.4	7.49	94	451	8.0	96	96.4
	4	19.79	278	289	8.0	95	97.5	314.7	7.44	94	468	8.0	95	97.6
	5	19.75	244	289	8.0	94	97.6	302.8	7.42	94	478	8.0	94	97.9

TABLE VIII (cont.)

Page 2 of 2
Metric Units

Oxygen Regen Cooling							RP-1 Regen Cooling									
F N	Pc kPa	MR	L' cm	T _{ox} °K	T _F °K	ε _C	NEL	ERE (%)	I _{sp} sec	L' cm	T _{ox} °K	T _F °K	ε _C	NEL	ERE (%)	I _{sp} sec
4448	6894	1	-	-	-	-	-	-	-	17.98	91	366	8.0	23	99.2	257.1
		2	12.32	333	289	8.0	22	97.9	334.8	-	-	-	-	-	-	-
		3	12.88	330	289	8.0	20	93.0	348.9	-	-	-	-	-	-	-
		4	17.98	343	289	8.0	19	96.7	347.5	-	-	-	-	-	-	-
		5	17.98	279	289	8.0	19	96.3	330.1	-	-	-	-	-	-	-
2758	1	-	-	-	-	-	-	-	-	17.78	91	342	8.0	62	98.5	253.8
		2	17.78	282	289	8.0	59	99.4	345.2	7.92	91	450	8.0	60	99.2	340.8
		3	17.78	244	289	8.0	55	96.4	353.2	-	[]	-	-	-	-	-
		4	17.78	206	289	8.0	54	97.2	340.4	-	-	-	-	-	-	-
		5	17.78	182	289	8.0	54	97.1	325.4	-	-	-	-	-	-	-
689	1	-	-	-	-	-	-	-	-	24.41	91	326	8.0	258	98.5	248.0
		2	24.41	277	289	8.0	257	99.5	331.4	20.0	91	456	8.0	256	100.0	334.0
		3	24.41	246	289	8.0	242	97.5	333.0	14.30	91	450	8.0	241	98.5	337.1
		4	24.41	214	289	8.0	241	98.4	320.0	12.22	91	450	8.0	241	99.1	322.3
		5	24.41	191	289	8.0	240	98.4	307.1	11.10	91	456	8.0	240	99.0	308.8

DUAL REGEN COOLING

F N	Pc kPa	MR	L' cm	T _{ox} °K	T _{RP-1} °K	ε _C	NEL	ERE (%)	I _{sp} sec
4448	6894	2	17.98	373	356	8.0	22	99.9	343.9
445	3447	2	8.66	397	312	16.75	7	95.7	322.4
	2758	2	8.05	397	307	13.1	7	94.6	317.7

Page 1 of 2
English Units

TABLE VIII
PARAMETRIC DATA AND RESULTS

$\frac{P}{F}$ (psi)	M_F	Oxygen			Regen			Cooling			RP-1			Regen			Cooling		
		L' (in)	T_{or} (°R)	T_F (°R)	e_c	NEL	ERE (%)	TSP sec.	L' (in)	T_{ex} (°R)	T_F (°R)	e_c	NEL	ERE (%)	TSP sec.	L' (in)	T_{ex} (°R)	T_F (°R)	e_c
100	1000	1	-	-	-	-	-	-	4.17	170	705	34.8	8	98.0	255.5	-	-	-	-
	2	-	-	-	-	-	-	-	-	-	-	-	-	-	-	-	-	-	-
	675	3	3.75	713	520	22.7	7	90.7	335.6	-	-	-	-	-	-	-	-	-	-
	900	4	4.00	620	520	30.0	7	92.9	330.5	-	-	-	-	-	-	-	-	-	-
	5	-	-	-	-	-	-	-	-	-	-	-	-	-	-	-	-	-	-
400	1	-	-	-	-	-	-	-	4.12	170	670	14.0	36	97.5	253.5	-	-	-	-
	2	3.09	693	520	13.1	7	92.3	311.2	-	-	-	-	-	-	-	-	-	-	-
	3	4.00	701	520	14.4	7	90.8	329.5	-	-	-	-	-	-	-	-	-	-	-
	4	4.12	712	520	14.5	7	91.6	316.9	-	-	-	-	-	-	-	-	-	-	-
	5	4.12	568	520	14.8	7	91.2	304.3	-	-	-	-	-	-	-	-	-	-	-
100	1	-	-	-	-	-	-	-	5.67	170	651	8.0	22	97.4	247.5	-	-	-	-
	2	5.25	717	520	8.0	24	98.1	314.5	1,60	170	811	8.0	24	95.6	363.4	-	-	-	-
	3	5.67	657	520	8.0	22	91.4	311.5	-	-	-	-	-	-	-	-	-	-	-
	4	5.31	504	520	8.0	21	94.3	301.0	-	-	-	-	-	-	-	-	-	-	-
	5	5.66	452	520	8.0	21	95.1	293.0	-	-	-	-	-	-	-	-	-	-	-
400	1	-	-	-	-	-	-	-	5.77	170	703	8.50	7	99.0	259.7	-	-	-	-
	2	4CJ	1	-	-	-	-	-	5.67	170	646	8.0	22	98.1	254.5	-	-	-	-
	2	5.67	635	520	8.0	22	98.6	338.9	2,381	170	810	8.0	22	97.9	331.3	-	-	-	-
	3	5.67	573	520	8.0	20	94.6	345.8	-	-	-	-	-	-	-	-	-	-	-
	4	5.67	464	520	8.0	20	95.4	333.1	-	-	-	-	-	-	-	-	-	-	-
	5	5.67	384	520	8.0	20	95.4	319.2	-	-	-	-	-	-	-	-	-	-	-
100	1	-	-	-	-	-	-	-	7.79	170	601	8.0	101	97.9	247.9	-	-	-	-
	2	7.79	657	520	8.0	102	99.2	327.2	4,24	170	811	8.0	101	99.7	330.1	-	-	-	-
	3	7.79	577	520	8.0	96	96.7	326.4	2,96	170	812	8.0	96	96.4	325.7	-	-	-	-
	4	7.79	500	520	8.0	95	97.5	314.7	2,93	170	842	8.0	25	97.6	315.1	-	-	-	-
	5	7.79	440	520	8.0	94	97.6	302.8	2,52	170	861	8.0	94	97.9	303.5	-	-	-	-

TABLE VIII (cont.)

Page 2 of 2
English Units

<u>F</u> (lbf)	<u>Pc</u> (psia)	Oxygen Regen Cooling						RP-1 Regen Cooling					
		<u>T_{ox}</u> (°R)	<u>T_F</u> (°R)	<u>E_C</u>	<u>E_{EL}</u>	<u>ERF</u> (%)	<u>I_{sp}</u> sec	<u>L'</u> (in)	<u>T_{ox}</u> (°R)	<u>T_F</u> (°R)	<u>E_C</u>	<u>E_{EL}</u>	<u>ERF</u> (%)
1000	1000	1	-	-	-	-	-	7.06	163	659	8.0	23	99.2 252.1
	2	4.35	600	520	8.0	22	97.9	334.8	-	-	-	-	-
	3	5.07	594	520	8.0	20	93.0	348.9	-	-	-	-	-
	4	7.29	618	520	8.0	19	96.7	347.5	-	-	-	-	-
	5	7.26	502	520	8.0	19	96.3	330.1	-	-	-	-	-
400	1	-	-	-	-	-	-	7.00	163	616	8.0	62	98.5 253.6
	2	7.29	509	520	8.0	59	99.4	345.2	3.12	163	810	8.0	60
	3	7.12	439	520	8.0	.5	96.4	353.8	-	-	-	-	-
	4	7.23	370	520	8.0	54	97.2	340.4	-	-	-	-	-
	5	7.36	328	520	8.0	54	97.1	325.4	-	-	-	-	-
100	1	-	-	-	-	-	-	9.61	163	596	8.0	258	98.5 248.5
	2	5.57	498	520	8.0	257	99.5	331.4	7.90	163	820	8.0	256
	3	5.61	443	520	8.0	242	97.5	333.0	5.63	163	810	8.0	241
	4	5.61	386	520	8.0	241	98.4	320.0	4.81	163	810	8.0	241
	5	9.61	343	520	8.0	240	98.4	307.1	4.37	163	820	8.0	240

CHAL REGEN COOLING

<u>F</u> (lbf)	<u>Pc</u> (psia)	<u>MR</u>	<u>L'</u> (in)	<u>T_{ox}</u> (°R)	<u>T_{RP-1}</u> (°R)	<u>E_C</u>	<u>E_{EL}</u>	<u>ERF</u> (%)	<u>I_{sp}</u> sec
1000	1000	2	7.08	672	640	8.0	22	99.9	343.9
100	500	2	3.41	715	561	16.75	7	95.7	322.4
100	400	2	3.17	714	552	13.1	7	94.6	317.7

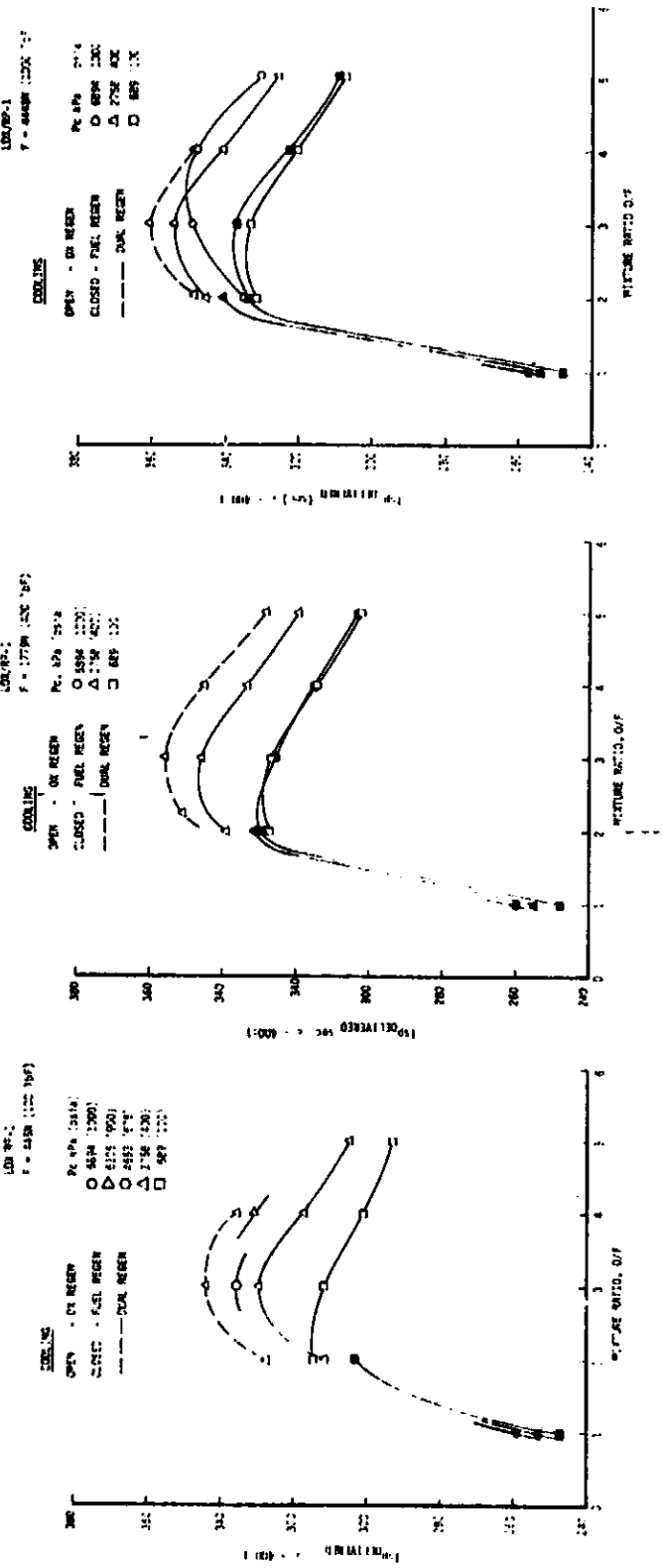


Figure 32. Delivered Performance Versus Mixture Ratio for 445N (100 lbF)

Figure 33. Delivered Performance Versus Mixture Ratio for 1779N (400 lbF)

Figure 34. Delivered Performance Versus Mixture Ratio for 4448N (1000 lbF)

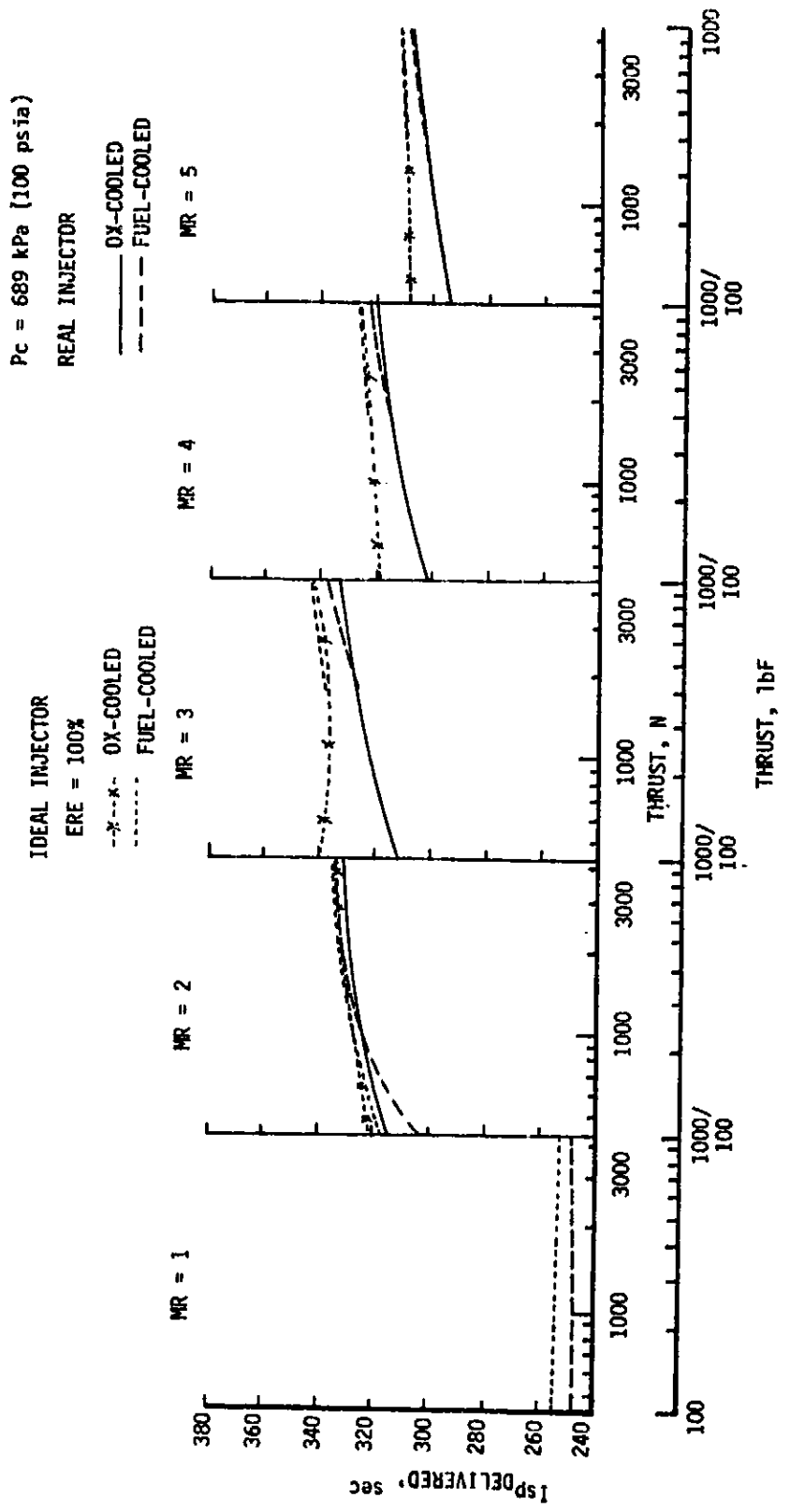


Figure 35. Delivered Performance Versus Thrust for 689 kPa (400 psia) Chamber Pressure

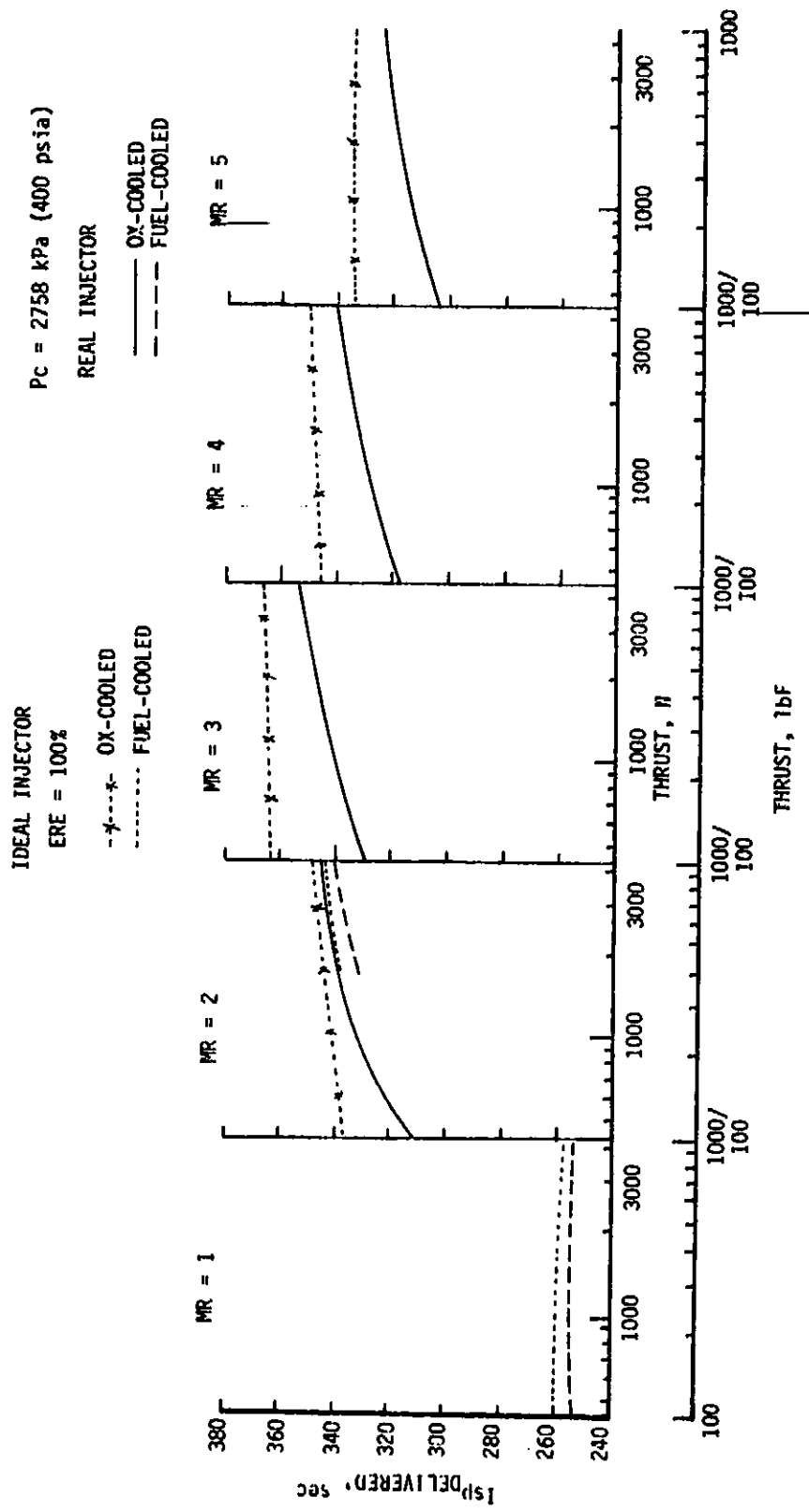


Figure 36. Delivered Performance Versus Thrust for 2758 kPa (400 psia) Chamber Pressure

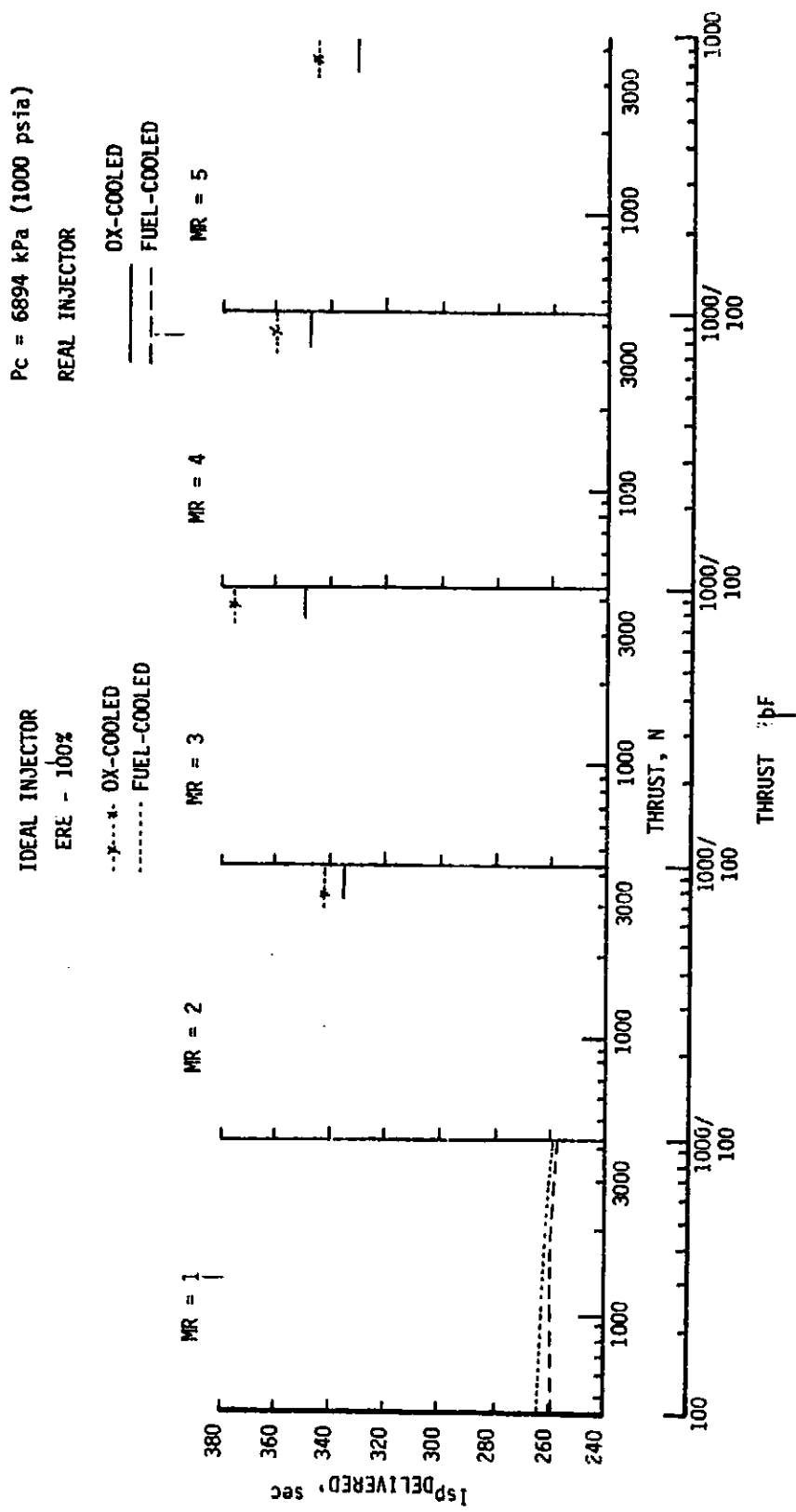


Figure 37. Delivered Performance Versus Thrust for 6894 kPa (1000 psia) Chamber Pressure

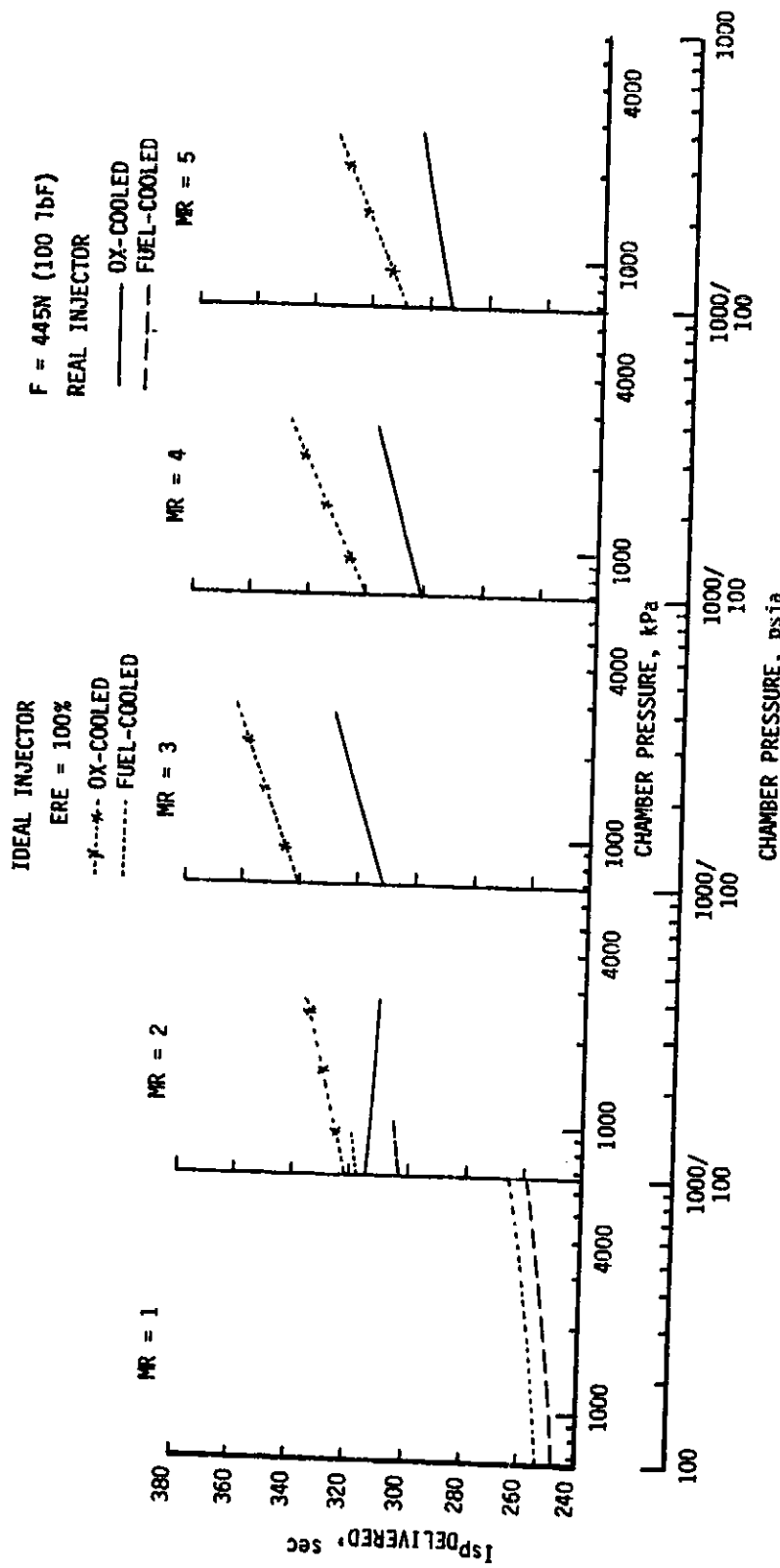


Figure 38. Delivered Performance Versus Chamber Pressure for
445 N (100 lb Thrust)

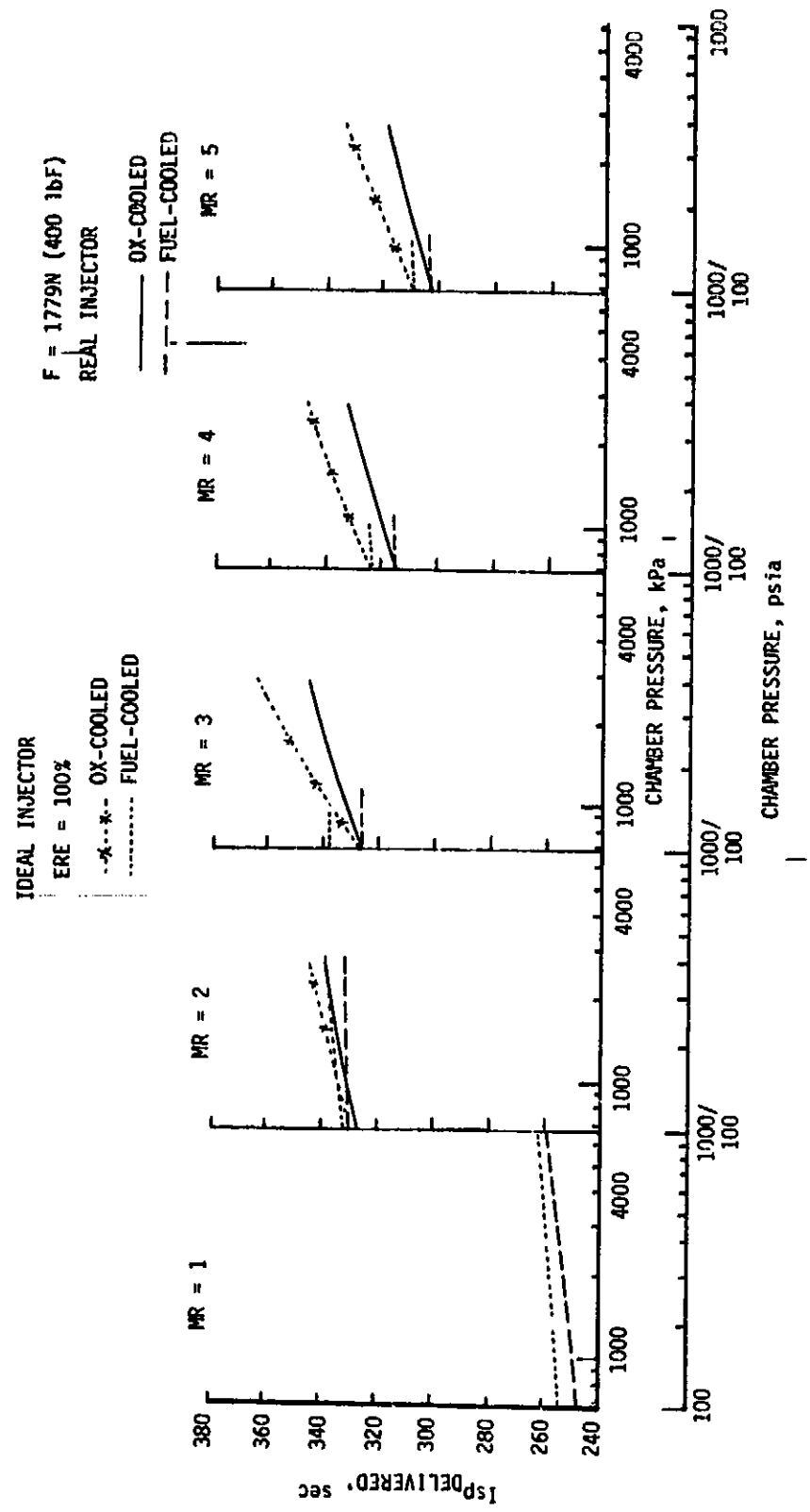


Figure 39. Delivered Performance Versus Chamber Pressure for 1779 N (400 lb Thrust)

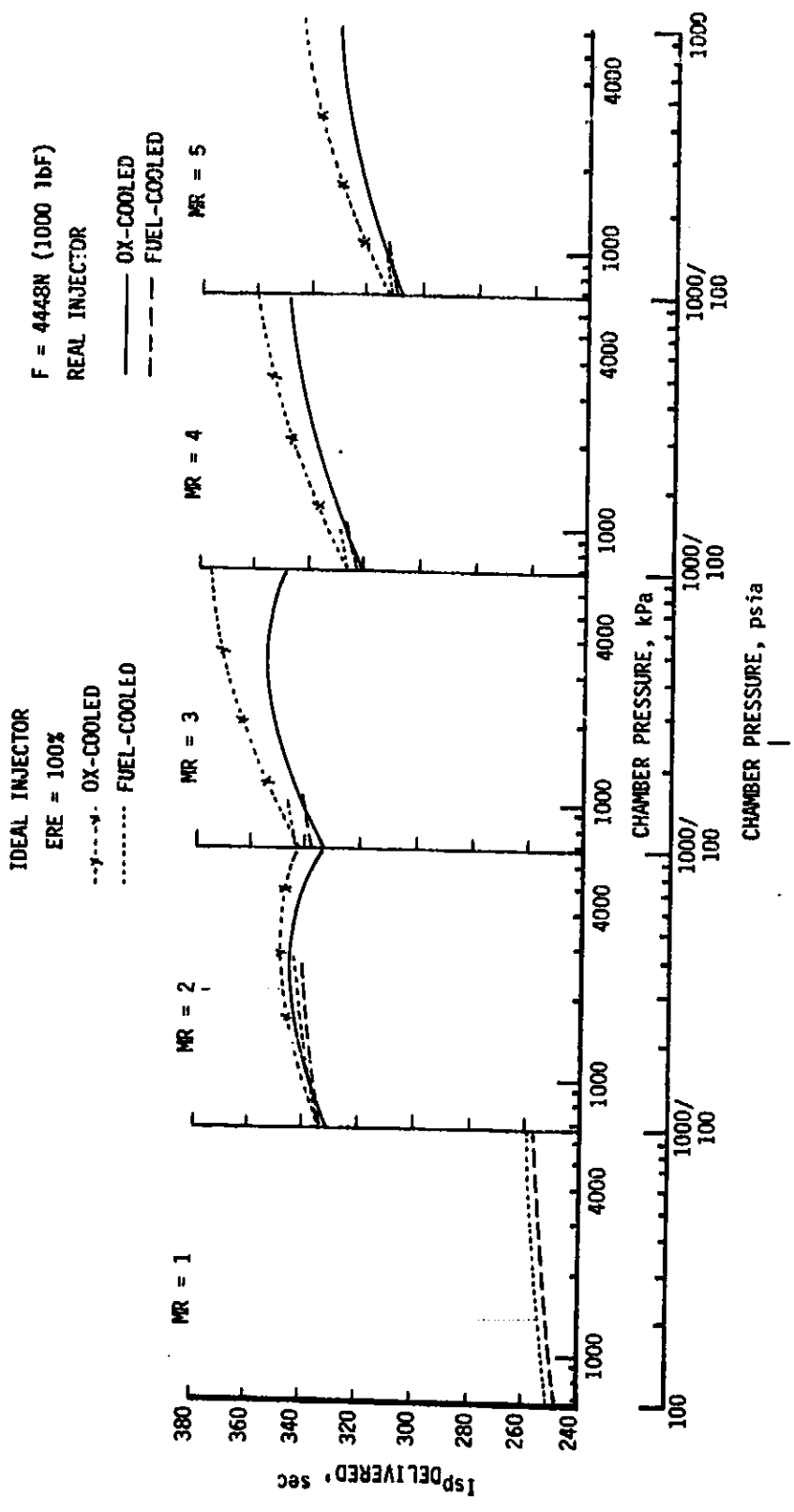


Figure 40. Delivered Performance Versus Chamber Pressure for 4448 N (1000 lb Thrust)

TABLE IX
MAX. PERFORMANCE SINGLE-REGEN COOLING

4448 (1000)	MR = 3.0 Fuel Regen Isp = 337	MR = 3.0 Ox Regen Isp = 354	MR = 3.5 Ox Regen Isp = 351
1779 (400)	MR = 2.0 Fuel Regen Isp = 330	MR = 3.0 Ox Regen Isp = 346	MR = 1.0 Fuel Regen Isp = 260*
445 (100)	MR = 2.0 Ox Regen Isp = 315	MR = 3.0 Ox Regen Isp = 330	** MR = 1.0 * Fuel Regen Isp = 259
	689 (100)	2758 (400)	6894 (1000)

Chamber Pressure, kPa (psia)

*Only MR considered where cooling solution was found

** p_c at max Isp = 4653 kPa (675 psia), Isp = 336, MR = 3.0
with Ox-regen cooling

III, C, Performance Sensitivity (cont.)

- Performance also decreases at mixture ratios greater than 3.0, except for the 4448N/6894 kPa (1000 lbF/1000 psia) (F/Pc) case.
- Fuel-regenerative cooling is only attractive from a performance standpoint at low chamber pressure 689 kPa (100 psia) and mid [1779N (400 lbF)] to high [4448N (1000 lbF)] thrust levels, with attainable peak Isp values of 330-340 seconds. At other conditions, the chamber L' that is dictated by cooling requirements is too short for reasonable combustion efficiency.
- Oxidizer regeneratively cooled engines can be designed for use in an O/F range from 2 to 5 and a thrust range from 445-4448N (100-1000 lbF) at chamber pressures from 689-2758 kPa (100-400 psia), with attainable peak Isp values of 315 to 354 seconds.
- High [6894 kPa (1000 psia)] chamber pressure operation is possible with oxidizer or dual-regenerative cooling, but only at higher thrust levels (~4448N/1000 lbF). The attainable Isp for this case is 360 seconds.
- Further improvements in performance are attainable through injector designs which provide either more or more efficient elements.

1. Performance Model

The predicted delivered specific impulse (I_{spDEL}) was obtained by calculating the influence of the known mechanisms that degrade the ideal (I_{spODE}) performance. These efficiencies/loss mechanisms were divided into five major categories: energy release efficiency (η_{ERE}), reaction kinetics efficiency (η_K), two-dimensional divergence efficiency (η_{2D}), loss due to the thrust decrement within the boundary layer, and loss due to film cooling.

A computer program had previously been developed to help facilitate parametric analysis by representing each loss mechanism in a subroutine with the appropriate data base.

During Task I, a Priem vaporization model and an empirical mixing loss correlation for LOX/RP-1 were incorporated into a subroutine which enabled the ERE to be internally calculated. The vaporization model was calibrated using data from the NASA-LeRC OFO triplet engines (NASA TM 79319). I_{spODE} and I_{spOK} data were obtained through the Two-Dimensional Kinetics Program (TDK), Reference 4, and were tabulated over a range of conditions that would encompass those desired for this program.

III, C, Performance Sensitivity (cont.)

The kinetic efficiency was obtained by comparing the one-dimensional kinetic specific impulse (I_{sp00K}) to the I_{spODE} ($\eta_K = I_{sp00K}/I_{spODE}$). The two-dimensional efficiency was obtained from charts which gave the η_{2D} for optimum Rao nozzles, as described in Reference 5. These charts were then tabulated to facilitate their use in the performance program. The performance loss due to boundary layer development was obtained by implementing the turbulent boundary layer chart procedures also given in Reference 5. These procedures were modified to incorporate the results of the BLIMP analysis performed in Task I. The boundary layer efficiency was calculated by assuming an adiabatic wall and propellants at the tank enthalpy. Past analyses had shown this approach to be quicker, and to result in the same efficiency as the more rigorous method of calculating the enthalpy loss to the regen coolant, than finding a new I_{spODE} by using the increased propellant enthalpy.

The performance model used also included a subroutine to calculate film-cooling efficiency, if required. The film-cooling efficiency was calculated by ratioing the mass-weighted performance for the core and coolant stream tubes by the performance at the injector mixture ratio. The performance mathematical modeling (loss accounting), shown in Figure 41, is consistent with the JANNAF simplified procedures specified in CPIA 246. Design and operating guidelines were based on previous task investigations and are shown in Figure 42.

2. Attainable Isp for RP-1 Regenerative Cooling

Fuel-regenerative cooling can be successfully applied to most operating points involving low chamber pressure and mid to high thrust. At low mixture ratio ($MR = 1$), fuel-regenerative cooling may be used over the entire chamber pressure and thrust range; however, the attainable delivered specific impulse is low (247 to 260 sec).

When using fuel-regenerative cooling at low chamber pressure and mixture ratios greater than 1, short combustion chamber lengths (L') are required to limit the propellant heat pickup in order to prevent coking in the cooling channels. These short chamber lengths limit performance by restricting the time for fuel vaporization, even when consideration is given to the effect of hot RP-1 (450°K/350°F) supplied to the injector. The allowable regeneratively cooled length, and hence engine L' , tend to increase with increasing thrust. As can be seen in Figure 35, this results in improved performance at higher thrust. At a mixture ratio of 2, increasing thrust from 445 to 4448N (100 to 1000 lbF) improved performance by 10%; increasing thrust from 445 to 4448N (100 to 1000 lbF) increased performance 3.5% and 1.7% at mixture ratios of 3 to 5, respectively. At a mixture ratio of 1, fuel-regenerative coolant proved to be the only viable cooling scheme.

- Loss allocation is consistent with JANNAF techniques
- Geometric sum of efficiencies multiplied by ODE Isp equals delivered Isp.

$$Isp_{DEL} = Isp_{ODE} \cdot \frac{\eta_{DIV}}{\eta_{f_inj}} \left\{ \eta_{EL} \cdot \eta_{MIX} \cdot \eta_{KIN} \cdot \eta_{VAP} \cdot \eta_{HL} \cdot \eta_{FC} - (1 - \eta_{BL}) \right\}$$

where

η_{DIV} = Divergence efficiency

η_{EL} = Mixing efficiency
MIX

η_{KIN} = Kinetic efficiency

η_{VAP} = Vaporization efficiency

η_{HL} = Heat loss (gain) efficiency

η_{FC} = Film cooling efficiency

η_{BL} = Boundary layer efficiency

Figure 41: Performance Mathematical Modelling (Loss Accounting)

- GEOOMETRY
 - MINIMUM CHAMBER DIAMETER = 3.81 cm (1.5 in.)
 - MINIMUM INJECTOR ORIFICE DIAMETER = 0.025 cm (0.010 in.)
 - INJECTION ELEMENT DENSITY = 6 ELEMENTS/IN.²
 - ELEMENT TYPE - OFO TRIPLET
 - 3.23 cm² (0.5 in.²) IGNITER AREA IN CENTER OF INJECTOR
 - 85% BELL NOZZLE

- OPERATING
 - INJECTOR PRESSURE DROP = $P_c^{0.75}$
 - VAPORIZATION AND MIXING LIMITED COMBUSTION EFFICIENCY
 - 0.2% CLOSURE ON PERFORMANCE ITERATION LOOPS
 - COOLING LOSS MODEL CONSISTENT WITH HEAT TRANSFER ASSUMPTIONS USING MASS-WEIGHTED FILM-COOLING AND CORE STREAM TUBES
 - ALL OTHER LOSSES AS DEFINED IN SIMPLIFIED PROCEDURE OF CPIA 246

Figure 42. Guidelines from Preliminary Investigations

III, C, Performance Sensitivity (cont.)

At this mixture ratio, performance was effectively constant over the entire thrust range but averaged 20-25% lower than that of the higher-mixture-ratio, oxidizer-cooled cases.

As seen in Figures 35, 36, and 37, fuel-regenerative cooling at mixture ratios of 2 and above does not offer any significant performance advantage over oxidizer-regenerative cooling and is only viable over limited ranges of low chamber pressure, high thrust, and mixture ratio. This same conclusion is evident from the cross-plotted data of Figures 38 through 40.

Use of a thermal liner in the cylindrical chamber allows for increases in the chamber length for the same total fuel heat pickup and thereby provides some performance improvement at low thrust. Performance data for chambers with and without a thermal liner are presented in Table X.

Inclusion of a chamber thermal liner improved performance from 7% for the low-thrust case to less than 0.3% at high thrust. The liner impacts performance less at high thrust because the original L' is in the asymptotic region of the ERE-versus- L' curve. Task I parametrics indicated the "knee" of the ERE-versus- L' curve to be at approximately 10.16 cm (4 in.), as shown in Figure 43.

3. Attainable Isp for Oxygen Regenerative Cooling

The thermal analyses determined that oxidizer regeneratively cooled engines are feasible except in the highest-Pc, low- to mid-thrust range. Generally, the cooling properties of oxygen allowed longer and larger chamber lengths and increased residence time for propellant vaporization. However, the lack of fuel preheating with oxidizer-only cooling slows the fuel vaporization and reduces the delivered performance. For the low-Pc, mid-regenerative cooling was within 1% of that for fuel-regenerative cooling (see Figures 33 and 34).

The oxidizer cooling results, shown in Figure 35, indicate that, at low P_c , performance will increase 5 to 7% as thrust is increased from 445 to 4448N (100 to 1000 lbF). A 7 to 11% performance increase is indicated for the mid-Pc condition (2758 kPa/400 psia) as can be seen from Figure 36. This increase in performance with increasing thrust is again due to increases in engine chamber L' . The limited applicability of regeneratively cooled concepts at high P_c (6894 kPa/1000 psia) is illustrated by the data contained in Figure 37. These data show that oxidizer-regenerative cooling can only be used in the 3558-4448N (800-1000 lbF) thrust range at $P_c = 6894$ kPa (1000 psia).

TABLE X
THERMAL LINER INFLUENCE ON PERFORMANCE

F N (1bF)	Pc kPa (psia)	MR	Without Liner		With Liner		Δ Isp %
			L' cm (in.)	Isp	L' cm (in.)	Isp	
445 (100)	689 (100)	2.0	4.06 (1.60)	303.4	10.80 (4.25)	325.2	7.2%
1779 (400)	2758 (400)	2.0	6.04 (2.38)	331.3	10.80 (4.25)	342.3	3.3%
	689 (100)	2.0	10.77 (4.24)	330.1	14.83 (5.84)	331.3	0.4%
		3.0	7.49 (2.95)	325.7	14.83 (5.84)	333.9	2.5%
		4.0	7.44 (2.93)	315.1	14.83 (5.84)	320.4	1.7%
		5.0	7.42 (2.92)	303.5	14.83 (5.84)	307.5	1.3%
4448 (1000)	689 (100)	3.0	14.30 (5.63)	337.1	18.31 (7.21)	337.5	0.1%
		4.0	12.22 (4.81)	322.3	18.31 (7.21)	323.2	0.3%
		5.0	11.71 (4.61)	308.8	18.31 (7.21)	309.6	0.3%

2224N (500 lbf), 276 to 5515 kPa (40 to 80 psia), MR 2.0 and 4.0

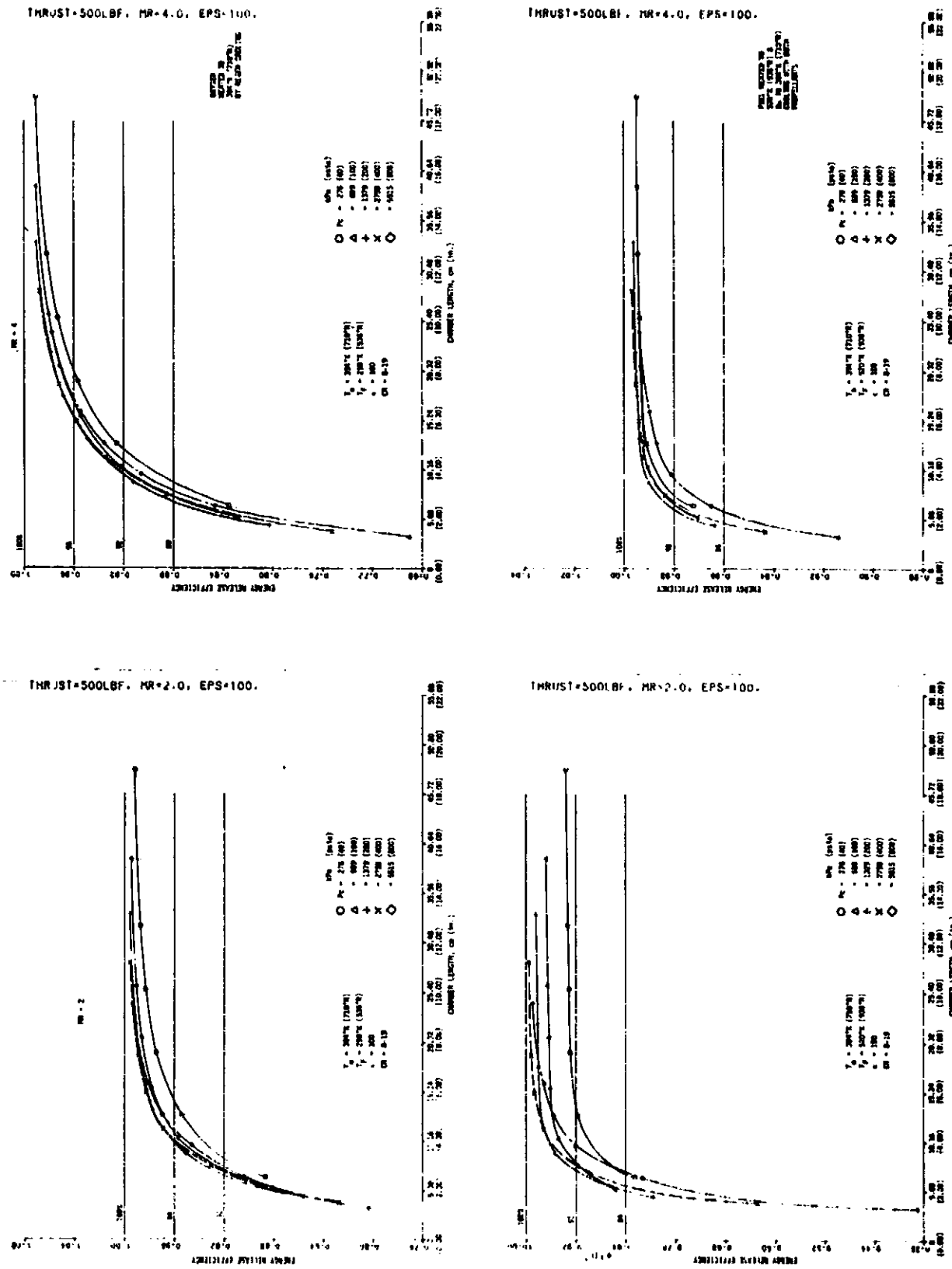


Figure 43. Energy Release Efficiency Sensitivity

III, C, Performance Sensitivity (cont.)

The wider applicability range of oxidizer as opposed to fuel regeneratively cooled engines is evident in the data presented in Figures 35 through 40. In general, the performance of an oxidizer regeneratively cooled engine tends to increase with increasing chamber pressure and thrust level. As shown in Figure 40, an exception to this trend is at the highest thrust level (4448N/1000 lbF) where the peak performance, for some mixture ratios, is achieved at chamber pressures of 2758-4136 kPa (400-600 psia). This peak performance for the high-thrust case occurs at less than the maximum chamber pressure due to the mixing and vaporization influences on the energy release efficiency which evolve from the element density and contraction ratio design criteria selected.

As P_c increases, the throat area decreases and, since a constant contraction ratio (8.0) is used, chamber diameter and the number of injector elements also decrease. The chamber diameter ranges from 17.8 cm (7 in.) at $P_c = 689$ kPa (100 psia) to 5.08 cm (2 in.) at $P_c = 6894$ kPa (1000 psia). At these small chamber diameters, fringe effects with their detrimental influence on mixing efficiency become more predominant. Thus, the ERE decreases, resulting in lower performance at high P_c . This trend is also evident in the data of Figure 34. In future analyses, an alternate approach could be to increase contraction ratio with chamber pressure.

4. Attainable Isp for Dual-Propellant Regenerative Cooling

At several operating points, regenerative cooling with a single coolant (either oxidizer or fuel) was not practical, or the allowable chamber L' was too short. To operate efficiently at these conditions, both propellants (dual-regenerative cooling) are needed to cool the engine. Performance was predicted for the three dual-regenerative cases given in Table VIII. As can be seen, dual-regenerative as opposed to oxidizer-regenerative cooling increases performance by 2% for the low-thrust, mid- P_c case and by 3% for the high-thrust, high- P_c case. These increases in performance result from increases in allowable engine L' and fuel injection temperature; both effects increase fuel vaporization efficiency.

The above results indicate that performance will benefit from heating the fuel when oxidizer-regenerative cooling is used. Additional studies were performed to determine how much the performance could be improved by heating the fuel for selected maximally-performing oxidizer-regenerative cases. Table XI lists the results of this analyses. For the low-thrust cases, performance improved 5 to 6%, depending on mixture ratio, over the oxidizer-only cooling cases. At high thrust, the performance improved 1% to 2%.

TABLE XI
 PERFORMANCE COMPARISON BETWEEN OXYGEN-
 REGENERATIVE AND DUAL-REGENERATIVE COOLING.

<u>N (lbF)</u>	<u>F kPa (psia)</u>	<u>MR</u>	<u>Isp</u>	<u>Isp</u>	<u>ΔIsp %</u>
			<u>Ox Regen</u>	<u>Dual Regen*</u>	
445 (100)	2758 (400)	2	311.2	-326.9	5%
		3	329.5	344.8	5%
		4	316.9	336.0	6%
1779 (400)	2758 (400)	2	338.9	344.2	2%
		3	345.8	355.6	3%
		4	333.1	344.8	4%
4448 (1000)	2758 (400)	2	345.2	347.0	1%
		3	353.8	360.5	2%
		4	340.4	347.4	2%
		5	325.4	331.4	2%
	
4448 (1000) 6894 (1000)	2758 (400)	2	334.8	340.9	2%
		3	348.9	354.8	2%
		4	347.5	352.6	1%
		5	330.1	334.7	1%
	

*Assumed Fuel Temperature Equaled 422°K (300°F)

III, C, Performance Sensitivity (cont.)

For these cases, the fuel temperature was assumed to be 422°K (300°F). Heat required to raise the fuel temperature was assumed to be obtainable by running the fuel through the nozzle skirt which would ordinarily be radiation-cooled. Further analyses need to be done on the thermal feasibility of this approach and on the weight penalties which may be incurred.

5. Performance Summary for LOX/RP-1

Significant performance advantages have been identified as being attainable when oxygen regenerative cooling is considered. The oxygen cooling eliminates the need for extensive fuel film-cooling and the associated loss in performance identified in previous studies. In past cases, the film-cooling requirements were dictated by the cold [561°K (550°F)] chamber walls needed to prevent coking.

Further improvements in attainable Isp (up to 5%) have been identified for the dual-regenerative cooling concept over oxidizer-only cooling.

The above conclusions are unique to low-thrust, high-pressure engines. The results are heavily influenced by the design criteria selected for chamber contraction ratio, element size, and density.

The resulting unusually large contraction ratios (ϵ_c = 8 to 30), and the known but not fully predictable interaction of ϵ_c on mixing efficiency, gas-side soot deposition, and the gas-side heat transfer coefficient, make experimental verification of these analyses mandatory.

IV. RESULTS OF PARAMETRIC STUDIES FOR LOX/HYDROGEN

A. SUMMARY

This section documents the LO₂/hydrogen portion of the Task IV analyses to determine the extent of applicability of regenerative cooling for LO₂/LH₂ engines at thrust levels ranging from 445 to 4448N (100 to 1000 lbF), chamber pressures from 689 to 6894 kPa (100 to 1000 psia), and mixture ratios from 2 to 8. The primary effort considered NBP propellants. A limited evaluation was also made of the effect of added enthalpy from a source external to the engine system for LO₂/LH₂.

Delivered specific impulse values were computed for $e = 400:1$ using simplified JANNAF techniques and included the effects on energy release efficiency of propellant vaporization and mixing defined in Appendix A. All performance values were based upon specific engine designs and configurations which were found to be viable on the basis of the above thermal analyses.

As in Task III, either single-propellant or dual-propellant cooling could be utilized, and channel fabrication technology was not limited by current capabilities.

The study results of the LO₂/LH₂ propellant system show that hydrogen cooling is feasible over the complete thrust/chamber pressure region of interest. For the most part, channel design parameters require only modest advancements in fabrication technology.

Enthalpy addition of the LO₂/LH₂ results in an additional but manageable thermal load to the hydrogen regenerative coolant. The additional energy results in a need for narrower cooling channels but improves the specific impulse up to 2.3% at an MR of 8 and 16.5% at an MR of 2.

B. THERMAL DESIGN

1. Scope and Analytical Basis

The analytical design methodology employed in Task III for the LO₂/RP-1 system (documented in Appendix A) was utilized in continuing the design studies for LO₂/LH₂.

The study envelope for the LO₂/LH₂ analyses was as follows:

$$\text{Engine Thrust, } F \quad - \quad 445\text{N (100 lbF)} \leq F \leq 4448\text{N} \\ (1000 lbF)$$

IV, B, Thermal Design (cont.)

Chamber Pressure, P_c - $689 \text{ kPa (100 psia)} \leq P_c \leq 6894 \text{ kPa}$
(1000 psia)

Mixture Ratio, O/F - $4 < MR < 8$ NBP Propellants
 $2 \leq MR \leq 8$ Heated Propellants

Chamber Material - Zirconium-Copper Alloy

Performance parameters, design guidelines, and thermochemical/gas dynamic parameters were the same as discussed in Section III.B.1, except for design guidelines specific to hydrogen.

- Coolant Pressure Drop

LO_2 and $\text{LH}_2 \Delta P \leq 1724 \text{ kPa (250 psia)}$

- Maximum Bulk Temperature

$\text{LO}_2 \quad T_b \leq 394^\circ\text{K (250°F)}$

$\text{LH}_2 \quad$ None directly (outlet temperature limited only by ΔP)

- Maximum Gas-Side Wall Temperature

LO_2 and $\text{LH}_2 \quad T_{wg} \leq 811^\circ\text{K (1000°F)}$

- Maximum Coolant-Side Wall Temperature

$\text{LO}_2 \quad T_w \leq 589^\circ\text{K (600°F)}$

$\text{LH}_2 \quad$ None directly

The pressure drop limitation was based on power-balance considerations for typical engine cycles. The coolant bulk temperature limit for oxygen was based on the reaction rates for copper oxidation. Hydrogen was not assigned a bulk temperature limit as a coolant. The gas-side copper wall temperature was limited to values consistent with a cycle life of 20 cycles and long hold-times at operating temperature. Copper oxidation was the sole constraining factor on coolant-side wall temperature.

2. Analysis Methodology

For the LO_2/LH_2 coolant combination, it was anticipated that cooling with hydrogen would be feasible over the entire F- P_c range of

IV, B, Thermal Design (cont.)

interest and that no recourse to oxygen cooling would be necessary. This pre-assessment of cooling capabilities led to the following logic for the performance of the thermal analysis:

a. The LO₂/LH₂ system was analyzed at three values of thrust [445, 1779, and 4448N (100, 400 and 1000 lbF)] for each of three mixture ratios (4, 6, and 8) and each of three chamber pressures [689, 2758, and 6894 kPa (100, 400, and 1000 psia)]. These analyses were performed for "single-regen" cooling with hydrogen as the coolant. The chamber was assumed to be regeneratively cooled from the point at which a radiation-cooled nozzle extension can be attached (or from an area ratio of 6:1 if the attach point ratio is less than 6:1) to the injector in a single-pass counterflow configuration.

b. In the event hydrogen could not be demonstrated as a feasible regenerative coolant at any design point noted above, analyses with oxygen as the coolant would be performed. "Dual-regen" cooling, defined as using both propellants as coolants in series, was to be utilized only if cooling with a single propellant proved to be unfeasible.

3. Hydrogen Regenerative Cooling Results

As anticipated, hydrogen was shown to be a feasible coolant over the complete F-Pc range of interest, thus no analyses for oxygen cooling were performed. Selected input data and calculated results for cooling with hydrogen are given in Table XII. (Table nomenclature is defined in Table VI.) Significant results are displayed in Figures 44 through 55. Data points not shown in complete detail in this thermal section had been found to be completely feasible in prior studies (Ref. 1) with the use of existing technology. For example, in Figure 44, the two lower operating pressures have low ΔP values and utilize standard channel sizes. The highest ΔP represents a design point which has been made possible by the use of a larger contraction ratio and smaller channels.

a. Coolant Pressure Drop

Cooling channel pressure drops for NBP hydrogen as a single-regen coolant are shown in Figures 44 through 46 as a function of mixture ratio for thrusts of 4448, 1779, and 445N (1000, 400, and 100 lbF), respectively. Pressure drop is low, even at the highest pressure and low thrust, and is relatively insensitive to thrust. The maximum ΔP occurs at a mixture ratio of 6; however, all values calculated are acceptable.

TABLE XII

SELECTED PARAMETERS CHARACTERIZING EN
COOLING WITH NBP HYDROGEN WITH LO₂

(Single Regen)

Code	MR	F N	P _c kPa	Coolant	P _{in} kPa	P _{in} /P _c	t _{wall} cm	CR	C _F **	Isp** sec	d/w*	L' cm	r _t cm	r _{ch} cm	e _A	ΔP kPa	T _b , in °K
4-1-1/F	4	445	689	F	2068	3.000	0.76	8.00	1.8223	440.7	4,2	17.98	1.062	3.002	6.00	0.69	22.3
4-1-4/F		2758	F	3894	1.412	0.076	12.90	1.8268	444.3	6,3		13.08	0.531	1.905	18.26	27.6	23.3
4-1-10/F		6894	F	9479	1.375	0.0635	33.28	1.8673	455.2	4		10.59	0.332	1.912	45.99	58.6	28.6
4-4-4/F	1779	2758	F	3894	1.412	0.76	8.00	1.8536	450.8	4		17.98	1.052	2.977	11.32	7.58	23.3
4-4-10/F		6894	F	9479	1.375	0.0635	8.32	1.8792	458.1	4		14.55	0.660	1.908	33.50	45.5	28.6
4-10-10/F	4448	6894	F	9479	1.375	0.0635	8.00	1.8813	458.6	4		17.98	1.044	2.954	46.86	68.9	28.6
6-1-1/F	6	445	689	F	2068	3.000	0.76	8.0	1.9494	439.4	4,2	17.98	1.026	2.903	6.00	2.07	22.3
6-1-4/F		2758	F	3894	1.412	0.76	14.06	1.9504	446.4	6		13.08	0.513	1.923	26.30	8.27	23.3
6-1-4/F		2758	F	3894	1.412	0.76	14.06	1.9504	446.4	4		13.08	0.513	1.923	26.30	14.5	23.3
6-1-10/F		6894	F	9479	1.375	0.0635	35.15	1.9891	459.1	4		10.59	0.322	1.905	65.42	173.7	28.6
6-4-4/F	1779	2758	F	3894	1.412	0.76	8.00	1.9783	452.8	4		17.78	1.019	2.883	16.72	8.27	23.3
6-4-10/F		6894	F	9479	1.375	0.0635	9.00	2.0012	461.9	4		14.55	0.640	1.923	45.43	90.3	28.6
6-10-10/F	4448	6894	F	9479	1.375	0.0635	8.00	2.0034	462.4	4		17.78	1.013	2.863	59.80	72.4	28.6
8-1-1/F	8	445	689	F	2068	3.000	0.76	8.00	1.9936	416.2	4	17.78	1.016	2.870	6.00	0	22.3
8-1-4/F		2758	F	3894	1.412	0.76	14.20	2.0085	427.0	4		13.08	0.505	1.905	23.97	8.96	23.3
8-1-10/F		6894	F	9479	1.375	0.0635	36.51	2.0663	443.9	4		10.59	0.315	1.905	61.68	159.9	28.6
8-4-4/F	1779	2758	F	3894	1.412	0.76	8.00	2.0377	433.2	4		17.78	1.003	2.840	15.28	5.51	23.3
8-4-10/F		6894	F	3894	1.375	0.0635	9.00	2.0784	446.5	4		14.55	0.629	1.887	42.69	72.4	28.6
8-10-10/F	4448	6894	F	3894	1.375	0.0635	8.00	2.0802	446.9	4		17.78	0.993	2.809	54.63	48.9	28.6

*When two numbers are given, the first refers to throat d/w, while the second refers to barrel d/w

**Employed for propellant flowrate determination of throat sizing

EOLDONIC FRAME

TABLE XII

CHARACTERIZING ENGINE REGENERATIVE
HYDROGEN WITH LO₂/LH₂ PROPELLANTS

(Single Regen)

Page 1 of 2
Metric Units

ΔP kPa	T _b , in °K	T _{b,out} - °K	ΔT_b °K	h_g, max kw/m ² °K $\times 10^{-3}$	Q _{g, max} kw/m ²	Q _{c, max} kw/m ²	Aspect Ratio d/w	Throat w/d cm/cm	Throat w/d cm/cm	No. of Channels
0.69	22.3	256	233	2924	5965	1030		0.1438/0.575	0.2654/0.737	55
27.6	23.3	287	263	8148	20,362	4559		0.0439/0.264	0.0493/0.295	75
58.6	28.6	276	245	19,503	41,819	19,823		0.0424/0.169	0.1562/0.625	23
7.58	23.3	202	178	6854	14,446	5393		0.0940/0.376	0.2037/0.815	72
45.5	28.6	247	216	14,884	32,014	11,848		0.0876/0.351	0.140/0.559	30
68.9	28.6	225	195	28,004	59,877	27,046		0.1013/0.405	0.2029/0.798	42
2.07	22.3	336	314	2492	6128	1030		0.1138/0.455	0.1140/0.137	63
8.27	23.3	402	379	8707	22,437	4788		0.0323/0.193	0.0970/0.582	84
14.5	23.3	402	379	8707	22,437	5867		0.343/0.137	0.1013/0.406	82
173.7	28.6	403	373	18,061	48,470	26,147		0.0299/0.120	0.1016/0.406	26
8.27	23.3	281	258	6236	16,064	4461		0.762/0.305	0.1527/0.610	80
90.3	28.6	345	315	12,943	34,841	20,052		0.0688/0.276	0.1006/0.401	33
72.4	28.6	310	280	20,209	53,880	21,212		0.0889/0.356	0.1491/0.597	44
0	22.3	349	327	2112	5180	850		0.1163/0.465	0.2068/0.828	62
8.96	23.3	426	404	7442	19,757	5066		0.0366/0.1466	0.0980/0.394	80
159.9	28.6	432	402	15,973	44,548	25,265		0.0284/0.1212	0.0955/0.381	26
5.51	23.3	299	276	5413	14,397	4151		0.0813/0.325	0.1529/0.612	77
72.4	28.6	373	343	11,413	31,899	17,421		0.0660/0.2644	0.0953/0.381	34
48.9	28.6	263	297	16,444	45,529	16,832		0.0899/0.360	0.1448/0.579	43

2
FOLDOUT FRAME

TABLE XII (cont.)

SELECTED PARAMETERS CHARACTERIZING EN
COOLING WITH NBP HYDROGEN WITH LO₂

(Single Regen)

Code	MR	F lbf	Pc psia	Coolant	P _{in} / psia	P _{in} /Pc	t wall in.	CR	C _F -	Isp** sec	d/w*	L' in.	r _t in.	r _{ch} in.	ε A	ΔP psi	T _b ,in °F	T _b °C
4-1-1/F	4	100	100	F	300	3.000	0.3	8.00	1.8223	440.7	4,2	7.08	0.418	1.182	6.00	0.1	-419.8	-40
4-1-4/F		400	F	564.8	1.412	0.3	12.90	1.8268	444.3	6,3	5.15	0.209	0.750	18.26	4.0	-418.0	56	
4-1-10/F		1000	F	1375	1.375	0.025	33.28	1.8673	455.2	4	4.17	0.131	0.753	45.99	8.5	-405.6	35	
4-4-4/F		400	400	F	564.8	1.412	0.3	8.00	1.8536	450.8	4	7.08	0.414	1.172	11.32	1.1	-418.0	-51
4-4-10/F		1000	F	1375	1.375	0.025	8.32	1.8792	458.1	4	5.73	0.260	0.751	33.50	6.6	-405.6	-11	
4-10-10/F		1000	1000	F	1375	1.375	0.025	8.00	1.8813	458.6	4	7.08	0.411	1.163	46.86	10.0	-405.6	-6
6-1-1/F	6	100	100	F	300	3.000	0.3	8.0	1.9494	439.4	4,2	7.08	0.404	1.143	6.00	0.3	-419.8	14
6-1-4/F		400	F	564.8	1.412	0.3	14.06	1.9504	446.4	6	5.15	0.202	0.757	26.30	1.2	-418.0	26	
6-1-4/F		400	F	564.8	1.412	0.3	14.06	1.9504	446.4	6	5.15	0.202	0.757	26.30	2.1	-418.0	26	
6-1-10/F		1000	F	1375	1.375	0.025	35.15	1.9891	459.1	4	4.17	0.127	0.750	65.42	25.2	-405.6	26	
6-4-4/F		400	400	F	564.8	1.412	0.3	8.00	1.9783	452.8	4	7.08	0.401	1.135	16.72	1.2	-418.0	46
6-4-10/F		1000	F	1375	1.375	0.025	9.00	2.0012	461.9	4	5.73	0.252	0.757	45.43	13.1	-405.6	16	
6-10-10/F		1000	1000	F	1375	1.375	0.025	8.00	2.0034	462.4	4	7.08	0.399	1.127	59.80	10.5	-405.6	96
8-1-1/F	8	100	100	F	300	3.000	0.3	8.00	1.9936	416.2	4	7.08	0.400	1.130	6.00	0.0	-419.8	16
8-1-4/F		400	F	564.8	1.412	0.3	14.20	2.0085	427.0	4	5.15	0.199	0.750	23.97	1.3	-418.0	30	
8-1-10/F		1000	F	1375	1.375	0.025	36.51	2.0663	443.9	4	4.17	0.124	0.750	61.68	23.2	-405.6	31	
8-4-4/F		400	400	F	564.8	1.412	0.3	8.00	2.0377	433.2	4	7.08	0.395	1.118	15.28	0.8	-418.0	78
8-4-10/F		1000	F	1375	1.375	0.025	9.00	2.0784	446.5	4	5.73	.248	0.743	42.69	10.5	-405.6	21	
8-10-10/F		1000	1000	F	1375	1.375	0.025	8.00	2.0802	446.9	4	7.08	0.391	1.106	54.63	7.1	-405.6	11

*When two numbers are given, the first refers to throat d/w, while the second refers to barrel d/w

**Employed for propellant flowrate determination and throat sizing

FOLDOUT FRAMES

TABLE XII (cont.)

CHARACTERIZING ENGINE REGENERATIVE
HYDROGEN WITH LO₂/LH₂ PROPELLANTS

Single Regen)

Page 2 of 2
English Units

AP psi	T _{b,in} °F	T _{b,out} °F	ΔT _b °F	h _{g,max}		Q _{g,max} Btu/in. ² -sec-°F x 10 ⁻³	Q _{c,max} Btu/in. ² -sec	Aspect Ratio d/w	Throat w/d in./in.	Throat w/d in./in.	No. of Channels
				Btu/in. ² -sec-°F	x 10 ⁻³						
0.1	-419.8	-0.1	419.7	0.994		3.65	0.63		0.0566/0.2263	0.1045/0.290	55
4.0	-418.0	56.2	474.2	2.77		12.46	2.79		0.0173/0.1040	0.0194/0.116	75
8.5	-405.6	35.9	441.5	6.63		25.59	12.13		0.0167/0.0667	0.0615/0.246	23
1.1	-418.0	-96.9	321.1	2.33		8.84	3.03		0.0370/0.1482	0.0802/0.321	72
6.6	-405.6	-16.3	389.3	5.06		19.59	7.25		0.0345/0.1380	0.0550/0.220	30
10.0	-405.6	-55.3	350.3	9.52		36.64	16.55		0.0399/0.1595	0.0799/0.314	42
0.3	-419.8	145.1	564.9	0.847		3.75	0.63		0.0448/0.1792	0.0449/0.054	63
1.2	-418.0	263.8	681.8	2.96		13.73	2.93		0.0127/0.0761	0.0382/0.229	84
2.1	-418.0	263.8	681.8	2.96		13.73	3.59		0.0135/0.0540	0.0399/0.160	82
25.2	-405.6	266.1	671.1	6.14		29.66	16.00		0.0118/0.0473	0.0400/0.160	26
1.2	-418.0	46.5	464.5	2.12		9.83	2.73		0.0300/0.1201	0.0601/0.240	80
13.1	-405.6	161.7	567.3	4.40		21.32	12.27		0.0271/0.1086	0.0396/0.158	33
10.5	-405.6	98.2	503.8	6.87		32.97	12.98		0.0350/0.1401	0.0587/0.235	44
0.0	-419.8	169.0	588.8	0.718		3.17	0.52		0.0458/0.1831	0.0814/0.326	62
1.3	-418.0	306.0	727.0	2.53		12.09	3.10		0.0144/0.0577	0.0386/0.155	80
23.2	-405.6	318.0	723.6	5.43		27.26	15.46		0.0112/0.0477	0.0376/0.150	26
0.8	-418.0	78.1	496.1	1.84		8.81	2.54		0.0320/0.1279	0.0602/0.241	77
10.5	-405.6	211.3	616.9	3.88		19.52	10.66		0.0260/0.1041	0.0375/0.150	34
7.1	-405.6	129.8	535.4	5.59		27.86	10.30		0.0354/0.1417	0.0570/0.228	43

FOLDOUT FRAME

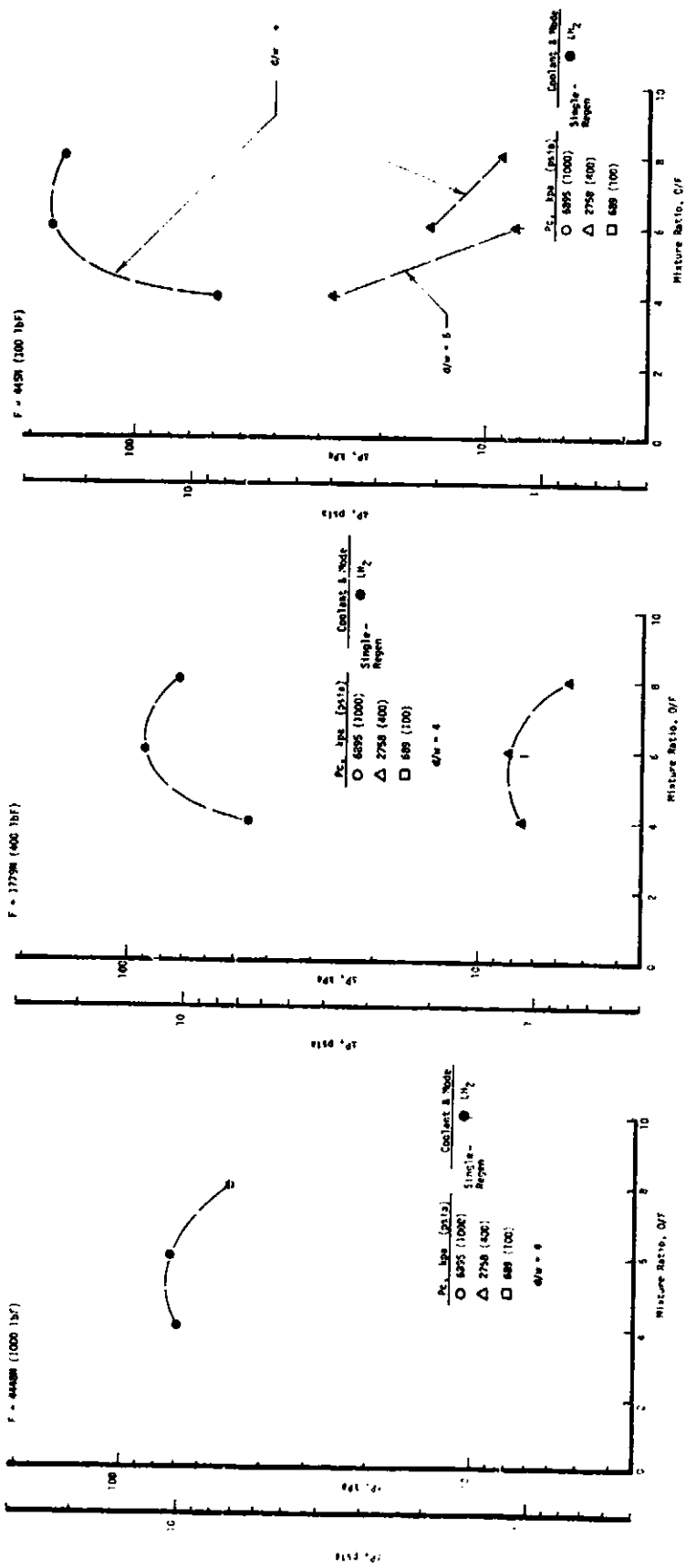


Figure 44. Coolant Pressure Drop for NBP Hydrogen Cooling Concepts,
 $F = 4448N$ (1000 lbf)

Figure 45. Coolant Pressure Drop for NBP Hydrogen Cooling Concepts
 $F = 1779N$ (400 lbf)

Figure 46. Coolant Pressure Drop for NBP Hydrogen Cooling Concepts
 $F = 445N$ (100 lbf)

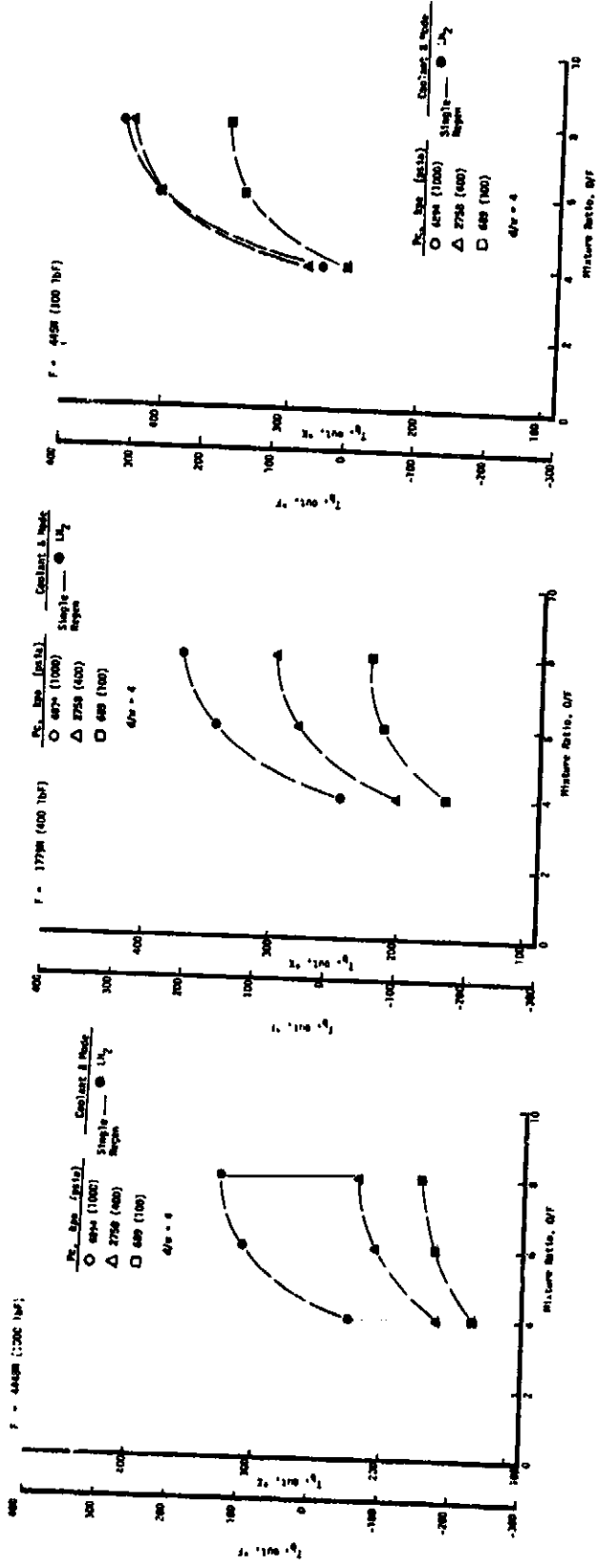


Figure 47. Coolant Discharge Temperature for NBP Hydrogen Cooling Concepts,
 $F = 4448N$ (1000 lbF)

Figure 48. Coolant Discharge Temperature for NBP Hydrogen Cooling Concepts,
 $F = 1779N$ (400 lbF)

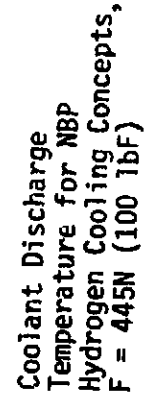


Figure 49. Coolant Discharge Temperature for NBP Hydrogen Cooling Concepts,
 $F = 445N$ (100 lbF)

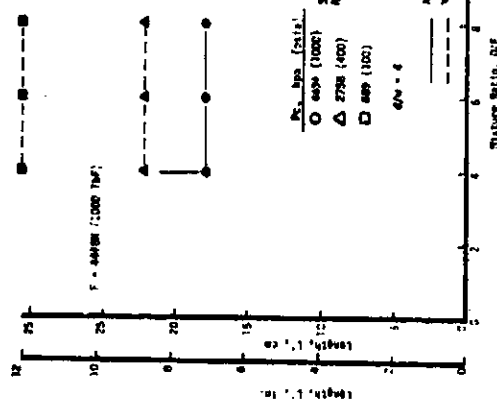


Figure 50. Minimum Chamber L' for NBP Hydrogen Cooling Concepts
 $F = 4448N$ (1000 lbf)

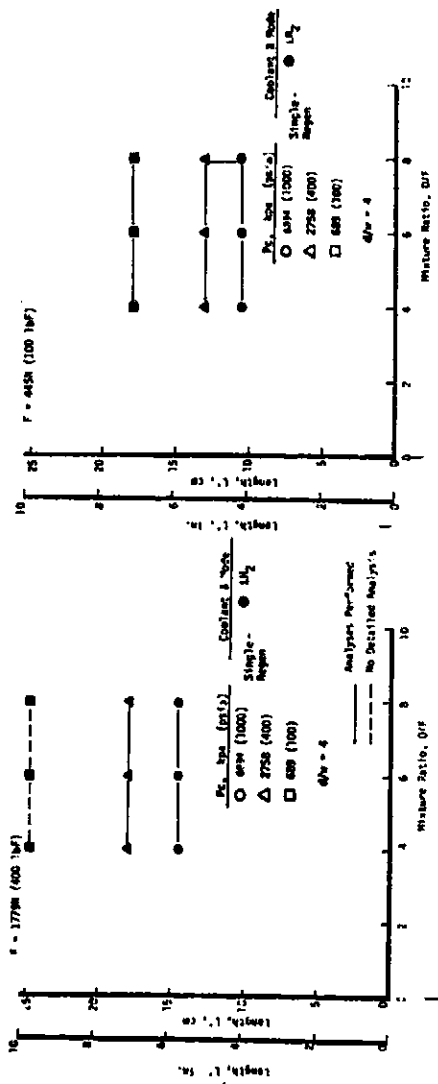


Figure 51. Minimum Chamber L' for NBP Hydrogen Cooling Concepts
 $F = 1779N$ (400 lbf)

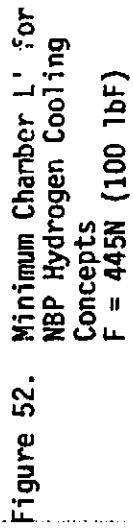


Figure 52. Minimum Chamber L' for NBP Hydrogen Cooling Concepts
 $F = 445N$ (100 lbf)

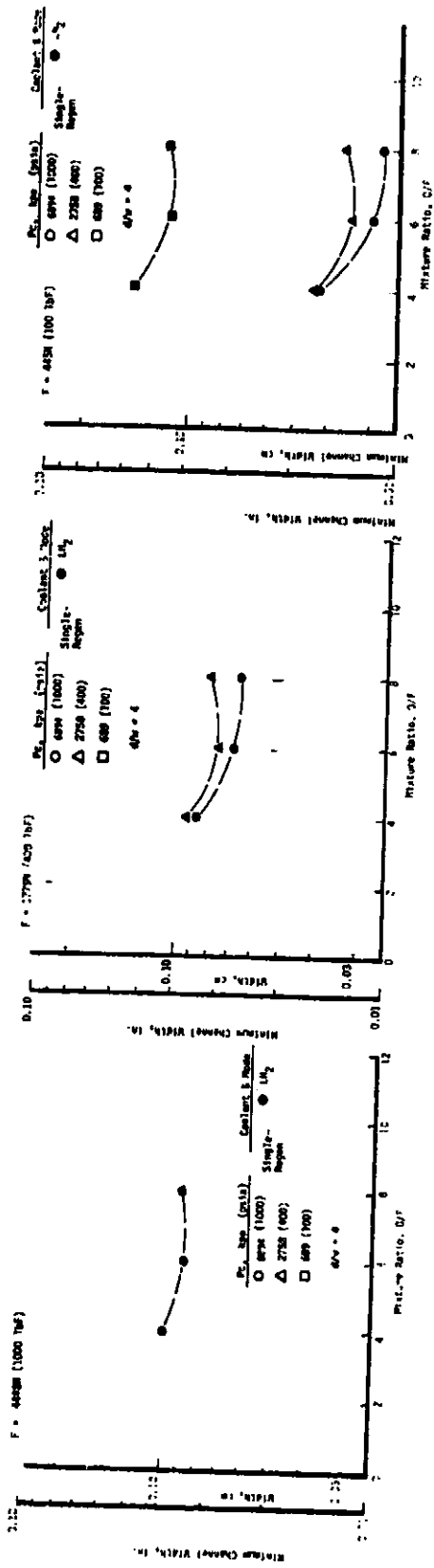


Figure 53. Minimum Coolant Channel Width Required for NBP Hydrogen Cooling Concepts, $F = 4448\text{N}$ (1000 lbf)

Figure 54. Minimum Coolant Channel Width Required for NBP Hydrogen Cooling Concepts, $F = 1779\text{N}$ (400 lbf)

Figure 55. Minimum Coolant Channel Width Required for NBP Hydrogen Cooling Concepts, $F = 445\text{N}$ (100 lbf)

Figure 55. Minimum Coolant Channel Width Required for NBP Hydrogen Cooling Concepts, $F = 445\text{N}$ (100 lbf)

IV, B, Thermal Design (cont.)

The data shown in Figure 46 illustrate the sensitivity of ΔP to channel aspect ratio (d/w) options for $P_c = 2758 \text{ kPa}$ (400 psia). Although the channel surface area (at the throat) increases by 31% if the aspect ratio is increased from 4:1 to 6:1, the total channel pressure drop decreases by 43%, largely as a result of lower coolant velocity 27.7 vs 36.1 m/s (90.8 vs 118.3 ft/sec) required at the higher aspect ratio. Since the coolant pressure drop was very small, no further attempts were made to minimize pressure loss. However, the trend is applicable to high-pressure systems where pressure drop becomes a limiting parameter.

b. Coolant Outlet Temperature

The temperature of the hydrogen discharged from the cooling jacket is displayed in Figures 47 through 49. This parameter is significant in that the energy level of the hydrogen is critical to those engine cycles using heated hydrogen as a turbine drive fluid. In this respect, the lower-thrust engines provide a higher outlet temperature fluid. In all cases, discharge temperature increased with chamber pressure. Since pressure drop is not limiting, the coolant temperature could be increased by adding chamber length to ensure a power-balanced expander engine cycle.

c. Chamber L'

Chamber L' requirements to meet minimum performance criteria are shown in Figures 50 through 52 for the three thrust levels studied. The required L' values decrease with increasing P_c and decreasing thrust and show no sensitivity to mixture ratio. The chambers are relatively long compared to those of the LO₂/RP-1 combination. Since bulk temperatures do not constrain L', even longer L' values may be advantageous to provide higher performance and higher temperature hydrogen as a turbine drive fluid. Detailed cooling analyses were not repeated where previous studies had already demonstrated cooling feasibility; instead, emphasis was placed on the high-pressure, low-thrust operating range where previous studies had failed to provide design solutions.

d. Channel Width

The results of earlier analyses, reported in References 1 through 3, showed that cooling with hydrogen was limited when conventionally sized chamber contraction ratios ($c_c = 3.3$) and channels (minimum width of 0.083 cm [0.032 in.]) were specified. Only the following design points showed cooling feasibility: (1) $F = 4448\text{N}$ (1000 lbF) at P_c 's of 689, 2758, and 6894 kPa (100, 400, and 1000 psia) at P_c 's of 689 and 2758 kPa (100 and 400 psia). Figures 53 through 55 show that minimum channel width

IV, B, Thermal Design (cont.)

increases as P_c decreases and thus substantiates the conclusions reached in the previous studies.

The minimum channel width, usually found at the maximum heat-flux point (at or near the throat station), is plotted in Figure 56 as a function of thrust for constant values of chamber pressure. The cross-plot in Figure 57 shows the coolable thrust and P_c design points possible for various channel widths greater than 0.025 cm (0.010 in.). The figure also shows the minimum channel widths at a mixture ratio of 6 for the study range of interest.

4. Effect of Added Enthalpy

The effect of added enthalpy from a "free" source was examined for the LO_2/LH_2 propellant system. Two cases were considered: first, it was assumed that energy was added to hydrogen alone; secondly, that energy was added to both hydrogen and oxygen to raise injector inlet temperature(s) to 922°K (1200°F) after the hydrogen supplied to the engine at NBP energy levels had cooled the chamber regeneratively. The design point for $F = 1779\text{N}$ (400 lbF) and $P_c = 2758 \text{ kPa}$ (400 psia) at a mixture ratio of 4 was selected for this analysis. Based on the results of the performance analyses, this mixture ratio was chosen to maximize the effect of enthalpy addition to hydrogen. The conclusions obtained are believed to be applicable to all other F , P_c , and MR combinations.

The results of these calculations are presented in Tables XIII and XIV. External heating of the hydrogen results in a 340°K (622°R) increase in the combustion temperature. Heating of the oxygen adds an additional 83°K (148°R) to the combustion temperature. Consequently, less than half the energy increase appears in temperature rise. The balance is absorbed in the dissociation to the ionic concentrations noted in Table XIII.

The increased energy level of the combustion gases results in a greater thermal load to the regenerative coolant, as shown in Table XIV. Pressure drop, though negligible, increases, as does the bulk temperature rise of the hydrogen. The flux levels increase, and the minimum channel widths required for proper cooling decrease.

5. Thermal Conclusions for Hydrogen Cooling

The following conclusions can be drawn from this analysis:

- (1) Hydrogen-regenerative cooling is feasible for the complete thrust and chamber pressure region of interest. Oxidizer cooling is not required.

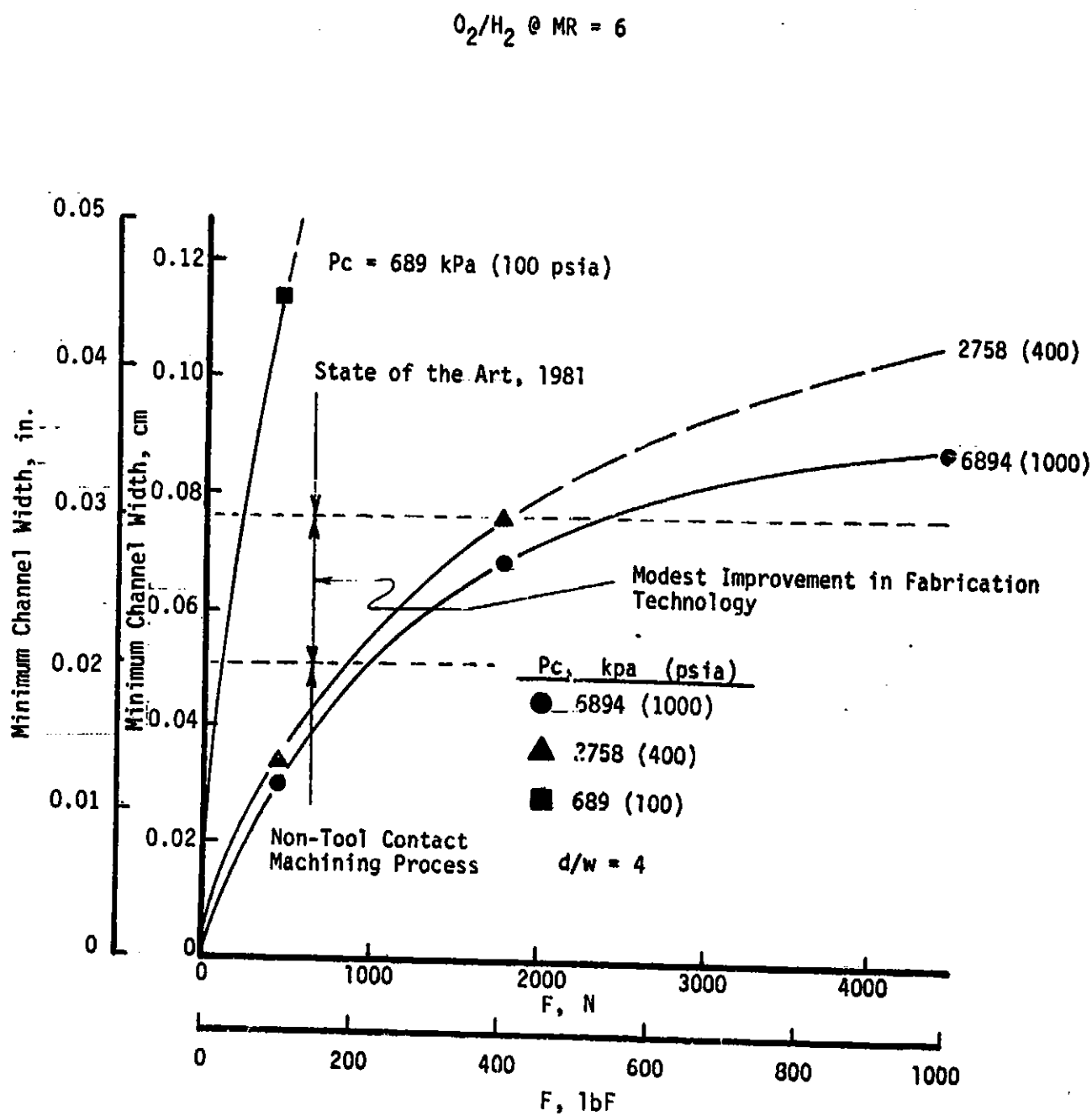


Figure 56. Minimum Channel Width Versus Thrust for Constant Chamber Pressures, O_2/H_2 at $MR = 6$

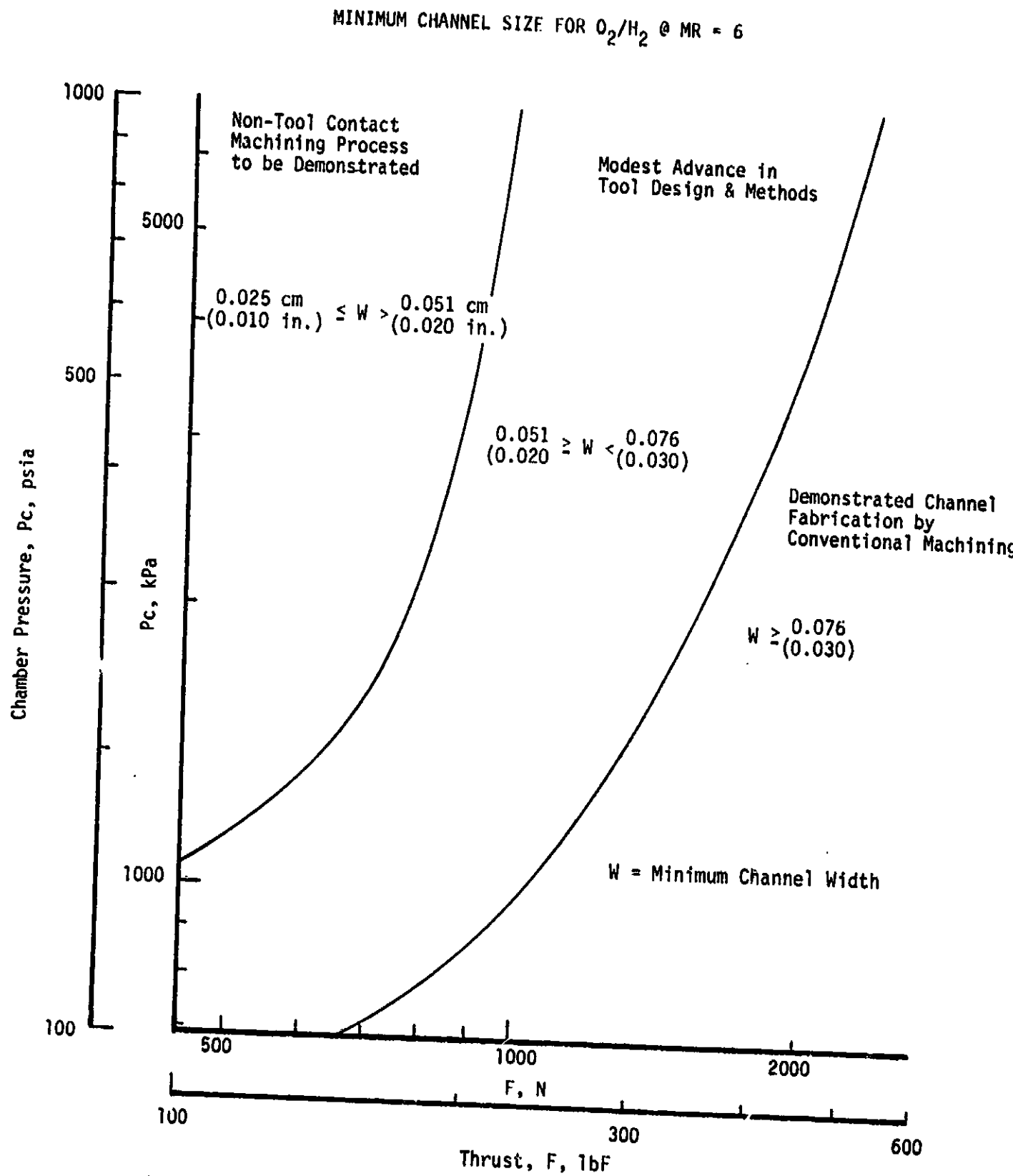


Figure 57. Ranges in Minimum Channel Size as a Function of Chamber Pressure and Thrust, O_2/H_2 at MR = 6

TABLE XIII
 EFFECT OF ENTHALPY ADDITION TO LO₂/LH₂ PROPELLANTS ON
 ONE-DIMENSIONAL EQUILIBRIUM PARAMETERS
 (P_c = 2758 kPa [400 psia], MR = 4)

	H ₂ and O ₂ @ NBP	H ₂ @ 922.2°K (1200°F) O ₂ @ NBP	H ₂ @ 922.2°K (1200°F) O ₂ @ 922.2°K (1200°F)
T _c , °K (°R)	2924 (5263)	3269 (5885)	3352 (6033)
H* cal/g (Btu/lbm)	-291.2 (-524.2)	357 (643.4)	549 (988.2)
C _p	1.5533	2.2762	2.5339
I _{sp} , sec	477.9	527.6	541.6
[H]*	0.01649	0.04417	0.05403
[O]*	0.00011	0.00102	0.00160
[OH]*	0.00525	0.01788	0.02282

*In Chamber

TABLE XIV
**EFFECT OF ENTHALPY ADDITION TO PROPELLANT(S)
FOR LOX/HYDROGEN SYSTEM**

PROPELLANTS NOMINAL P _c /F <u>CASE No.</u>	O ₂ /H ₂ 400/400	O ₂ /H ₂ 400/400	O ₂ /H ₂ 400/400
	1 $\frac{H_2}{O_2}$ NBP	2 $H_2 @ 922^{\circ}\text{K}$ (1200 °F) $O_2 @ \text{NBP}$	3 $\frac{H_2}{O_2} @ (1200^{\circ}\text{F})$
Thrust, N (lbf)	1779 (400)	1779 (400)	1779 (400)
P _c , kPa (psia)	2758 (400)	2758 (400)	2758 (400)
Throat-Radius, cm (in.)	1.052 (0.414)	1.029 (0.405)	1.024 (0.403)
Contraction Ratio	8.00	8.00	8.00
MR	4	4	4
\dot{m}_{ox} , kg/sec (lbm/sec)	0.323 (0.712)	0.287 (0.6318)	0.279 (0.6158)
\dot{m}_f , kg/sec (lbm/sec)	0.081 (0.178)	0.072 (0.1579)	0.070 (0.1539)
ΔP_{cj} , kPa (psi)	7.58 (1.1)	17.92 (2.6)	19.30 (2.8)
P _{cj-in} , kPa (psia)	3894 (564.8)	3894 (564.8)	3894 (564.8)
P _{cj-out} , kPa (psia)	3886 (563.7)	3876 (562.2)	3874 (562.0)
T _{cj-in} , °K (°F)	23 (-418.0)	23 (-418.0)	23 (-418.0)
T _{cj-out} , °K (°F)	202 (-96.9)	250 (-9.6)	264 (14.6)
Regen c	11.32	7.28	8.21
h _g , max, kw/m ² °K (Btu/in. ² -sec °F)	6.854 (0.00233)	7.442 (0.00253)	7.354 (0.00250)
h _l , max, kw/m ² °K (Btu/in. ² -sec °F)	8.237 (0.00280)	10.149 (0.00345)	10.560 (0.00359)
Q/A _g max, kw/m ² (Btu/in. ² -sec)	14447 (8.84)	18320 (11.21)	18679 (11.43)
Q/A _l max, kw/m ² (Btu/in. ² -sec)	4952 (3.03)	5965 (3.55)	6079 (3.72)
Q _{total} , kw (Btu/sec)	232.3 (220.3)	261.9 (248.4)	269.6 (255.7)
T _r , °K (°F)	2924 (4803.3)	3275 (5425.3)	3352 (5573.3)
Wall Thickness, cm (in.)	.762 (0.3)	.762 (0.3)	.762 (0.3)
V _{cj-max} , m/sec (ft/sec)	24.5 (80.3)	32.9 (107.8)	35.1 (115.3)
M _{cj-max} ,	0.039	0.051	0.054
No. Channels	72	89	89
Min. Channel Depth, cm (in.)	0.142 (0.056)	0.124 (0.049)	0.137 (0.054)
Limiting Criterion	T _{wg}	T _{wg}	T _{wg}
Cooling Channel Geometry			
Depth/Width @ Max Flux Point, cm (in.)	0.376/0.094 (0.148/0.037)	0.251/.064 (0.099/0.025)	0.249/0.061 (0.098/0.024)
Depth/Width @ Max Bulk Temperature, cm (in.)	0.815/0.203 (0.321/0.080)	0.610/0.155 (0.240/0.061)	0.582/0.147 (0.229/0.058)

LEGEND

- \dot{m}_{ox} = Total Weight Flow Oxygen
- \dot{m}_f = Total Weight Flow Fuel
- \dot{m}_{cj} = Coolant Weight Flow
- ΔP_{cj} = Cooling Jacket Inlet Pressure Drop
- P_{cj} = Cooling Jacket Inlet Pressure
- ΔT_{cj} = Cooling Jacket Temperature Rise
- T_{cj} = Cooling Jacket Inlet Temperature
- \dot{m}_{fcc} = Fuel Film-Cooling Weight Flow
- T_{wg} = Gas-Side Wall Temperature
- T_{wl} = Liquid-Side Wall Temperature
- h_g = Gas-Side Heat Transfer Coefficient
- h_l = Liquid-Side Heat Transfer Coefficient
- Q/A_g = Gas-Side Heat Flux
- Q/A_l = Liquid-Side Heat Flux
- T_r = Recovery Temperature
- V_{cj} = Maximum Coolant Jacket Velocity
- M_{cj-max} = Maximum Coolant Jacket Mach Number

IV, B, Thermal Design-(cont.)

(2) Minimum channel widths are within the realm of current fabrication technology or require only moderate advances in the state of the art.. No channel widths less than 0.025 cm (0.010 in.) were required for NBP propellants, as compared to the widths for RP-1 and oxygen, which, in some cases, were below 0.013 cm (0.005 in.).

(3) Hydrogen channel aspect ratios of 4:1 gave satisfactory results.

(4) Coolant pressure loss was sufficiently low, relative to operating pressure, to make the additional pumping power a negligible design parameter.

C. PERFORMANCE SENSITIVITY

Parametric performance analyses were conducted to determine the advantages of using LOX/hydrogen propellants instead of LOX/RP-1. The potential for improved performance by adding enthalpy to the propellants from "free" energy sources (i.e., waste heat or solar heat) was also investigated.

The parametric operating points investigated in the performance analyses are as follows:

Thrust, F	445, 1779, 4448N (100, 400, 1000 lbF)
-----------	--

Chamber Pressure, P _c	689, 2758, 6894 kPa (100, 400, 1000 psia)
----------------------------------	--

Mixture Ratio, O/F

NBP	4, 6, 8
Heated	2, 4, 6, 8

Expansion Ratio	400:1
-----------------	-------

1. Performance Model

The vaporization model was calibrated for oxygen-hydrogen using like doublet element data from the Extended Temperature Range Thruster Program (Ref. 6). The mixing limitations are representative of all oxygen-hydrogen class injectors, including those with coaxial elements.

IV, C, Performance Sensitivity (cont.)

The performance computer program was further modified to calculate the change in Isp resulting from enthalpy addition. Incorporated in the performance computer program was a subroutine containing data tables relating the ratio of change in Isp to change in enthalpy as a function of mixture ratio, chamber pressure, and expansion ratio. These data tables were compiled from a series of ODE and ODK runs for different propellant enthalpies.

2. Attainable Isp for NBP LOX/Hydrogen

Table XV summarizes the design point conditions and attainable Isp for LOX/hydrogen propellants. The delivered specific impulse is predicted to decrease with increasing mixture ratio for a constant thrust and chamber pressure, as shown in Figure 58. The peak delivered performance (455-468 sec) occurs at a mixture ratio equal to 4.

Another interesting result which evolved from the selected design guidelines is that, for thrusts of both 4448 and 1779N (1000 and 400 lbF), performance increases between chamber pressures of 689 to 2758 kPa (100 to 400 psia) and then decreases between 2758 to 6894 kPa (400 to 1000 psia). This trend may be seen in Figures 58 through 60. At a mixture ratio of 4, performance will increase approximately 1.3% from $P_c = 689$ kPa (1000 psia) to $P_c = 2758$ kPa (400 psia) and will decrease slightly ($\approx 0.3\%$) between $P_c = 2758$ kPa (400 psia) to $P_c = 6894$ kPa (1000 psia). The variation becomes more pronounced with increasing mixture ratio. At a MR of 8, performance increases approximately 2.5% between P_c 's of 689 and 2758 kPa (100 and 400 psia) and decreases up to 2.8% between P_c 's of 2758 and 6894 kPa (400 and 1000 psia).

This trend occurs because of a decrease in energy release efficiency (ERE) with increasing chamber pressure for a constant thrust. From $P_c = 689$ kPa (100 psia) to $P_c = 2758$ kPa (400 psia), an increase in kinetic efficiency (η_{KIN}) offsets the decrease in ERE. However, from $P_c = 2758$ kPa (400 psia) to $P_c = 6894$ kPa (1000 psia), the increase in η_{KIN} is less than the decrease in ERE. The net effect is an increase in predicted performance from $P_c = 689$ kPa (100 psia) to $P_c = 2758$ kPa (400 psia) and a decrease from $P_c = 2758$ kPa (400 psia) to $P_c = 6894$ kPa (1000 psia).

The reason ERE decreases with increasing chamber pressure is primarily due to a decrease in element mixing efficiency which results from the interaction of selected injector face element density [$0.93/cm^2$ (6/in.²)] and chamber contraction ratios of 8 minimum but not less than 3.8 cm (1.5 in.) diameter. As P_c increases, the throat area decreases and, since a constant contraction ratio (8.0) is used, chamber diameter and number of injector elements also decrease (NEL, Table XV). At these small chamber diameters, fringe effects with their detrimental influence on mixing

TABLE XV
LOX/LH₂ PARAMETRIC DATA AND RESULTS
FUEL-REGEN CASES

$\frac{F}{I_{sp}}$	$\frac{P_c}{kPa}$	$\frac{L'}{cm.}$	T_{ox} (in.)	T_f (°K) (°R)	$\frac{\epsilon_c}{\epsilon_L}$	$\frac{NEL}{\epsilon_c}$	$\frac{FRE}{\%}$	$\frac{Delivered}{I_{sp}}$ (sec)
445 (1000)	6894 (1000)	4	17.98 (7.08)	91 (163)	225 (404.7)	8.0	22	99.6
		6	17.98 (7.08)	91 (163)	310 (558.2)	8.0	20	98.4
		8	17.98 (7.08)	91 (163)	327 (589.8)	8.0	19	94.5
2758 (400)		4	22.20 (8.74)	91 (163)	157 (282.0)	8.0	60	99.8
		6	22.20 (8.74)	91 (163)	207 (373.0)	8.0	56	99.6
		8	22.20 (8.74)	91 (163)	219 (394.0)	8.0	54	98.1
689 (100)		4	30.53 (12.02)	91 (163)	128 (230.0)	8.0	252	99.9
		6	30.53 (12.02)	91 (163)	159 (286.0)	8.0	236	99.9
		8	30.53 (12.02)	91 (163)	169 (304.0)	8.0	230	99.4
2779 (400)	6894 (1000)	4	14.55 (5.73)	91 (163)	247 (443.7)	8.32	7	99.3
		6	14.55 (5.73)	91 (163)	345 (621.7)	9.0	7	96.7
		8	14.55 (5.73)	91 (163)	373 (671.3)	9.36	7	92.5
2758 (400)		4	17.98 (7.08)	91 (163)	202 (363.1)	8.0	22	99.8
		6	17.98 (7.08)	91 (163)	281 (506.5)	8.0	21	99.6
		8	17.98 (7.08)	91 (163)	299 (538.1)	8.0	19	97.2
689 (100)		4	24.74 (9.74)	91 (163)	164 (296.0)	8.0	99	99.9
		6	24.74 (9.74)	91 (163)	215 (387.0)	8.0	93	99.9
		8	24.74 (9.74)	91 (163)	224 (405.0)	8.0	91	99.2
445 (1000)	6894 (1000)	4	10.59 (4.17)	91 (163)	275 (495.9)	33.28	7	99.4
		6	10.59 (4.17)	91 (163)	403 (726.1)	35.26	7	97.7
		8	10.59 (4.17)	91 (163)	432 (788.0)	37.2	7	93.6
2758 (400)		4	13.08 (5.15)	91 (163)	287 (516.2)	13.19	7	99.7
		6	13.08 (5.15)	91 (163)	407 (723.8)	13.96	7	99.0
		8	13.08 (5.15)	91 (163)	426 (766.0)	14.72	7	95.9
689 (100)		4	17.98 (7.08)	91 (163)	255 (459.9)	8.0	23	99.9
		6	17.98 (7.08)	91 (163)	336 (605.1)	8.0	21	99.9
		8	17.98 (7.08)	91 (163)	349 (629.0)	8.0	20	99.0

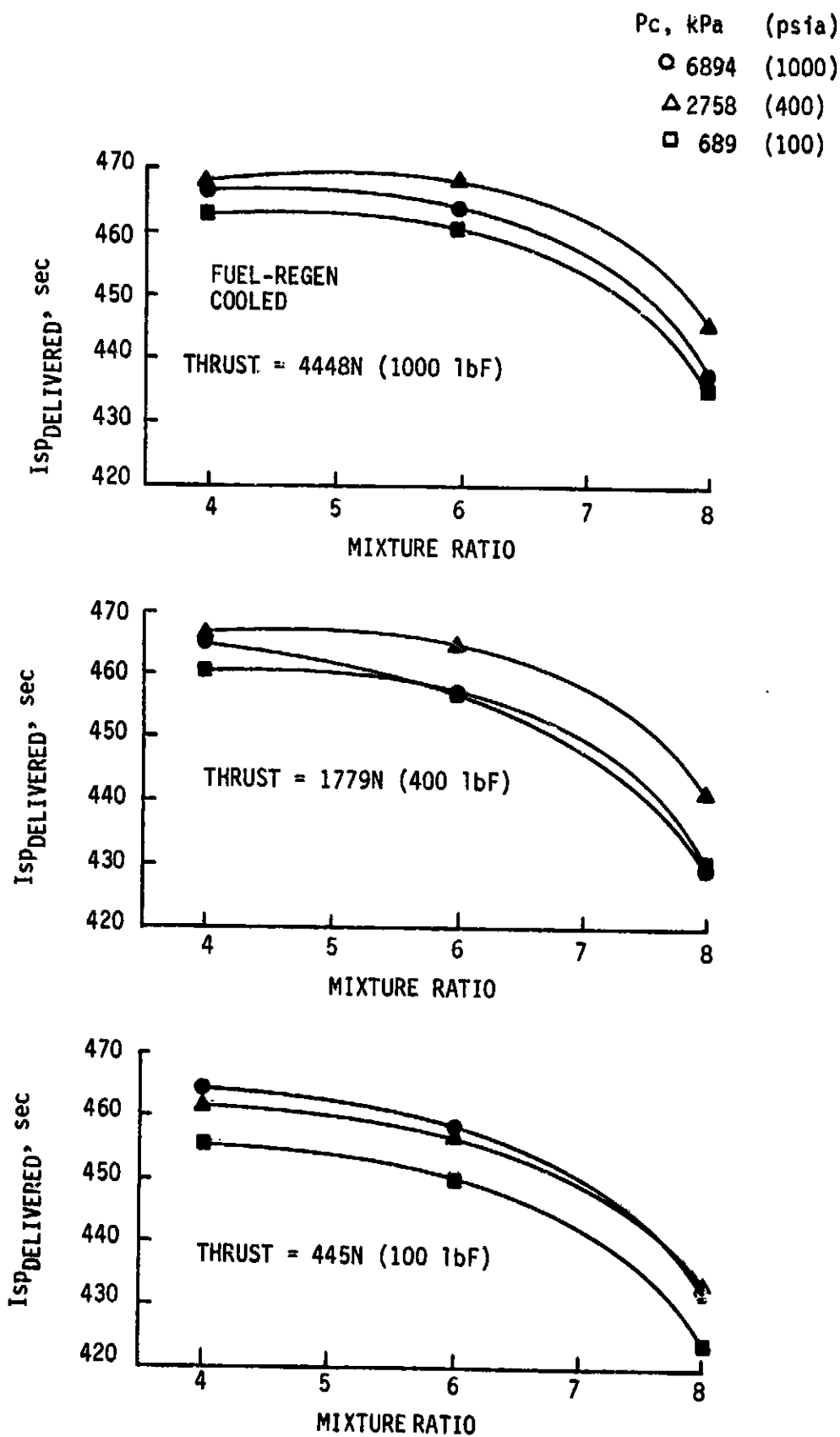


Figure 58. Predicted Performance for LOX/LH₂ as a Function of Mixture Ratio for 4448, 1779, and 445N (1000, 400, and 100 lbF)

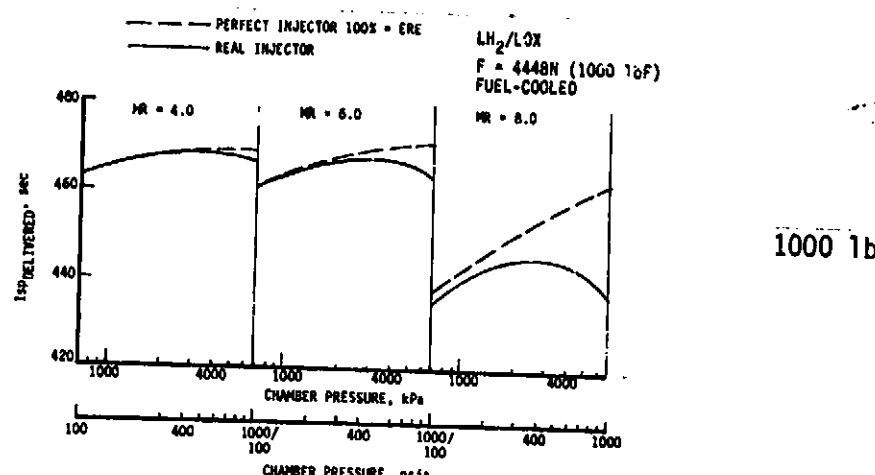


Figure 59. LOX/LH₂ Delivered Performance vs Chamber Pressure for 4448N (1000 lbf)

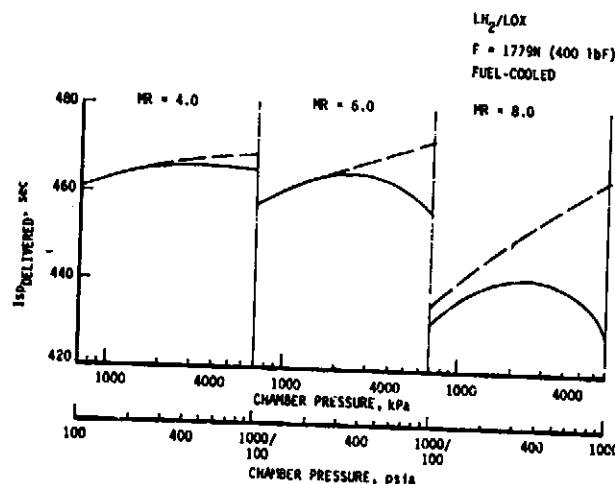


Figure 60. LOX/LH₂ Delivered Performance vs Chamber Pressure for 1779N (400 lbf)

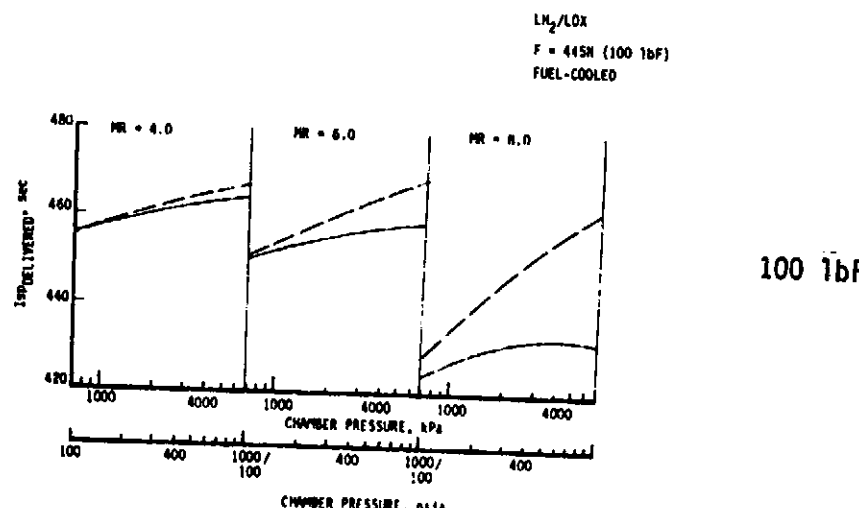


Figure 61. LOX/LH₂ Delivered Performance vs Chamber Pressure for 445N (100 lbf)

IV, C, Performance Sensitivity (cont.)

efficiency are predicted to become more predominant. Also, having fewer elements inhibits interelement mixing and propellant vaporization.

At $F = 445\text{N}$ (100 lbF), the minimum chamber diameter and number of elements had been reached for both $P_c = 2758 \text{ kPa}$ (400 psia) and $P_c = 6894 \text{ kPa}$ (1000 psia); therefore, increasing P_c from 2758 to 6894 kPa (400 to 1000 psia) does not significantly reduce ERE. The low-thrust, high-pressure designs result in contraction ratios of up to 37.

For the 445N (100 lbF) thrust case (Figure 61), the increase in η_{KIN} is greater than the decrease in ERE from $P_c = 2758 \text{ kPa}$ (400 psia) to $P_c = 6894 \text{ kPa}$ (1000 psia). These trends indicate that further improvements in Isp are attainable at high thrust if either a finer injector element pattern, or contraction ratios greater than eight, or both are utilized.

Figures 62 through 64 are cross-plots of predicted performance as a function of thrust and mixture ratio for constant chamber pressures. For $P_c = 689 \text{ kPa}$ (100 psia) and $P_c = 2758 \text{ kPa}$ (400 psia), performance will increase with increasing thrust. This occurs because the throat area increases with increasing thrust, resulting in both η_{KIN} and ERE improving with thrust. Kinetic efficiency improves because the engine gets larger, providing longer residence times and thus more potential for recombination. Energy release efficiency improves because larger throat areas mean larger chamber diameters and a greater number of elements, thus improving mixing efficiency. For $P_c = 6894 \text{ kPa}$ (1000 psia), the minimum chamber diameter and minimum number of elements occur at both 445 and 1779N (100 and 400 lbF) thrust. Although the number of elements at both thrust levels is the same, the element orifice diameter increases from 445 to 1779N (100 to 400 lbF). This increase in orifice size decreases interelement mixing and vaporization, thus lowering ERE. At thrusts from 1779 to 4448N (400 to 1000 lbF), chamber diameter and element number increases result in improved mixing and ERE.

3. Effect of Added Enthalpy

The potential for performance improvement by adding heat from a "free" source was investigated using LOX/hydrogen for the following operating points:

Thrust, F	1779N (400 lbF)
Chamber Pressure, P_c	2758 kPa (400 psia)
Mixture Ratio, O/F	2, 4, 6, 8
Expansion Ratio	400:1

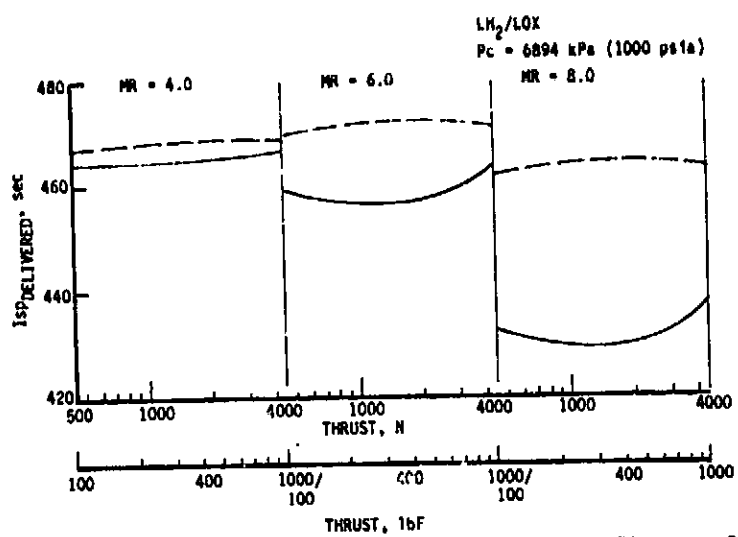


Figure 62. LOX/LH₂ Delivered Performance vs Thrust for 6894 kPa (1000 psia) Chamber Pressure

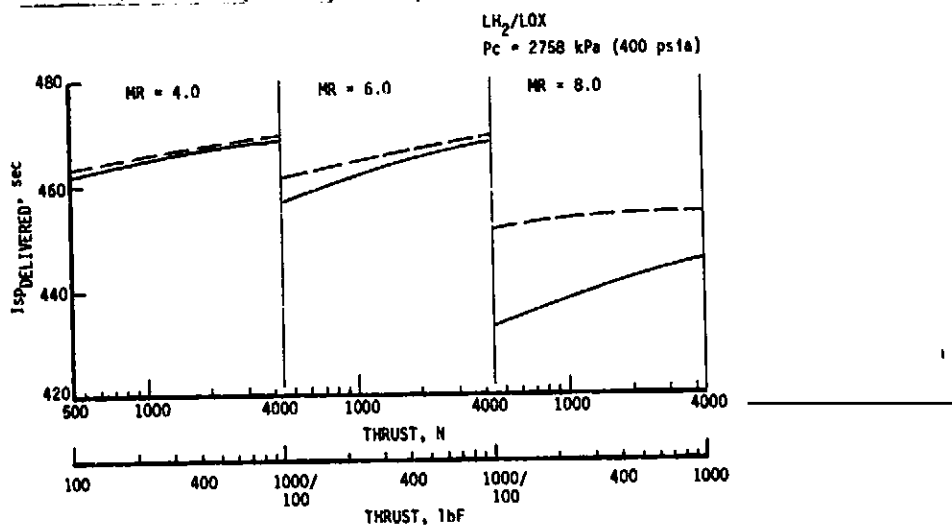


Figure 63. LOX/LH₂ Delivered Performance vs Thrust for 2758 kPa (400 psia) Chamber Pressure

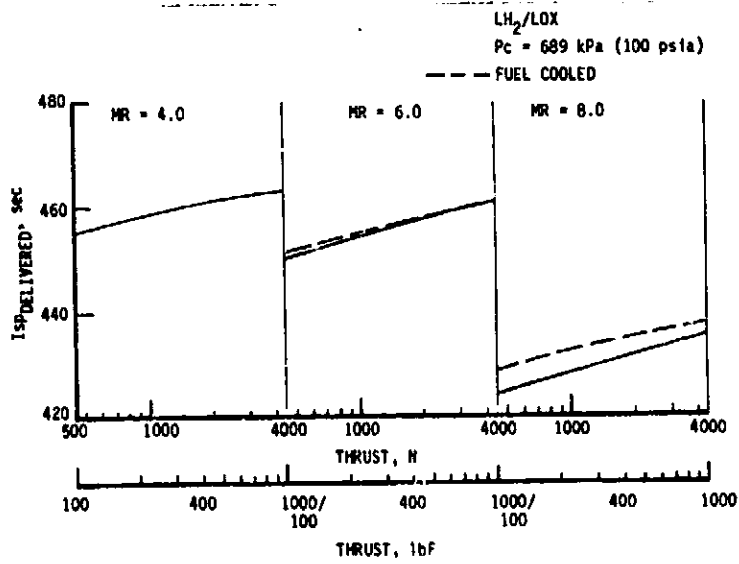


Figure 64. LOX/LH₂ Delivered Performance vs Thrust for 639 kPa (100 psia) Chamber Pressure

IV, C, Performance Sensitivity (cont.)

Table XVI lists the results of this analysis. Performance will improve from 2.3% (at MR = 8) to 16.5% (at MR = 2) if the hydrogen is heated 922.2°K (1200°F) after it has been used in regenerative cooling. Another 2% to 3% performance improvement may be realized by also heating the oxygen to 922.2°K (1200°F).

Without enthalpy addition, the peak performance occurred at a mixture ratio of 4. With enthalpy addition, the maximum performance occurred at a mixture ratio of 2 and increased further as the mixture ratio was lowered.

Although the heating of hydrogen results in significant performance improvements, the same may not be true of hydrocarbons. At these high temperatures, coking may occur in the propellant lines which has a detrimental effect on engine operation.

4. Performance Conclusions for LOX/Hydrogen

The following general conclusions may be drawn from this analysis:

- The maximum Isp for LOX/hydrogen is approximately 25 to 30% higher than that for LOX/methane and 30 to 35% higher than that for LOX/RP-1.
- The peak performance generally occurs at a mixture ratio of 4 ± 1 for the thrust and chamber pressure ranges analyzed.
- When real injector effects for a fixed element type and density are considered, maximum specific impulse is obtained at approximately the intermediate chamber pressure levels [≈ 2758 kPa (≈ 400 psia)]. However, when allowance is made for the development of improved injectors or the use of larger element quantities, significant improvements in attainable Isp are possible at pressures higher than 2758 kPa (400 psia). While the higher attainable performance is not expected to alter the cooling conclusions, it could result in slightly smaller channel sizes.
- In all cases, maximum specific impulse is obtained at the maximum thrust level [4448N (1000 lbF)] analyzed in this study.

TABLE XVI
 ADDED ENTHALPY RESULTS FOR
 LOX/LH₂ PROPELLANTS

P_c = 2758 kPa (400 psia)

F = 1779N (400 lbf)

e = 400:1

MR	Isp _R	ΔT _F	Isp _{H1}	% ΔIsp ₁	ΔT _{ox}	Isp _{H2}	% ΔIsp ₂
2	433.8	778 (1400)	505.5	16.5	832 (1497)	518.1	19.4
4	466.4	720 (1296.9)	496.9	6.5	832 (1497)	508.4	9.0
6	464.9	641 (1153.5)	479.9	3.2	832 (1497)	489.3	5.2
8	441.6	623-(1121.9)	451.6	2.3	832 (1497)	459.9	4.1

			<u>UNITS</u>
Isp _R	-	Reference Case - 1 NBP	sec
Isp _{H1}	-	Only hydrogen is heated by "free" source	sec
ΔT _F	-	Temperature rise by "free" source	Deg-R
Isp _{H2}	-	Both hydrogen and oxygen are heated	sec
ΔT _{ox}	-	Temperature rise from tank condition	Deg-R
% ΔIsp ₁	-	$\frac{Isp_{H1}}{Isp_R} * 100$	
% ΔIsp ₂	-	$\frac{Isp_{H2}}{Isp_R} * 100$	

V. RESULTS OF PARAMETRIC STUDIES FOR LOX/METHANE

A. SUMMARY

The LOX/LCH₄ propellant combination presents the most challenging design task for optimization as both propellants are reasonably good coolants of almost equal capability. However, unlike hydrogen, neither is completely satisfactory for the entire operating range. Oxygen cooling was found to be more difficult than with the LOX/RP-1 system due to a combination of higher gas-side heat flux and lower total propellant flows available for the higher-performing LOX/methane propellants.

For the oxygen-methane system, methane cooling is limited to lower P_c 's, low MR, and higher thrusts. Oxygen cooling is favored at nominal and high MR's and higher thrusts. The attainable specific impulse is maximum at a mixture ratio between 3.0 and 3.5. The present study shows that fuel should be the primary coolant at an MR of 3.0 while oxygen is preferred at an MR of 3.5. At optimum mixture ratio, a large region at low thrust and high P_c requires cooling augmentation; this region shrinks as the thrust level increases. The use of dual-regen cooling provides a good solution to design points which are limited by bulk temperature rises. The second coolant allows the added chamber length required for high performance to be attained without requiring use of film cooling.

B. THERMAL DESIGN

1. Scope and Analytical Basis

The study envelope for the LO₂/LCH₄ analyses of Task IV was identical to that given in Section IV.B.1 for LO₂/LH₂, except that the mixture ratio range was from 2 to 5. In this study, no credit was taken for possible gas-side heat-flux reduction resulting from carbon deposition from oxygen-methane combustion. The maximum bulk temperature for methane is limited primarily by pressure drop. The decomposition temperature of methane is above the allowable wall temperature and thus is not a limiting factor.

2. Analysis Methodology

The cooling capability trends for the LO₂/LCH₄ system resemble those previously determined for the LO₂/RP-1 propellant combination. Methane cooling was evaluated at mixture ratios of 2, 3, and 3.5, in that order, while oxygen cooling was studied starting at MR = 5 and proceeding to MR = 3.5. Selected input data and calculated results for cooling with methane and with oxygen are presented in Tables XVII and XVIII, respectively. Significant results are shown graphically in Figures 65 through 83.

TABLE XVII

SELECTED PARAMETERS CHARACTERIZING
COOLING WITH NBP METHANE WITH LO₂
(Single Regen)

Code	MR	F	Pc	Coolant	P _{in}	P _{in} /Pc	t _{wall}	CR	C _F ^{**}	Isp ^{**}	Channel Dimensions			
											d/w	Aspect Ratio	Throat w/d	Barrel w/d
		N	kPa		kPa						cm/cm	cm/cm	cm/cm	cm
2-1-4/F	2	445	2758	F	7583	2.75	0.76	13.05	1.8465	321.1	10	0.0301/0.308	0.0301/0.109	13.21
				F	7583	2.75	0.76	13.05	1.8465	321.1	5	0.0338/0.169	0.0338/0.071	13.21
				F	17235	6.25	0.76	13.05	1.8465	321.1	10	0.0335/0.336	0.0335/0.056	13.21
2-4-4/F	1779	2758	F	7583	2.75	0.76	8.00	1.8557	322.7	20	0.0663/1.325	0.0663/0.163	17.98	
2-10-4/F 2-10-10/F	4448 6894	2758	F	7583 9652	2.75 1.40	0.76 0.0635	8.00 8.00	1.8563 1.8534	322.8 322.3	20 20	0.0442/0.881 0.0373/0.747	0.0803/1.549 0.0554/0.904	22.10 18.03	
3-4-1/F 3-4-4/F	3 1779	689 2758	F	5515 7583	8.00 2.75	0.76 0.76	8.00 8.00	1.9853 2.0047	358.2 367.0	20 20	0.0963/1.923 0.0427/0.853	0.0963/1.090 0.0427/0.089	24.64 15.11	
3-10-4/F	4448	2758	F	7583	2.75	0.76	8.00	2.0096	367.9	20	0.0564/1.128	0.0564/0.831	22.10	
3.5-4-1/F	3.5 1779	689 689	F	5515 5515	8.00 8.00	0.76 0.76	8.00 8.00	2.0000 2.0000	352.7 352.7	20 7	0.0919/1.841 0.1016/0.710	0.0925/1.328 0.1016/0.406	24.64 24.64	
3.5-4-4/F		2758	F	7583	2.75	0.76	8.00	2.0490	367.4	20	0.0442/0.886	0.0442/0.079	14.48	
		2758	F	7583	2.75	0.76	8.00	2.0490	367.4	20	0.0411/0.825	0.0414/0.066	15.16	
3.5-10-1/F 3.5-10-4/F	4448 2758	689 2758	F	5515 7583	8.00 2.75	0.76 0.76	8.00 8.00	2.0204 2.0574	356.3 368.9	5 20	0.2169/1.084 0.0569/1.137	0.2177/0.218 0.0569/0.457	30.46 22.10	

*MR = Thrust, N - $\frac{444.8}{6894}$ - $\frac{\text{Pc, kPa}}{6894}$ / Coolant

**Values employed to calculate propellant flow and throat size

EOLDOUT ERAMIS

TABLE XVII

CHARACTERIZING ENGINE REGENERATIVE
METHANE WITH LO_2/LCH_4 PROPELLANTS
(Single Regen)

SI Units

Barrel w/d cm/cm	L' cm	r _t cm	r _{ch} cm	c _A -	ΔP kPa	T _{b,in} °K	T _{b,out} °K	ΔT _b °K	h _{g,max} kw/m ² °K x 10 ⁻³	q _{g,max} kw/m ²	q _{c,max} kw/m ²	No. of Channels
.O301/0.109	13.21	0.528	1.905	13.82	103	114.3	557	442	7589	16881	1879	86
.O338/0.071	13.21	0.528	1.905	13.82	55	114.3	557	442	7589	16881	3072	83
.O335/0.056	13.21	0.528	1.905	13.82	153	114.3	572	458	7589	16881	1634	83
.O663/0.163	17.98	1.052	2.974	9.27	142	114.3	398	283	5501	11390	2762	88
.O803/1.549	22.10	1.664	4.704	15.54	15	114.3	347.4	233	10149	22732	6896	142
.O554/0.904	18.03	1.052	2.977	42.54	105	114.3	437	322	23621	53716	10132	70
.O963/1.090	24.64	2.035	5.753	6.00	2.8	114.3	435	320	1665	4216	670	110
.O427/0.089	15.11	1.011	2.863	13.09	396	114.3	497	383	4942	13563	5229	105
.O564/0.831	22.10	1.598	4.521	13.55	14	114.3	447	332	4648	13123	1896	124
.O925/1.328	24.64	2.027	5.733	6.00	2.8	114.3	458	344	1574	4020	654	171
.O1016/0.406	24.64	2.027	5.733	6.00	9.0	114.3	458	344	1574	4020	801	106
.O442/0.079	14.48	1.001	2.832	6.00	481	114.3	496	382	4707	13041	3840	103
.O414/0.066	15.16	1.001	2.832	12.76	631	114.3	525	411	4707	13025	4167	106
.2177/0.218	30.48	3.188	9.017	6.00	13	114.3	331	217	1253	3203	899	89
.O569/0.457	22.10	1.580	4.468	12.96	24	114.3	472	357	4324	12387	2402	122

FOLDOUT FRAME 2

TABLE XVII (Cont)

**SELECTED PARAMETERS CHARACTERIZING
COOLING WITH NBP METHANE WITH LO₂**
(Single Regen)

Code	MR	F 1bf	Pc psia	Coolant	P _{in} psia	P _{in} /Pc	t _{wall} in.	CR	C _F —	I _{sp} ** sec	Channel Dimensions			
											Aspect Ratio d/w	Throat w/d in./in.	Barrel w/d in./in.	L' in.
2-1-4/E	2	100	400	F	1100	2.75	0.3	13.05	1.8465	321.1	10	0.0121/0.1213	0.0121/0.043	5.20
				F	1100	2.75	0.3	13.05	1.8465	321.1	5	0.0133/0.0666	0.0133/0.028	5.20
				F	2500	6.25	0.3	13.05	1.8465	321.1	10	0.0132/0.1321	0.0132/0.022	5.20
2-4-4/F		400	400	F	1100	2.75	0.3	8.00	1.8557	322.7	20	0.0261/0.5217	0.0261/0.064	7.08
2-10-4/F 2-10-10/F	1000	400	F	1100	2.75	0.3	8.00	1.8563	322.8	20	0.0174/0.3470	0.0316/0.610	8.70	
			1000	F	1400	1.40	0.025	8.00	1.8534	322.3	20	0.0147/0.2940	0.0218/0.356	7.10
3-4-1/F	3	400	100	F	800	8.00	0.3	8.00	1.9853	358.2	20	0.0379/0.2570	0.0379/0.479	9.70
3-4-4/F		400	F	1100	2.75	0.3	8.00	2.0047	367.0	20	0.0168/0.3359	0.0168/0.035	5.95	
3-10-4/F		1000	400	F	1100	2.75	0.3	8.00	2.0096	367.9	20	0.0222/0.4442	0.0222/0.327	8.70
3.5-4-1/F	3.5	400	100	F	800	8.00	0.3	8.00	2.0000	352.7	20	0.0362/0.7249	0.0364/0.523	9.70
			100	F	800	8.00	0.3	8.00	2.0000	352.7	7	0.0400/0.2797	0.0400/0.160	9.70
3.5-4-4/F		400	F	1100	2.75	0.3	8.00	2.0490	367.4	20	0.0174/0.3479	0.0174/0.031	5.70	
			400	F	1100	2.75	0.3	8.00	2.0490	367.4	20	0.0162/0.3249	0.0163/0.026	5.97
3.5-10-1/F 3.5-10-4/F	1000	100	F	800	8.00	0.3	8.00	2.0204	356.3	5	0.0854/0.4269	0.0857/0.086	12.00	
			400	F	1100	2.75	0.3	8.00	2.0574	368.9	20	0.0224/0.4477	0.0224/0.180	8.70

*MR = $\frac{\text{Thrust}, \text{1bf}}{100} - \frac{\text{Pc/psia}}{1000}$ / Coolant

**Values employed to calculate propellant flow and throat size

FOLDOUT FRAME

TABLE XVII (Cont.)

**CHARACTERIZING ENGINE REGENERATIVE
METHANE WITH LO_2/LCH_4 PROPELLANTS**
(Single Regen)

English Units

Barrel w/d in./in.		L' in.	r _t in.	r _{ch} in.	c _A -	ΔP psi	T _{b,in} °F	T _{b,out} °F	ΔT _b °F	h _{g, max} Btu/in ² -sec-°F x 10 ⁻³	Q _{g, max} Btu/in ² -sec	Q _{c, max} Btu/in ² -sec	No. of Channels
0.0121/0.043	5.20	0.208	0.750	13.82	14.9	-254.2	542.2	796.4	2.58	10.33	1.15	86	
0.0133/0.028	5.20	0.208	0.750	13.82	8.0	-254.2	542.2	796.6	2.58	10.33	1.88	83	
0.0137/0.022	5.20	0.208	0.750	13.82	22.2	-254.2	570.0	824.2	2.58	10.32	1.11	83	
0.0261/0.064	7.08	0.414	1.171	9.27	20.6	-254.2	255.9	510.1	1.87	6.97	1.69	88	
0.0316/0.610	8.70	0.655	1.852	15.54	2.2	-254.2	165.3	419.5	3.45	13.91	4.22	142	
0.0218/0.356	7.10	0.414	1.172	42.54	15.3	-254.2	325.8	580.0	8.03	32.87	6.20	70	
0.0379/0.429	9.70	0.801	2.265	6.00	0.4	-254.2	322.7	576.9	0.566	2.58	0.41	110	
0.0168/0.035	5.95	0.398	1.127	13.09	57.5	-254.2	434.4	688.6	1.68	8.30	3.20	105	
0.0222/0.327	8.70	0.629	1.780	13.55	2.0	-254.2	344.0	598.2	1.58	8.03	1.16	124	
0.0364/0.523	9.70	0.798	2.257	6.00	0.4	-254.2	364.7	618.9	0.535	2.46	0.40	171	
0.0400/0.160	9.70	0.798	2.257	6.00	1.3	-254.2	364.8	619.0	0.535	2.46	0.49	106	
0.0174/0.031	5.70	0.394	1.115	6.00	69.8	-254.2	433.6	687.8	1.60	7.98	2.35	103	
0.0163/0.026	5.97	0.394	1.115	12.76	91.6	-254.2	485.7	739.9	1.60	7.97	2.55	106	
0.0857/0.086	12.00	1.255	3.550	6.00	1.9	-254.2	135.6	389.8	0.426	1.96	0.55	89	
0.0224/0.180	8.70	0.622	1.759	12.96	3.5	-254.2	389.3	643.5	1.47	7.58	1.47	122	

FOLDOUT FRAME

TABLE XVIII

SELECTED PARAMETERS CHARACTERIZING ENGINE REGEN COOLING WITH LO_2/LCH_4 PROPELLANTS

(Single Regen)

Code*	MR	F N (lbF)	Pc kPa (psia)	P _{in} kPa (psia)	P _{in} /Pc -	t _{w+1} cm (in.)	CR	C _F ** sec	Isp** sec	L' cm (in.)	r _t cm (in.)	r _{ch} cm (in.)	A cm ²	ΔP kPa (psi)	T _{b,in} °K (°F)	T _{b,out} °K (°F)	
3.5-1-1/0	3.5	445 (100)	689 (100)	0 (900)	6205 (900)	9.0 (0.3)	0.76 (0.3)	8.00	1.9654	346.6	13.21 (5.20)	1.021 (0.402)	2.891 (1.138)	6.00	154 (22.3)	94.5 (-289.9)	394 (250.1)
3.5-1.4/0		2758 (400)	0 (1030)	7101 (1030)	2.575 (0.3)	0.76 (0.3)	14.33	2.0273	363.5	6.73 (2.65)	0.503 (0.198)	1.905 (0.750)	20.31	1737 (251.9)	97.0 (-285.3)	394 (250.1)	
3.5-4-1/0		1779 (400)	689 (100)	0 (900)	6205 (900)	9.0 (0.3)	0.76 (0.3)	8.00	2.0000	352.7	24.64 (9.70)	2.027 (0.798)	5.733 (2.257)	6.00	47 (6.8)	94.5 (-289.9)	309 (96.5)
3.5-4-4/0		2758 (400)	0 (1030)	7101 (1030)	2.575 (0.3)	0.76 (0.3)	8.00	2.0490— —367-4		17.42 (6.86)	1.001 (0.394)	2.832 (1.115)	12.76	529 (76.8)	97.0 (-285.3)	394 (250.1)	
3.5-10-1/0		4448 (1000)	689 (100)	0 (900)	6205 (900)	9.0 (0.3)	0.76 (0.3)	8.00	2.0204	356.3	30.48 (12.00)	3.188 (1.255)	9.017 (3.550)	6.00	31 (4.5)	94.5 (-289.9)	217 (-68.1)
3.5-10-4/0		2758 (400)	0 (1030)	7101 (1030)	2.575 (0.3)	0.76 (0.3)	8.00	2.0574	368.9	22.10 (8.70)	1.580 (0.622)	4.468 (1.759)	12.96	239 (34.6)	97.0 (-285.3)	292 (65.9)	
3.5-10-6/0		4136 (600)	0 (1350)	9307 (1350)	2.25 (0.025)	0.0635 (0.025)	8.00	2.0602	371.5	20.19 (7.95)	1.288 (0.507)	3.645 (1.435)	28.77	1194 (173.2)	96.8 (-285.7)	389 (240.6)	
3.5-10-8/0		5515 (800)	0 (2200)	15,167 (2200)	2.75 (0.025)	0.0635 (0.025)	8.00	2.0616	373.0	14.68 (5.78)	1.115 (0.439)	3.157 (1.243)	46.03	2729 (395.8)	101 (-278.2)	394 (250.1)	
4-1-1/0	4	445 (100)	689 (100)	0 (900)	6205 (900)	9.0 (0.3)	0.76 (0.3)	8.00	1.9596	337.0	14.81 (5.83)	1.024 (0.403)	2.896 (1.140)	6.00	33 (4.8)	94.5 (-289.9)	394 (250.1)
4-1-4/0		2758 (400)	0 (1030)	7101 (1030)	2.575 (0.3)	0.76 (0.3)	14.35	2.0304	355.1	9.19 (3.62)	0.503 (0.198)	1.905 (0.750)	19.12	929 (134.8)	96.8 (-285.7)	394 (250.1)	
4-4-1/0		1779 (400)	689 (100)	0 (900)	6205 (900)	9.0 (0.3)	0.76 (0.3)	8.00	1.9968	343.4	24.64 (9.70)	2.029 (0.799)	5.738 (2.259)	6.00	16 (2.3)	94.5 (-289.9)	275 (35.4)
4-4-4/0		2758 (400)	0 (1030)	7101 (1030)	2.575 (0.3)	0.76 (0.3)	8.00	2.0544	359.3	18.03 (7.70)	1.001 (0.394)	2.827 (1.113)	12.01	325 (47.2)	96.8 (-285.7)	364 (195.2)	
4-10-1/0		4448 (1000)	689 (100)	0 (900)	6205 (900)	9.0 (0.3)	0.76 (0.3)	8.00	2.0195	347.3	30.48 (12.00)	3.188 (1.255)	9.019 (3.551)	6.00	7.6 (1.1)	94.5 (-289.9)	198 (-103.0)
4-10-4/0		2758 (400)	0 (1030)	7101 (1030)	2.575 (0.3)	0.76 (0.3)	8.00	2.0636	360.9	22.10 (8.70)	1.577 (0.621)	4.460 (1.756)	12.64	185 (26.8)	96.8 (-285.7)	262 (10.9)	
4-10-6/0		4136 (600)	0 (1350)	9307 (1350)	2.25 (0.025)	0.0635 (0.025)	8.00	2.0715	364.7	20.19 (7.95)	1.285 (0.506)	3.635 (1.431)	28.53	655 (95.0)	96.8 (-285.7)	351 (173.2)	
4-10-8/0		5515 (800)	0 (2200)	15,167 (2200)	2.75 (0.025)	0.0635 (0.025)	8.00	2.0754	366.9	16.97 (6.68)	1.113 (0.438)	3.145 (1.238)	44.64	1916 (277.9)	101 (-278.2)	394 (250.0)	
5-1-1/0	5	445 (100)	689 (100)	0 (900)	6205 (900)	9.0 (0.3)	0.76 (0.3)	8.00	1.9584	320.6	17.65 (6.95)	1.024 (0.403)	2.896 (1.140)	6.00	27 (3.9)	94.5 (-289.9)	394 (250.0)
5-1-4/0		2758 (400)	0 (1030)	7101 (1030)	2.575 (0.3)	0.76 (0.3)	14.30	2.0236	336.8	11.84 (4.66)	0.503 (0.198)	1.905 (0.750)	17.21	297 (43.1)	95.2 (-288.7)	394 (250.0)	
5-1-10/0		6894 (1000)	0 (2200)	15,167 (2200)	2.2 (0.025)	0.0635 (0.025)	36.30	2.0540	345.7	8.38 (3.30)	0.315 (0.124)	1.905 (0.750)	46.87	1721 (249.6)	101 (-278.2)	394 (250.0)	
5-4-1/0		1779 (400)	689 (100)	0 (900)	6205 (900)	9.0 (0.3)	0.76 (0.3)	8.00	1.9945	326.5	24.64 (9.70)	2.029 (0.799)	5.740 (2.260)	6.00	7.6 (1.1)	94.5 (-289.9)	232 (-42.9)
5-4-4/0		2758 (400)	0 (1030)	7101 (1030)	2.575 (0.3)	0.76 (0.3)	8.00	2.0464	340.6	18.03 (7.10)	1.001 (0.394)	2.835 (1.116)	19.22	261 (37.3)	95.2 (-288.7)	280 (44.7)	
5-4-10/0		6894 (1000)	0 (2200)	15,167 (2200)	2.2 (0.025)	0.0635 (0.025)	9.12	2.0641	347.4	13.28 (5.23)	0.630 (0.248)	1.905 (0.750)	39.84	815 (118.2)	101 (-278.2)	394 (250.0)	
5-10-1/0	5	4448 (1000)	689 (100)	0 (900)	6205 (900)	9.0 (0.3)	0.76 (0.3)	8.00	2.0164	330.1	30.48 (12.00)	3.190 (1.256)	9.027 (3.554)	6.00	3.4 (0.5)	94.5 (-289.9)	180 (-135.2)
5-10-4/0		2758 (400)	0 (1030)	7101 (1030)	2.575 (0.3)	0.76 (0.3)	8.00	2.0554	342.1	22.10 (8.70)	1.580 (0.622)	4.470 (1.760)	11.99	104 (15.1)	95.2 (-288.7)	218 (-68.4)	
5-10-10/0		6894 (1000)	0 (2200)	15,167 (2200)	2.2 (0.025)	0.0635 (0.025)	8.00	2.0653	347.6	18.03 (7.10)	0.998 (0.393)	2.819 (1.110)	50.62	381 (55.3)	101 (-278.2)	377 (218.8)	

*MR = Thrust, N = P_c, kPa/coolant
445.8 6894MR = Thrust, lbF = P_c, psia/coolant
100 1000

**Values employed to calculate propellant flow and throat size.

FOLDOUT FRAME

TABLE XVIII

METERS CHARACTERIZING ENGINE REGENERATIVE
BOLING WITH LO_2/LCH_4 PROPELLANTS

(Single Regen)

r_t cm (in.)	r_{ch} cm (in.)	A	ΔP kPa (psi)	T_b , in °K (°F)	$T_{b,out}$ °K (°F)	ΔT_b °K (°F)	h_g, \max kw/m ² °K (Btu/in. ² sec-°F) $\times 10^{-3}$	Q_g, \max kw/m ² (Btu/in. ² sec)	Q_c, \max kw/m ² (Btu/in. ² sec)	Aspect Ratio d/w	Throat w/d cm/cm (in./in.)	Throat w/d cm/cm (in./in.)	No. of Channels
1.021 (0.402)	2.891 (1.138)	6.00	154 (22.3)	94.5 (-289.9)	394 (250.0)	300 (539.9)	1903 (0.647)	5442 (3.33)	1079 (0.66)	10	0.0147/0.147 (0.0058/0.0580)(0.0095/0.095)	0.0241/0.241	143
0.503 (0.198)	1.905 (0.750)	20.31	1737 (251.9)	97.0 (-285.3)	394 (250.0)	297 (535.3)	6648 (2.26)	18,679 (11.43)	3105 (1.90)	20	0.0066/0.133 (0.0026/0.0525)(0.0060/0.120)	0.0152/0.305	113
2.027 (0.798)	5.733 (2.257)	6.00	47 (6.8)	94.5 (-289.9)	309 (96.5)	215 (386.4)	1574 (0.535)	4298 (2.63)	801 (0.49)	7	0.0388/0.273 (0.0153/0.1074)(0.0280/0.196)	0.0711/0.498	171
1.001 (0.394)	2.832 (1.115)	12.76	529 (76.8)	97.0 (-285.3)	394 (250.0)	297 (535.3)	4707 (1.60)	13,433 (8.22)	3268 (2.00)	20	0.0208/0.419 (0.0082/0.1648)(0.0094/0.137)	0.0239/0.348	131
3.188 (1.255)	9.017 (3.550)	6.00	31 (4.5)	94.5 (-289.9)	217 (-68.9)	123 (221.0)	1253 (0.426)	3432 (2.10)	1128 (0.69)	5	0.0046/0.423 (0.0333/0.1664)(0.0501/0.217)	0.1273/0.551	168
1.580 (0.622)	4.468 (1.759)	12.96	239 (34.6)	97.0 (-285.3)	292 (65.9)	195 (351.2)	4324 (1.47)	12,976 (7.94)	3546 (2.17)	20	0.0348/0.444 (0.0137/0.1749)(0.0181/0.362)	0.0460/0.919	149
1.288 (0.507)	3.645 (1.435)	28.77	1194 (173.2)	96.8 (-285.7)	389 (240.0)	292 (525.7)	9266 (3.15)	29,170 (17.85)	3987 (2.44)	20	0.0234/0.467 (0.0092/0.1838)(0.0154/0.141)	0.0391/0.358	98
1.115 (0.439)	3.157 (1.243)	46.03	2729 (395.8)	101 (-278.2)	394 (250.0)	293 (528.2)	15,032 (5.11)	45,235 (27.68)	9086 (5.56)	20	0.0198/0.396 (0.0078/0.1558)(0.0104/0.180)	0.0264/0.460	89
1.024 (0.403)	2.396 (1.140)	6.00	33 (4.8)	94.5 (-289.9)	394 (250.0)	300 (539.9)	1830 (0.622)	5180 (3.17)	997 (0.61)	20	0.0155/0.307 (0.0061/0.1210)(0.0105/0.133)	0.0267/0.338	142
0.503 (0.198)	1.905 (0.750)	19.12	929 (134.8)	96.8 (-285.7)	394 (250.0)	298 (535.7)	6324 (2.15)	17,829 (10.91)	2631 (1.61)	20	0.0076/0.155 (0.0030/0.0602)(0.0058/0.117)	0.0147/0.297	112
2.029 (0.799)	5.738 (2.259)	6.00	16 (2.3)	94.5 (-289.9)	275 (35.4)	181 (325.3)	1497 (0.509)	4069 (2.49)	605 (0.37)	20	0.0386/0.770 (0.0152/0.3031)(0.0275/0.535)	0.0699/1.359	172
1.001 (0.394)	2.827 (1.113)	12.01	325 (47.2)	96.8 (-285.7)	364 (195.2)	267 (480.9)	4501 (1.53)	12,763 (7.81)	2729 (1.67)	20	0.0236/0.474 (0.0093/0.1865)(0.0109/0.217)	0.0277/0.551	127
3.188 (1.255)	9.019 (3.551)	6.00	7.6 (1.1)	94.5 (-289.9)	198 (-103.0)	104 (186.9)	1194 (0.406)	3252 (1.99)	654 (0.34)	20	0.0775/1.551 (0.0305/0.6106)(0.0446/0.664)	0.1133/1.687	176
1.577 (0.621)	4.460 (1.756)	12.64	185 (26.8)	96.8 (-285.7)	262 (10.9)	164 (296.6)	4265 (1.45)	12,714 (7.78)	3007 (1.84)	20	0.0389/0.776 (0.0153/0.3054)(0.0203/0.405)	0.0516/1.029	144
1.285 (0.506)	3.635 (1.431)	28.53	655 (95.0)	96.8 (-285.7)	351 (173.2)	255 (458.9)	9237 (3.14)	28,958 (17.72)	3710 (2.27)	20	0.0259/0.517 (0.0102/0.2034)(0.0169/0.227)	0.0429/0.577	95
1.113 (0.438)	3.145 (1.238)	44.64	1916 (277.9)	101 (-278.2)	394 (250.0)	293 (528.2)	14,443 (4.91)	43,731 (26.76)	7599 (4.65)	20	0.0216/0.433 (0.0085/0.1704)(0.0121/0.151)	0.0307/0.384	87
1.024 (0.403)	2.896 (1.140)	6.00	27 (3.9)	94.5 (-289.9)	394 (250.0)	300 (539.9)	1750 (0.595)	4739 (2.90)	833 (0.51)	20	0.0213/0.425 (0.0084/0.1673)(0.0220/0.439)	0.0559/1.115	132
0.503 (0.198)	1.905 (0.750)	17.21	297 (43.1)	95.2 (-288.7)	394 (250.0)	299 (538.7)	6119 (2.08)	16,358 (10.01)	2353 (1.44)	20	0.0107/0.212 (0.0042/0.0835)(0.0130/0.259)	0.0330/0.658	107
0.315 (0.124)	1.905 (0.750)	46.87	1721 (249.0)	101 (-278.2)	394 (250.0)	293 (528.2)	12,619 (4.29)	31,458 (19.25)	8383 (5.13)	20	0.0102/0.206 (0.0040/0.0810)(0.0119/0.156)	0.0302/0.396	32
2.029 (0.799)	5.740 (2.260)	6.00	7.6 (1.1)	94.5 (-289.9)	232 (-42.9)	137 (247.0)	1456 (0.495)	3612 (2.21)	490 (0.30)	20	0.0526/1.051 (0.0207/0.4137)(0.0436/0.680)	0.1107/1.727	151
1.001 (0.394)	2.835 (1.116)	17.72	261 (37.3)	95.2 (-288.7)	280 (44.7)	185 (333.4)	4354 (1.48)	11,603 (7.10)	2696 (1.65)	20	0.0315/0.632 (0.0124/0.2487)(0.0209/0.405)	0.0531/1.029	117
0.630 (0.248)	1.905 (0.750)	39.84	815 (118.2)	101 (-278.2)	394 (250.0)	293 (528.2)	10,354 (3.47)	30,821 (18.86)	4086 (2.53)	20	0.0251/0.502 (0.0099/0.1977)(0.0136/0.259)	0.0345/0.658	49
3.190 (1.256)	9.027 (3.554)	6.00	3.4 (0.5)	94.5 (-289.9)	180 (-135.2)	86 (154.7)	1162 (0.395)	2893 (1.77)	425 (0.26)	20	0.1059/2.119 (0.0417/0.8341)(0.0648/0.479)	0.1646/1.217	147
1.580 (0.622)	4.470 (1.760)	11.99	104 (15.1)	95.2 (-288.7)	218 (-68.4)	122 (220.3)	4324 (1.47)	12,289 (7.52)	2010 (1.23)	20	0.0508/1.015 (0.0200/0.3995)(0.0328/0.475)	0.0833/1.207	129
0.998 (0.393)	2.819 (1.110)	50.62	381 (55.3)	101 (-278.2)	377 (218.8)	276 (497.0)	16,914 (5.75)	47,817 (29.26)	6847 (4.19)	20	0.0292/0.5850 (0.0115/0.2303)(0.0216/0.364)	0.0549/0.925	72

FOLDOUT FRAME

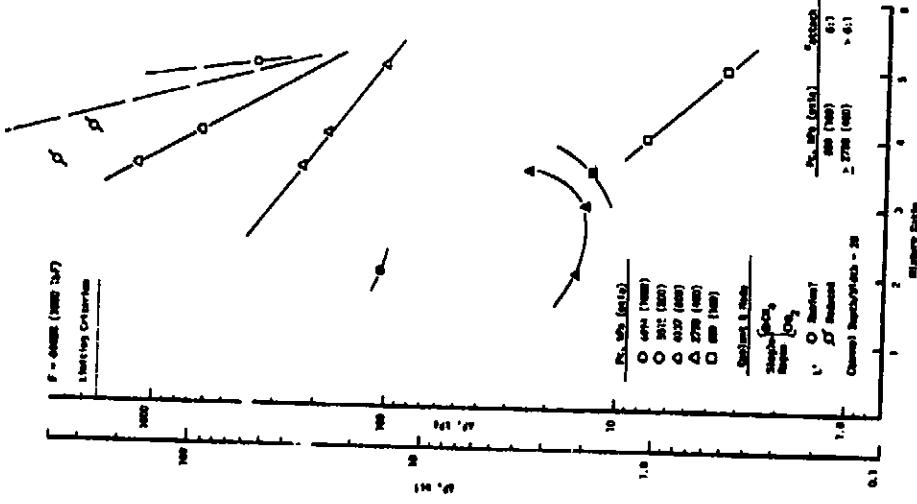


Figure 65. Coolant Pressure Drop for NBP Methane and Oxygen Cooling vs Mixture Ratio, $F = 4448N$ (1000 lbF)

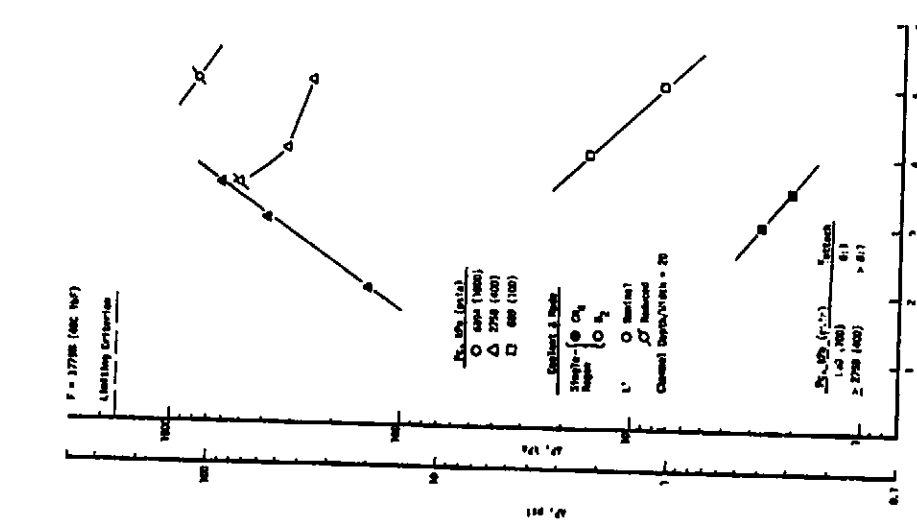


Figure 66. Coolant Pressure Drop for NBP Methane and Oxygen Cooling vs Mixture Ratio, $F = 1779N$ (400 lbF)

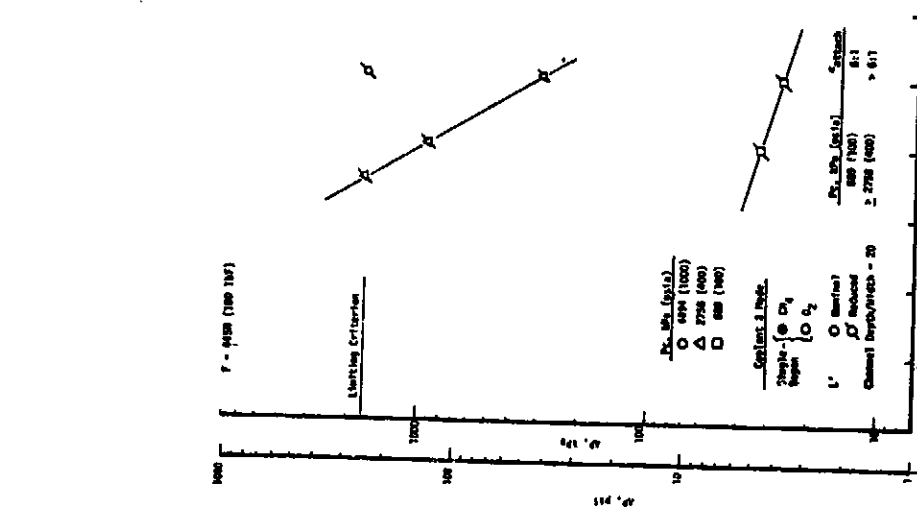


Figure 67. Coolant Pressure Drop for NBP Methane and Oxygen Cooling vs Mixture Ratio, $F = 445N$ (100 lbF)

ORIGINAL PAGE IS
OF POOR QUALITY

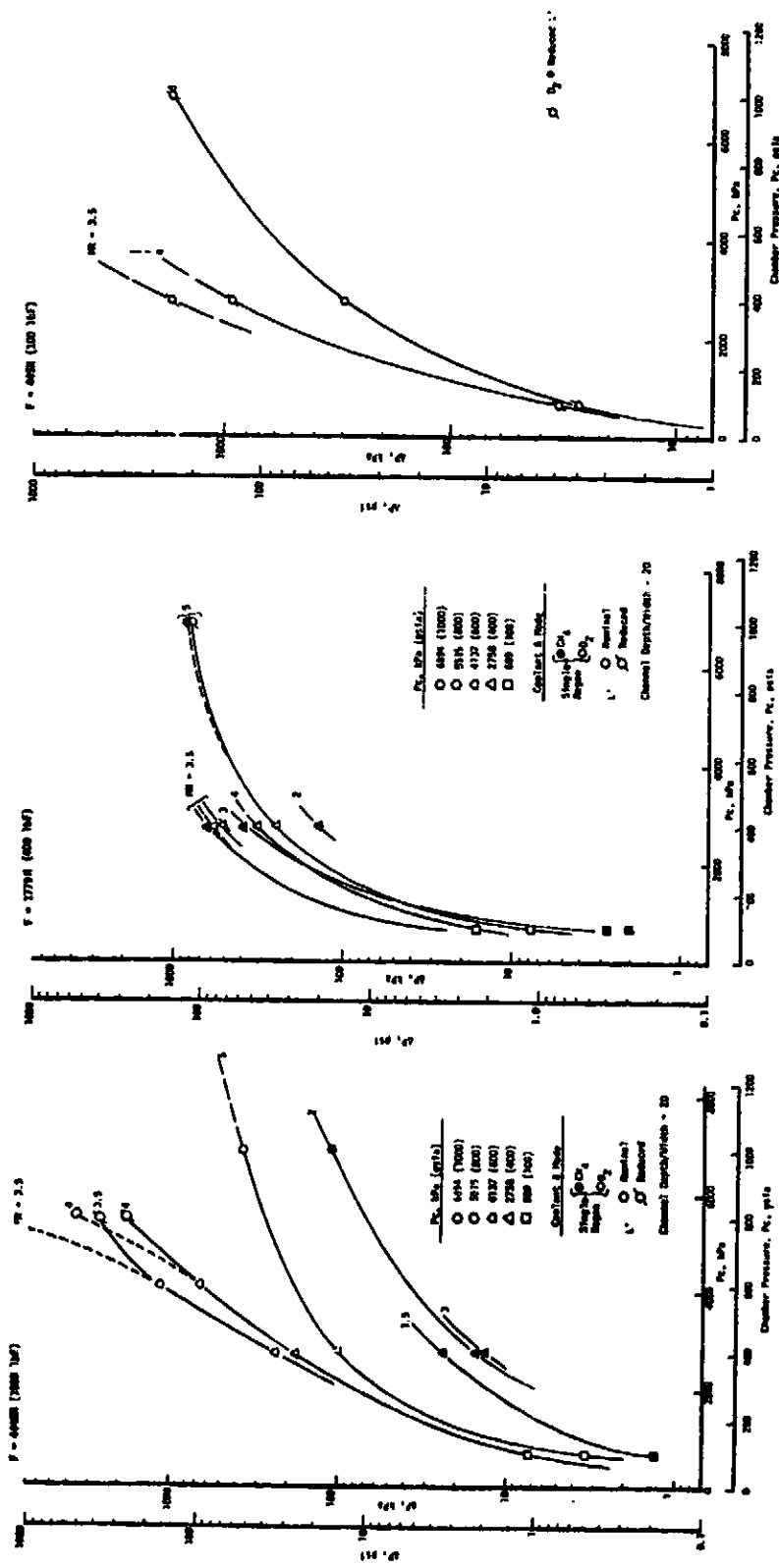


Figure 68. Coolant Pressure Drop for NBP Methane and Oxygen Cooling,
 $F = 4448\text{N}$ (1000 lbf)

Figure 69. Coolant Pressure Drop for NBP Methane and Oxygen Cooling, $F = 1779\text{N}$ (400 lbf)

Figure 70. Coolant Pressure Drop for NBP Methane and Oxygen Cooling, F = 445N (100 lbf)

ORIGINAL PAGE IS
OF POOR QUALITY

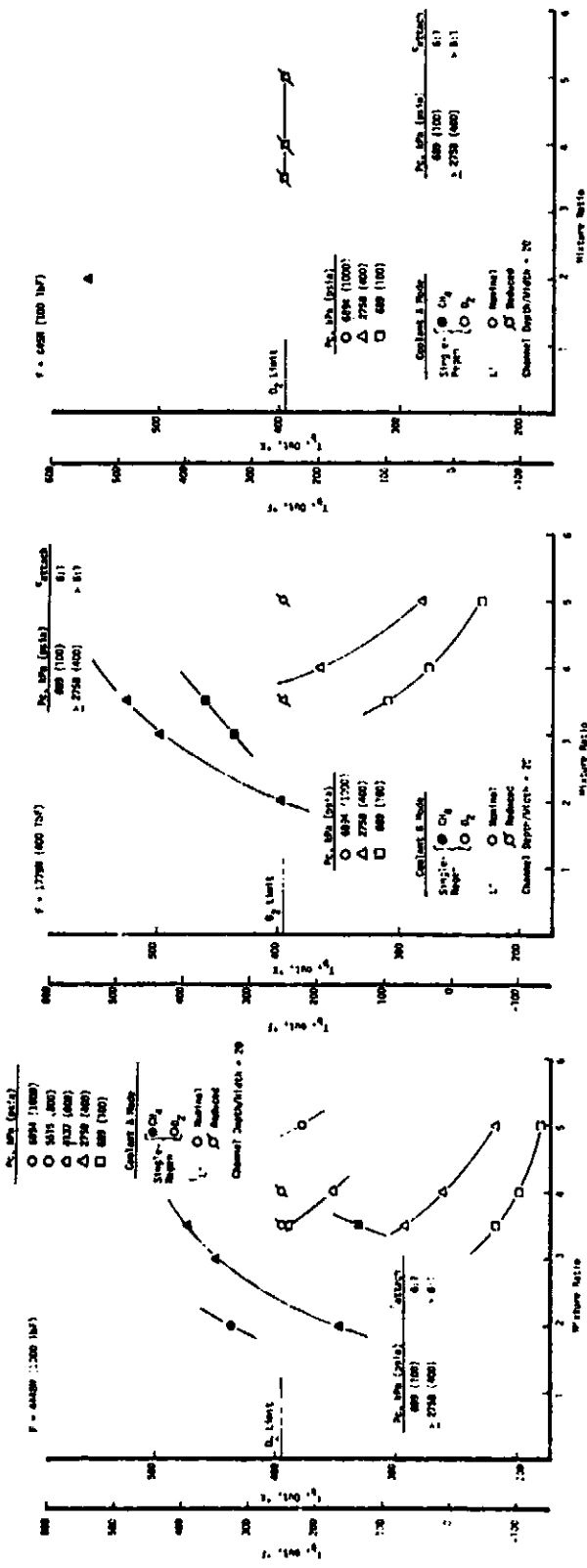


Figure 71. Coolant Discharge Temperature for NBP Methane and Oxygen Cooling,
 $F = 4448\text{N}$ (1000 lbf)

Figure 72. Coolant Discharge Temperature for NBP Methane and Oxygen Cooling,
 $F = 1779\text{N}$ (400 lbf)

Figure 73. Coolant Discharge Temperature for NBP Methane and Oxygen Cooling,
 $F = 445\text{N}$ (100 lbf)

ORIGINAL PAGE IS
OF POOR QUALITY

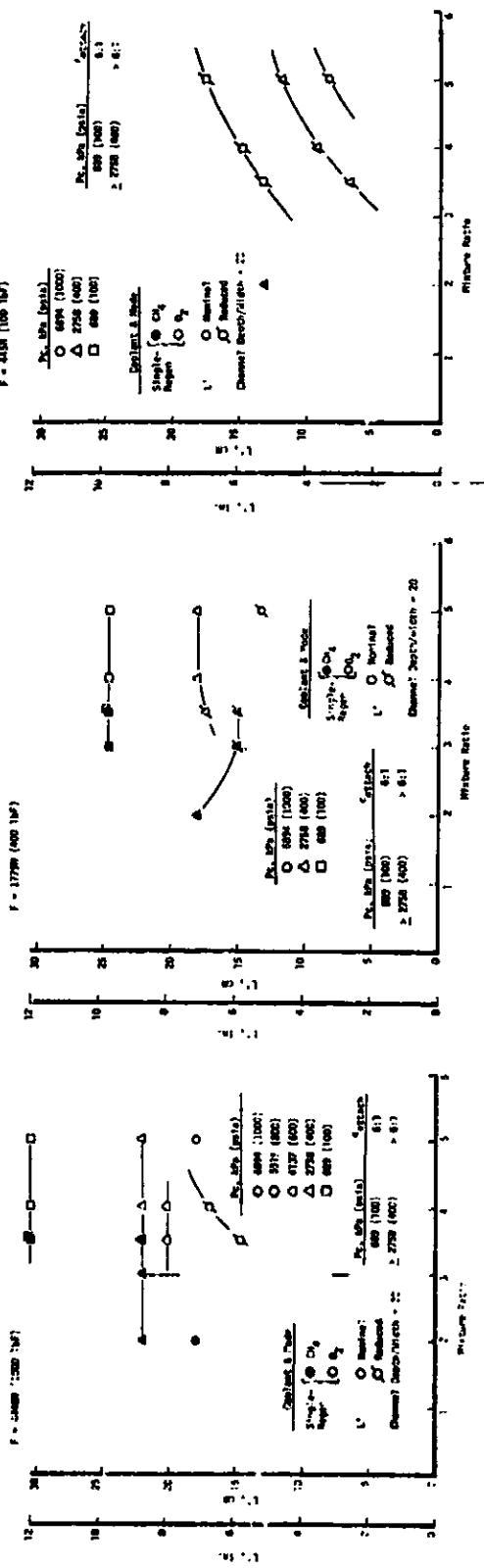


Figure 74. Chamber L' for NBP Methane and Oxygen,
 $F = 4448N (1000 \text{ lbf})$

Figure 75. Chamber L' for NBP Methane and Oxygen,
 $F = 1779N (400 \text{ lbf})$

Figure 76. Chamber L' for NBP Methane and Oxygen,
 $F = 445N (100 \text{ lbf})$

ORIGINAL PAGE IS
OF POOR QUALITY

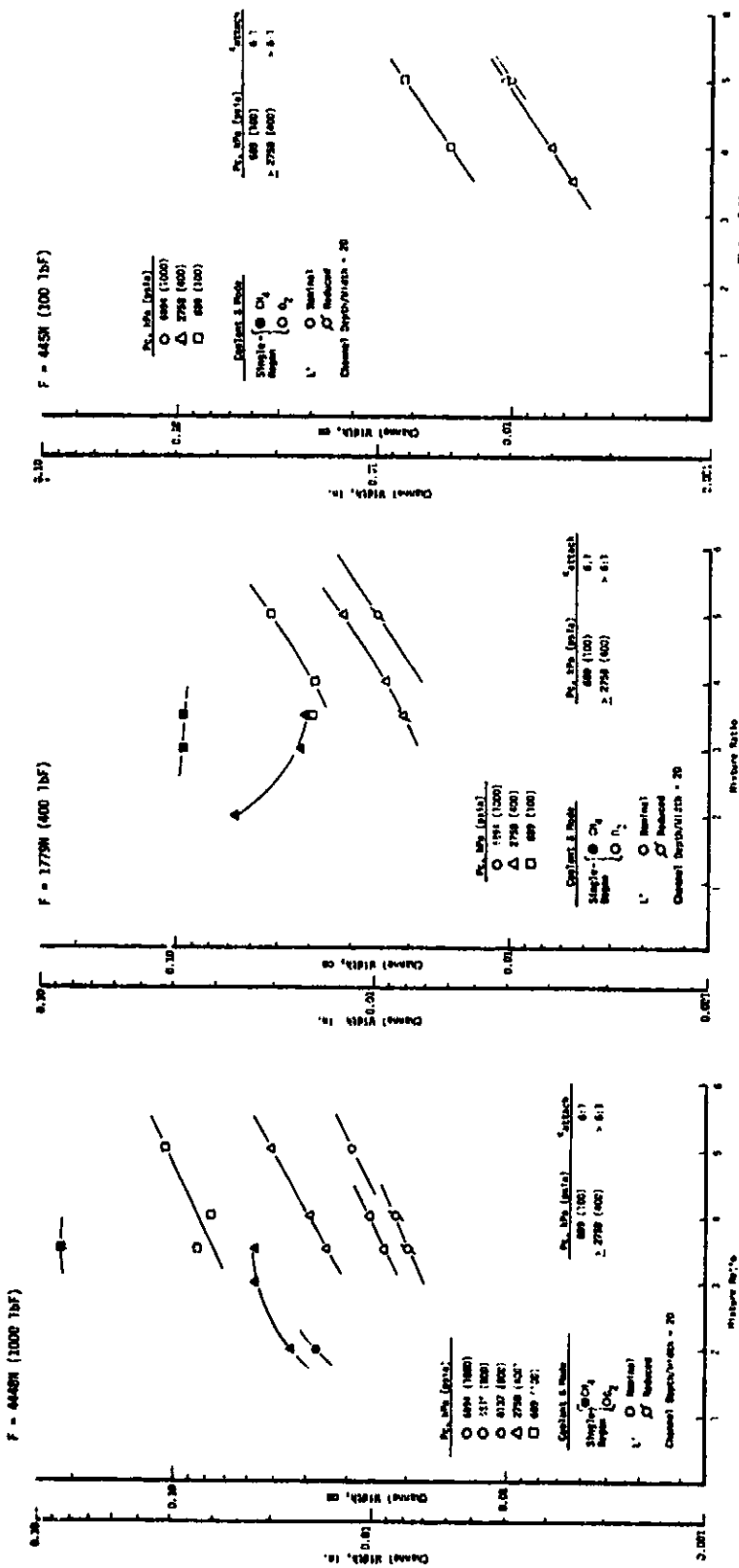


Figure 77. Coolant Channel Width Required for NBP Methane and Oxygen Cooling,
 $F = 4448N$ (1000 lbF)

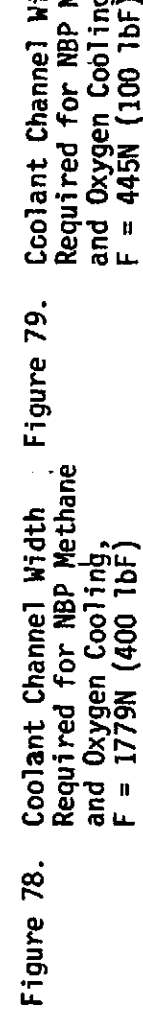


Figure 78. Coolant Channel Width Required for NBP Methane and Oxygen Cooling,
 $F = 1779N$ (400 lbF)

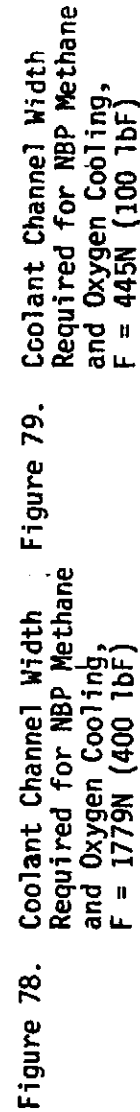


Figure 79. Coolant Channel Width Required for NBP Methane and Oxygen Cooling,
 $F = 445N$ (100 lbF)

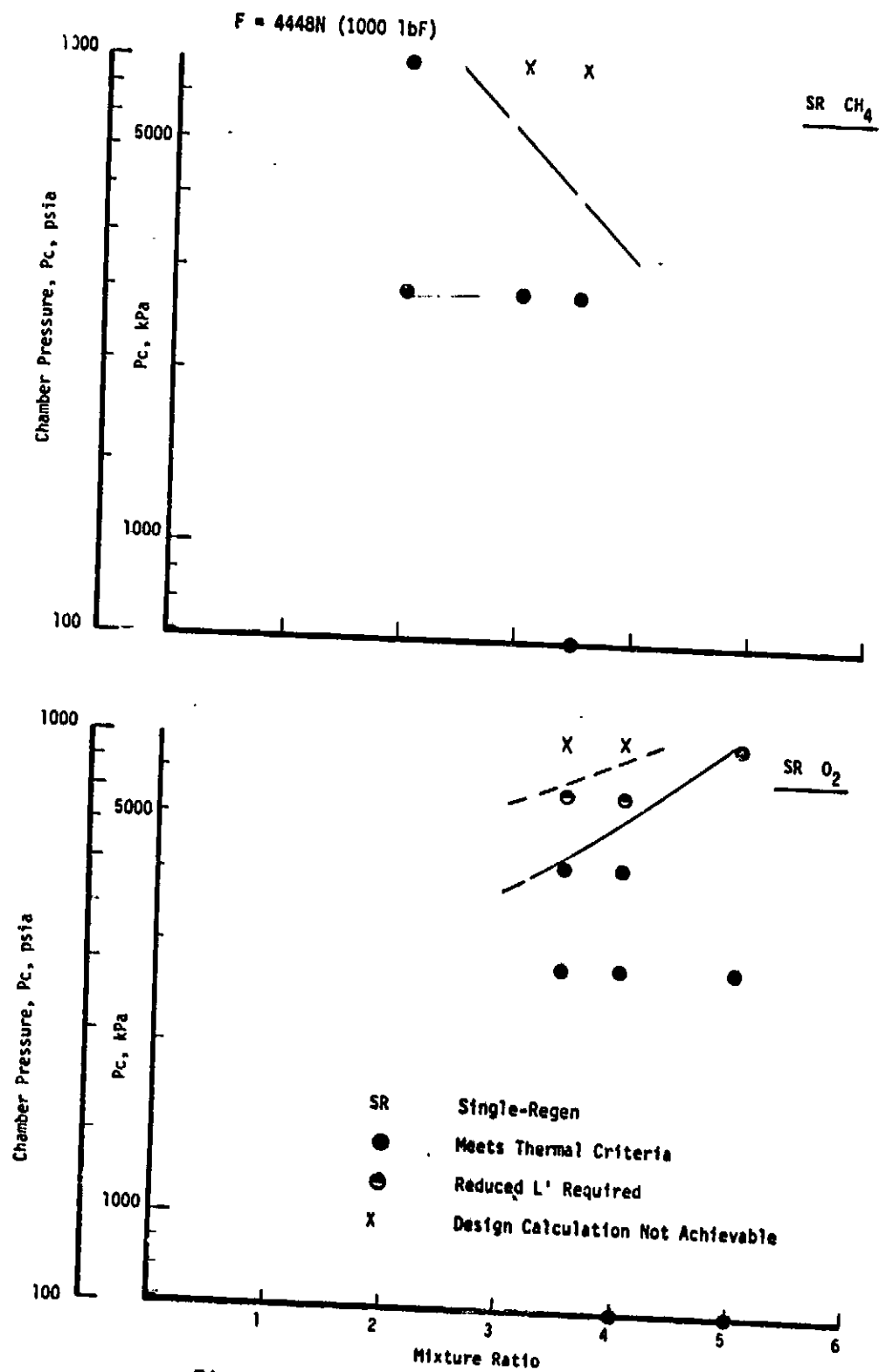


Figure 80. LO_2/LCH_4 Regenerative Cooling Analysis Matrix,
 $F = 4448\text{N} (1000 \text{ lbF})$

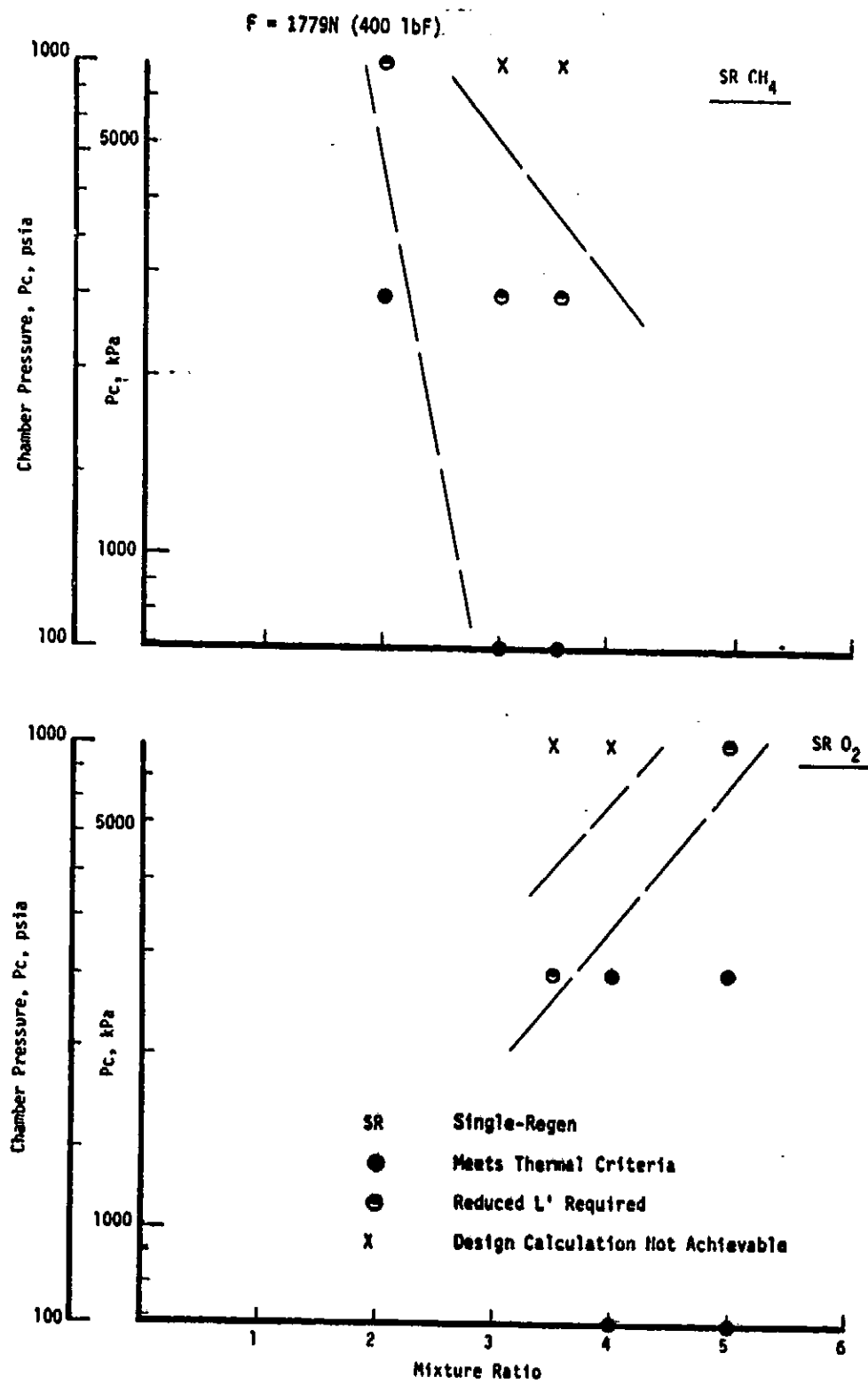


Figure 81. L_2/LCH_4 Regenerative Cooling Analysis Matrix,
 $F = 1779\text{N} (400 \text{lbf})$

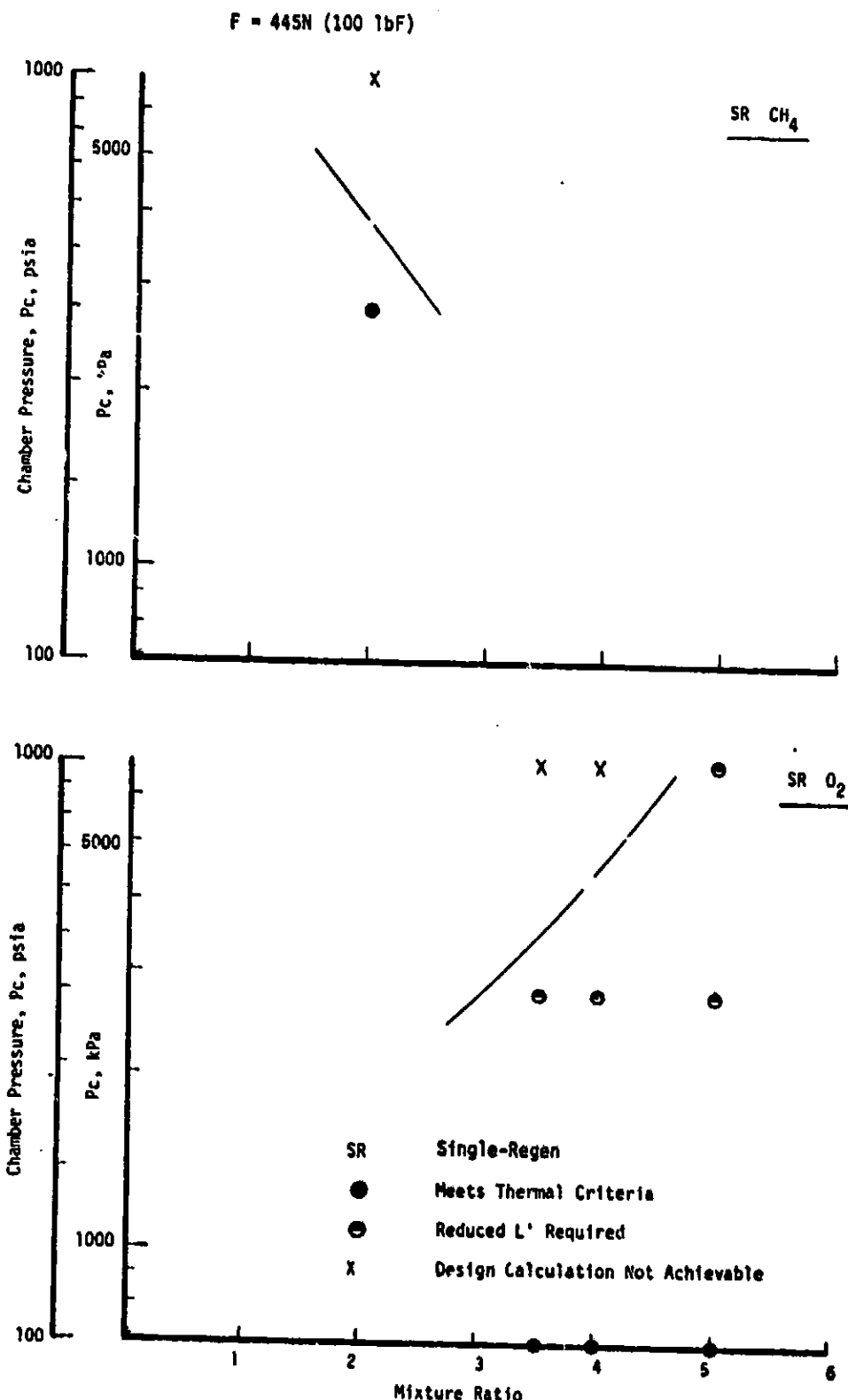


Figure 82. LO_2/LCH_4 Regenerative Cooling Analysis Matrix,
 $F = 445N$ (100 lbF)

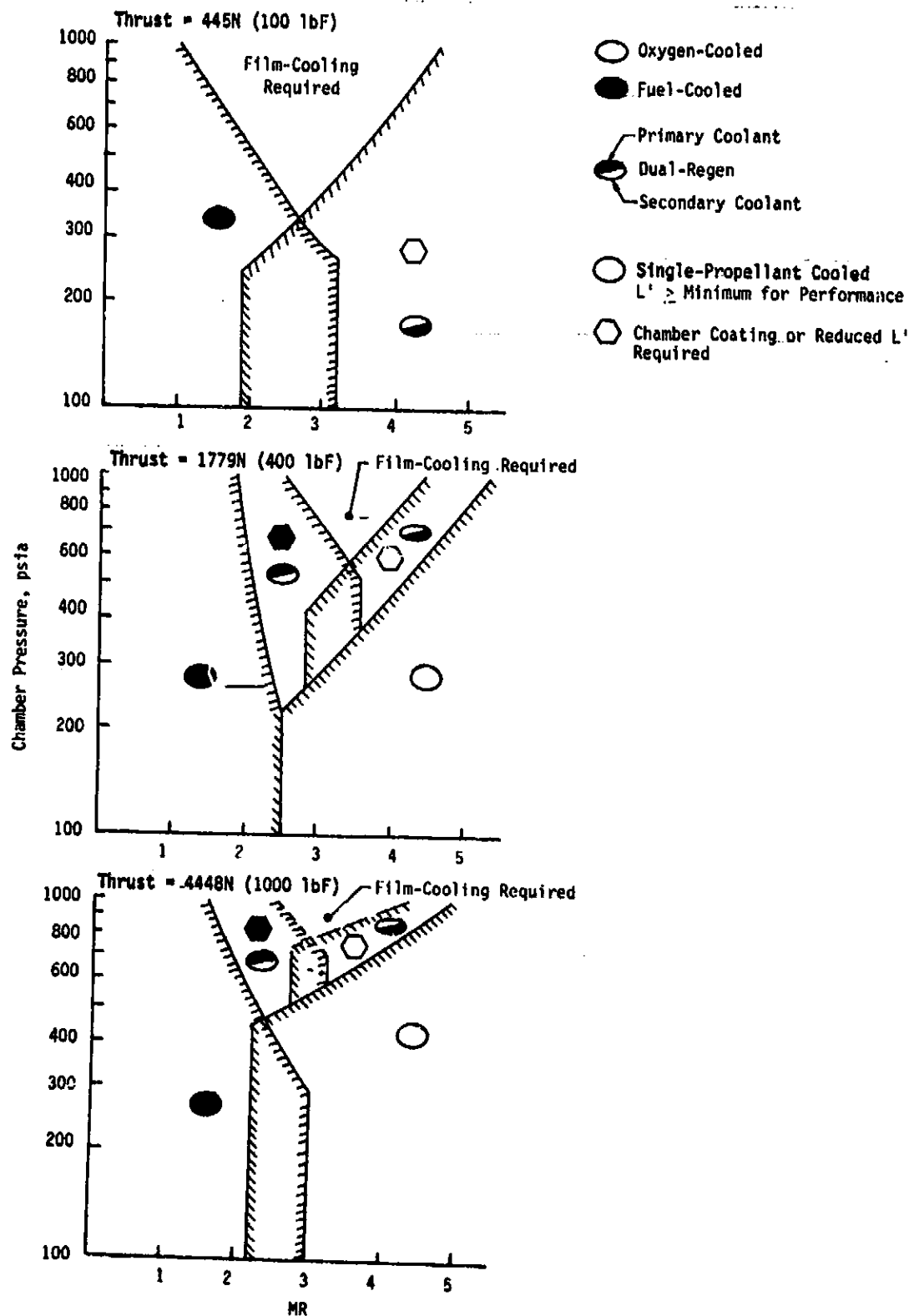


Figure 83. Thrust/Chamber Pressure/Mixture Ratio Operating Limits for Regenerative Cooling Concepts for LO_2/LCH_4 Engines

V, B, Thermal Design (cont.)

3. Single-Propellant Regenerative Cooling Results (Fuel or Oxygen)

a. Coolant Pressure Drop

Channel pressure losses for NBP methane and oxygen as single regenerative coolants in a channel c' aspect ratio = 20 are shown in Figure 65 for a thrust of 4448N (1000 lbF). Acceptable cooling with lower aspect ratio channels was not possible at many design points. At low chamber pressures (< 2758 kPa [400 psia]), methane gives low pressure drops over the mixture ratio range investigated; data trends indicate a rapid increase in ΔP as MR is increased. At a P_c of 6894 kPa (1000 psia), a fuel cooling solution could be achieved only at mixture ratios of 2 or less within the limits of practical ΔP values.

With oxygen cooling, the imposed pressure drop limit of $\Delta P < 1724$ kPa (250 psi) allowed a maximum P_c of about 4137 kPa (600 psia) at an MR of 3.5. For higher P_c values, operation at high mixture ratio or at reduced L' is required if the pressure drop limitation criterion is not to be exceeded. Dual-regen cooling overcomes the need for the reduced L' .

These cooling data, shown cross-plotted in Figure 68, define ΔP versus P_c for lines of constant MR. Methane cooling at the maximum P_c and at the highest thrust can be accomplished only at a low mixture ratio (MR = 2); oxygen cooling is practical only at a high mixture ratio (MR = 5). At lower pressures and at an optimum MR of 3.5, methane cooling offers the advantage of a lower pressure drop.

Pressure drop data for a thrust of 1779N (400 lbF) are shown in Figures 66 and 69. These lower-thrust oxygen data exhibit the same trends as for the high-thrust case, but with the data displaced toward higher ΔP 's. The lack of adequate methane coolant flow at the lower thrust levels leads to higher coolant temperatures, eliminating the reduced pressure loss advantage over oxygen.

In order to remain within the bulk temperature rise limit for oxygen cooling, reduced L' engines are required for a thrust of 445N (100 lbF). A channel aspect ratio of 20 is required in order to hold the pressure loss to the specified limits. The data, shown in Figure 67, are solely for oxygen and continue the trends established at the higher thrusts (Figures 65 and 66). The low fuel coolant flow makes methane cooling impractical at low thrust. The cross-plot of Figure 70 gives the limiting P_c value at $F = 445N$ (100 lbF) for an oxygen coolant ΔP of 250 psi as follows:

V, B, Thermal Design (cont.)

<u>MR</u>	<u>Pc, kPa (psia)</u>
3.5	2758 (400)
4.0	3448 (500)
5.0	6894 (1000)

The limited data on the effect of aspect ratio indicate that the optimization of this parameter is a complex function which is dependent on thrust, mixture ratio, pressure, cycle fatigue effects, and coolant properties. This can be observed by comparing the two cases coded* 2-1-4/F and 3.5-4-1/F taken from Table XVII:

<u>Case 2-1-4/F</u>			
<u>d/w</u>	<u>ΔP, kPa (psi)</u>	<u>d/w</u>	<u>ΔP, kPa (psi)</u>
5	55.16 (8.0)	7	8.96 (1.3)
10	102.73 (14.9)	20	2.76 (0.4)

In the first case, increasing the channel aspect ratio (d/w) increases the pressure drop; in the second case, ΔP is decreased. It is apparent that a more detailed investigation is required to establish the criteria for optimization of channel aspect ratio.

b. Coolant Outlet Temperature

Figures 71 through 73 show the respective outlet bulk temperatures of methane and oxygen as single-regen coolants at the three thrust levels specified for this study. At $F = 4448N$ (1000 lbf), oxygen becomes bulk-temperature-limited at $MR = 3.5$ for chamber pressures above 4137 kPa (600 psia). Increasing the mixture ratio lowers the flux and increases the coolant flow. Oxygen is not bulk-temperature-limited at a mixture ratio of 5 for the highest P_c studied. Methane outlet temperatures range from 328 to 478°K (130 to 400°F) and are suitable for use as a turbine drive fluid in an expander cycle.

*Code = MR - Thrust, lbf - $\frac{P_c, \text{ psia}}{100}$ / Coolant

V, B, Thermal Design (cont.)

Both oxygen and methane discharge temperatures are higher at the mid-thrust level of 1779N (400 lbF) (Figure 72) than they were at 4448N (1000 lbF) (Figure 71). Reduced L' values are required for single-propellant cooling at the higher chamber pressures analyzed. At the lowest thrust level, oxygen outlet bulk temperatures are at the upper limit at all pressures and reduced L' values are required at every design point, as shown in Figure 73. This limitation can be overcome by cooling with both propellants or by the use of thermal liners, discussed in subsequent sections of this report.

c. Chamber L'

The chamber L' values required to meet the coolant ΔP and temperature rise criteria are shown in Figures 74 through 76 for the three thrusts studied. The reduced L' values shown for oxygen result from the maximum bulk temperature limitation. No L' reduction is required for F = 4448N (1000 lbF). Only the highest P_c requires a reduced L' at F = 1779N (400 lbE), whereas every design point at F = 445N (100 lbF) is limited by maximum oxygen temperature. No L' reductions are required if dual-regen cooling is employed.

d. Channel Width

The minimum channel widths calculated for each design point are shown in Figures 77 through 79. These data are cross-plotted in Figures 80-82 using the coordinates thrust versus P_c for a mixture ratio of 3.5 (the optimum performance MR). The cross-plots define the minimum fuel or oxidizer sizes required for a particular design point. The data for oxygen are similar to those determined for oxygen in the LO₂/RP-1 studies (reported in Section III.B) but result in a narrower channel. For example, at P_c = 2758 kPa (400 psia) and MR = 4, minimum channel widths are as follows:

Thrust, F N (lbF)	Minimum Channel Widths	
	LO ₂ /LCH ₄ cm (in.)	LO ₂ /RP-1 cm (in.)
4448 (1000)	0.0389 (0.0153)	0.0513 (0.0202)
1779 (400)	0.0236 (0.0093)	0.0333 (0.0131)
445 (100)	0.0076 (0.0030)	0.0117 (0.0046)

The smaller channels result from the higher heat flux of LOX/methane as compared to the LOX/RP-1 combination.

V, B, Thermal Design (cont.)

Because of the lower fuel density, methane channel widths are larger than those determined for RP-1. The minimum channel width calculated for $F = 1779\text{N}$ (400 lbF) (the lowest practical thrust level), $P_c = 2758 \text{ kPa}$ (400 psia), and $MR = 2$ was 0.0663 cm (0.0261 in.) for a channel aspect ratio of 20:1. The channel width for RP-1 at the same F - P_c - MR combination was 0.0099 cm (0.0039 in.) for a channel aspect ratio of 8:1. The methane data also show a lower sensitivity to mixture ratio than was noted for RP-1. The differences in slope for channel width vs MR at 2758 kPa (400 psia) for the 4448N (1000 lbF) and 1779N (400 lbF) thrust levels are most likely due to coolant bulk temperature/flowrate interactions.

4. Dual-Propellant Regenerative Cooling and Coating Applicability

With single-propellant cooling, the oxygen or methane become heat-absorption-limited based on the allowable coolant discharge temperature. These limitations become significant at low thrust, higher P_c 's, and optimum MR where the total heat flux is high. Operation at a reduced L' provides a simple cooling solution for many of these design points; however, the accompanying performance loss makes this approach undesirable.

The bulk temperature rise limits of a single-propellant coolant can be overcome by (1) dual-regen cooling in which both propellants are used in series flow, or (2) utilization of a thermal resistance liner in the chamber to reduce the heat flow to the coolant.

A comparison of fuel-only (single-regen) and oxidizer-fuel (dual-regen) cooling is given in Table XIX for operation at $F = 1779\text{N}$ (400 lbF), $P_c = 2758 \text{ kPa}$ (400 psia), and $MR = 3.5$. The use of oxygen to cool from the skirt attachment point area ratio ($\epsilon = 12.76$) to the coolant change point area ratio ($\epsilon = 6$) results in a small oxygen pressure drop and temperature rise but provides a 7% decrease in ΔT_b for the methane which cools the throat and chamber. Thus dual-regen cooling for this case results in a lower fuel coolant temperature which can be converted to a longer chamber L' , which, in turn, results in higher performance.

A reduction in coolant discharge temperature from the chamber by either (a) dual-regen cooling which distributes the total heat load to both propellants, or (b) use of chamber coatings or liners which reduce the total heat flow to the coolant, increases the region of regenerative cooling feasibility of the F - P_c - MR maps (shown in Figure 83).

TABLE XIX
 COMPARISON OF SELECTED PARAMETERS FOR SINGLE-REGEN (FUEL)
 AND DUAL-REGEN (OXYGEN-FUEL SERIES) CHAMBER COOLING

PROPELLANTS	O ₂ /CH ₄	O ₂ /CH ₄	
NOMINAL P _c /F	2758/1779 (400/400)	2758/1779 (400/400)	
CASE NO.	Single Regen CH ₄	O ₂	CH ₄
• Thrust, N (lbF)	1779 (400)	1779 (400)	
• P _c , kPa (psia)	2758 (400)	2758 (400)	
• I _{sp} , sec	367.4	367.4	
• Throat Radius, cm (in.)	1.001 (0.394)	1.001 (0.394)	
• Contraction Ratio	8:1	8:1	
• L', cm (in.)	15.16 (5.97)	14.48 (5.70)	
• MR	3.5	3.5	
• w _{ox} , kg/sec (lbm/sec)	0.386 (0.85)	0.386 (0.85)	
• w _f , kg/sec (lbm/sec)	0.109 (0.24)	0.109 (0.24)	
• ΔP _{c.j.} , kPa (psi)	631 (91.6)	3.45 (0.5)	481 (69.8)
• P _{c.j.,-in} , kPa (psia)	7583 (1100)	7101 (1030)	7583 (1100)
• P _{c.j.,-out} , kPa (psia)	6952 (1008.4)	7097 (1029.5)	7102 (1030.2)
• ΔT _{c.j.,} °K (°F)	411 (739.9)	6.7 (12.4)	382 (687.8)
• T _{c.j.,-in} , °K (°F)	114 (-254.2)	97.0 (-285.3)	114 (-254.2)
• T _{c.j.,-out} , °K (°F)	525 (485.7)	104 (-272.9)	496 (433.6)
• Regen ε	12.76:1	12.76:6	6:1
• T _{wg,max} , °K (°F)	816 (1008)	233 (-40)	816 (1009)
• T _{wt,max} , °K (°F)	747 (884)	222 (-60)	492 (885)
• h _{g,max} , kw/m ² °K (Btu/in ² -sec °F)	4.707 (0.00160)	0.6236 (0.000212)	4.707 (0.00160)
• h _{t,max} , kw/m ² °K (Btu/in ² -sec °F)	13.943 (0.00474)	6.295 (0.00214)	17.179 (0.00584)
• Q/A _{g,max} , kw/m ² (Btu/in ² -sec)	13025 (7.97)	1945 (1.19)	13041 (7.98)
• Q/A _{t,max} , kw/m ² (Btu/in ² -sec)	4167 (2.55)	343 (0.21)	3857 (2.36)
• Q _{total} , watt (Btu/sec)	162264 (153.9)	4428 (4.2)	151405 (143.6)
• T _r , °K (°F)	3569 (5964.3)	3477 (5498)	3314 (5964.3)
• Wall Thickness, cm (in.)	0.762 (0.300)	0.762 (0.300)	
• V _{c.j.-max} , m/sec (ft/sec)	86.9 (285)	1.65 (5.4)	111.6 (366)
• M _{c.j.-max}	0.154	0.002	0.196
• No. Channels	106	131	103
• Min. Chan. Depth, cm (in.)	0.066 (0.026)	0.612 (0.241)	0.079 (0.031)
• ΔP _{c.j./P_c}	0.229	0.00125	0.1745
• Limiting Criterion	Gas-Side Wall Temp.	Channel Aspect Ratio of 20	Gas-Side Wall Temp.

V, B, Thermal Design (cont.)

5. Thermal Conclusions for NBP LO₂/LCH₄ Cooling

The analyses of the oxygen/methane propellant system further substantiate the conclusion drawn from the LO₂/RP-1 and LO₂/LH₂ studies that TCA cooling channel widths are highly sensitive to thrust, chamber pressure, mixture ratio, and channel aspect ratio. The analysis of methane and oxygen as coolants has shown that regenerative cooling feasibility depends largely on selecting proper channel widths and aspect ratios. The use of smaller, high-aspect-ratio channels provides an effective method of extending the range of regenerative cooling which, in turn, means higher performance due to elimination of losses associated with the use of less efficient cooling methods. It must be emphasized, however, that these results are applicable only for a high thermal conductivity alloy such as copper which allows for very effective fin heat transfer and, thus, excellent flux transformation.

The analysis matrices for the three thrust levels studied are given in Figures 80 through 82. Each design point analyzed is coded to indicate design feasibility status; approximations for boundaries have been sketched to delineate regions of differing feasibility.

The use of methane as a single-regen coolant provides design feasibility at P_c's of roughly 3448 kPa (500 psia) or less at MR's from 2 to 3.5 -- the most likely range for use of methane. As shown in Figure 65, pressure drop becomes very large at higher P_c's and mixture ratios above 2.

The use of oxygen as a single-regen coolant is feasible at high mixture ratios at P_c's between 4137 and 6894 kPa (600 and 1000 lbF). Oxygen cooling is marginal at higher P_c's at the lower mixture ratio and does not appear feasible at 6894 kPa (1000 psia) for MR's of 3.5 and 4. Again the data of Figure 65 show that very high pressure drops and narrow channels are required to approach this region on the F-Pc-MR map.

At 1779N (400 lbF), the feasible design region has decreased while the marginal and nonfeasible areas have increased (Figure 81).

The analyses performed at F = 445N (100 lbF) showed even less cooling capability for oxygen; this is evident in Figure 82. In all cases, the bulk temperature limitation of single-propellant cooling results in a reduced chamber L' and reduced Isp.

One detailed dual-regen analysis was performed for F = 1779N (400 lbF), P_c = 2758 kPa (400 psia), and MR = 3.5. Oxygen was selected to regeneratively cool the divergent nozzle from $\epsilon = 12.76$ to $\epsilon = 6$. Pressure drop and temperature rise were found to be minimal, i.e., 1.4 kPa (0.2 psia)

V, B, Thermal Design (cont.)

and 6.9°K (12.4°F). Methane was then selected to cool the balance of the regeneratively cooled chamber. In comparing these results to single-regen cooling with methane, the ΔP was reduced from 632 kPa (91.6 psia) to 481 kPa (69.8 psia) and the outlet bulk temperature from 525.4°K (485.7°F) to 496.4°K (433.6°F). Channel minimum widths increased slightly from 0.041 cm (0.016 in.) to 0.044 cm (0.017 in.).

The net results for the Task IV study of the oxygen-methane propellant combination are displayed in Figure 83 which provides F-Pc-MR operating maps delineating approximate cooling concept areas. At the highest thrust, regenerative cooling must be augmented by other performance-degrading concepts only at the highest Pc's near the optimum mixture ratio. This augmented region increases as thrust is decreased.

C. PERFORMANCE SENSITIVITY

1. Performance Model

The performance model used was essentially the same as in the previous sections for LOX/RP-1 and LOX/hydrogen. Calibration for oxygen-methane used OFO triplet element data from the NASA-LeRC Hydrocarbon Fuel Engine Injector Evaluation (Ref. 7).

2. Attainable Isp for NBP LOX/LCH₄

Unlike the oxygen-hydrogen engines which can successfully use fuel-regenerative cooling at all operating points, only a limited number of operating points are possible with methane or oxygen cooling. As can be seen from Table XX and Figure 84, fuel-regen cooling is feasible for mixture ratios less than 3.5 at a Pc of 2758 kPa (400 psia) and thrusts of 4448 and 1779N (1000 and 400 lbF). By increasing the mixture ratio from 2 to 3.5 at the two thrust levels, performance increased 12.3% and 9.9%, respectively.

Table XXI documents the results of the oxygen regen-cooled cases. Oxygen regen-cooling can be used for mixture ratios greater than 3.5 [Pc = 2758 kPa (400 psia)] in the mid-Pc design range. By varying the mixture ratio from 3.5 to 5, performance decreased by 4.3% at 445N (100 lbF) thrust and 6.8% at 4448N (100 lbF) thrust. With MR = 3.5, either oxygen or fuel regen-cooling could be used at Pc = 2758 kPa (400 psia).

The benefits of dual-regen cooling in improving performance are tabulated in Table XII. As can be seen in Figure 84, the most significant performance improvements occur at the lowest thrust level. Figures 85

TABLE XX
LOX/LCH₄ RESULTS FOR

FUEL-REGEN-COOLED CASES

<u>N (1bf)</u>	<u>p_c kPa (psi a)</u>	<u>M_K</u>	<u>L' cm (in.)</u>	<u>T_f °K (°R)</u>	<u>ε_c</u>	<u>NEI</u>	<u>EFE %</u>	<u>Delivered Isp (sec)</u>
4448 (1000)	6894 (1000)	2.0	15.49 (6.10)	394 (710.0)	8.0	23	1.00	332.6
	2758 (400)	2.0	22.10 (8.70)	347 (624.3)	8.0	61	1.00	333.5
1779 (400)	3.0	18.97 (7.47)	394 (710.0)	8.0	57	0.995	374.8	
	3.5	17.70 (6.97)	394 (710.0)	8.0	55	0.985	374.6	
689 (100)	2.0	17.83 (7.02)	394 (710.0)	8.0	22	1.00	333.5	
	3.0	11.51 (4.53)	394 (710.0)	8.0	21	0.986	366.7	
689 (100)	3.5	11.51 (4.53)	394 (710.0)	8.0	20	0.965	366.6	
	3.0	22.02 (8.67)	394 (710.0)	8.0	93	0.999	368.6	
689 (100)	3.5	20.75 (8.17)	394 (710.0)	8.0	92	0.998	363.4	

$T_{ox} = 90.6 \text{ °K (163 °R)}$

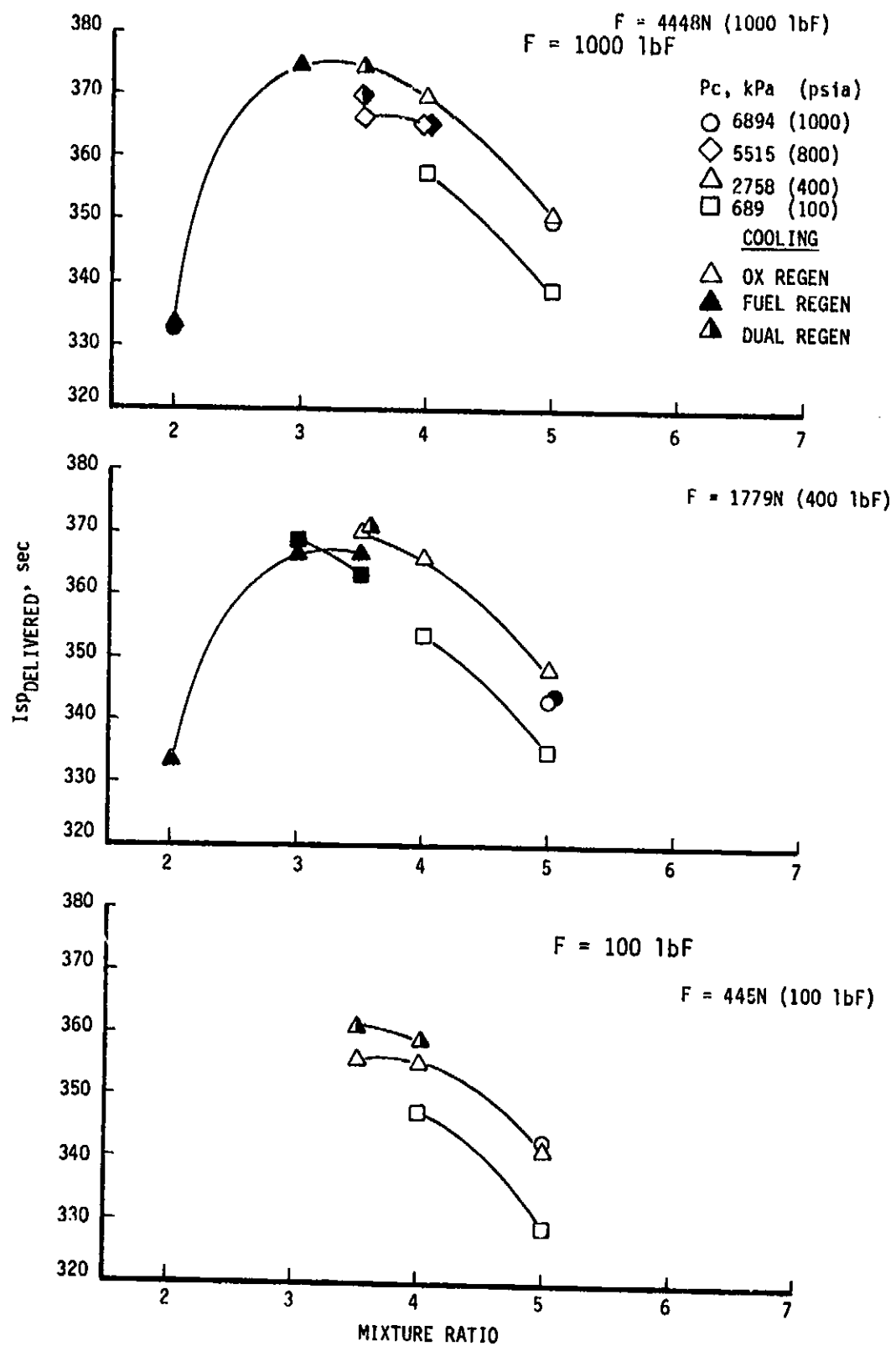


Figure 84. Predicted LOX/LCH₄ Performance as a Function of Mixture Ratio for 4448, 1779, and 445N (1000, 400, and 100 lbF)

TABLE XXI

 LOX/LCH₄ RESULTS FOR
 OXYGEN-REGEN-COOLED CASES

<u>F</u>	<u>P_c</u>	<u>L'</u>	<u>T_{ox}</u>	<u>ε_c</u>	<u>NEI</u>	<u>ERE %</u>	<u>Delivered Isp (sec)</u>
<u>N (lbF)</u>	<u>kPa (psia)</u>	<u>MR</u>	<u>cm (in.)</u>	<u>°K (°R)</u>			
4448 (1000)	5515 (800)	3.5	14.68 (5.78)	394 (710.0)	8.0	26	0.956 366.3
	5515 (800)	4.0	16.97 (6.68)	394 (710.0)	8.0	25	0.953 365.1
6894 (1000)	5.0	18.03 (7.10)	377 (678.8)	8.0	20	0.973	349.8
2758 (400)	3.5	22.10 (8.70)	292 (525.9)	8.0	55	0.987	374.9
	4.0	22.10 (8.70)	262 (470.8)	8.0	54	0.979	369.6
	5.0	22.10 (8.70)	256 (460.0)	8.0	55	0.995	350.9
689 (100)	4.0	30.48 (12.0)	198 (357.0)	8.0	231	0.986	357.4
	5.0	30.48 (12.0)	180 (324.8)	8.0	234	0.996	339.0
1779 (400)	6894 (1000)	5.0	13.28 (5.23)	394 (710.0)	9.20	7	0.951
	2758 (400)	3.5	12.19 (4.80)	394 (710.0)	14.33	38	0.975
	4.0	18.03 (7.10)	364 (655.2)	8.0	19	0.969	365.8
	5.0	18.03 (7.10)	280 (504.7)	8.0	20	0.989	343.2
689 (100)	4.0	24.64 (9.70)	275.2 (495.4)	8.0	91	0.986	369.7
	5.0	24.64 (9.70)	232 (417.4)	8.0	93	0.995	353.6
445 (100)	6894 (100)	5.0	8.38 (3.30)	394 (710.0)	36.62	7	0.944
	2758 (400)	3.5	7.24 (2.85)	394 (710.0)	14.40	7	0.945
	4.0	9.19 (3.62)	394 (710.0)	14.75	7	0.945	355.3
	5.0	11.84 (4.66)	394 (710.0)	14.40	7	0.976	341.1
689 (100)	4.0	14.81 (5.83)	394 (710.0)	8.0	21	0.983	347.3
	5.0	17.65 (6.95)	394 (710.0)	8.0	21	0.994	329.0

 $T_{fuel} = 111 \text{ °K (200 °R)}$

TABLE XXII
 LOX/LCH₄ RESULTS FOR DUAL-REGEN COOLING

F N (1bF)	p _c kPa (psia)	MR	L' cm (in.)	ϵ_c	NEL	ERF %	Delivered Isp (sec)
4448 (1000)	5615 (800)	3.5	18.29 (7.2)	8.0	26	0.962	368.9
	5515 (800)	4.0	22.10 (8.7)	8.0	25		366.2
1779 (400)	2758 (400)	3.5	14.48 (5.7)	14.3	38	0.979	371.1
	6894 (1000)	5.0	14.48 (5.7)	9.2	7	0.954	344.3
445 (100)	2758 (400)	3.5	13.21 (5.2)	14.4	7	0.961	361.8
	2758 (400)	4.0	13.21 (5.2)	14.7	7	0.955	358.4
689 (100)	4.0	14.73 (5.8)	8.0	21	0.983	347.3	
	6894 (1000)	5.0	10.67 (4.2)	36.6	7	0.961	344.7
2758 (400)	5.0	13.21 (5.2)	14.4	7	0.978	341.6	
	689 (100)	5.0	17.78 (7.0)	8.0	21	0.994	329.0

V, C, Performance Sensitivity (cont.)

through 87 show that when real injector ERE is considered, the peak performance generally occurs at $P_c = 2758 \text{ kPa}$ (400 psia) for a constant thrust. The general trend is that performance increases from $P_c = 689 \text{ kPa}$ (100 psia) to $P_c = 2758 \text{ kPa}$ (400 psia) and then decreases from $P_c = 2758 \text{ kPa}$ (400 psia) to $P_c = 6894 \text{ kPa}$ (1000 psia). At high P_c , chamber diameter, element quantity, and ERE decrease as indicated in Tables XXI and XXII, resulting in lower performance.

The potential Isp improvements attainable by utilizing more efficient injectors are indicated by the dotted curves. More efficient injectors can be achieved by improved element design or by use of a larger quantity of smaller elements per unit area of injector face. The real injector prediction lines are based on 0.93 elements/cm² (6 elements/in.²) surface face. Another approach to improving the injector efficiency by adding elements would be to keep the element density fixed and increase the chamber contraction ratio to allow more elements to be packaged.

The respective maximum LOX/LCH₄ Isp for real and ideal injectors for coolable chambers are compared in the following table:

<u>Thrust, F N (lbF)</u>	<u>Injector</u>	<u>MR</u>	<u>Chamber Pressure, P_c kPa (psia)</u>	<u>Isp, sec</u>	<u>Cooling</u>
4448N (1000)	Ideal	3.5 to 4	5515N (800)	383	--
	Real	3.5	2758N (400)	375	Fuel or Oxygen
1779N (400)	Ideal	3.5	2758N (400)	380	--
	Real	3.5	2758N (400)	371	Dual-Regen
445N (100)	Ideal	3.5	2758N (400)	377	--
	Real	3.5	2758N (400)	362	Dual-Regen
	Real	3.5	2758N (400)	356	Oxygen

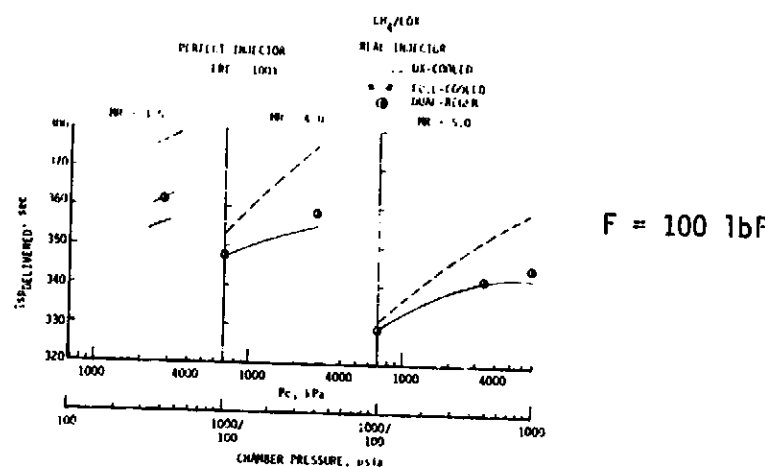


Figure 85.—Delivered Performance vs Chamber Pressure for 485H (100 lbF)

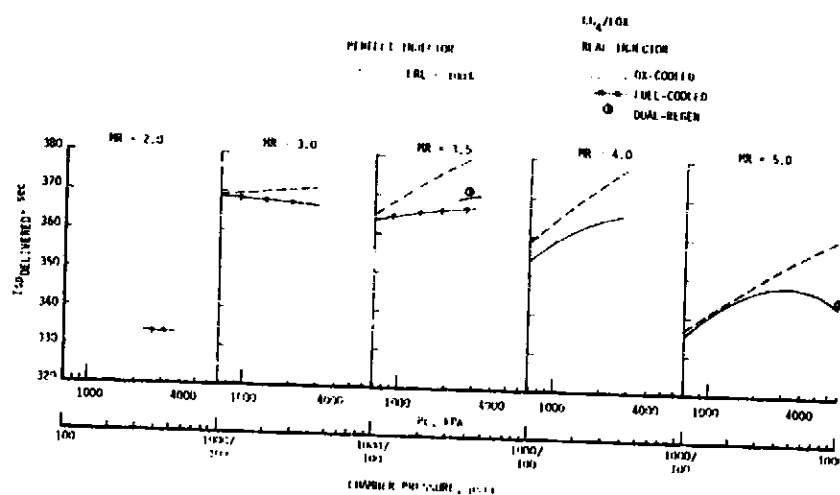


Figure 86. Delivered Performance vs Chamber Pressure for 1779N (400 lbF)

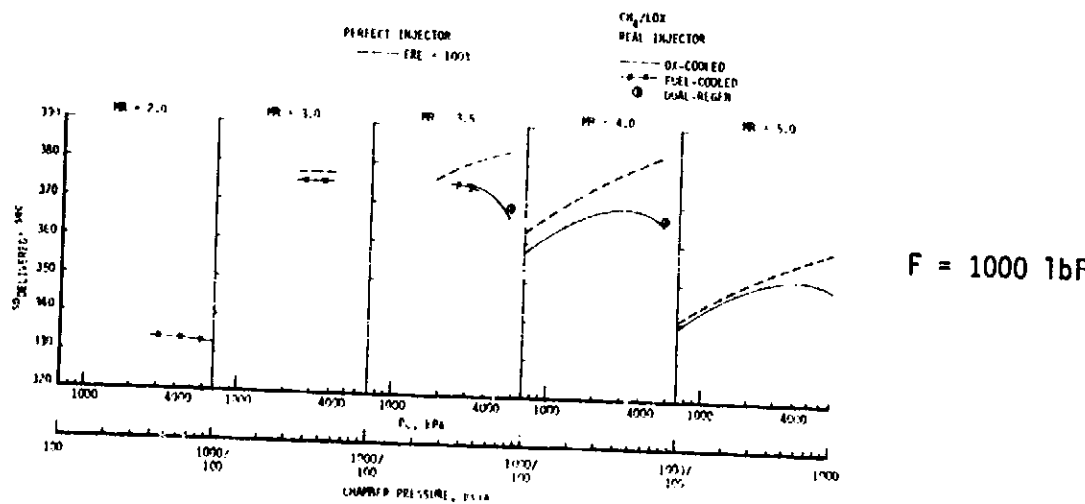


Figure 87. Delivered Performance vs Chamber Pressure for 4448N (1000 lbF)

V, C, Performance Sensitivity (cont.)

3. Performance Conclusions for LOX/Methane

From these data, the following general conclusions may be made:

- ° The peak performance generally occurs at a mixture ratio of 3.5 ± 0.5 for LOX/methane.
- ° When real injector effects are considered, maximum specific impulse is obtained at the intermediate chamber pressure levels [2758 kPa (≈ 400 psia)] except for the low-thrust [445N (≈ 100 lbf)] high chamber pressure condition. In all cases, maximum specific impulse is obtained at the maximum steady thrust level [6894N (1000 lbf)].
- ° When higher-efficiency injectors become available, the maximum Isp will occur at the highest coolable chamber pressure.

PRECEDING PAGE BLANK NOT FILMED

REFERENCES

1. Mellish, J.A. and Bassham, L.B., Low-Thrust Chemical Rocket Engine Study, Final Report, Contract NAS 3-21940, ALRC, 14 January 1981.
2. Thompson, W.R., Thrust Chamber Cooling Analysis (Task II), Low-Thrust Chemical Rocket Engine Study, TAR 9751:0424, Contract NAS 3-21940, ALRC, 5 March 1980.
3. ——— Thompson, W.R., Follow-On Thrust Chamber Cooling Analysis, Low-Thrust Chemical Rocket Engine Study, TAR 9751:0528, Contract NAS 3-21940, ALRC, 14 August 1980.
4. Nickerson, G.R. et al., The Two-Dimensional Kinetic (TDK) Rocket Nozzle Analysis Reference Computer Program, December 1973.
5. Pieper, J.L., ICRPG Liquid Propellant Thrust Chamber Performance Evaluation Manual, CPIA 178, September 1968.
6. Blubaugh, A.L. and Schoenman, L., Extended Temperature Range ACPS Thruster Investigation, Final Report, Contract NAS 3-16775, CR-134655, August 1974.
7. Pavli, A.J., Design and Evaluation of High-Performance Rocket Engine Injectors for Use with Hydrocarbon Fuels, NASA TM-79319, 1979.

PRECEDING PAGE BLANK NOT FILMED

APPENDIX A

SIMPLIFIED THERMAL MODEL

PRECEDING PAGE BLANK NOT FILMED

APPENDIX A

I. Introduction

II. Thermal Design Model and Inputs

1. Modified Channel Thermal Design Program (SCALEF)
2. Gas-Side Heat Transfer
3. Attachment Area Ratio for a Radiation-Cooled Nozzle Extension
4. Engine Contour
5. Channel Design Constraints
6. Propellant Properties
7. Coolant Correlations
8. Coolant Limitations

References

FIGURE LIST

Figure No.

- A-1 Generalized Heat Transfer Model for Regeneratively and Radiation-Cooled Chambers
- A-2 Schematic of SCALER and SCALEF Wall Conduction Model
- A-3 Gas-Side Heat Transfer - Turbulent Regime
- A-4 Simplified Gas-Side Heat Transfer Characteristics for Low-Thrust Engines, Considering Boundary Layer Laminarization and Transition Flow
- A-5 Gas-Side Boundary Layer Flow Regimes
- A-6 Attachment Area Ratio for Radiation-Cooled Skirt
- A-7 Chamber and Initial Nozzle Selection Contour
- A-8 Sensitivity of Attainable Specific Impulse, Chamber L', and Chamber Heat Flux to Chamber Contraction Ratio
- A-9 Allowable Channel Aspect Ratio as a Function of Hot Gas-Side Wall Temperature for Zr-Cu Aged at 867°K (1100°F)
- A-10 Effect of Chamber Pressure on Pressure Drop and Channel Aspect Ratio with Supercritical Oxygen as Coolant
- A-11 Unique Design Requirements for Regeneratively Cooled Chambers at Low Thrusts and High Chamber Pressures
- A-12 Sensitivity of Channel Design Characteristics to Throat Land Width
- A-13 Allowable Coolant Pressure Drop for LO₂/LCH₄

PROGRESS REPORT NUMBER 1

I. INTRODUCTION

The primary objective of the Task I thermal analysis effort was to identify candidate cooling concepts and to develop a simplified thermal design process. The resulting design model for regeneratively cooled chambers is capable of providing preliminary designs for a wide range of design variables with a simplified input and at lower computational cost per case. Cooling analyses utilizing any of the three candidate fuels, oxygen, or combined fuel and oxygen cooling are possible.

The objectives of Task II were to evaluate the thermal model and the selected design criteria by performing preliminary regenerative cooling channel design studies on the LO₂/RP-1 system. Thrusts of 667, 1779, and 3114N (150, 400 and 700 lbF), P_c's of 689, 2758 and 5515 kPa (100, 400, and 800 psia) were studied at mixture ratios of 2 and 4 as specified in the contractual statement of work. These calculations resulted in chamber geometric proportioning criteria, such as contraction ratio ϵ_c , and other specifications used to complete the balance of the study.

II. THERMAL DESIGN MODEL AND INPUTS

◦ DEVELOPMENT AND VERIFICATION OF ANALYTIC MODELS (TASKS I AND II)

The primary objective of the thermal analysis effort in Task I was to modify existing computer thermal design programs to provide (1) automated optimization of channel design variables at two critical locations -- the maximum heat flux point and the maximum bulk temperature point -- and (2) simplification of computational techniques to facilitate parametric studies of engine design variables at minimum cost in computer and engineering time. This methodology was then evaluated in the Task II preliminary studies of the LO₂/RP-1 propellant combination. This program modification and its more significant features and input variables are discussed below.

1. Modified Channel Thermal Design Program (SCALEF)

A generalized heat transfer model for regeneratively and radiation-cooled chambers is depicted in Figure A-1. In this study, lower-performing mass transfer cooling, such as film and transpiration cooling, was advised only when a regenerative cooling configuration meeting thermal criteria could not be developed. The gas-side film resistance accounted for boundary layer laminarization effects. Soot resistance (hot-wall carbon deposition) was not included in the model; a clean chamber wall condition was assumed. A manufactured thermal liner with a specified resistance was employed to reduce the chamber heat flux in those cases where the total heat load to the coolant was excessive. Such liners were applied only to the cylindrical chamber region where the heat flux was low. The fin model of the chamber wall includes a simplified two-dimensional effect, as shown in Figure A-2. The coolant film resistance was based on appropriate design correlations for single-phase fluid in forced convection.

The need for a more flexible and rapid design feasibility program to facilitate parametric thermal analysis was recognized from the onset of this study effort. The ALRC SCALER thermal design code program was modified to provide greater internal cooling channel optimization parameters, such as variable width and depth at the critical points of maximum heat flux and maximum coolant temperature, and to accept some loss in station design detail. The resulting computer program, SCALEF (documented in Ref. A-1), provides the following features:

directly from (1) The hot-gas heat transfer coefficient is calculated

$$h_g = C_g DB (T_f) [W_T F_{2D} (T_e/T_f)]^{0.8} D^{-1.8},$$

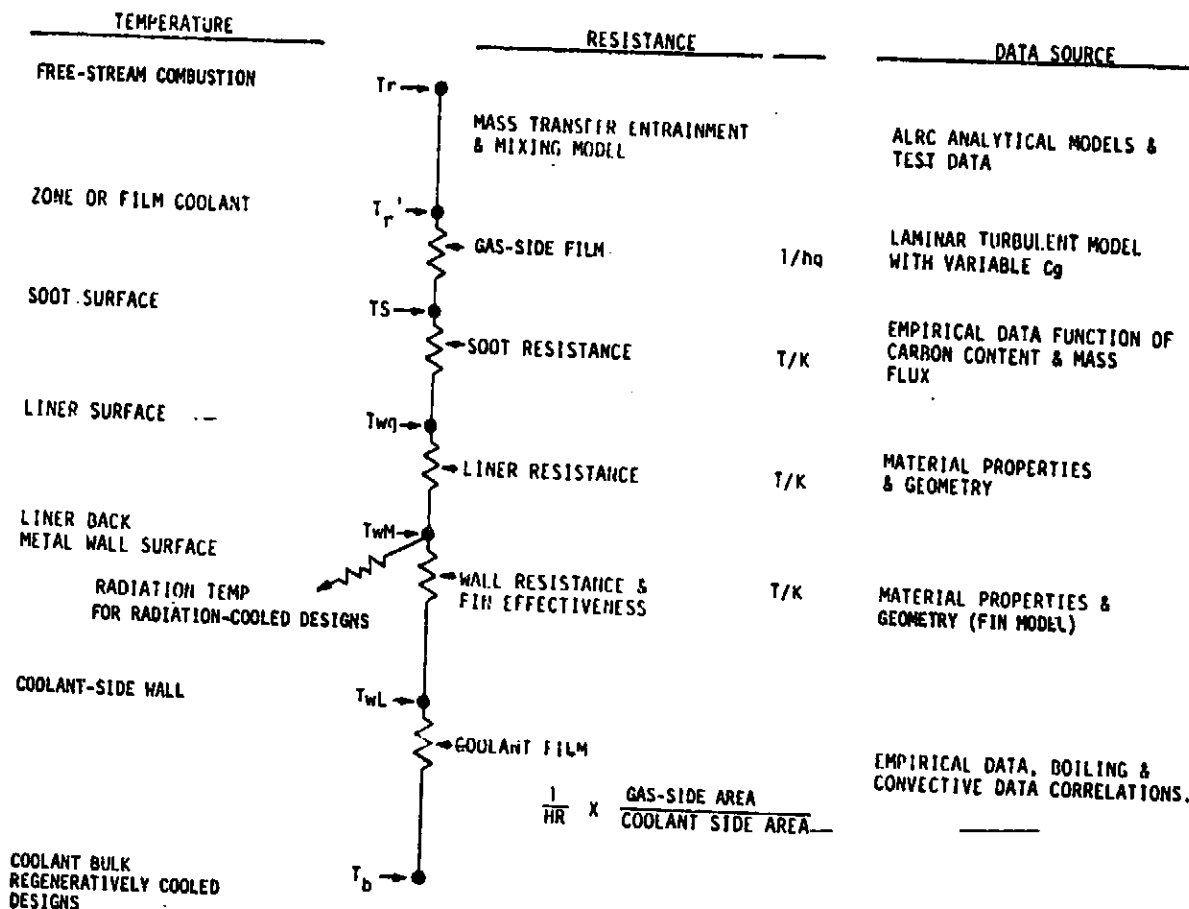


Figure A-1. Generalized Heat Transfer Model for Regeneratively and Radiation-Cooled Chambers

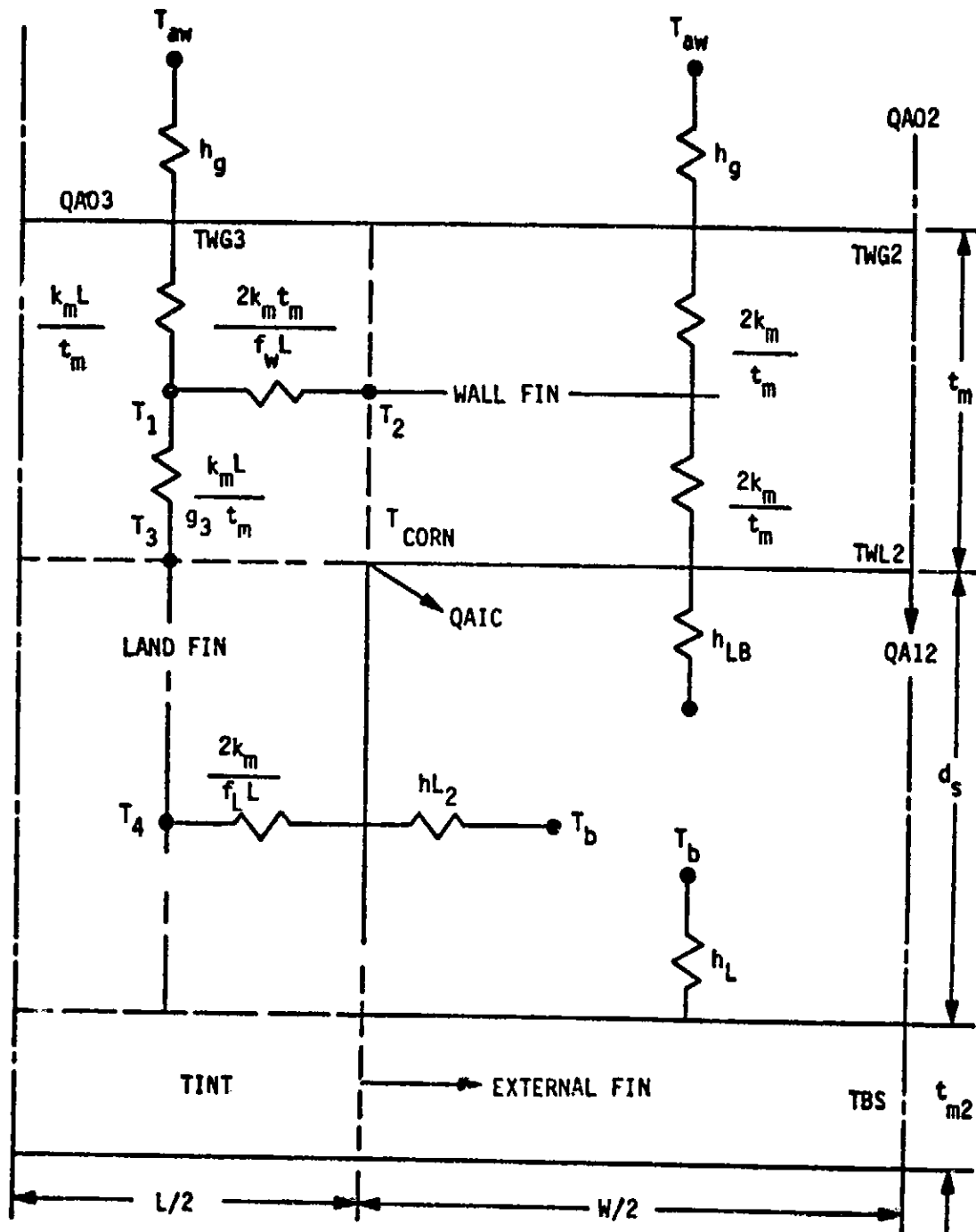


Figure A-2. Schematic of SCALER and SCALEF Wall Conduction Model

II, Summary (cont.)

with the film temperature defined as $0.5(T_r + T_{wg})$ and DB being the temperature-dependent Dittus-Boelter properties factor.* The C_g's are input both as a function of area ratio (convergent section) and as station-specified values (nozzle). This parameter reflects the combined effect of combustion and nozzle pressure gradients. Laminarization criteria and synthesis of the reverse transition regime are identical to previous analyses employed in Contract NAS 321940 (documented in Ref. A-2). These criteria are based on a fixed convergence angle of 30 degrees and were not altered for this program even though a slightly larger angle of 40 degrees was used.

(2) Simplified chamber contour and station definition permits input of the contraction ratio through use of dimensionless contour parameters. Chamber cylindrical and convergent section geometries are generated internally based on the specified contraction ratio, convergence angle, and three dimensionless radii of curvature (cylindrical to conical, throat upstream, and throat downstream). The number of subdivisions in the barrel, in the curve at the start of convergence, and at the conical section are specified input. The divergent nozzle is a scaled Rao contour for a 90% bell nozzle.

(3) Addition of the two-point design option provides an iterative solution to optimum channel size and quantity for minimum pressure drop in a relatively inexpensive fashion. This option requires the following inputs: (a) the nozzle channel width, (b) the nozzle land width at the initial (coolant inlet) station, and (c) the land width in the throat region (normally the maximum heat flux point). The throat channel width and the land and channel widths in the cylindrical barrel section are calculated. A single-pass counterflow cooling system is assumed, with the first point located in the constant channel width section (normally at the maximum flux point) and the second point located in the barrel (normally at the maximum bulk temperature location). The coolant bulk temperature at each station is calculated by an energy balance method based on the difference between the known gas temperature and the desired wall temperature, the gas-side heat transfer coefficient, and the coolant flowrate and properties. This is accomplished without concern for the cooling channel geometry at stations other than at the two critical design points. At Point No. 1, the program accounts for the radius change across the gas-side wall in calculating the

*The "DB factor," as used herein, consists of the fluid properties and correlation constants of the Dittus-Boelter equation. It is calculated as $0.026 (4/\pi)^{0.8} \mu^{0.2} Cp^{0.2} Pr^{-0.6}$ (evaluated at the bulk temperature).

II, Summary (cont.)

channel width and the corresponding number of channels to satisfy wall temperature criteria. At Point No. 2, a similar calculation of the land width and corresponding channel width is performed by using the number of channels defined for Point No. 1.

In these calculations, the channel depth is related to the channel width at each point by a specified constraint. Three options are provided for this constraint:

- (1) Channel Aspect Ratio (Depth/Width)
- (2) Coolant Mass Velocity
- (3) Friction Pressure Gradient

In this study, the first option (specified d/w) was selected as the design constraint.

2. Gas-Side Heat Transfer

Boundary layer laminarization, specification of the experimental C_g profile employed to characterize the gas-side coefficient, and consideration of carbon deposition from hydrocarbon propellants were addressed in modifying the SCALER program.

a. Gas-Side Boundary Layer

Throat Reynolds numbers in the present low-thrust study cover a range which yields three distinct boundary layer flow regimes as a result of flow acceleration in the convergent section. At high Reynolds numbers, the flow remains turbulent and, as shown in Figure A-3, heat transfer coefficients are calculated from a standard pipe-flow correlation. The dip shown in the turbulent correlation coefficient accounts for the effects of flow acceleration. At low Reynolds numbers, acceleration effects are strong enough that the boundary layer undergoes a reverse transition to laminar flow. At moderate Reynolds numbers, the reverse transition process is started but not completed, and the throat boundary layer is in a transition state. These regimes are shown in Figure A-4, in which the solid curve gives the throat Stanton number as a function of the diameter-based Reynolds number. The reverse transition regime spans the Reynolds number range of $6-13 \times 10^5$. This range, as well as the coefficient of the laminarized characteristics and the shape of the transition curve, is based on References A-3 and A-4.

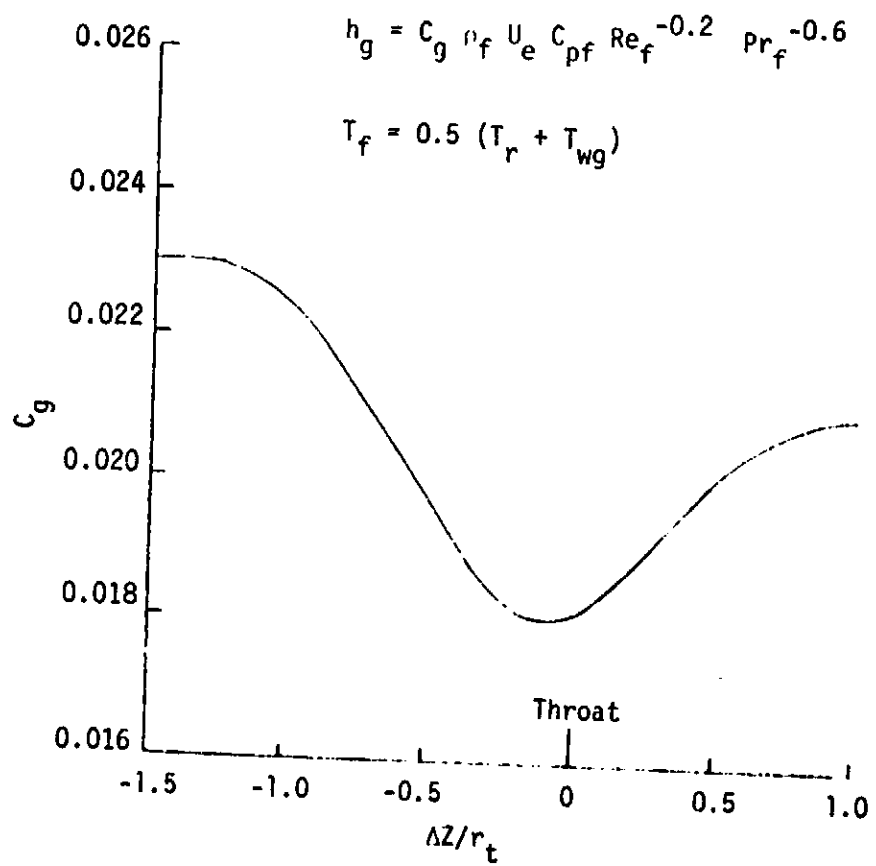


Figure A-3. Gas-Side Heat Transfer - Turbulent Regime

ORIGINAL PAGE IS
OF POOR QUALITY

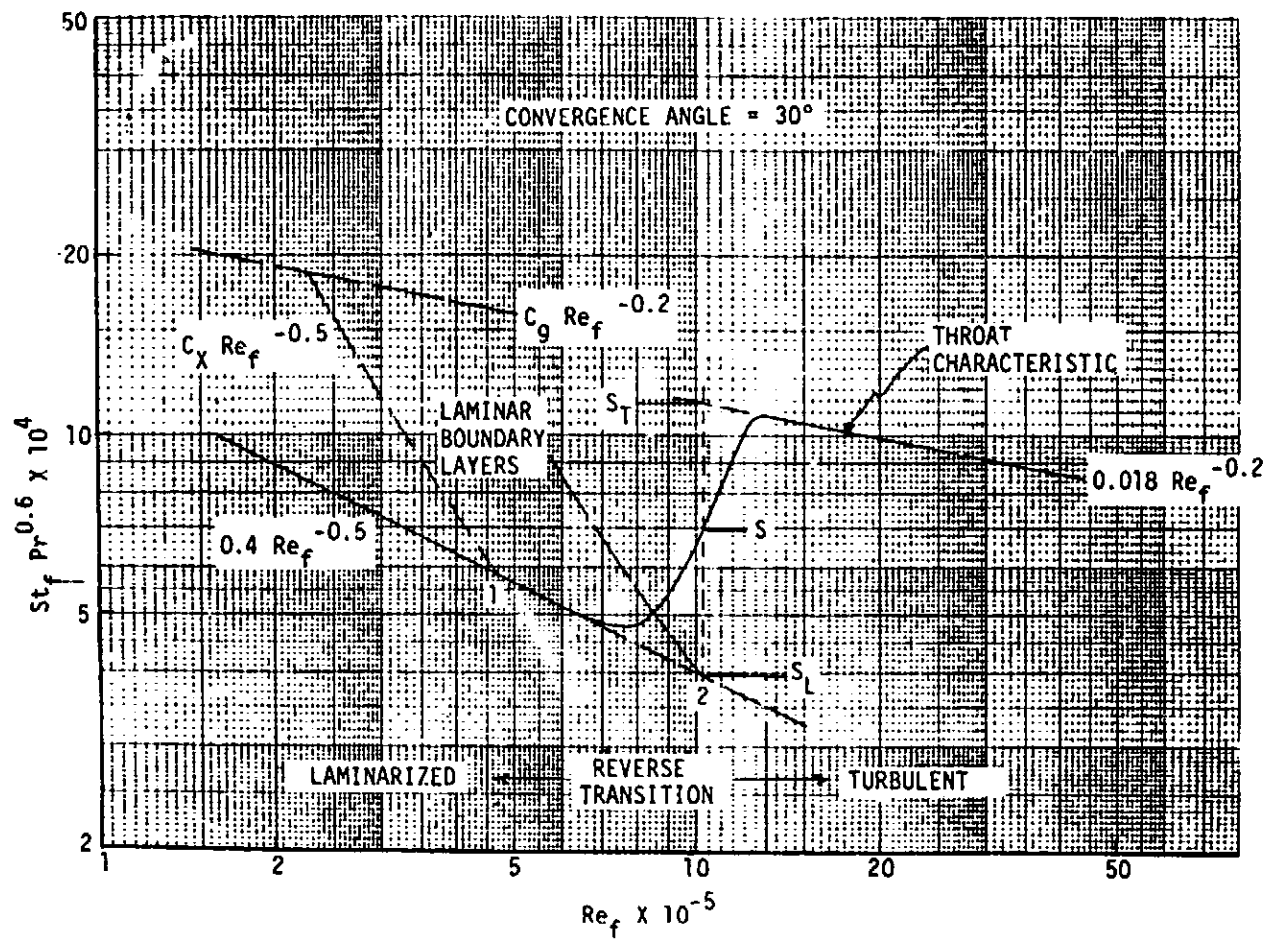


Figure A-4. Simplified Gas-Side Heat Transfer Characteristics for Low-Thrust Engines, Considering Boundary Layer Laminarization and Transition Flow

II, Summary (cont.)

Figure A-4 also illustrates the calculation procedure used upstream of the throat when reverse transition, or complete laminarization, occurs at the throat. Consider first the laminarized case with the throat at Point No. 1. A laminar boundary layer analysis (Ref. A-5) is used to predict the Stanton number upstream of the throat. This analysis employs a length-based Reynolds number, with the effective starting point of the laminar boundary layer calculated such that the predicted throat Stanton number equals the empirical value from the solid curve of Figure A-4, i.e.,

$$C_{x_t} R_{ext}^{-0.5} = 0.4 R_{eft}^{-0.5}$$

This boundary layer analysis applies downstream of the point in the convergent section where the local turbulent and laminar Stanton numbers are equal, i.e.,

$$C_g R_{ef}^{-0.2} = C_x R_{ex}^{-0.5}.$$

The C_g employed is the local turbulent correlation shown in Figure A-3.

When the throat Reynolds number is in the reverse transition region, as illustrated by the vertical dashed lines in Figure A-4 at $Re \sim 10 \times 10^5$, a fictitious laminar boundary layer analysis, based on an extension of the laminarized throat characteristics, is used. In this case, the boundary layer analysis is forced to match the fictitious Stanton number at Point No. 2 in Figure A-4. Local heat transfer coefficients are then calculated by weighting the laminar and turbulent coefficients as follows:

$$h_g = h_{gL} \frac{S_T - S}{S_T - S_L} + h_{gL} \frac{S - S_L}{S_T - S_L}$$

in which S is the actual throat Stanton number, while S_T and S_L are the throat values obtained by extension of the turbulent and laminar characteristics, respectively. These three Stanton numbers are identified in Figure A-4.

The reverse transition region limits, defined in Figure A-4, divide the $F\text{-}P_c$ box of interest herein into three regions, as shown in Figure A-5. It is apparent that only a very small region at high thrust and high chamber pressure results in turbulent flow in the throat boundary layer for hydrocarbons and even less for hydrogen. Furthermore, much of the operating box of interest is in the fully laminarized regime.

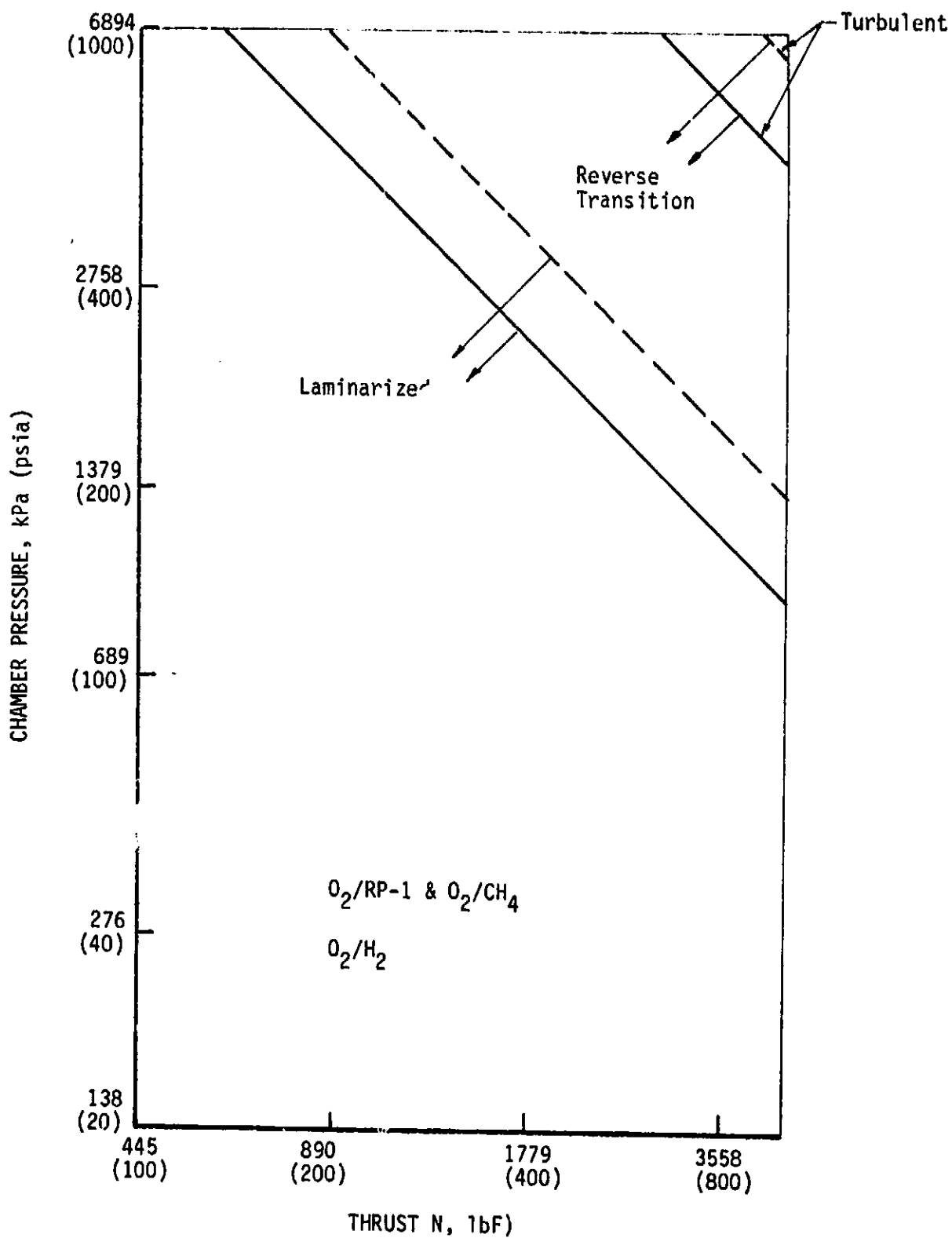


Figure A-5. Gas-Side Boundary Layer Flow Regimes

II, Summary (cont.)

b. Gas-Side Carbon Deposition

Carbon deposition on the gas-side walls of rocket thrust chambers is not well-characterized, with experimental data indicating a high degree of dependency on injector design and hardware and operating conditions. In this study, no credit for reduction in heat load to the coolant was taken on the basis of this mechanism. However, it was postulated that a thermal resistance liner could be used in the cylindrical section when high barrel heat loads result in an unacceptable coolant bulk temperature rise.

3. Attachment Area Ratio for a Radiation-Cooled Nozzle Extension

The area ratio at which a radiation-cooled nozzle extension can be attached was calculated by assuming 1786°K (2755°F) as the operating temperature for the skirt material. Predicted wall temperatures were based on the simple energy balance:

$$h_g (T_{aw} - T_{wg}) = \epsilon \epsilon (1 + f_i) (T_{wg})^4$$

in which —

ϵ = coating emissivity (typical value = 0.85)

f_i = internal view factor to end planes from an axisymmetric view factor program

The proper attachment area ratio is calculated separately for each propellant combination and operating point. Model checkout calculations for LO₂/RP-1 at mixture ratios of 2 and 4 showed the attachment area ratio to be primarily a function of P_c (i.e., heat flux) and to be insensitive to MR and thrust, as shown in Figure A-6. At chamber pressures below about 689 kPa (100 psia), temperatures were below 1756°K (2700°F), permitting full wall chamber cooling by radiation alone. At the maximum P_c, the attachment area ratios for a radiation-cooled skirt are in the 40:1 to 50:1 range.

4. Engine contour

a. Chamber Contour Selection

The basic nondimensional chamber contours used in this study are shown in Figure A-7. The convergent section contours were selected to minimize boundary layer turbulence within the limits of standard design practice. This goal dictates the use of a large convergence angle with a conical section of sufficient length. Therefore, a 40° convergence angle,

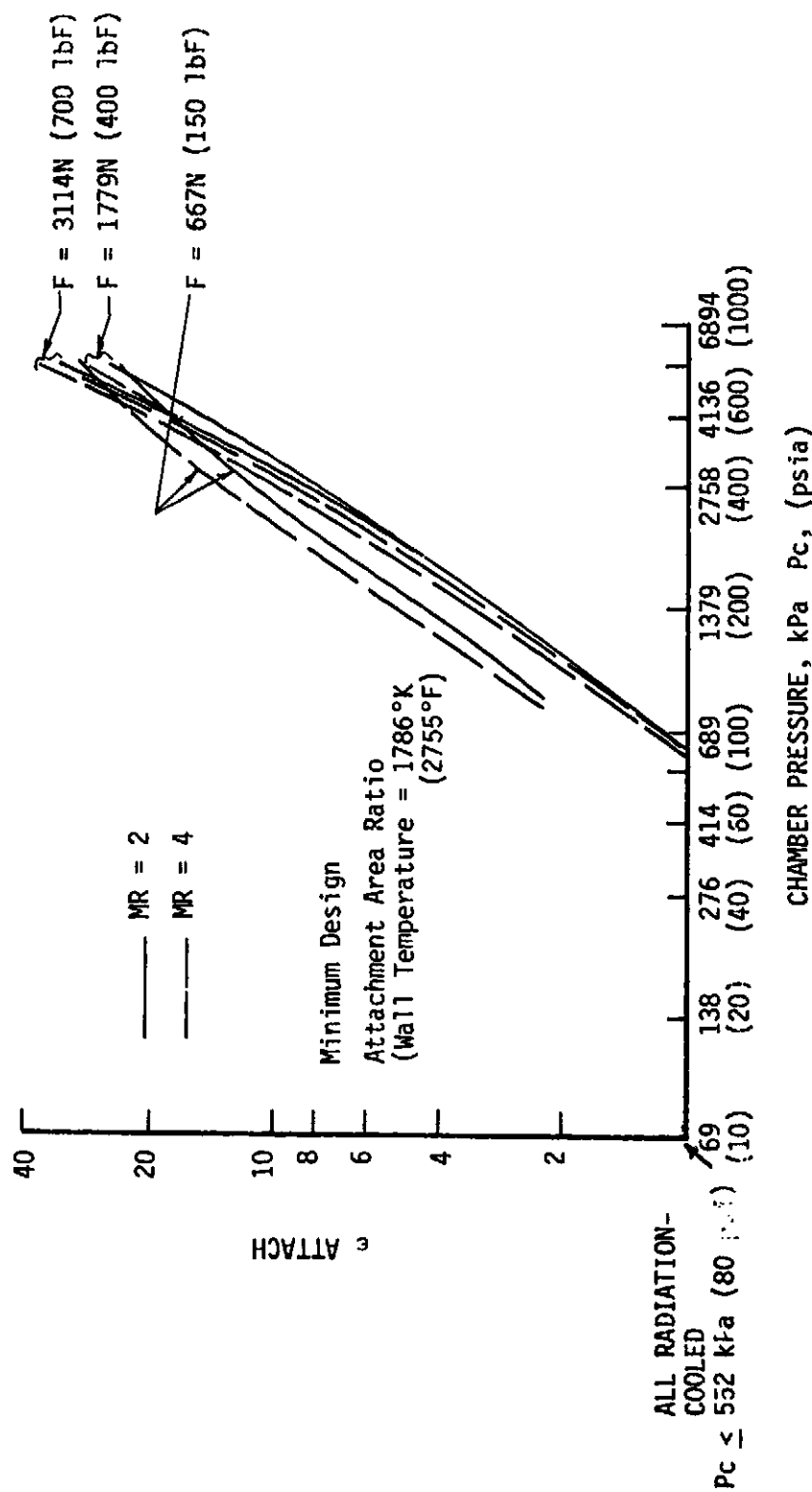


Figure A-6. Attachment Area Ratio for Radiation-Cooled Skirt

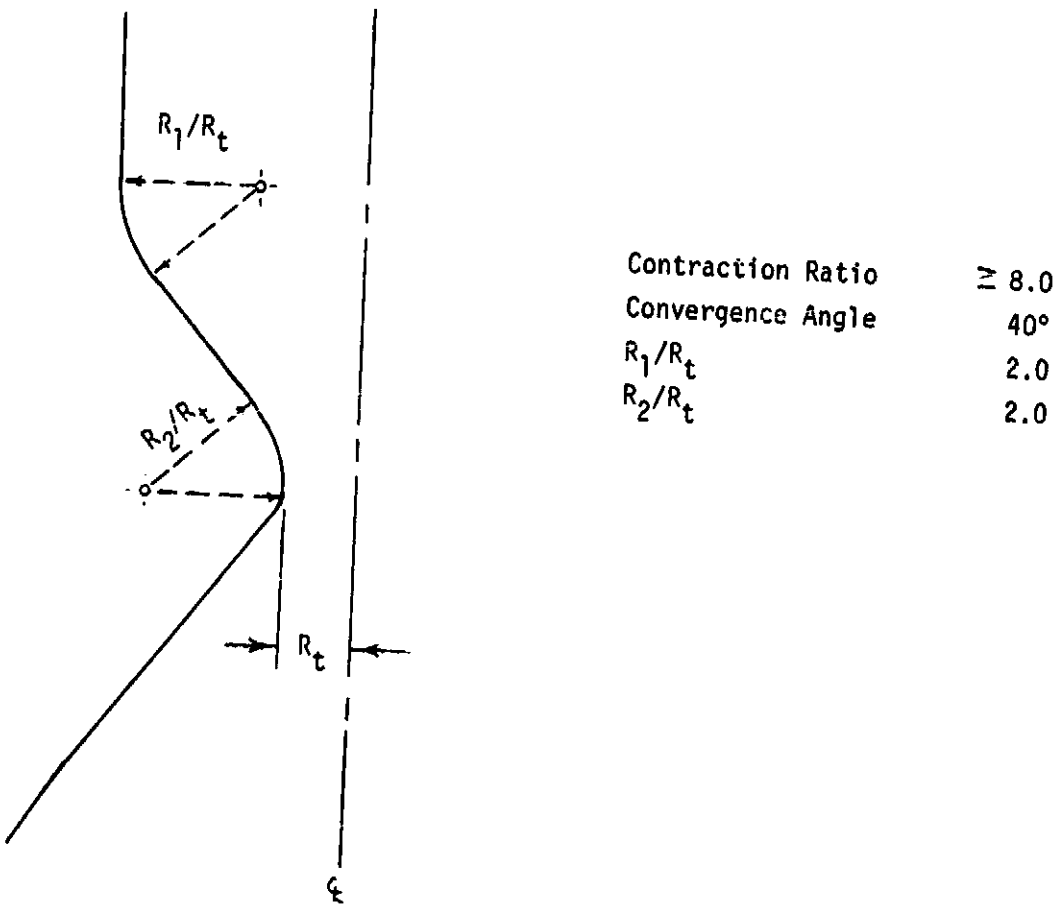


Figure A-7. Chamber and Initial Nozzle Section Contour

II, Summary (cont.)

along with a radius of curvature at the start of convergence large enough to prevent flow separation and local perturbations in the local heat-transfer coefficient, was selected.

b. Nozzle Contour Selection

A standard nondimensional contour for a 400:1 area ratio, 85% bell nozzle was selected. The cooled surface area, length, and local diameter are proportioned to the throat diameter calculated for the specific thrust, pressure, and mixture ratio, using preliminary I_{sp} and C_F values.

c. Minimum Contraction Ratio

The sensitivity of attainable specific impulse, chamber L' , and chamber heat flux was assessed for the LO₂/RP-1 propellant combination at a mixture ratio of 2 and a chamber pressure of 6894 kPa (1000 psia). The results of this analysis are shown in Figure A-8. All three parameters benefit as the contraction ratio is increased from the 3.3:1 value utilized in the earlier study (documented in Ref. A-2). Practical considerations regarding engine size and injector/igniter design and fabrication resulted in a recommendation of a minimum contraction ratio of 8:1.

d. Minimum Chamber Diameter

At low thrusts, increasing the chamber pressure results in smaller throat diameters. For example, for LO₂/RP-1 propellants at $F = 445\text{N}$ (100 lbF) and $P_c = 6894 \text{ kPa}$ (1000 psia), a throat diameter of 0.62 cm (0.244 in.) is calculated. For a contraction ratio of 8, the resulting chamber diameter would be only 1.75 cm (0.690 in.). This is not considered realistic for the following reasons.

Injector design requires a centrally located igniter for the non-hypergolic propellants and, for combustion efficiency, two concentric rows of injector elements. The igniter requires a flow area encompassing 2% of the throat area, but with a diameter not less than 0.152 cm (0.06 in.). A thrust per element ranging from 26.7N (6 lbF) to 44.5N (10 lbF) was considered along with a minimum element density of 0.93/cm² (6/in.²). Packaging and manifolding of this minimum-size injector resulted in an injector diameter of 3.81 cm (1.50 in.) which dictated the contraction ratio at many design points.

Consequently, the study philosophy was to design chambers with a contraction ratio of 8:1 until the minimum chamber diameter of

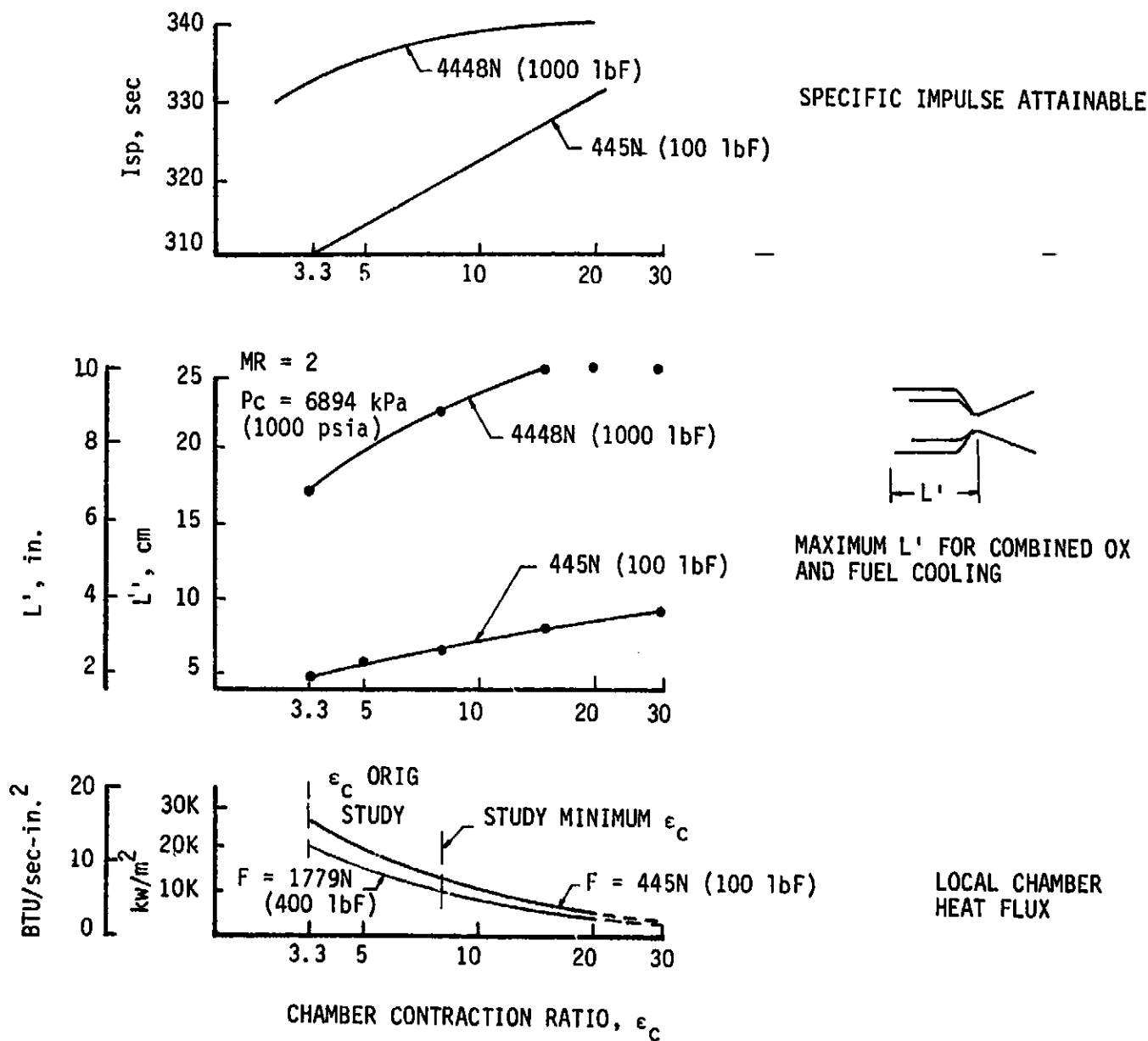


Figure A-8. Sensitivity of Attainable Specific Impulse, Chamber L', and Chamber Heat Flux to Chamber Contraction Ratio

II, Summary (cont.)

3.81 cm (1.50 in.) was reached. This, then, became the limiting constraint with increasing P_c and as the contraction ratio was increased as required. For the case noted above, the resulting contraction ratio was over 37:1.

5. Channel Design Constraints

A basic coolant channel configuration currently employed for regeneratively-cooled designs utilizes rectangular coolant passages milled in a zirconium-copper liner with an electroformed nickel closeout. This type of construction minimizes cooling problems at higher chamber pressures and maximizes fin effectiveness in high-conductivity metals in transforming the gas-side heat flux to a lower coolant-side flux. These channel-walled chambers normally extend to the area (ϵ_A) at which a radiation-cooled nozzle can be utilized. At the lower chamber pressures, however, ϵ_A approaches the throat (Figure A-6). In order to eliminate a flange near the throat station for these cases, the nozzle cooling channels are extended to an area ratio of 6:1, at which point fabricability methods for joining the nozzle extension to the cooled chambers are straightforward.

a. Creep and Cycle Life Considerations

The designs considered are based on a service life of five full thermal cycles times a safety factor of four. The maximum chamber wall temperature is limited to 811°K (1000°F) and the temperature differential between the Zr-Cu gas-side and Ni closeout is 700°K (800°F). This results in a maximum strain of not over 1.6% for each cycle. The equations built into the program allow slightly higher strain levels if the gas-side temperature is less than 811°K (1000°F).

b. Channel Dimensions and Geometry

Conventional fabrication technology limits assumed in past studies restricted the minimum channel widths and depths and the minimum land width to about 0.076 cm (0.030 in.). The maximum channel aspect ratio (depth/width) is typically 4 or 5, again based on machining limitations. With these restrictions, as reported in Reference A-2, only limited regions of the F- P_c map could be shown to have cooling feasibility. No limits based on fabrication considerations were specified for these variables in the present study. However, minimum channel dimension of around 0.013 to 0.025 cm (0.005 to 0.010 in.), depending on the coolant, are suggested due to a plugging potential and the limits of coolant filtration.

The allowable gas-side channel width-to-wall thickness ratio requirements for Zr-Cu are shown in Figure A-9. The design program utilizes the input wall thickness unless the gas-side wall temperature

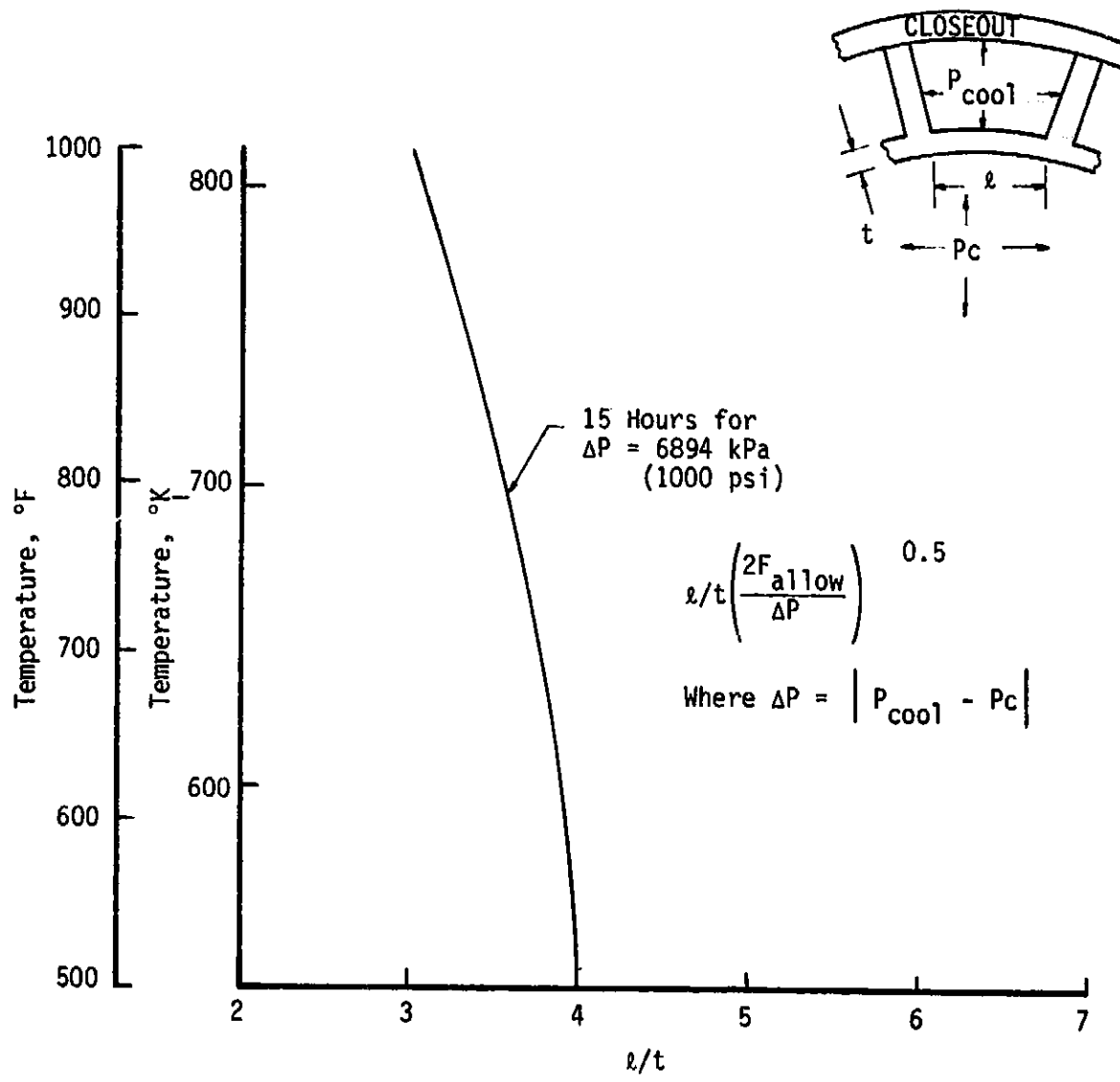


Figure A-9. Allowable Channel Aspect Ratio as a Function of Hot Gas-Side Wall Temperature for Zr-Cu Aged at 867°F (1100°F)

II, Summary (cont.)

requires use of a thicker wall for structural reasons, based on a wall-thickness-to-channel-width ratio for the respective pressure and temperature. Actual pressure differentials across the hot wall and hot gas-side wall temperature material strengths are used in the program to determine wall thickness at each station.

The calculations of Task II indicated that the required cooling channel width at the throat with either RP-1 or oxygen as coolant would be significantly less than the conventional minimum width of 0.076 cm (0.030 in.). In addition, high-aspect-ratio channels are required for oxygen. The high cooling surface attained by high aspect ratio channels more than compensates for the reduced heat transfer coefficient as velocity is decreased, particularly at high chamber pressures. These trends are illustrated in Figures A-10 and A-11.

Figure A-11 also illustrates the effect of increased wall thickness on the flux transformation for low-thrust, high-Pc engines. The coolant-side flux is appreciably reduced by the radial dimension effect on these small engines.

Also evaluated was the effect of varying land width over a range from 0.030 to 0.089 cm (0.012 to 0.035 in.) with RP-1 as the coolant. As throat land width was increased, the number of coolant channels decreased and pressure drop increased. Fabrication and structural considerations led to the selection of a minimum land width of 0.063 cm (0.025 in.) for this study (Figure A-12).

c. Coolant Flow Arrangement

A single-pass, counterflow regenerative-cooling configuration was selected as the preferred cooling concept. Both the fuel and the oxidizer were evaluated with the coolant inlet located at the radiation-cooled extension attachment point. This type of cooling arrangement, termed "single-regen" cooling, can become bulk-temperature or pressure-drop-limited as the fluxes increase with increasing P_c and as the flow decreases with reduced thrust. Cooling with both propellants in series, termed "dual-regen" cooling, provides an increased heat load capability. For the LOX/RP-1 propellant combination, fuel cooling was considered from the attachment point to an area ratio of 6:1 (based on manifolding requirements). Oxidizer cooling was utilized from this point through the high-flux throat region to the injector in order to avoid coolant-side fouling possible with RP-1. In some cases, a thermal barrier or liner in the barrel was utilized to reduce the bulk temperature rise of the coolant.

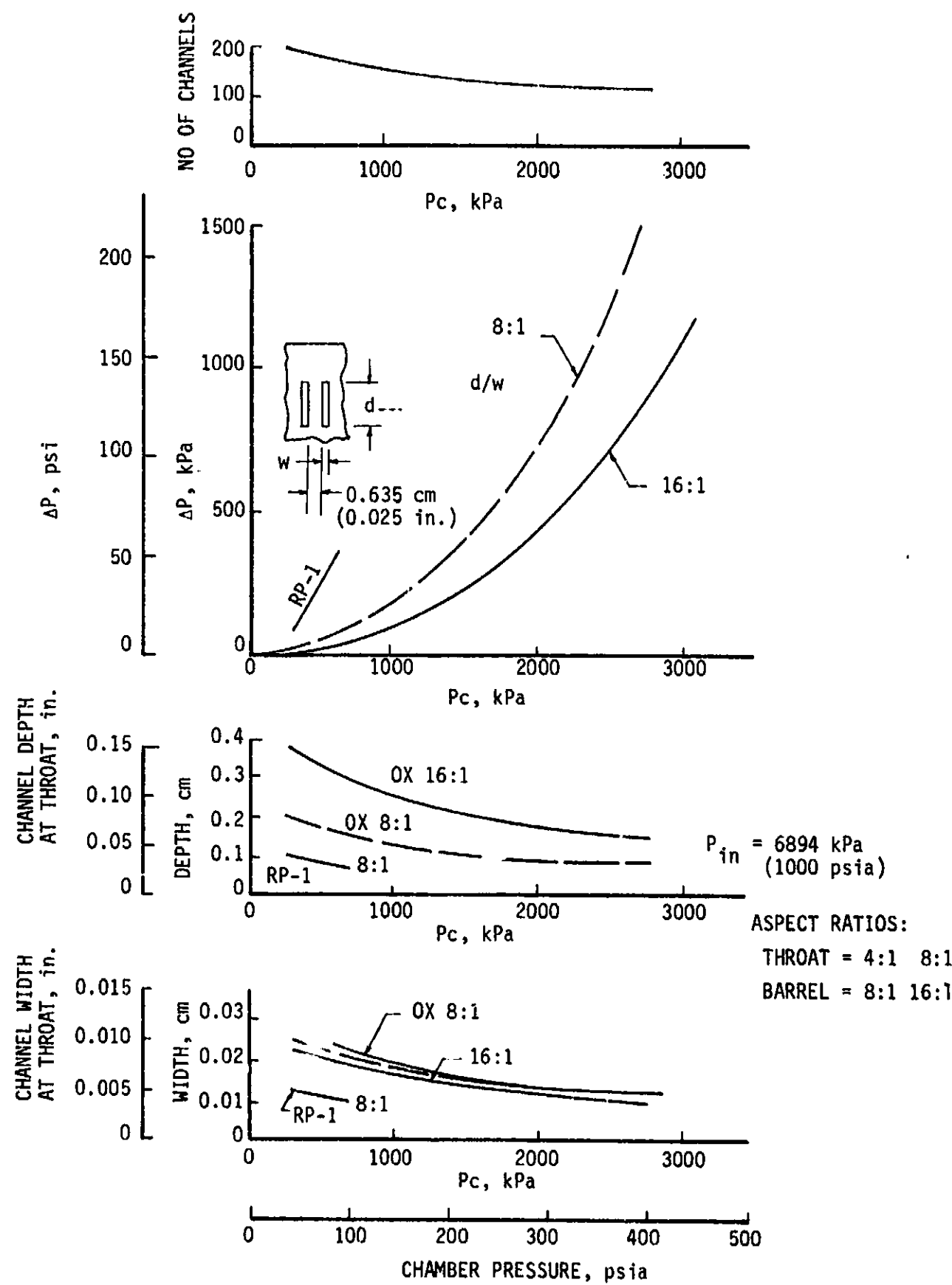


Figure A-10. Effect of Chamber Pressure on Pressure Drop and Channel Aspect Ratio with Supercritical Oxygen as Coolant 169

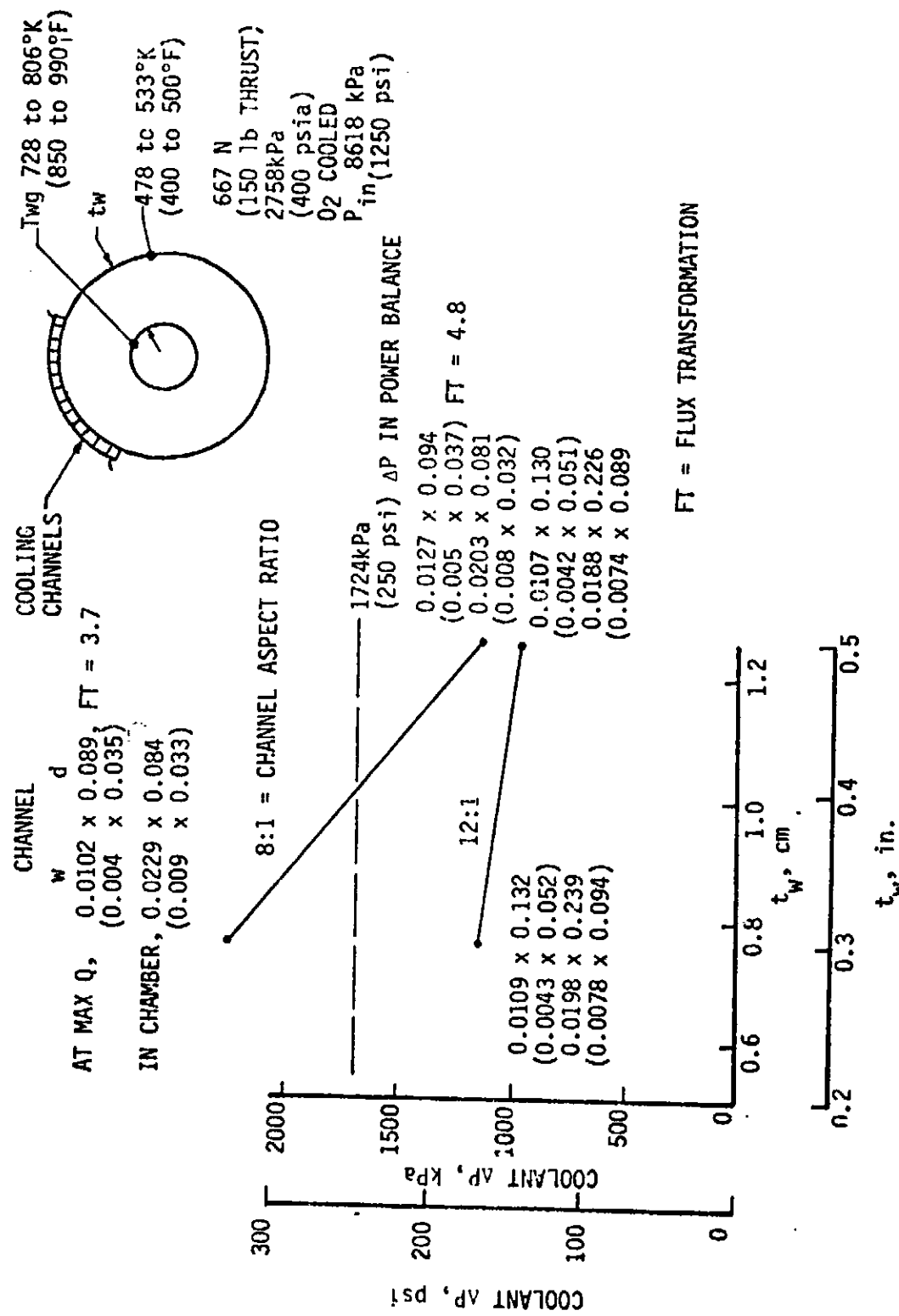


Figure A-11. Unique Design Requirements for Regeneratively Cooled Chambers at Low Thrusts and High Chamber Pressures

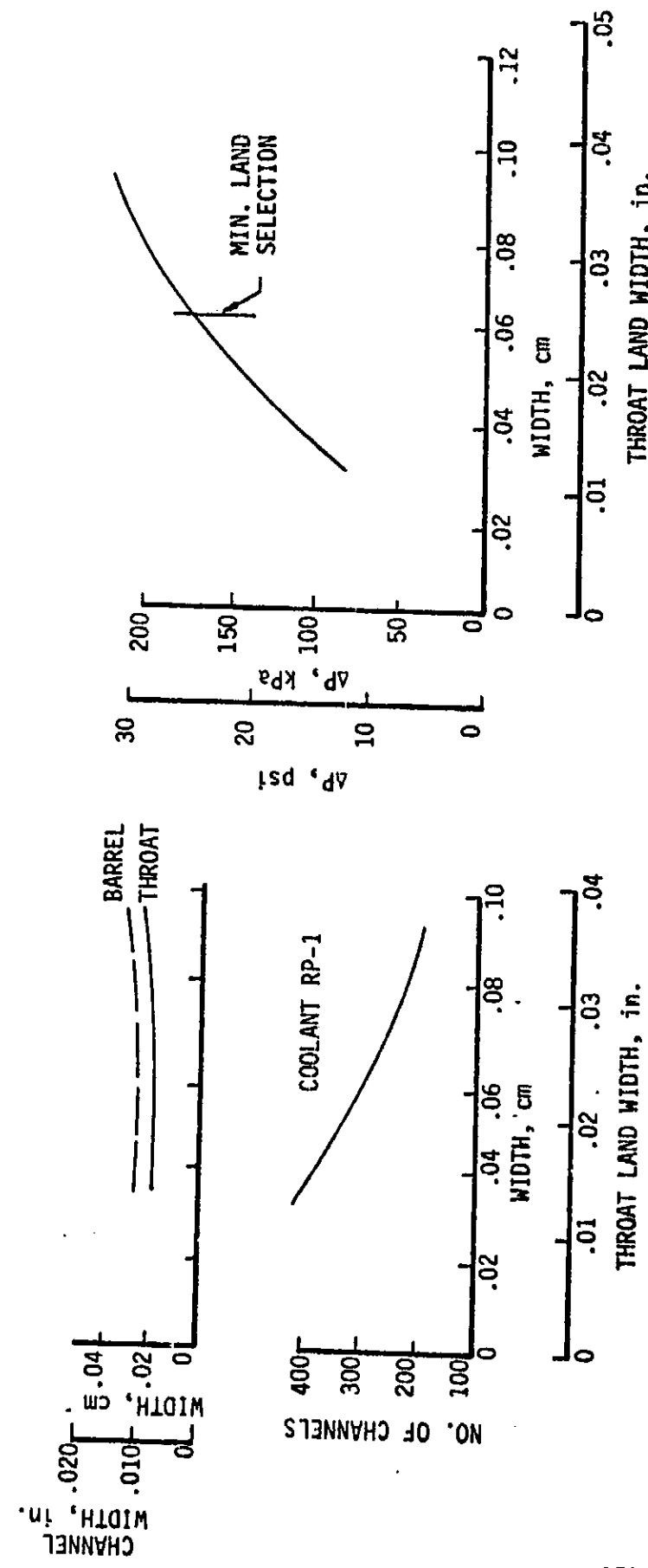
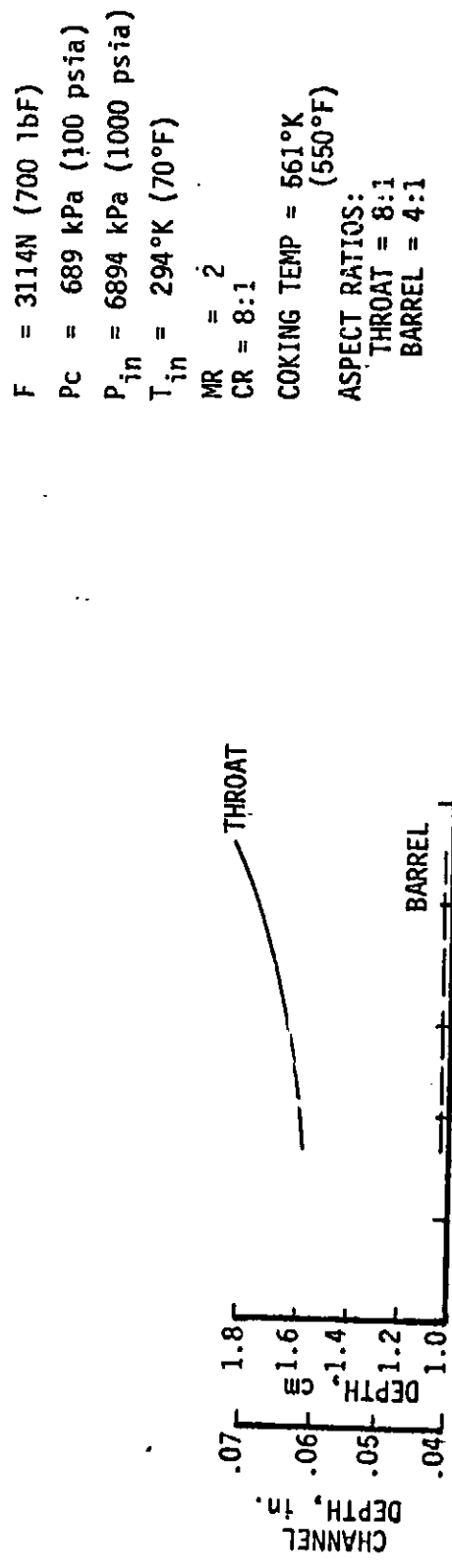


Figure A-12. Sensitivity of Channel Design Characteristics to Throat Land Width

II, Summary (cont.)

d. Coolant State

Fluid in the coolant channels is single-phase at all times. The oxygen is in a supercritical state, as are the hydrogen and methane analyzed in Task IV.

e. Coolant-Side Wall Temperature

Two of the four coolants studied required a limit to the allowable coolant-side wall temperature. Both hydrocarbon fuels, RP-1 and methane, thermally decompose or "coke." The threshold for carbonaceous deposit formation with RP-1 is approximately 561°K (550°F), based on Jet Fuel Thermal Oxidation Test (ASTM D 3241-73T) data for the similar Jet A-1 fuel. Coking of methane does not limit channel design as the thermal decomposition range is estimated to be 1033-1367°K (1400-2000°F), well above the wall temperatures allowed by life cycle and creep considerations.

Studies on copper oxidation, reported in Reference A-6, show no evidence of oxidation below about 533°K (500°F) whereas the reaction rate becomes pronounced at a temperature of 755°K (900°F). In this study, it was assumed that 589°K (600°F) was the maximum allowable temperature for copper surfaces in contact with oxygen.

f. Coolant Outlet Temperature

The maximum allowable coolant bulk temperature is directly related to the allowable coolant-side wall temperature discussed above. With wall temperatures limited to 561 and 589°K (550 and 600°F), respectively, for RP-1 and oxygen, rule-of-thumb allowances for the wall-to-bulk temperature differentials and density changes determined 450 and 394°K (350 and 250°F), respectively, to be reasonable maximum allowable bulk temperatures for the two coolants. While methane is not reaction-limited at low pressures, the rapid decrease in density with increasing temperature indicates that 478-533°K (400-500°F) is a practical limit. However, the pressure effect is strong; thus each methane cooling case was analyzed without considering a limiting bulk temperature.

g. Coolant Velocity

For supercritical hydrogen, oxygen, and methane, the maximum acceptable fluid velocity was not permitted to exceed a local Mach number of 0.3. For subcooled liquid RP-1, the maximum liquid velocity was taken to be 61 m/s (200 ft/sec).

II, Summary (cont.)

h. Channel Pressure Drop

The acceptability of the magnitude of the cooling channel pressure drop is largely a function of system considerations which, as such, are beyond the scope of this study. However, since coolant pressure drop is a primary factor in assessment of any design, it was necessary to specify a limiting value for pressure loss for each coolant in order to arrive at a reasonable acceptability bound for each. The minimum channel outlet pressure was prescribed by the allowable pressure drop across the injector, defined as $P_c 0.75$. Coolant channel pressure drops were specified as follows:

- LO₂/RP-1

System power balance studies for oxygen cooling of turboalternator expander cycle engines led to a specification for ΔP_{max} for oxygen of 1722 kPa (250 psi). Since RP-1 became bulk-temperature-limited in most cases, a maximum ΔP criterion was not necessary.

- LO₂/LH₂

A preliminary selection of 1722 kPa (250 psi) for the allowable maximum pressure drop for either hydrogen or oxygen became unnecessary as hydrogen ΔP 's were much lower and oxygen is not indicated as a coolant for this propellant combination.

- LO₂/LCH₄

With either or both propellants as coolants, the allowable pressure drops were based on a preliminary power balance analysis of a mixed expander/turboalternator cycle. Cooling channel outlet pressures were maintained supercritical. Minimum coolant channel pressure drops were functions of P_c as shown in Figure A-13.

6. Coolant Properties

The thermal coolant channel design analysis program requires both coolant thermodynamic data (density, enthalpy, specific heat, and sonic velocity) and transport data (thermal conductivity and viscosity) as well as saturation pressures and temperatures. Standard NBS properties were employed for oxygen, hydrogen, and methane. Property data for RP-1 were intensively reviewed, and the results are reported in Reference A-7.

7. Coolant Correlations

Coolant heat transfer correlations for single-phase fluids in forced convection are semi-empirical; consequently the usual uncertainties

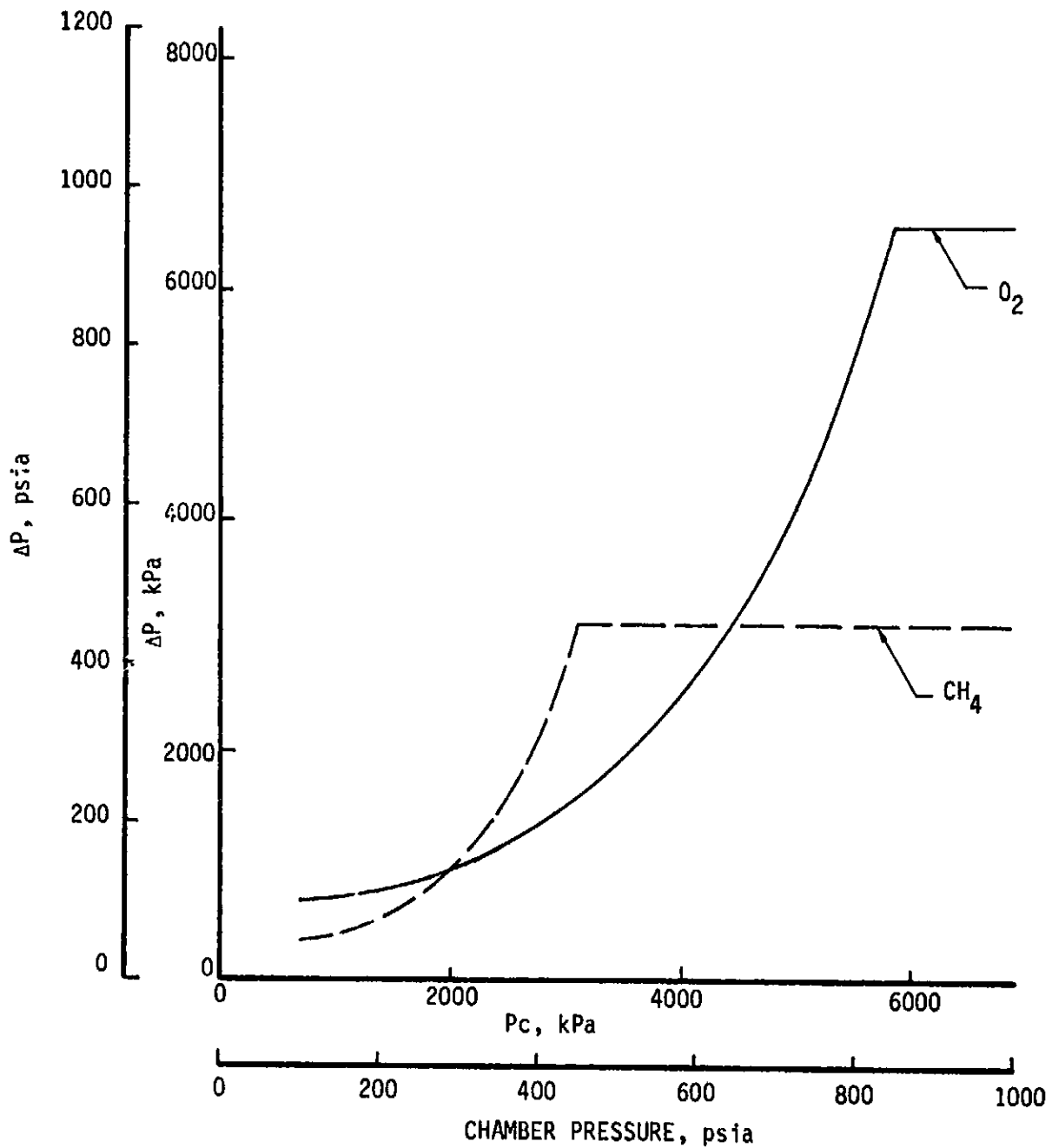


Figure A-13. Allowable Coolant Drop for LO_2/LCH_4

II, Summary (cont.)

regarding their use beyond the range of supporting test data must be considered. The critical points, normal boiling points, and typical temperatures for the four coolants of interest are presented below:

	<u>Oxygen</u>	<u>RP-1</u>	<u>Methane</u>	<u>Hydrogen</u>
Crit. Press., kPa (psia)	5102 (740)	2172 (315)	4598 (667)	1296 (188)
Crit. Temp, °K (°F)	154 (-182)	677 (758)	191 (-117)	33 (-400)
NBP, °K (°F)	90 (-298)	490 (422)	112 (-259)	21 (-423)
Typical Inlet Temp., °K (°F)	90 (-298)	289 (60)	112 (-259)	21 (-423)

a. Oxygen

The results of a recently concluded heated-tube test program over a reduced pressure ratio range of 0.39 to 6.76 and a heat flux range of 1961 to 89,881 kw/m² (1.2 to 55 Btu/in.²-sec), together with earlier data, led to the following correlation:

$$Nu_b = Nu_{ref} \left(\frac{\rho_b}{\rho_w} \right)^{-0.5} \left(\frac{k_b}{k_w} \right)^{0.5} \left(\frac{C_p}{C_{p_b}} \right)^{0.67} \left(\frac{P}{P_{crit}} \right)^{0.2}$$

where $Nu_{ref} = 0.0025 Re_b^{0.4} Pr_b^{0.4}$

Over 95% of the data used fits this equation within $\pm 30\%$ (Ref. A-8).

b. RP-1

The forced convection characteristics of RP-1 as developed for water, RP-1, and diethylcyclohexane (DECH) were predicted by the Hines equation (Ref. 9):

$$Nu_b = 0.0055 Re_b^{0.95} Pr_b^{0.4}$$

c. Methane

Heat transfer to methane at supercritical pressures was assumed to be characterized by the recently developed equation for its homologous propane (Ref. A-10):

II, Summary (cont.)

$$Nu_b = 0.00545 Re_b^{0.90} Pr_b^{0.4} \left(\frac{\rho_b}{\rho_w}\right)^{0.11} \left(\frac{k_b}{k_w}\right)^{0.27}$$

$$\quad \quad \quad 0.53 \quad \quad \quad 0.23$$

$$\left(\frac{C_p}{C_{p_b}}\right) \quad \left(\frac{\mu_b}{\mu_w}\right) \quad \left(1 + \frac{2}{L/D}\right)$$

d. Hydrogen

Hydrogen as a coolant in the supercritical pressure range is characterized by the Hess and Kunz correlation of Reference A-11:

$$Nu_f = 0.0208 \left[\frac{\rho_f v_b D}{\mu_f} \right]^{0.8} Pr_f^{0.4} (1 + 0.01457 \frac{v_w}{v_b})^{-}$$

The correction factor below for tube curvature effects, as developed in Reference A-12, was applied to all of the above correlations:

$$h_c = h_s \left[Re \left(\frac{D_e}{2R_c} \right)^2 \right]^{.05}$$

where:

h_c = coefficient corrected for curvature effects

h_s = straight-tube coefficient

Re = Reynolds number

D_e = Channel equivalent diameter

R_c = Radius of curvature

8. Coolant Limitations

Of the four coolants studied, only hydrogen does not possess an innate characteristic which limits its use in regenerative cooling.

a. Oxygen

As discussed in Section II.5.e, copper is subject to a significant rate of oxidation at wall temperatures estimated at 589°K (600°F).

II, Summary (cont.)

b. RP-1

Thermal decomposition of RP-1 limits this coolant to wall and bulk temperatures of 561 and 450°K (550 and 350°F), respectively, as discussed in Section II.5.e and f. In context with the narrow channels determined in this study, the problem of contamination by biological and chemical reactions must also be considered.

c. Methane

Although the coking temperature of around 978°K (1300°F) is above copper metal temperature limitations, the lack of any appreciable subcooling, along with the sensitivity of bulk density to relatively small pressure decreases and temperature increases, constrains the channel design process.

REFERENCES

- A-1. Ewen, R.L., Modification of the SCALER Program for the Low-Thrust Isp Sensitivity Study, Contract NAS 3-22665, TAR 9751:0646, ALRC, 9 April 1981.
- A-2. Thompson, W.R. and Ewen, R.L., Thrust Chamber Cooling Analysis (Task II), Low-Thrust Chemical Rocket Engine Study, Contract NAS 3-21940, TAR 9751: 0424, ALRC, 5 March 1980.
- A-3. Liquid Rocket Engine Self-Cooled Combustion Chambers, NASA SP-8124, September 1977.
- A-4. Boldman, D.R., et al., Laminarization of a Turbulent Boundary Layer as Observed from Heat Transfer and Boundary Layer Measurements in Conical Nozzles, NASA TN D-4788, September 1968.
- A-5. Back, L.H. and Witte, A.B., Prediction of Heat Transfer from Laminar Boundary Layer with Emphasis on Large Free-Stream Velocity Gradients and Highly Cooled Walls, JPL Technical Report No. 32-728, June 1965.
- A-6. Bouillon, F., et al., "Oxidation of Copper and The Solubility of Oxygen in the Metal", Acta Met., Vol. 10, No. 7, pp. 647-652, 1962 (NASA STAR Abstract N77-24241).
- A-7. Schoenman, L., Low Thrust Isp Sensitivity Study, Monthly Progress Narrative 22665-M-I, Contract NAS 3-22665, January 1981.
- A-8. Spencer, R.G. and Rousar, D.C., Supercritical Oxygen Heat Transfer, NASA CR-135339, Contract NAS 3-20384, ALRC, November 1977.
- A-9. Hines, W.S., Turbulent Forced Convection Heat Transfer to Liquids at Very High Heat Fluxes and Flowrates, Rocketdyne Research Report 61-14, 1961.
- A-10. Gross, R.S., Task I Data Dump, Combustion Performance and Heat Transfer Characterization of LOX/Hydrocarbon-Type Propellants, Contract NAS 9-15958, ALRC, August 1980.
- A-11. Hess, H.L. and Kunz, H.R., "A Study of Forced Convection Heat Transfer to Supercritical Hydrogen," J. Heat Transfer, Vol. 87, No. 1, pp. 41-48, February 1965.
- A-12. Ito, H., "Friction Factors for Turbulent Flow in Curved Pipes," J. Basic Engineering, Vol. 81, p. 123, June 1959.

PRECEDING PAGE BLANK NOT FILMED

APPENDIX B
SIMPLIFIED PERFORMANCE MODEL

TABLE OF CONTENTS

- I. Introduction
- II. Summary
 - A. Performance Model Description
 - B. Calibration and Sensitivity Study Results
- III. Technical Discussion
 - A. Task I - Analyses
 - 1. Model Formulation and Calibration
 - 2. Task I - Results
 - B. Task II - Analyses

References

PRECEDING PAGE BLANK NOT FILMED

LIST OF TABLES

Table No.

- B-I Energy Release Efficiency Calibration to NASA-LeRC LOX/RP-1 OFO Triplet Engine
- B-II BLIMP-TBL Chart Comparison
- B-III Comparison of BLIMP and the Simplified TBL Chart Losses
- B-IV Evaluation of Regen Cooling/Performance Interactions for Selected Task II Thrust and Chamber Pressures

LIST OF FIGURES

Figure No.

- B-1 Performance Model Qualification Calibration
- B-2 Performance Mathematical Modeling (Loss Accounting)
- B-3 Performance Efficiency Definitions
- B-4 Influence of Chamber Pressure and Thrust on Thrust Loss Due to Boundary Layer Development
- B-5 BLIMP vs TBL Chart Thrust Loss Correction Factor
- B-6 Influence of Reynolds Number and Wall Temperature Ratio on Boundary Layer Thrust Loss
- B-7 Influence of Contraction Ratio on Specific Impulse
- B-8 Influence of Thrust/Chamber Pressure Ratio on Number of Injection Elements
- B-9 Heated Fuel Allows Use of a Shorter Chamber
- B-10 Predicted Performance Losses for Low-Thrust, Low-Pc Engine
- B-11 Predicted Performance Losses for High-Thrust, High-Pc Engine
- B-12 Predicted Specific Impulse - Dual-Regen Cooling
- B-13 Predicted Specific Impulse - Fuel-Regen Cooling with Barrier Cooling
- B-14 Predicted Specific Impulse - Radiation Cooling
- B-15 Influence of Mixture Ratio on Predicted Specific Impulse - Dual-Regen Case
- B-16 Influence of Mixture Ratio on Specific Impulse - Fuel-Regen Plus Barrier Cooling
- B-17 Influence of Mixture Ratio on Specific Impulse - Radiation Cooling

I. INTRODUCTION

This appendix documents the performance modeling conducted during Tasks I and II of the study program. Included in this appendix is a brief description of the performance prediction methodology, calibration techniques relating to the energy release and boundary layer losses, and a presentation of the results of sensitivity analyses relating to the impact of chamber pressure, thrust, and mixture and area ratio on predicted delivered specific impulse.

The overall objectives of the Task I and II performance studies were:

- Task I - Calibrate simplified analysis techniques and select chamber geometry criteria
- Contraction Ratio
 - Length
- Task II - Define area ratio and mixture ratio influences on the attainable specific impulse of LOX/RP-1 and the recommended study ranges for Task III

II. SUMMARY

A. PERFORMANCE MODEL DESCRIPTION

The performance model was based on simplified JANNAF techniques, then calibrated to existing engines and/or more rigorous analytical techniques. This model yields reasonable performance trends and is inexpensive to run.

The predicted delivered specific impulse (I_{spDEL}) was obtained by calculating the influence of known mechanisms that degrade the ideal (I_{spODE}) performance. These efficiencies/loss mechanisms were divided into five major categories: energy release efficiency (η_{ERE}), reaction kinetics efficiency (η_K), two-dimensional divergence efficiency (η_{2D}), loss due to the thrust decrement within the boundary layer, and loss due to film cooling.

A computer program had previously been developed to help facilitate parametric analysis by representing each loss mechanism in a subroutine with the appropriate data base.

During Task I, a Priem vaporization model (Ref. B-1) and empirical mixing loss correlation for LOX/RP-1 were incorporated into a subroutine which enabled the ERE to be internally calculated. The vaporization model was calibrated using data from the NASA-LeRC OFO triplet engines (NASA TM 79319). I_{spODE} and I_{spODK} data were obtained using the Two-Dimensional Kinetics Program (TDK), Reference B-2, and tabulated over a range of conditions that would encompass those desired for this analysis.

The kinetic efficiency was obtained by comparing the one-dimensional kinetics specific impulse (I_{spODK}) to the I_{spODE} ($\eta_K = I_{spODK}/I_{spODE}$). The two-dimensional efficiency was obtained from charts which gave the η_{2D} for optimum Rao nozzles as described in Reference B-3. These charts were tabulated to facilitate their use in the performance program. The performance loss due to boundary layer development was obtained by implementing the turbulent boundary layer chart procedures also given in Reference B-3. These procedures were modified to incorporate the results of the BLIMP analysis conducted during Task I (Ref. B-4). The boundary layer efficiency was calculated by assuming an adiabatic wall chamber and propellants at the tank enthalpy levels. Past analyses have shown this approach to be quicker and to result in the same efficiency predictions as the more rigorous method of calculating the enthalpy loss to the regen coolant, then finding a new I_{spODE} by using the increased propellant enthalpy.

The performance model also includes a subroutine to calculate film-cooling efficiency, if required. Film-cooling efficiency is calculated by ratioing the mass weighted performance for the core and coolant stream tubes by the performance at the injector mixture ratio. The performance mathematical modeling (loss accounting) is consistent with the JANNAF simplified procedures specified in CPIA 246.

II, Summary (cont.)

B. CALIBRATION AND SENSITIVITY STUDY RESULTS

The energy release efficiency was calibrated to the NASA-LeRC OFO triplet LOX/RP-1 engine. The measured performance (% C*) of this engine was 99.1%; the parametric model prediction was 99.0%. The boundary layer loss used in the model was calibrated to BLIMP analyses and resulted in thrust loss correction factors from 0.4 to 1.2, depending on engine throat Reynolds number. The range of ODE specific impulse and various performance losses for LOX/RP-1 and area ratios of 10 to 1000, chamber pressures of 276 to 5515 kPa (40 to 800 psia), and thrusts of 667 to 890N (150 to 200 lbF) at mixture ratios of 2 and 4 are shown in the following table:

RANGE OF COMPONENT PERFORMANCE LOSSES

	<u>RANGE</u>
ODE Specific Impulse	(300 - 380 lbF-sec/lbm)
Kinetic Loss	2 - 15%
Divergence Loss	0.1 - 1.5%
Boundary Layer Loss	0.3 - 4.0%
Energy Release Loss	0.2 - 12%
Film-Cooling Loss	0 - 10%

As can be seen, the kinetic loss represents the largest potential performance decrement. However, both the energy release loss (vaporization and mixing) and the cooling loss are also potentially large losses. These can be controlled (to some extent) by engine/injector design.

During the Task I study, the chamber contraction ratio (CR), length (L'), and propellant temperature were evaluated. The results of these studies, based on element packaging and performance considerations, indicated that a minimum contraction ratio of 8 or minimum chamber diameter of 3.81 cm (1.5 in.) is necessary for good performance (ERE > 95%). Also, it was concluded that this performance level was compatible with the recommended (regenerative) cooling schemes. Further, heated fuel (RP-1) was predicted to yield significant performance improvements. Based on these analyses, an injection element density of 0.93 cm²(6/in.²) (OFO triplets) was selected as both yielding good performance and being in the current range of state-of-the art design practice.

During the Task II study, three engines with thrust/chamber pressure ratios of 667/276, 2669/2068, and 3113/5515N/kPa (150/40, 600/300, and 700/800 lbF/psia) were evaluated at mixture ratios of 2 and 4 over an area ratio range of 10 to 1000. This study resulted in chamber lengths of 14.73,

II, B, Calibration and Sensitivity Study Results (cont.)

12.7, and 10.41 cm (5.8, 5.0, and 4.1 in.), respectively, for the three engines. These lengths were within the regenerative cooling capability envelope (with LOX or LOX + RP-1) and resulted in predicted energy release efficiencies of 97.4 to 100%.

In addition to regenerative cooling, radiation and thermal barrier (O/F control) cooling were investigated. These cooling techniques result in lower performance than the regeneratively cooled cases at equivalent lengths, but performance could be improved by using longer lengths. The area ratio survey indicated approximately a 1% Isp increase with each doubling of ϵ above $\epsilon = 200:1$. Since good experimental data exist at a 400:1 area ratio (Ref. B-5), this area ratio ($\epsilon = 400:1$) was recommended for Task III analysis. The mixture ratio survey indicated the mixture ratio for maximum delivered specific impulse to be between 2.0 and 3.0.

III. TECHNICAL DISCUSSION

A. TASK I - ANALYSES

1. Model Formulation and Calibration

The simplified performance model formulated for this phase of the study was structured to fulfill the following four requirements:

- Represent state-of-the-art technology with regard to computer codes and modeling assumptions.
- Be sufficiently detailed to allow realistic trends of performance with both engine design and operating variables.
- Be amenable to parametric analysis (i.e., easy to input and fast to run).
- Be capable of being calibrated to known data or more rigorous analysis in those areas where current state-of-the-art simplified techniques were deemed inadequate.

The performance model uses the one-dimensional equilibrium specific impulse as the reference performance. From this reference performance, the various performance losses are subtracted to yield the predicted specific impulse. The performance losses considered and the codes used are shown in Figure B-1. The mathematical modeling (loss accounting) is shown on Figure B-2. This loss accounting is consistent with the JANNAF recommended techniques of Reference B-6. The two performance losses requiring special consideration in order to provide sufficient accuracy for meaningful performance trends were the energy release loss and the boundary layer loss.

a. Energy Release Loss Model

The energy release loss model can consider both vaporization-limited and mixing-limited performance. The vaporization-limited combustion model uses the work of Priem (Ref. B-1) to model the impact on engine performance due to incomplete propellant vaporization. This loss accounts for both the effects of a total mass flow rate deficit and the significant increase (shifts) in combustion mixture ratio compared to overall injector mixture ratio as a result of the vaporization limitation. A mathematical representation of the vaporization loss is given in Figure B-3. For LOX/RP-1 propellants, the vaporization model uses an empirically derived reduction in atomization efficiency by applying a 1.5 factor to the propellant droplet size. The mixing efficiency component of the energy release

- ODE and ODK Performance - Use JANNAF reference codes to generate parametric data as a function of P_c , mixture ratio, and area ratio. The ODK performance is scaled for thrust influences by using throat correction factors.
- Divergence Loss - Computes ΔV as a function of area ratio and % bell nozzle. Loss is consistent with results from nozzle design program output.
- Boundary Layer Loss - Use turbulent boundary layer (TBL) chart program calibrated by comparison with BLIMP laminar/turbulent analyses.
- Energy Release Loss - Use Priedem vaporization model and mixing criteria. Loss calibrated by comparison to the NASA/LERC hydrocarbon fuel engine.
- Film Cooling Loss - Use mass flowrate weighted coolant and core stream tube Isp to define loss per JANNAF simplified multizone technique.

Figure B-1. Performance Model Qualification Calibration

- Loss allocation is consistent with JANNAF techniques
- Geometric sum of efficiencies multiplied by ODE Isp equals delivered Isp

$$ISP_{DEL} = ISP_{ODE} \left\{ \frac{\eta_{DIV}}{\eta_{EL}/f_{inj}} \left(\eta_{KIN} \eta_{VAP} \eta_{HL} \eta_{FC} - (1 - \eta_{BL}) \right) \right\}$$

where

η_{DIV} = Divergence efficiency

η_{EL} = Mixing efficiency
 MIX

η_{KIN} = Kinetic efficiency

η_{VAP} = Vaporization efficiency

η_{HL} = Heat loss (gain) efficiency

η_{FC} = Film-cooling efficiency

η_{BL} = Boundary layer efficiency

Figure B-2. Performance Mathematical Modeling (Loss Accounting)

$$\begin{aligned}
1. \eta_{DIV} &= \frac{\dot{I}_{sp,ODE}}{\dot{I}_{sp,ODE}} \cdot \frac{\dot{M}_T}{\dot{M}_T} \\
2. \eta_{EL\ MIX} &= \frac{\left(\frac{\dot{I}_{sp,ODE}}{O/F_1} \times \dot{M}_1 \right) + \left(\frac{\dot{I}_{sp,ODE}}{O/F_2} \times \dot{M}_2 \right)}{\dot{I}_{sp,ODE} \cdot (\dot{M}_1 + \dot{M}_2)} \quad (O/F_1, O/F_2, \dot{M}_1, \dot{M}_2 \text{ does not account for } O/F \text{ shift caused by film cooling}) \\
3. \eta_{KIN} &= \frac{\left(\frac{\dot{I}_{sp,ODK}}{O/F_{V1}} \times \dot{M}_{V1} \right) + \left(\frac{\dot{I}_{sp,ODK}}{O/F_{V2}} \times \dot{M}_{V2} \right) + \left(\dot{I}_{sp,ODK} \times \dot{M}_{BV} \right)}{\left(\frac{\dot{I}_{sp,ODE}}{O/F_{V1}} \times \dot{M}_{V1} \right) + \left(\frac{\dot{I}_{sp,ODE}}{O/F_{V2}} \times \dot{M}_{V2} \right) + \left(\frac{\dot{I}_{sp,ODE}}{O/F_{BV}} \times \dot{M}_{BV} \right)} \\
4. \eta_{VAP} &= \frac{\left(\frac{\dot{I}_{sp,ODE}}{O/F_{V1}} \times \dot{M}_{V1} \right) + \left(\frac{\dot{I}_{sp,ODE}}{O/F_{V2}} \times \dot{M}_{V2} \right) + \left(\frac{\dot{I}_{sp,ODE}}{O/F_{BV}} \times \dot{M}_{BV} \right)}{\left(\frac{\dot{I}_{sp,ODE}}{O/F_1} \times \dot{M}_1 \right) + \left(\frac{\dot{I}_{sp,ODE}}{O/F_2} \times \dot{M}_2 \right) + \left(\frac{\dot{I}_{sp,ODE}}{O/F_B} \times \dot{M}_B \right)} \\
5. \eta_{BLL} &= 1 - \frac{\dot{I}_{F,BLL}}{\dot{M}_T \cdot \dot{I}_{sp,ODE} / O/F_{inj}} \\
6. \eta_{HL} &= \frac{\dot{I}_{sp,ODE} / HL\ O/F_{inj}}{\dot{I}_{sp,ODE} / O/F_{inj}} \\
7. \eta_{FC} &= \frac{\eta_{ST} W/FC}{\eta_{ST} W/O FC} = \left(\frac{\dot{M}_1 + \dot{M}_2}{\dot{M}_T} \right) \frac{\left(\frac{\dot{I}_{sp,OD}}{O/F_1} \times \dot{M}_1 \right) + \left(\frac{\dot{I}_{sp,OD}}{O/F_2} \times \dot{M}_2 \right) + \left(\frac{\dot{I}_{sp,OD}}{O/F_B} \times \dot{M}_B \right)}{\left(\frac{\dot{I}_{sp,ODE}}{O/F_1} \times \dot{M}_1 \right) + \left(\frac{\dot{I}_{sp,ODE}}{O/F_2} \times \dot{M}_2 \right) + \left(\frac{\dot{I}_{sp,ODE}}{O/F_B} \times \dot{M}_B \right)}
\end{aligned}$$

NOTE: All efficiencies are thrust ratios; losses are $(1 - \text{efficiencies})$

$$\dot{M} = \text{Mass Flowrate} \quad \dot{M}_T = \dot{M}_1 + \dot{M}_2 + \dot{M}_B$$

SUBSCRIPTS

1,2 = Stream Tubes 1 and 2 (Core)

B = Barrier Stream Tube

V = Vaporized Property

T = Total Property

III, A, Task I - Analyses (cont.)

model considers the influence of element size, element spacing, and engine size by using ALRC-developed empirical correlations derived from engine test data. The influence of element size is modeled within the code as the impact of hole size tolerance on interelement mixture ratio distribution. For a fixed orifice tolerance, the magnitude of possible element-to-element injection mixture ratio maldistribution increases with decreasing orifice size. The influence of element spacing on propellant core mixing efficiency is proportional to the ratio of chamber length to the product of contraction ratio and thrust per element raised to a power. Thus long chambers with small, densely packed injection elements result in predicted high interelement mixing efficiencies within the core. The engine size modeling considered the ratio of active injector core area to total injector area. Thus large injectors with a high ratio of active pattern-to-total-injector area yield a higher potential mixing efficiency than smaller injectors due to reduction of barrier or fringe mixing inefficiencies. Mixing loss is generally a small decrement to energy release efficiency, and the approach used herein has been found in previous programs to be conservative, i.e., to overpredict the mixing component of the energy release loss. The energy release model also considers the impact of the vaporization and mixing losses on the kinetic specific impulse. The operating and design parameters which influence the energy release loss and which may be evaluated with the model include the following:

Chamber Length	Element Type	Propellant Temperature
Chamber Contraction Ratio	Element Size	Injection Velocity
Nozzle Expansion Ratio	Propellant Type	Chamber Pressure
		Mixture Ratio

Basically, the performance program input is the desired chamber pressure, mixture ratio, propellant combination, element type, element density, expansion and contraction ratios, chamber and nozzle lengths, and reference engine vaporization data. The program iterates to determine engine size (throat radius) and performance, using a 0.2% energy release closure criterion. The following guidelines for the LOX/RP-1 engine resulted from preliminary investigations:

* Geometry

Minimum Chamber Diameter - 3.81 cm (1.5 in.)

Minimum Injector Orifice Diameter 0.025 cm
(0.010 in.)

Injection Element Density $0.93/\text{cm}^2$ (6/in.²)

Element Type OFO Triplets, or Equivalent

3.23 cm^2 (0.5 in.²) Igniter Area in Center of
Injector

85% Bell Nozzle

III, A, Task I - Analysis (cont.)

• Operating Parameters

Injector Pressure Drop = $P_c 0.75$

Vaporization-limited and Mixing-Limited Combustion Efficiency

0.2% Closure on Performance Iteration Loops

Cooling Loss Model Consistent with Heat Transfer Assumptions Using Mass-Weighted Film Cooling and Core Stream Tubes

All Other Losses as Defined in Simplified Procedure of CPIA 246

The energy release loss model was calibrated to the NASA-LeRC LOX/RP-1 OFO triplet engine described in Reference B-7. The pertinent engine parameters and calibration results are shown on Table B-I. These data show excellent agreement of the predicted parametric model performance ($\%C^* = 99.0$) to the measured value (99.1%).

b. Boundary Layer Loss Model

The purpose of this work was to qualify the simplified procedure (TBL chart) used for predicting performance loss due to boundary layer development. This was accomplished by comparing TBL (turbulent boundary layer) chart predictions to losses calculated by the more rigorous JANNAF procedure used for the BLIMP program. Twenty-five operating points were simulated with the BLIMP program. Thrust, chamber pressure, combustion chamber length to throat diameter ratio, wall temperature to gas-side stagnation temperature ratio, and flow transition (laminar to turbulent) criteria were varied during these simulations. Table B-II lists the cases simulated and the resulting thrust loss; all cases were for an area ratio of 100:1.

The first seven BLIMP runs were used to determine the influence of using laminar or turbulent boundary layers when solving for thrust loss. These runs indicated that the thrust loss with turbulent flow was approximately twice the loss experienced with laminar flow for the same operating point.* Since the type of flow significantly influences the calculated thrust loss, these runs were also used to determine a transition criterion based on momentum thickness Reynolds number (Re_θ) that is consistent with the criterion used in the thermal analysis.

*Subsequent analyses showed that the relationship of laminar to turbulent boundary layer thrust loss varies as a function of Reynolds number.

TABLE B-1

ENERGY RELEASE EFFICIENCY CALIBRATION TO NASA-LeRC LOX/RP-1 OFO TRIPLET ENGINE

	Engine Configuration	OFO Triplet	ALRC Parametric Model
○ Engine Configuration			
Chamber Length, L', cm (in.)	24.94 (9.82)		
Chamber Contraction Ratio	4.30		
Throat Diameter, cm (in.)	6.60 (2.60)		
Chamber Pressure, kPa (psia)	4136 (600)		
Mixture Ratio	2.7		
○ Injector Type			
Oxidizer Orifice Diameter, cm (in.)	0.185 (0.073)		
Fuel Orifice Diameter, cm (in.)	0.170 (0.067)		
Number of Elements	37		
○ Injector Pressure Drop			
Oxidizer, kPa (psia)	627 (91)		
Fuel, kPa (psia)	634 (92)		
○ Performance, % C*			
Experimental	NASA-LeRC Prediction		
99.1	98.9		
		99.0	

TABLE B-11
BLIMP - TBL CHART COMPARISON*

CASE NO.	1	2	3	4	5
F, N (1bf)	4448 (1000)	4448 (1000)	4448 (1000)	5400 (1214)	5400 (1214)
Pc, kPa (psia)	2671 (387.5)	2671 (387.5)	2671 (387.5)	1206 (175)	1206 (175)
F/Pc	1.67 (2.58)	1.67 (2.58)	1.67 (2.58)	4.48 (6.93)	4.48 (6.93)
F x Pc	11.88 x 10 ⁶ (387,500)	11.88 x 10 ⁶ (387,500)	11.88 x 10 ⁶ (387,500)	6.51 x 10 ⁶ (212,370)	6.51 x 10 ⁶ (212,370)
R*, cm (in.)	6159 (0.6362)	1.6159 (0.6362)	1.6159 (0.6362)	2.588 (1.019)	2.588 (1.019)
y	1.213	1.213	1.213	1.213	1.213
a ₁	15°	15°	15°	15°	15°
CR	2.5	2.5	2.5	2.5	2.5
L _{cyl} /D*	4.0	4.0	2.0	4.0	4.0
RTHETA	1.095	1.095	1.0	1.095	1.095
T _w /T _s	0.2	0.2	0.2	0.2	0.2
ΔF BLIMP, N (1bf)	42.48 (9.55)	88.78 (19.96)	41.54 (9.34)	112.76 (25.35)	57.87 (13.01)
ΔF TBL, N (1bf)	125.66 (28.25)	125.66 (28.25)	114.76 (25.80)	137.18 (30.84)	137.18 (30.84)
Δε _{TBL}	6.72 x 10 ⁵	6.72 x 10 ⁵	6.72 x 10 ⁵	4.33 x 10 ⁵	4.33 x 10 ⁵
F RATIO	0.3381	0.7065	0.3520	0.8220	0.4219
Flow	Laminar	Mixed	Laminar	Mixed	Laminar
Trans. Pt.		c = 1		c = 1	
Trans. Re _{em}	1000	360	1000	360	800
z ΔF BLIMP	0.96	2.00	0.93	2.09	1.07

Negative c = upstream of throat

*Area Ratio = 100:1

$$F \text{ RATIO} = \frac{\Delta F_{BLIMP}}{\Delta F_{TBL}}$$

TABLE B-II (cont.)

CASE No.	6	7	8	9	10
F, N (1bF)	6672 (1500)	12365 (2780)	445 (100)	445 (100)	445 (100)
Pc, kPa (psia)	2944 (427)	2944 (427)	137.9 (20)	137.9 (20)	137.9 (20)
F/PC	2.27 (3.51)	2.27 (3.51)	3.23 (5.0)	3.23 (5.0)	3.23 (5.0)
F x PC	19.64×10^6 (640,000)	36.4×10^6 (1,187,000)	61.3×10^3 (2,000)	61.3×10^3 (2,000)	61.3×10^3 (2,000)
R*, cm (in.)	1.886 (0.7426)	2.567 (1.0106)	2.230 (0.8781)	2.230 (0.8781)	2.230 (0.8781)
y	1.213	1.213	1.213	1.213	1.213
x_1	15°	15°	15°	15°	15°
CR	2.5	2.5	2.5	2.5	2.5
L_{cy1}/D^*	4.0	4.0	4.0	4.0	4.0
RTHETA	1.095	1.095	1.0	1.0	1.0
T_w/T_s	0.2	0.2	0.2	0.2	0.2
$\zeta_F BLIMP, N (1bF)$	128.8i (28.96)	212.56 (47.79)	15.21 (3.42)	12.32 (2.77)	8.32 (1.87)
$\zeta_F TBL, N (1bF)$	180.14 (40.50)	311.58 (70.05)	18.99 (4.27)	15.70 (3.53)	11.03 (2.48)
Re _{TBL}	8.46×10^5	1.22×10^7	4.97×10^4	4.97×10^4	4.97×10^4
F RATIO	0.7151	0.7108	0.8009	0.7847	0.7544
Flow	Mixed	Mixed	Laminar	Laminar	Laminar
Trans Pt.	$\epsilon = -1.36$	$\epsilon = -1.36$	360	360	360
Trans Re _{em}					
$\frac{\epsilon F BLIMP}{F}$	1.93	1.79	3.42	2.77	1.87

Transition Criteria

$$R_{e_{em}} = 443$$

Area Ratio = 100:1

$$\text{F RATIO} = \frac{\Delta F BLIMP}{\Delta F TBL}$$

TABLE B-II (cont.)

CASE No.	<u>11</u>	<u>12</u>	<u>13</u>	<u>14</u>	<u>15</u>
F, N (1bf)	4448 (1000)	4448 (1000)	4448 (1000)	445 (100)	445 (100)
P_c, kPa (psia)	137.9 (20)	137.9 (20)	137.9 (20)	6894 (1000)	6894 (1000)
F/P_c	32.25 (50)	32.25 (50)	32.25 (50)	0.065 (0.10)	0.065 (0.10)
$F \times P_c$	613×10^3 (20,000)	613×10^3 (20,000)	613×10^3 (20,000)	3.07×10^6 (100,000)	3.07×10^6 (100,000)
R^*, cm (in.)	7.053 (2.7768)	7.053 (2.7768)	7.053 (2.7768)	0.319 (0.1257)	0.319 (0.1257)
γ	1.213	1.213	1.213	1.213	1.213
γ_1	15°	15°	15°	15°	15°
CR	2.5	2.5	2.5	2.5	2.5
L_{cy1}/D^*	2.0	2.0	2.0	2.0	2.0
ATHETA	1.0	1.0	1.0	1.0	1.0
T_w/T_s	0.2	0.5	0.5	0.2	0.5
$\Delta F_{BLIMP}, N$ (1bf)	85.58 (19.24)	69.21 (15.56)	46.79 (10.52)	5.822 (1.309)	4.71 (1.059)
$\Delta F_{TBL}, N$ (1bf)	150.83 (33.91)	124.90 (28.08)	87.45 (19.66)	13.26 (2.98)	10.99 (2.47)
Re_{TBL}	1.57×10^5	1.57×10^5	1.57×10^5	3.39×10^5	3.39×10^5
F RATIO	0.5674	0.5541	0.5351	0.4393	0.4287
Flow	Laminar	Laminar	Laminar	Laminar	Laminar
Trans Pt.					
Trans Re_{ϵ_m}					
$\frac{\epsilon}{F} \frac{\Delta F_{BLIMP}}{F}$	1.92	1.56	1.05	1.31	1.06
Transition Criteria	$R_{e_{\epsilon_m}} = 443$				

*Area Ratio = 100:1

F RATIO = $\frac{\Delta F_{BLIMP}}{\Delta F_{TBL}}$

TABLE B-II (cont.)

CASE No.	16	17	18	19	20
F, N (1bF)	445 (100)	4448 (1000)	4448 (1000)	4448 (1000)	2.224 (0.5)
Pc, kPa (psia)	6894 (1000)	6894 (1000)	6894 (1000)	6894 (1000)	1034 (150)
F/Pc	0.065 (0.1)	0.645 (1.0)	0.645 (1.0)	0.645 (1.0)	0.002 (0.003)
$\xi \times P_c$	3.07×10^6 (100,000)	30.66×10^6 (1,000,000)	30.66×10^6 (1,000,000)	30.66×10^6 (1,000,000)	2300 (75)
R ^w , cm (in.)	0.319 (0.1257)	1.009 (0.3974)	1.009 (0.3974)	1.009 (0.3974)	0.058 (0.0227)
γ	1.213	1.213	1.213	1.213	1.213
γ_1	15°	15°	15°	15°	15°
CR	2.5	2.5	2.5	2.5	2.5
L_{cy}/D^*	2.0	2.0	2.0	2.0	2.0
RTHETA	1.0	1.0	1.0	1.0	1.0
T_w/T_s	1.0	0.2	0.5	1.0	0.2
ΔF_{BLIMP} , N (1bF)	3.19 (0.7162)	81.49 (18.32)	67.43 (15.16)	17.93 (4.03)	0.173 (0.0389)
ΔF_{TBL} , N (1bF)	7.70 (1.73)	105.28 (23.67)	87.14 (19.59)	61.03 (13.72)	0.133 (0.03)
Re _{TBL}	3.39×10^5	1.08×10^6	1.07×10^6	1.07×10^6	9.49×10^3
F RATIO	0.4140	0.7740	0.7739	0.2937	1.295
Flow	Laminar	Mixed	Laminar	Laminar	
Trans Pt.	$\epsilon = 1.0$	$\epsilon = 1.0$	$\epsilon = 1.0$	$\epsilon = 1.0$	
Trans Re _{em}					
$\frac{\Delta F_{BLIMP}}{f}$	0.72	1.83	1.52	0.40	7.78
Transition Criteria	$R_{e_{em}} = 443$				
					Negative ϵ means upstream of throat
					$F \text{ RATIO} = \frac{\Delta F_{BLIMP}}{\Delta F_{TBL}}$

*Area Ratio = 100:1

TABLE B-II (cont.)

CASE No.	<u>21</u>	<u>22</u>	<u>23</u>	<u>24</u>	<u>25</u>
F, N (1bf)	2.224 (0.5)	8896 (2,000)	8896 (2,000)	88960 (20,000)	88960 (20,000)
Pc, kPa (psia)	1034 (150)	10341 (1500)	10341 (1500)	13788 (2,000)	13788 (2,000)
F/Pc	0.002 (0.003)	0.86 (1.33)	0.86 (1.33)	6.45 (10)	6.45 (10)
F x P _c	2330 (75)	92 x 10 ⁶ (3,000,000)	92 x 10 ⁶ (3,000,000)	1226.6 x 10 ⁶ (40,000,000)	1226.6 x 10 ⁶ (40,000,000)
R*, cm (in.)	0.058 (0.0227)	1.166 (0.4589)	1.166 (0.4589)	3.193 (1.2570)	3.193 (1.2570)
r _t	1.213	1.213	1.213	1.213	1.213
15°	15°	15°	15°	15°	15°
CR	2.5	2.5	2.5	2.5	2.5
L _{cg} /D*	2.0	2.0	2.0	2.0	2.0
P/THETA	1.0	1.0	1.0	1.0	1.0
T _w /T _s	1.0	0.2	1.0	0.2	1.0
F _{BLIMP} , N (1bf)	0.095 (0.0213)	153.36 (34.48)	57.02 (12.82)	1285 (288.7)	578 (129.9)
F _{TBL} , N (1bf)	0.089 (0.02)	188.77 (42.44)	109.42 (24.6)	1458 (327.8)	845 (190.07)
Re _{TBL}	9.49 x 10 ³	1.85 x 10 ⁶	1.85 x 10 ⁶	6.73 x 10 ⁶	6.73 x 10 ⁵
F RATIO	1.054	0.9124	0.5211	0.8806	0.6834
Flow	Laminar	Mixed	Mixed	Mixed	Mixed
Trans Pt.		c = -1.36	c = 35	c = -1.984	c = -1.36
Trans Re _{e_m}					
$\frac{\chi f_{BLIMP}}{F}$	4.26	1.72	0.64	1.44	0.65
Transition Criteria	$R_{e_{em}} = 443$				

Negative ϵ means upstream of throat
 $R_{e_{em}}$

*Area Ratio = 100:1

$$F \text{ RATIO} = \frac{\Delta F_{BLIMP}}{\Delta F_{TBL}}$$

III, A, Task I - Analysis (cont.)

The BLIMP User's Manual suggests a transition Re_{θ} of 360 as a nominal guess. The manual notes that this value is for a zero pressure gradient flat surface (not contoured) and that for accelerating flows, as in a rocket nozzle, the transition value will increase. A transition Re_{θ} of 443 was found to result in a transition criterion consistent with that of the thermal analysis.

Having established a transition criterion, reference cases to be simulated were chosen to be at the corners of the study parametric box. These cases (No. 8-19 in Table B-II) assumed wall-temperature to gas-stagnation temperature ratios of 0.2, 0.5, and adiabatic wall (1.0) and were run at the operating points listed below:

Pc, kPa (psia)	138 (20)	138 (20)	6894 (1000)	6894 (1000)
Thrust, N (lbF)	445(100)	4448(1000)	445(100)	4448(1000)

Six additional cases were run to provide a better definition of data trends. The three operating points listed below were run for a wall temperature ratio of 0.2 and an adiabatic wall (Cases 19-25):

Pc, kPa (psia)	1034 (150)	10341 (1500)	13788 (2000)
Thrust, N (lbF)	2.224 (0.5)	8896 (2000)	88960 (20,000)

Figure B-4 shows the percentage of thrust loss as a function of chamber pressure, thrust, and wall temperature. In general, as thrust, chamber pressure, and/or wall temperature ratio increase, the percentage of thrust loss decreases with either laminar or turbulent flow.

Figure B-5 shows the correlation between the BLIMP and TBL chart predictions as a function of throat Reynolds number calculated by TBL chart. This shows that the majority of operating points at low-thrust are in the laminar and transition region. For the low-thrust sensitivity study, the correlation shown in Figure B-5 was used to anchor the TBL chart estimate to the BLIMP prediction.

The data shown on Figure B-5 indicate that wall-to-free-stream temperature ratio differences have a negligible influence on the correlation below a throat Reynolds number of about 4×10^5 . At throat Reynolds numbers above this value to about $Re = 1.1 \times 10^6$, the boundary layer is in the transition region, and large differences in the correlation are evident dependent on the assumed wall-to-free-stream temperature ratio. However, in this region, the total boundary layer loss is small (1 to 2%) and the resulting performance uncertainty introduced by using the recommended correlation is less than 0.5%.

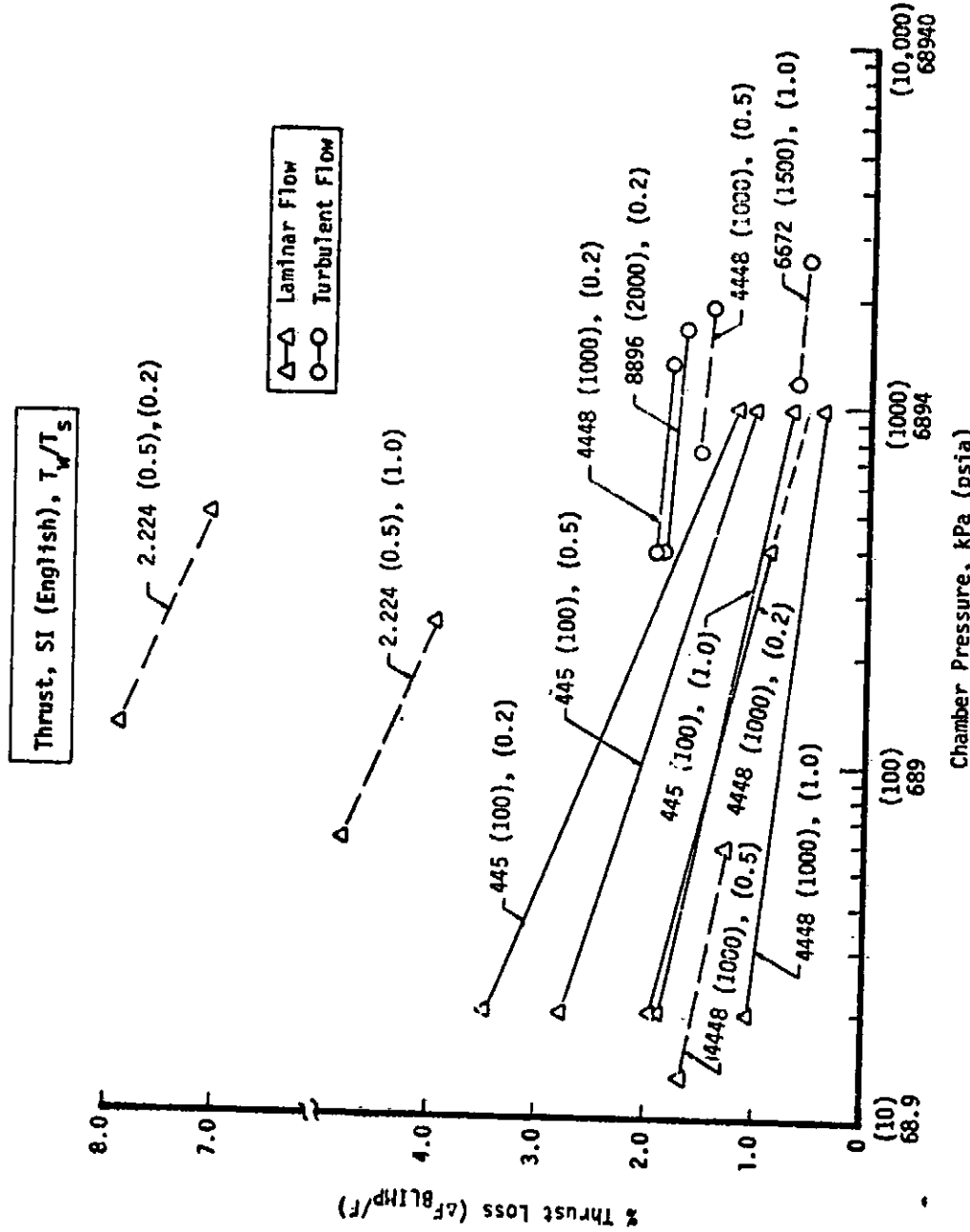


Figure 8-4. Influence of Chamber and Thrust on Thrust Loss Due to Boundary Layer Development

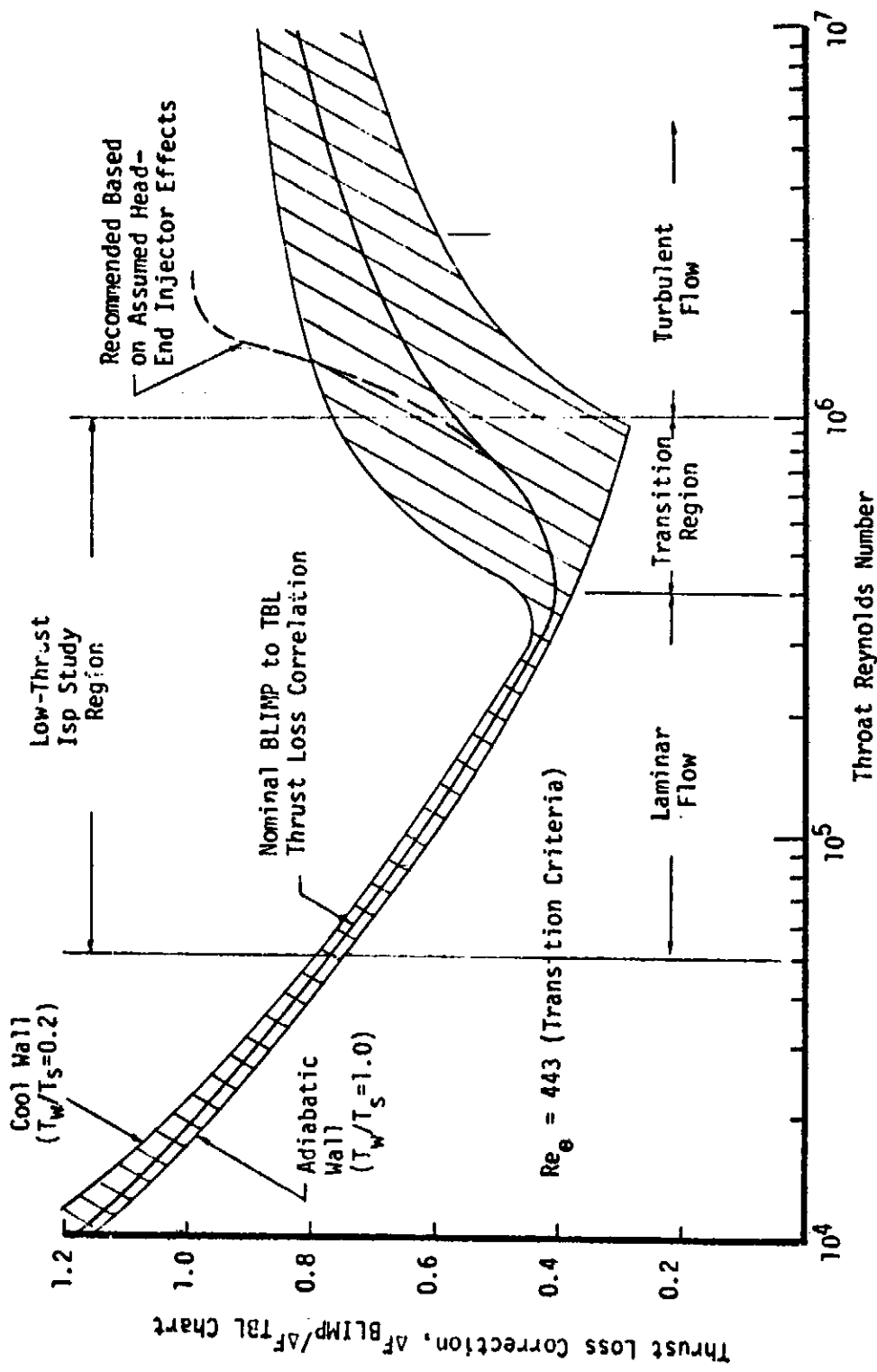


Figure B-5. BLIMP vs TBL Chart Thrust Loss Correction Factors

III, A, Task I - Analysis (cont.)

A question still remains about the validity of applying the correlation shown in Figure B-5 to high-Pc, high-thrust engines. Using the transition criteria of $Re_0 = 443$, the BLIMP solution shows the flow to be laminar at the start and becoming turbulent as it nears or enters the throat. This mix-flow situation results in a predicted performance loss less than that shown on the TBL chart which considers the flow to be fully turbulent. However, if injector influences are considered to promote free-stream turbulence, the boundary layer is probably turbulent from very near the starting point. In this case, a lower transition Reynolds number may be appropriate to ensure a fully turbulent boundary layer. Table B-III shows that for the fully turbulent cases, the BLIMP (using the recommended Cebeci-Smith correlation) and TBL chart predictions agree very well. Therefore, in the turbulent flow region (from $Re = 1.1 \times 10^6$ to $Re = 2 \times 10^6$), the correlation indicated by the dashed line on Figure B-5 is recommended in order to avoid a discontinuity between the transition and fully turbulent regions. For Reynolds numbers greater than 2×10^6 , a BLIMP-to-TBL-chart ΔF ratio of 1.0 is recommended.

Based on the BLIMP/TBL chart comparisons shown in Table B-III, the impact of differences in isentropic exponent (γ) on the boundary layer loss appears to be well modeled. Also, comparing the data for the turbulent cases, the influence of viscosity on the boundary layer loss is adequately modeled for a variety of propellants and mixture ratios. The correlation for the laminar and transition cases, shown in Figure B-5, was obtained by using a constant BLIMP/TBL chart reference viscosity. The influence of viscosity changes on the boundary layer loss is a Reynolds number effect which should be accounted for in the correlation of Figure B-5. However, cases which would allow a direct assessment of the combined influence of γ and viscosity on the boundary layer correction in the laminar flow region have not been run. The thrust loss correction factor in the laminar region follows the theoretical trend, which is based on the local skin friction being a function of Reynolds number to the 1/5 and 1/2 power for the turbulent and laminar conditions, respectively. The trends of thrust loss with throat Reynolds number and wall temperature ratio are shown in Figure B-6. The value of viscosity used to compute the Reynolds number and the value of γ are functions of engine operating conditions and are computed within the boundary layer routine.

2. Task I Results

a. Influence of Contraction Ratio on Isp

The influence of chamber contraction ratio on attainable specific impulse is shown in Figure B-7. This figure shows the predicted Isp as a function of contraction ratio for both 445 and 4448N

TABLE B-III
COMPARISON OF BLIMP AND THE SIMPLIFIED TBL CHART LOSSES

	Thrust, N (lbf)	88960 (20k)	88960 (20k)	88960 (20k)	88960 (20k)	102304 (23k)	102304 (23k)	66720 (15k)	66720 (15k)
ρ_c , kPa (psi)	13788 (2000)	13788 (2000)	13788 (2000)	13788 (2000)	13995 (2030)	15767 (2287)	15767 (2287)	5872 (1300)	5872 (1300)
Propellant	10x/10P-1	10x/10P-1	10x/10P-1	10x/10P-1	Q ₂ /H ₂				
Q/r	2.1	2.1	2.8	2.8	6.356	6.378	6.378	6.0	6.0
Area Ratio	400	400	400	400	190	405	405	782	782
Turbulence Mode:	Geberi-Smith	Geberi-Smith	Geberi-Smith	Geberi-Smith	Kendall	Kendall	Kendall	Geberi-Smith	Geberi-Smith
R_e	1.23	1.23	1.23	1.23	1.203	1.25	1.25	1.992	1.992
τ_w	1.221	1.221	1.293	1.293	1.19	1.19	1.21	1.19	1.19
T_w/T_s	0.243	0.171	0.219	0.154	0.156	0.170	0.170	0.16	0.16
η_1	13	13	13	13	17	17	17	11	11
η_2	CR	2.8	3.8	3.8	3.66	3.66	3.66	3.66	3.66
L_{Cf}/D^*	0	0	0	0	0.75	0.75	0.75	6.5	6.5
η_{NETA}	0.95	0.95	0.95	0.95	1.0	1.0	1.0	1.07	1.07
η_{BLIMP} , N (lbf)	1664 (374)	1766 (460)	2046 (479)	2131 (535)	1579 (491)	2184 (574)	2553 (806)	903 (208)	7208 (208)
η_{BLIMP} , N (lbf)	1717 (386)	1726 (451)	2068 (412)	1833 (518)	2324 (412)	1090 (245)	1090 (245)	1659 (373)	1659 (373)
ΔI_{sp} BLIMP	7.3	7.7	8.9	9.2	12.7	12.1	17.0	4.5	18.7
ΔI_{sp} Simplified	7.5	7.5	8.8	9.0	10.7	10.7	10.9	5.4	18.2
Flow Field	Turb	Turb	Turb	Turb	Turb	Turb	Turb	Turb	Turb

COMPARISON RESULTS

TURBULENCE MODEL	MALL TEMP.	NO. OF LINES	AVE. 1SD %
Geberi-Smith	Cool Wall	8	0.5
Kendall	Cool Wall	3	4.7
Geberi-Smith	Hot Wall	1	0.6
Both Models	Adiabatic	3	0.6

Transition Criterion $Re_t = 360$

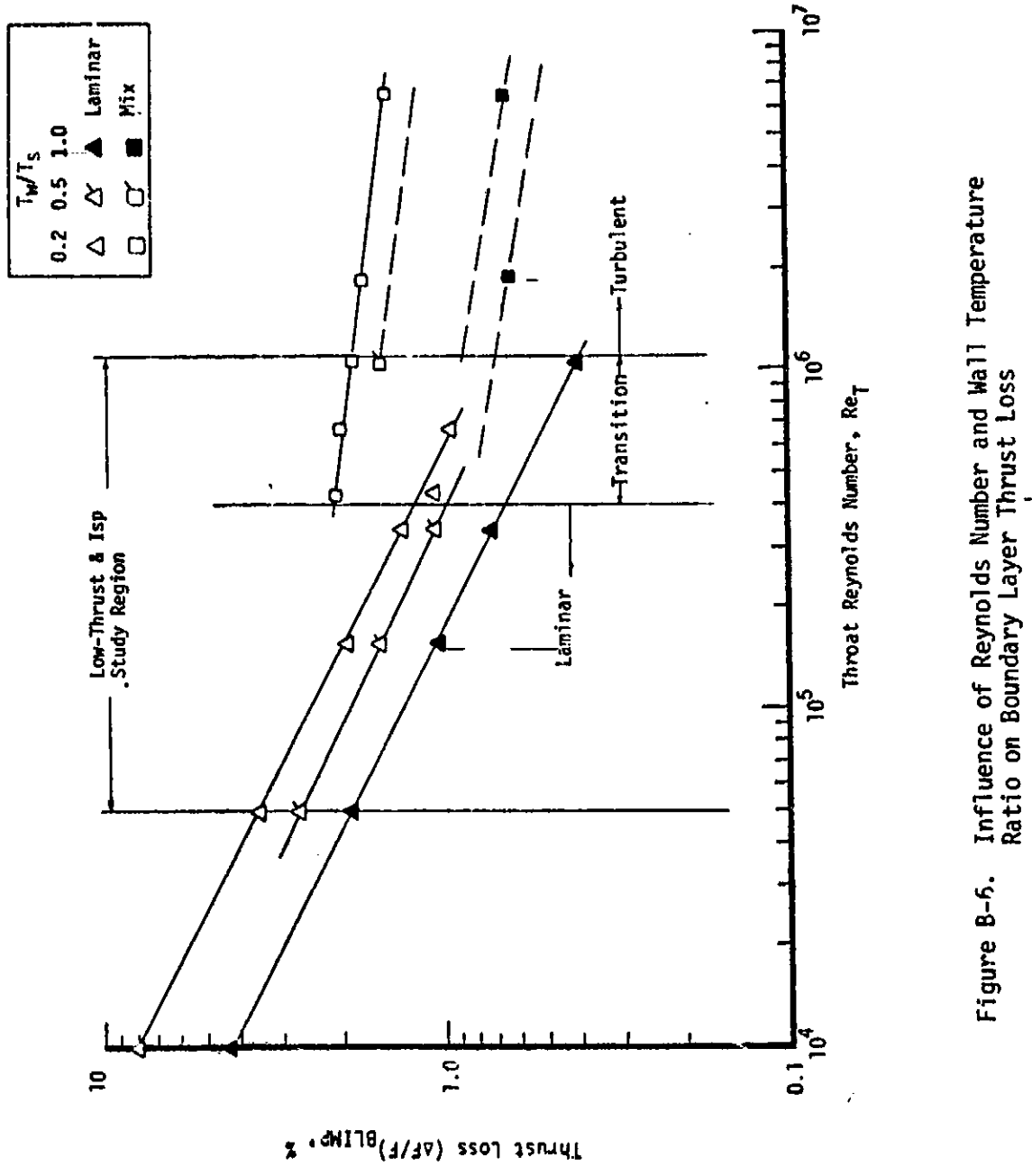


Figure B-6. Influence of Reynolds Number and Wall Temperature Ratio on Boundary Layer Thrust Loss

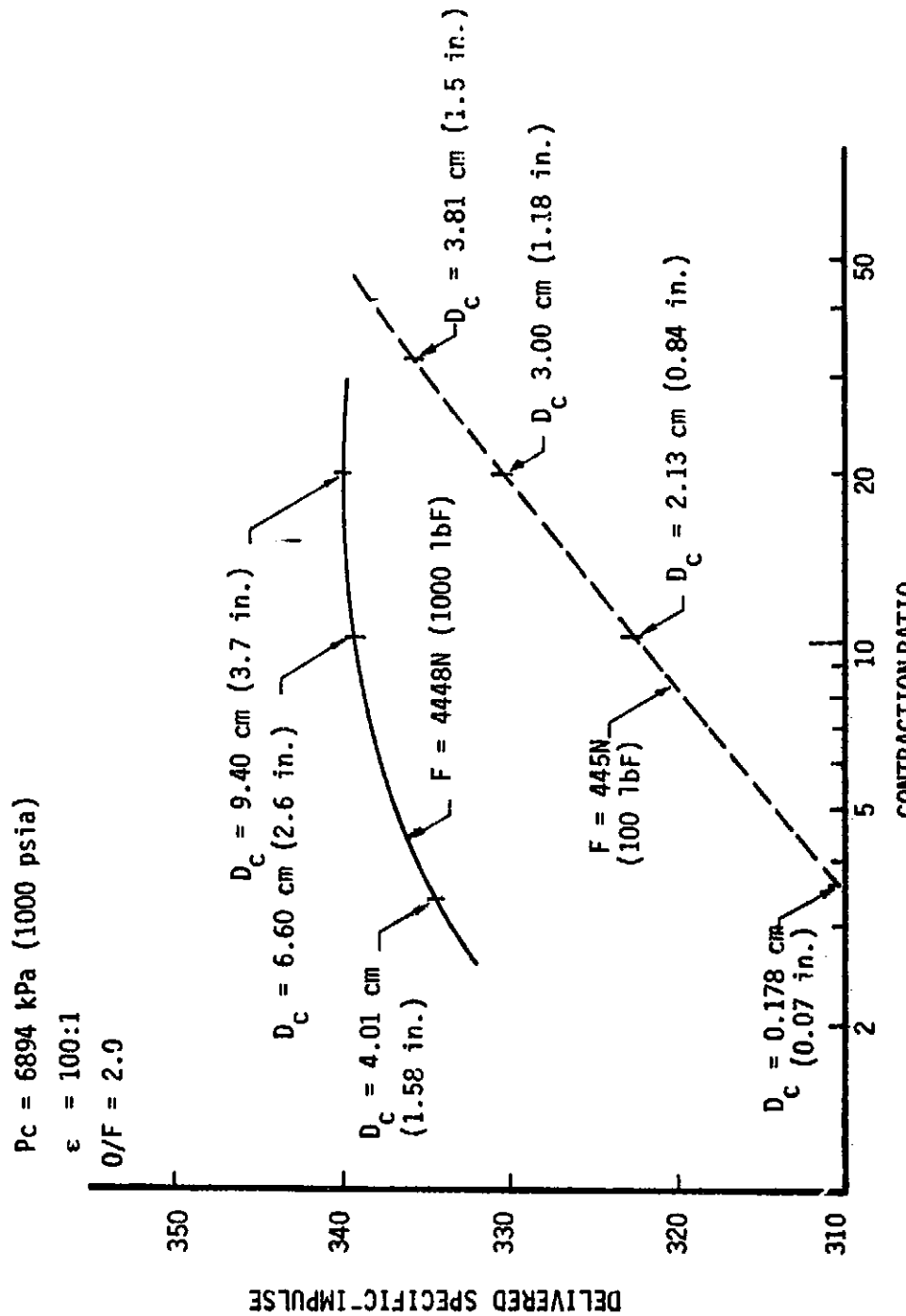


Figure B-7. Influence of Contraction Ratio on Specific Impulse

III, A, Task I - Analysis (cont.)

(100 and 1000 lbF) thrust engines assuming $0.93/\text{cm}^2$ ($6/\text{in.}^2$) ODE element density over the injector surface. For the 445N (100 lbF) thrust case, the Isp decreases significantly with contraction ratio due to the reduction in the injector area available for elements. For the larger 4448N (1000 lbF) engine, the chamber diameter is sufficiently large [$D_c = 4.01 \text{ cm}$ (1.58 in.]) at the small contraction ratios that the Isp reduction caused by a reduction in the number of elements is only about 2%. The influence of thrust/chamber pressure ratio on the number of injection elements is shown in Figure B-8 for an element density of 6 and 12 and contraction ratios equal to or greater than 8.

b. Influence of Chamber Length and Fuel Temperature on Energy Release Efficiency

The influences of chamber length and fuel temperature on energy release efficiency are shown in Figure B-9. These data show that the use of heated fuel allows shorter chambers for a given performance level. This increase in performance results from improved fuel vaporization efficiency at the higher fuel temperatures.

c. Predicted Performance Trends with Area Ratio

Predicted performance trends as a function of area ratio are shown for a low-thrust/low-chamber-pressure engine and a high-thrust/high-chamber-pressure engine in Figures B-10 and B-11, respectively. Included in the figures are the ODE Isp and the predicted losses. As would be expected, the low-thrust/low-Pc case has significantly higher kinetic and boundary layer losses. The energy release loss for both cases is seen to decrease with increasing area ratio. This reduction in energy release loss is caused by a shift in the maximum ODE Isp to higher mixture ratios as area ratio is increased. The shift in optimum mixture ratio tends to reduce the component of energy release loss associated with the difference between combustion mixture ratio and propellant mixture ratio at the injector. As can be seen from the two figures, the Isp continuously increases with area ratio, and there is no pronounced "knee" or change in slope although the slope decreases continuously with increasing area ratio. At an area ratio of 400:1, the attainable Isp values for the low- and high-thrust/Pc cases are (318 and 342 lbF-sec/lbm), respectively. Nearly all of this performance difference is due to larger kinetic and boundary layer losses for the low-thrust/Pc case.

B. TASK II - ANALYSES

During the Task II sensitivity studies, evaluations were conducted for three NASA-approved engine sizes:

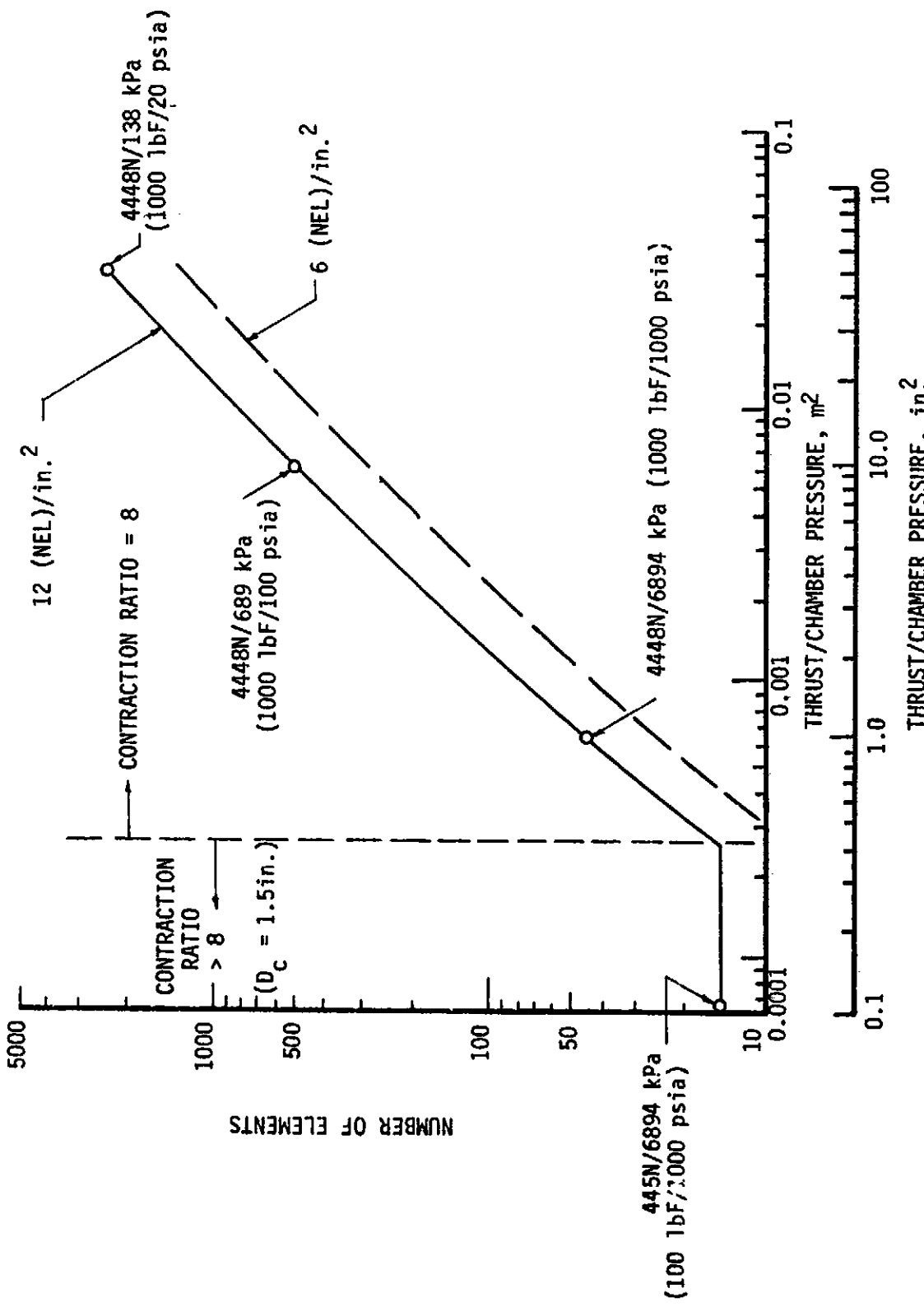


Figure B-8. Influence of Thrust/Chamber Pressure Ratio on Number of Injection Elements

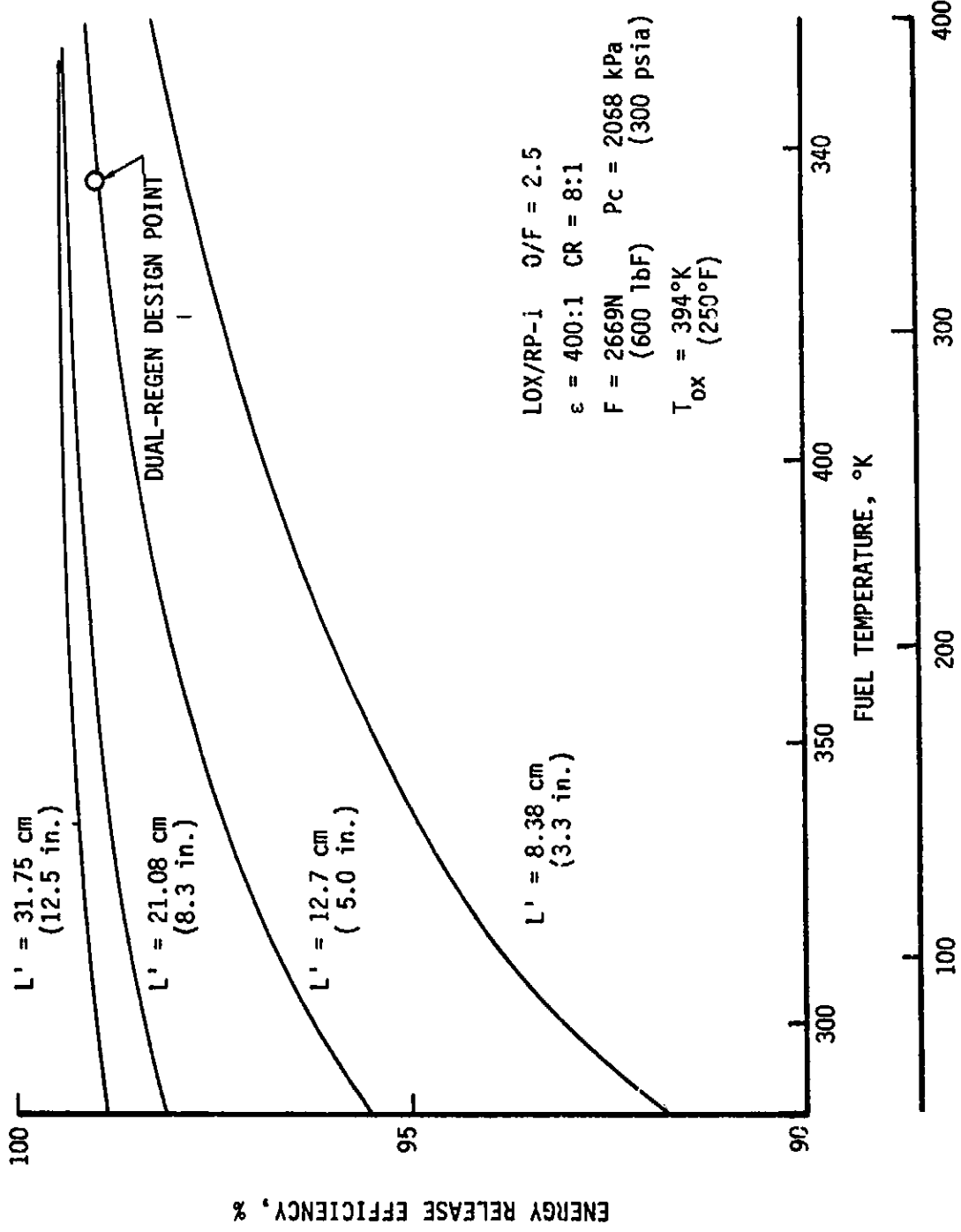


Figure B-9. Heated Fuel Allows Use of Shorter Chambers

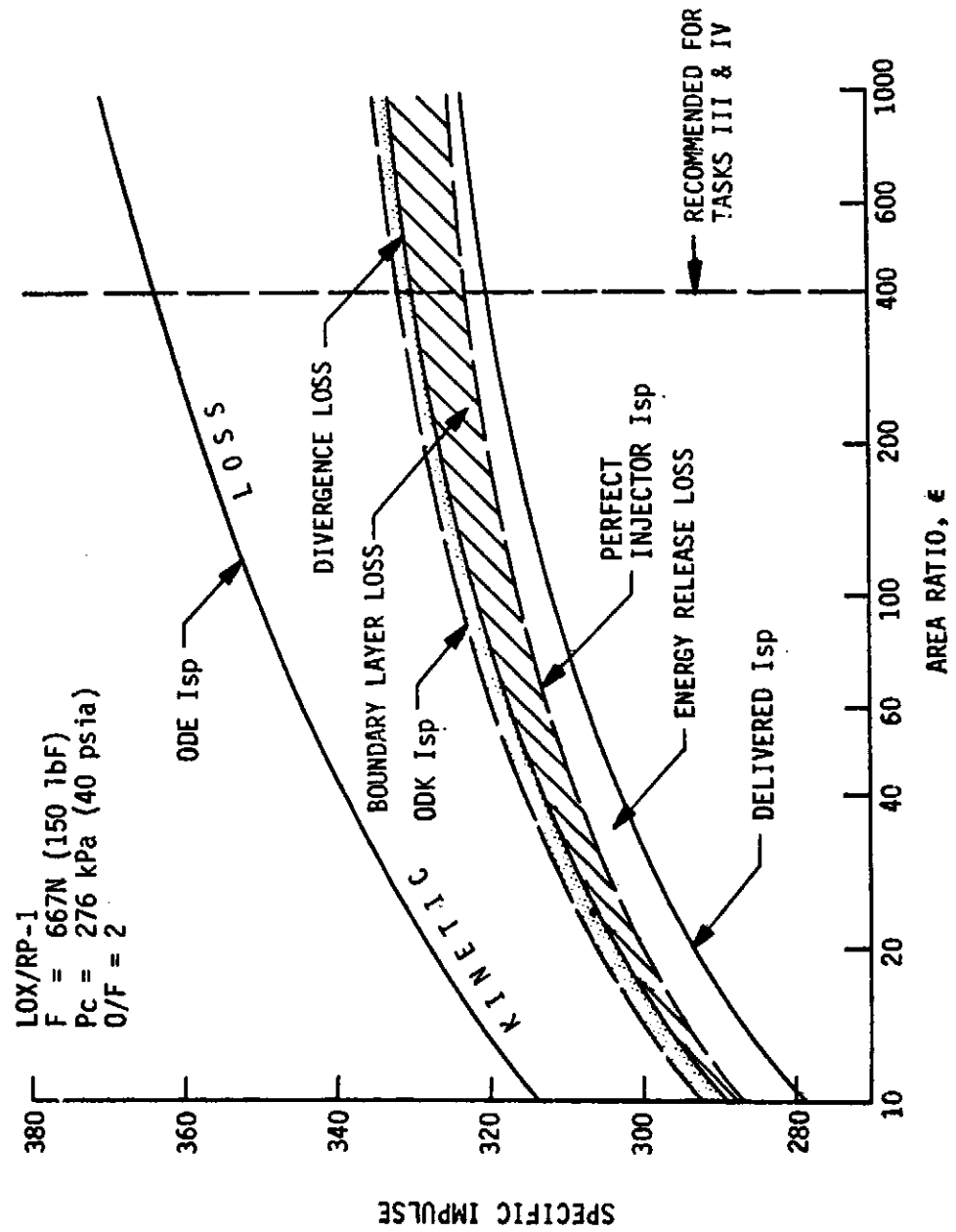


Figure B-10. Predicted Performance Losses for Low-Thrust, Low-Pc Engine

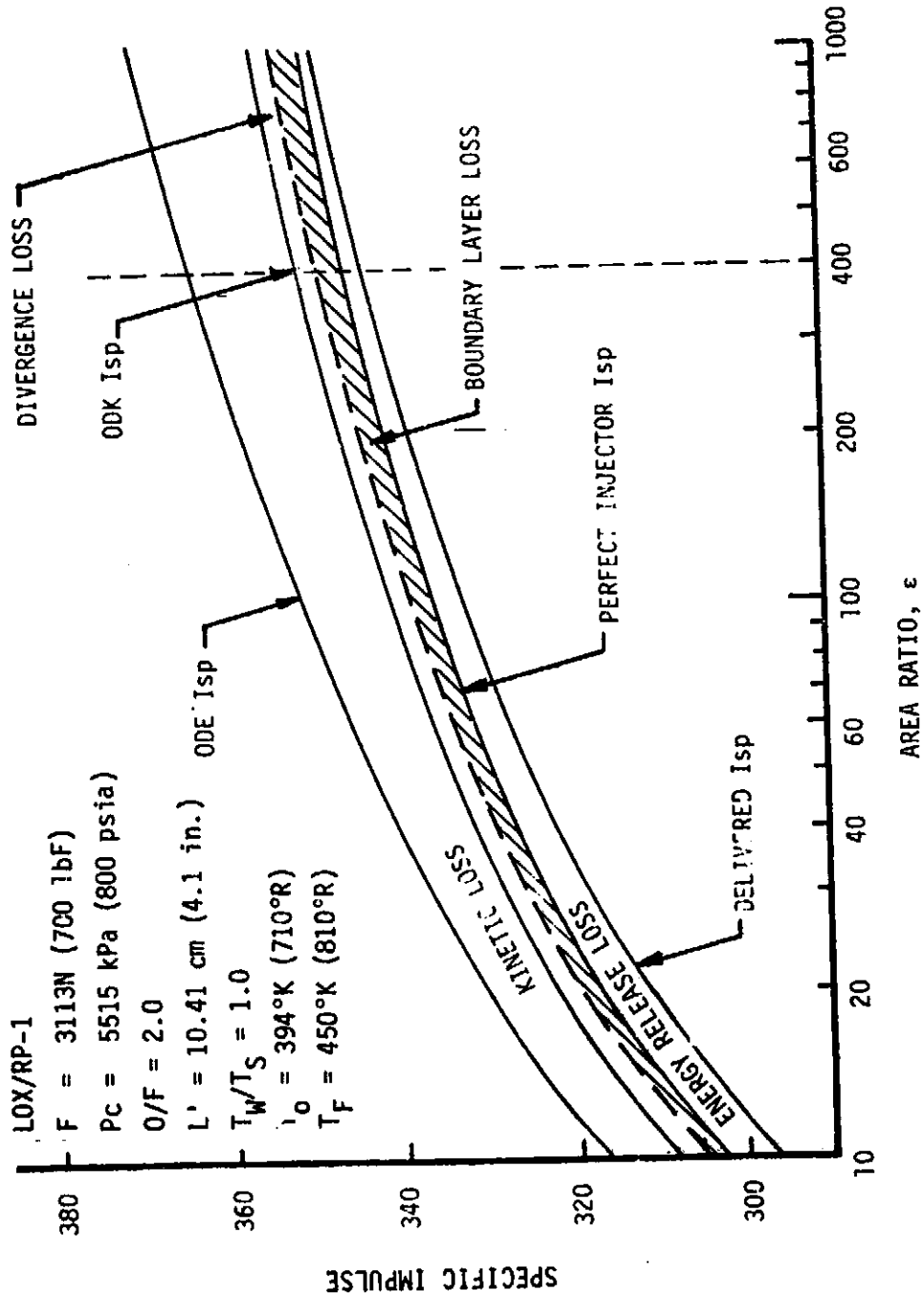


Figure B-11. Predicted Performance Losses for High-Thrust, High-Pc Engine

III, B, Task II - Analyses (cont.)

	1	2	3
Thrust, N(1bf)	667(150)	2669(600)	3114(700)
Chamber Pressure, kPa(psia)	276(40)	2068(300)	5515(800)

Attainable specific impulse was evaluated for these engines as a function of area ratio (10 to 1000) for two mixture ratios (2.0 and 4.0) and three cooling concepts:

1. Dual regen (oxidizer + fuel)
2. Fuel regen plus barrier
3. Radiation

Also, the attainable Isp for the above three cooling concepts was evaluated as a function of mixture ratio at a selected area ratio of 400:1.

A summary of the pertinent operating and design parameters for these engines is presented on Table B-IV. For all cases, the engines could be regeneratively cooled with either oxidizer or fuel + oxidizer. The energy release efficiencies with the dual regenerative cooling (oxidizer + fuel) were calculated to range from 97.4 to 100%. With oxidizer-only regenerative cooling, the efficiencies would be from 1 to 5% lower because of lower fuel vaporization resulting from lower fuel-injection temperatures.

Trends of attainable specific impulse as a function of area ratio for engines using dual-regenerative, fuel-regenerative + barrier, and radiation cooling are shown on Figures B-12, -13, and -14, respectively.

The performance with all engine concepts is predicted to increase with increasing area ratio. As mentioned previously, an area ratio of 400:1 is recommended for the Task III studies. The high- and mid-thrust/Pc engines [3114/5515 and 2669/2068N/kPa (700/800 and 600/300 1bf/psia)] are significantly higher performing than the low-thrust/Pc engine [667/276N/kPa (150/40 1bf/psia)] and are roughly of equal performance. Also, at a mixture ratio of 2.0, the three cooling concepts offer roughly equivalent performances at the high and mid-range of thrust and chamber pressure, with the dual-regen case offering the highest performance (342-350 sec) followed by the fuel-regenerative + barrier cooling case (340-342 sec) and the radiation-cooled case (238 sec). For both the fuel-regenerative + barrier cooling and the radiation-cooled cases, the high- and mid-thrust/Pc engines show significant performance reductions (10-30 sec) at O/F = 4.0 compared to O/F = 2.0.

TABLE B-IV
EVALUATION OF REGEN COOLING/PERFORMANCE INTERACTIONS FOR SELECTED
TASK II THRUST AND CHAMBER PRESSURES

CASE	1	2	3	COMMENTS
Thrust, F - N (lbf)	667 (150)	2669 (600)	3114 (700)	Lowest, Highest
Chamber Pressure, P_c - kPa (psia)	276 (40)	2068 (300)	5515 (800)	Lowest, Highest and Mid-Range P_c from Task I Study
$F \times P_c$	0.184×10^6 (6000)	5.519×10^6 (180,000)	17.173×10^6 (560,000)	$\sim 100:1$ Variation in $F \times P_c$
F/P_c	2.42 (3.75)	1.29 (2.0)	0.565 (0.875)	
Throat, Reynolds No.	8×10^4	2×10^5	6×10^5	Laminar, Reverse Transition, and Turbulent Cases
Max. Cooled Chamber Length, in.				
Fuel Regen Only (MR = 2/4)	3.0/2.0	$\sim 4.0/\sim 2.0$	0.8/0.0	Short Chamber Lengths, Low Performance
Ox. Regen Only (MR = 2/4)	8.0/10.0	$>10.0/\sim 10.0$	5.0/7.1	Poor Fuel Vaporization, Fair Performance, ERE 96 to 98% if Max. Length is used
Ox. + Fuel Regen (MR = 2/4)	$>10.0/\sim 10.0$	$>10.0/\sim 10.0$	8.0/8.8	Adequate Chamber Length, Good Fuel Vaporization and Performance, ERE 97.4 to 100%
Chamber Length, L' , Selected for Performance Evaluation, cm (in.)	14.73 (5.8)	12.7 (5.0)	10.41 (4.1)	$L' = 0.6 \times ALRC$ Design Guidelines
Energy Release Efficiency, ERE, % at Selected L' for Data Regen	97.4 - 99.5	98.9 - 100	97.5 - 99.8	ERE For $T_g = 394^\circ K$ ($710^\circ R$) $T_f = 450^\circ K$ ($810^\circ R$), Heated Fuel Increases ERE By ~1 to 5%

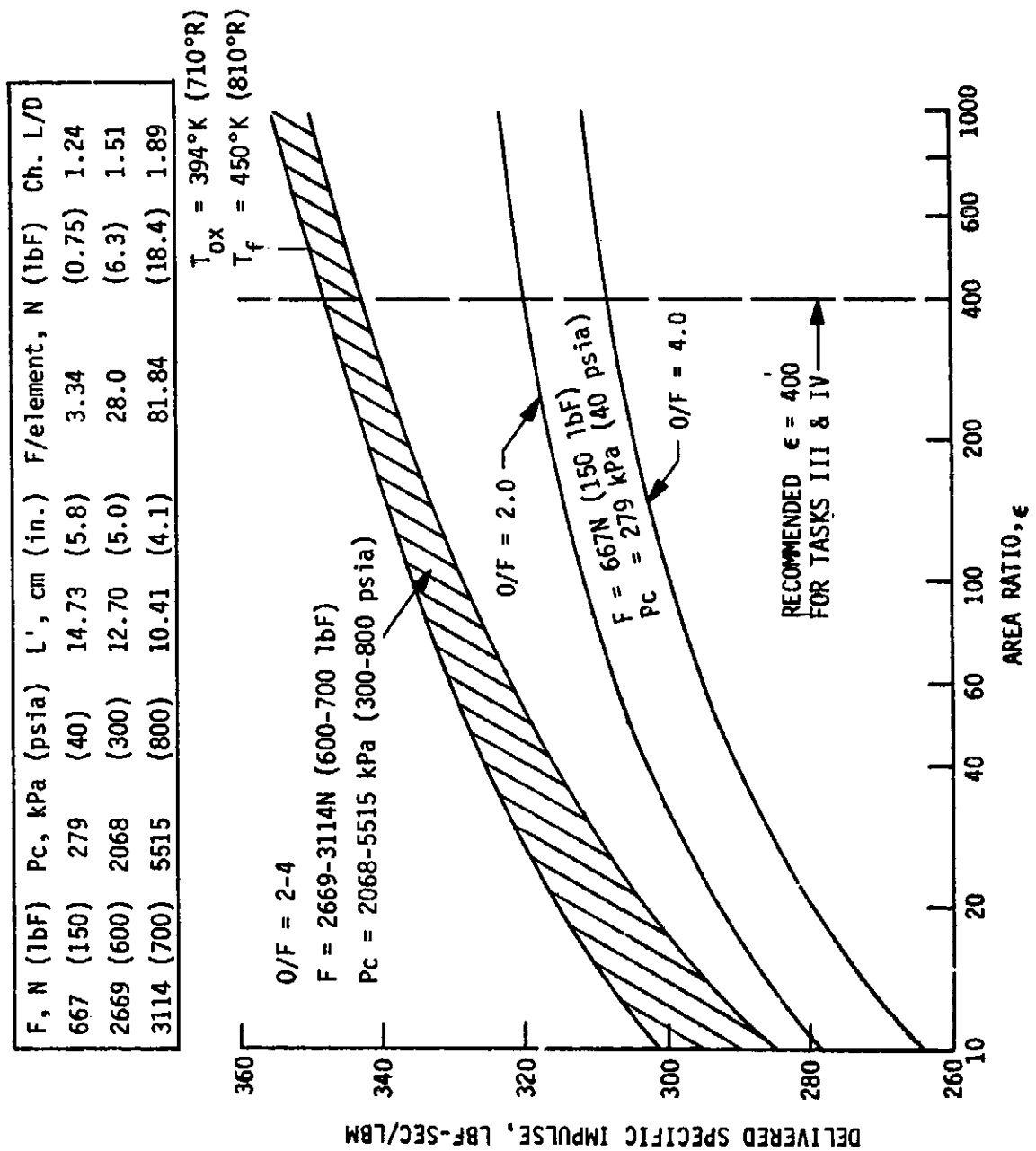


Figure B-12. Predicted Specific Impulse - Dual-Regen Cooling

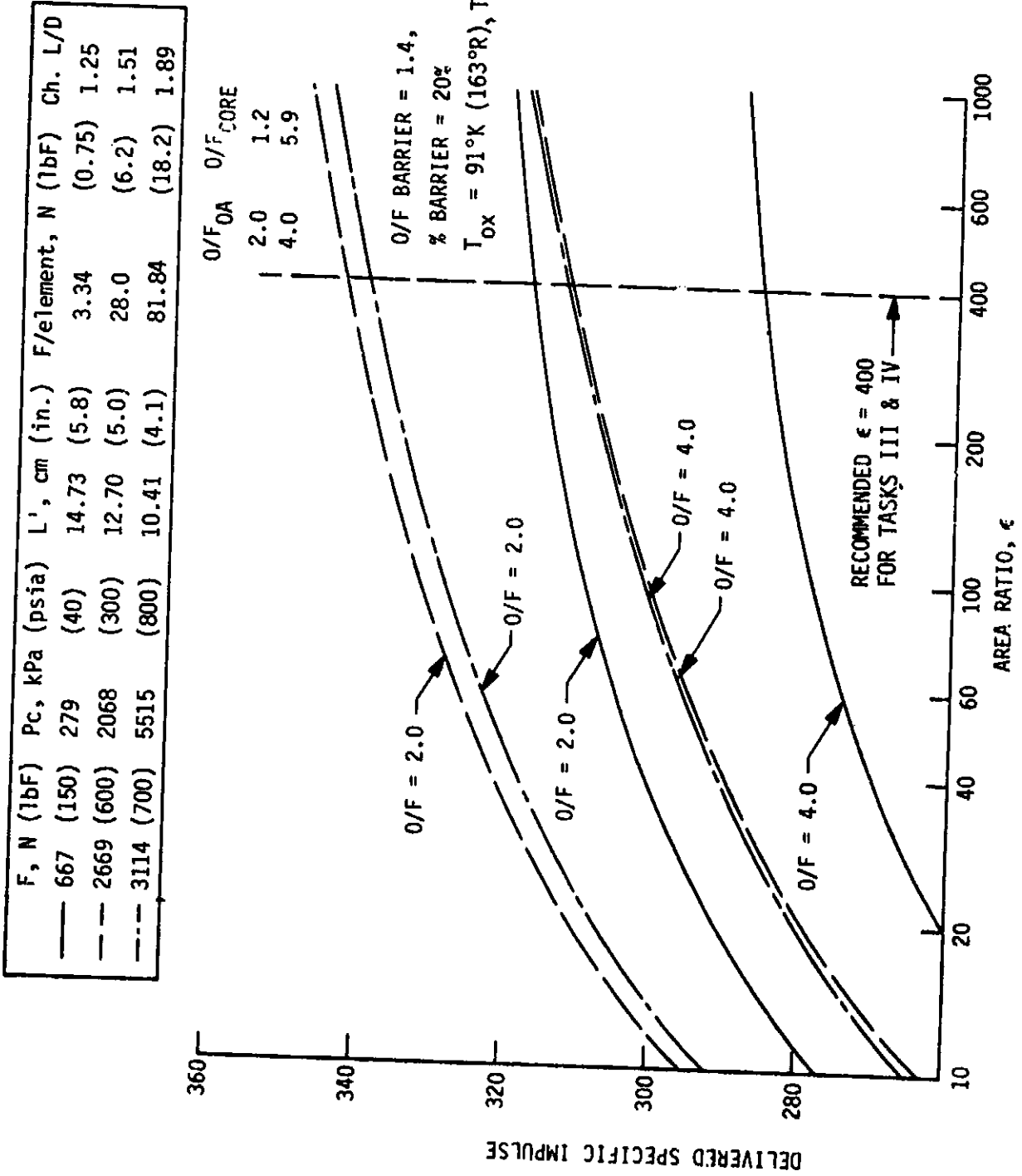


Figure B-13. Predicted Specific Impulse - Fuel-Regen Cooling with Barrier Cooling

Note: $T_w/T_s = 0.2$, $T_{ox} = 91^\circ\text{K}$ (163°R), $T_f = 294^\circ\text{K}$ (530°R)

F, N (1bf)	P_c, kPa	L', cm (in.)	$F/\text{element}, N$ (1bf)	Ch. L/D
667 (150)	279 (40)	14.73 (5.8)	3.34	(0.75) 1.24
2669 (600)	2068 (300)	12.70 (5.0)	28.0	(6.3) 1.51

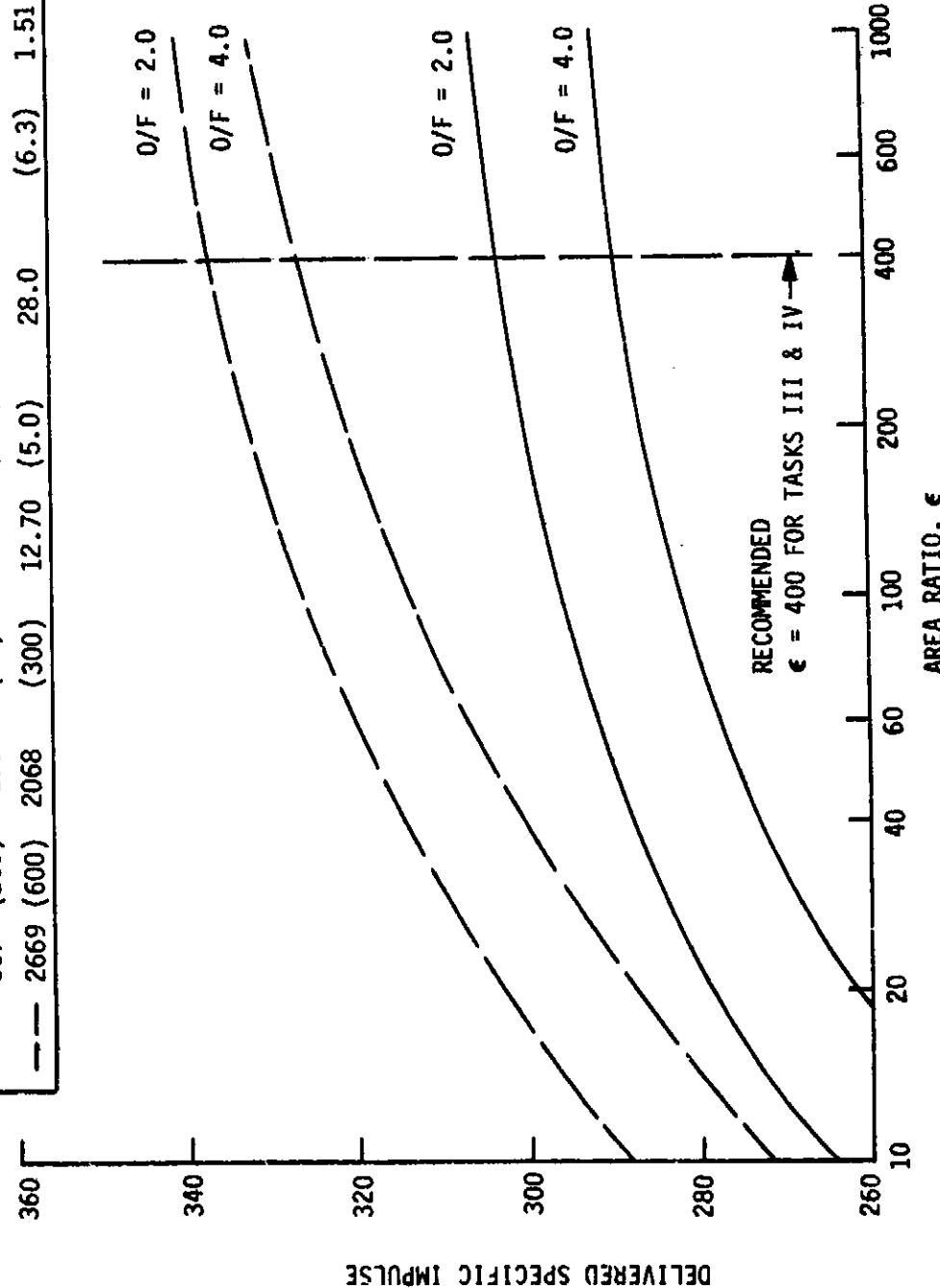


Figure B-14. Predicted Specific Impulse - Radiation Cooling

III, B, Task II - Analyses (cont.)

This performance reduction for the fuel regenerative + barrier cooling case is caused by the injector core mixture ratio of 5.9 at an overall O/F = 4.0 (Figure B-13) which is significantly lower-performing than the core mixture ratio of 2.2 at an overall O/F = 2.0. For the radiation-cooled case, the high mixture ratio results in lower performance because the fuel vaporization limitation of the unheated fuel causes a significant increase in the combustion mixture ratio compared to the overall injector mixture ratio. In turn, this results in an increase in the energy release loss. The lower performance predicted for the lowest-thrust/Pc cases is due primarily to the increase in kinetic loss.

Trends of attainable specific impulse as a function of mixture ratio for engines using dual-regenerative, fuel-regenerative + barrier, and radiation cooling are shown in Figures B-15, -16, and -17, respectively, at an area ratio of 400:1. These data show that the optimum performance for all engines occurs within an O/F range of 2.0 to 3.0. The trends of performance as a function of thrust and chamber pressure are, of course, the same as discussed during the evaluation of the specific impulse versus area ratio data. Of particular interest is a comparison of the data from Figures B-15 and B-16 which show the marked decrease in Isp for the barrier cooling case over the dual-regen case at the higher mixture ratios. This reduction in Isp at the higher mixture ratios for the barrier cooling case is caused by the extremely high and nonoptimum core mixture ratios. The data contained on Figure B-17 illustrate the potential benefit of heating the fuel for the radiation-cooled cases. With heated fuel, the performance of the low-thrust/low-Pc radiation-cooled engine is approximately equal to that of the dual-regen cooled engine. The same performance improvement for the radiation-cooled engine could also be achieved by increasing the chamber length.

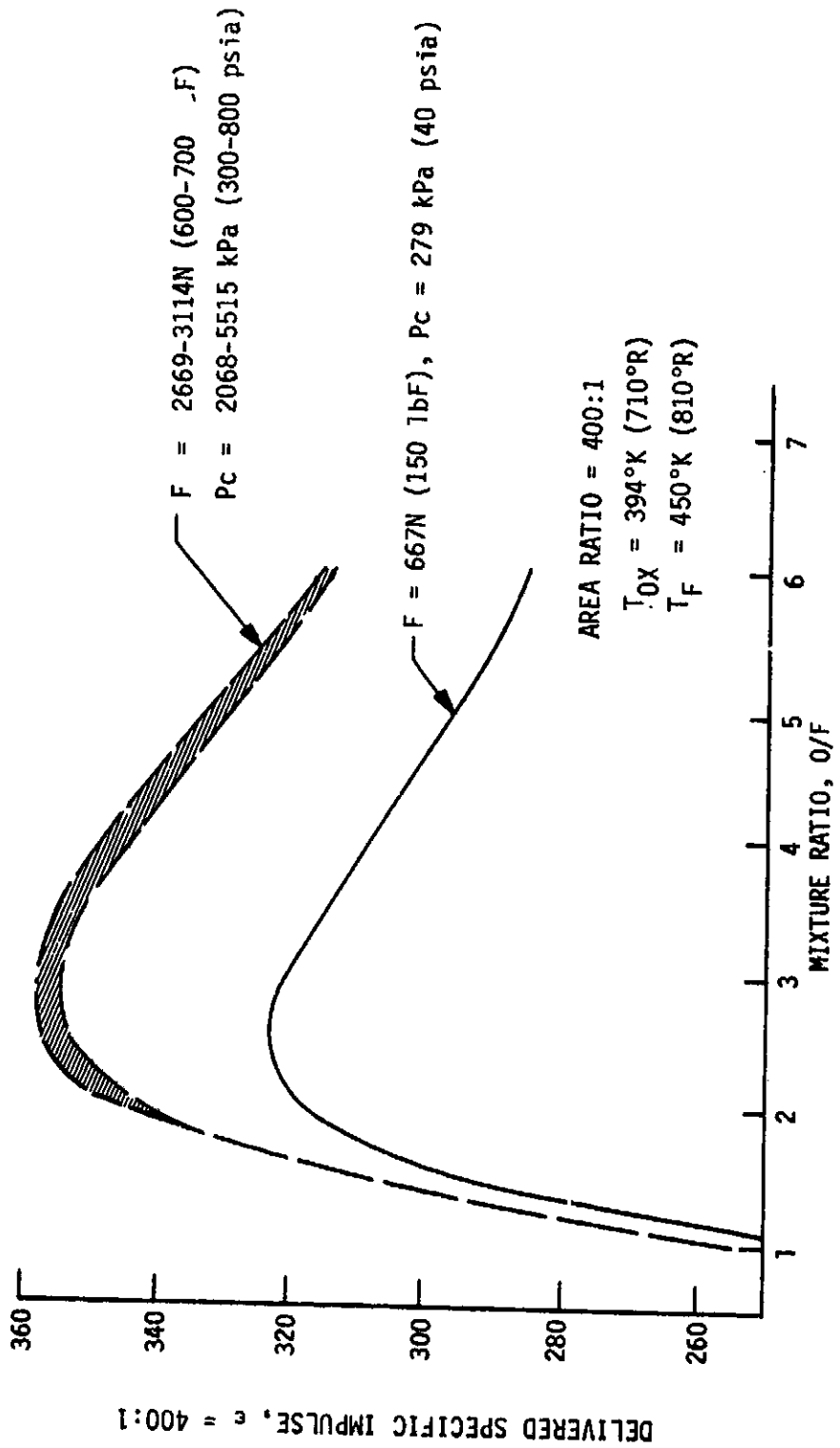


Figure B-15. Influence of Mixture Ratio on Predicted Specific Impulse - Dual-Regen Case

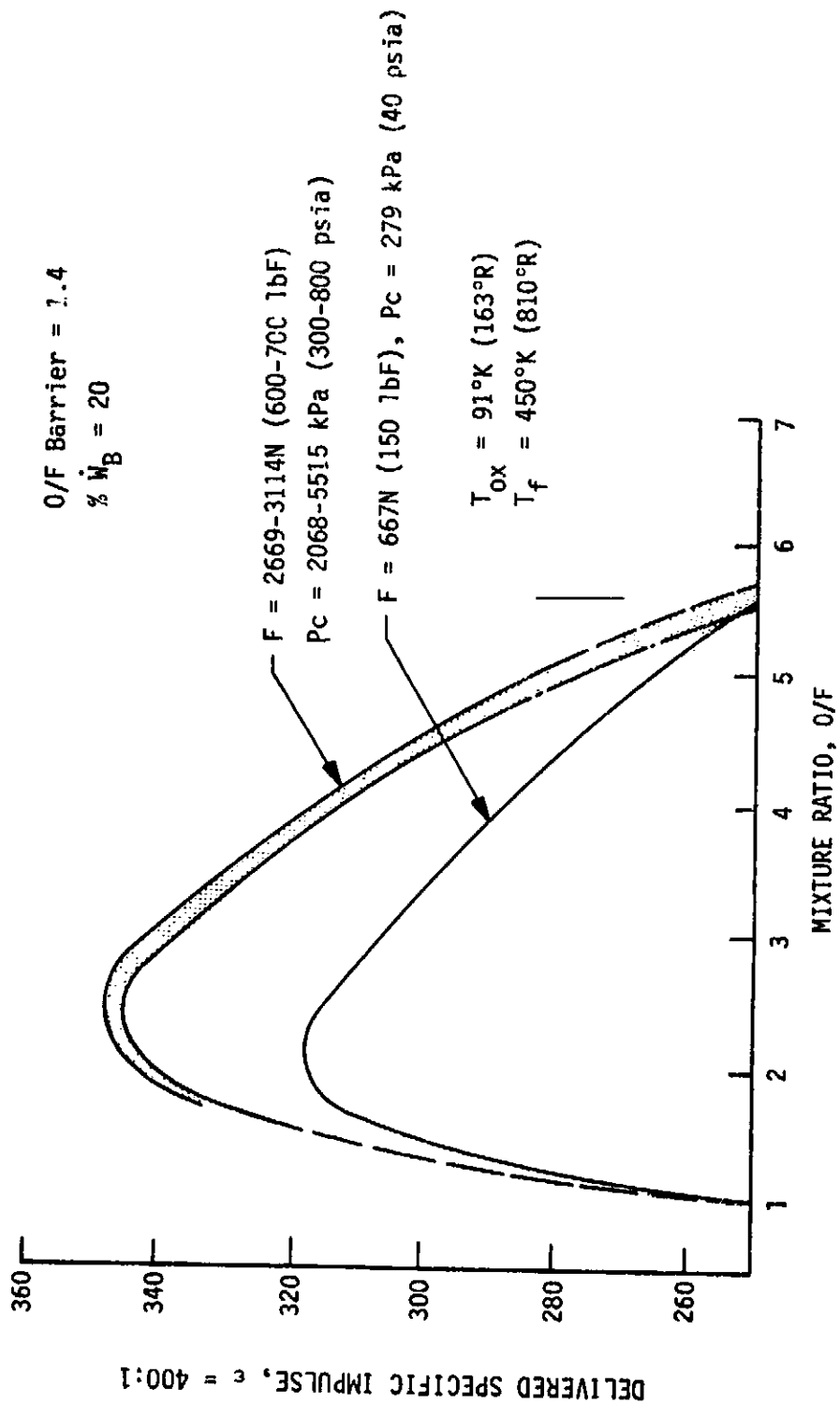


Figure B-16. Influence of Mixture Ratio on Specific Impulse -
Fuel-Ragen Plus Barrier Cooling

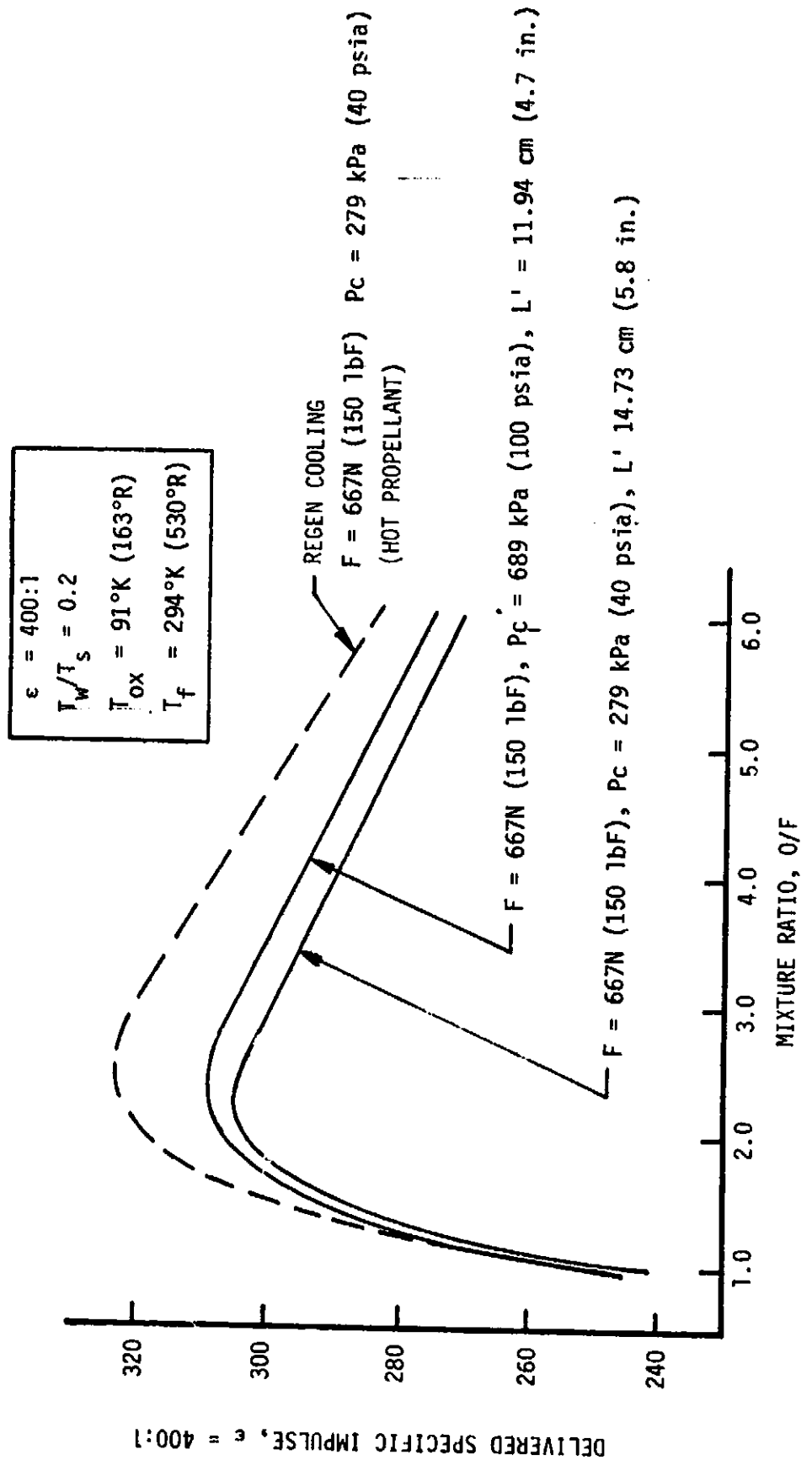


Figure B-17. Influence of Mixture Ratio on Specific Impulse - Radiation Cooling |

PRECEDING PAGE BLANK NOT FILMED

REFERENCES

- B-1. Priem, R.J. and Heidmann, M.F., Propellant Vaporization as a Design Criteria for Rocket Engine Combustion Chambers, NASA TR-R-67, 1960.
- B-2. Nickerson, G.R. et al., The Two-Dimensional Kinetic (TDK) Rocket Nozzle Analysis Reference Computer Program, December 1973.
- B-3. Pieper, J.L., "ICRPG Liquid Propellant Thrust Chamber Performance Evaluation Manual," CPIA 178, September 1968.
- B-4. Meagher, G.M., Low-Thrust Isp Sensitivity Study: Comparison Between BLIMP and TBL Chart of Predicted Performance Loss Due to Boundary Layer Influence, ALRC Thermodynamic Analysis Report 9751:0618, 5 March 1981.
- B-5. Pieper, J.L., Evaluation of Attainable Specific Impulse for The OTV Expander Cycle Point Design, ALRC Thermodynamic Analysis Report 9751:0499, 24 June 1980.
- B-6. JANNAF Liquid Rocket Engine Performance Prediction and Evaluation Manual, CPIA Publication No. 246, April 1975.
- B-7. Pavli, A.J., Design and Evaluation of High-Performance Rocket Engine Injectors for Use with Hydrocarbon Fuels, NASA TM 79319, September 1979.

PRECEDING PAGE BLANK NOT FILMED

APPENDIX C

COMPUTER PERFORMANCE TABULATIONS

PRECEDING PAGE BLANK NOT FILMED

DATE 101681										PAGE 3									
FUEL/FILM ARATIO	NEL	MR	XFILMCL	THTS	CRTD	XBELL	ZISP	ERE	FC EFF	KIN EFF	DIV EFF	BL EFF	BL FLOW RATE	DELT P	(PSI)	(PSI)	(PA)		
ENGLISH (PSIA)	CHAR PRESS	THRUST (LBF)	ISP DEL (SEC)	CSTAR (FT/SEC)	LPRIME (IN)	LNOZ (IN)	RTHROAT (IN)	REXIT (IN)	OX DIA (IN)	FUEL DIA (IN)	DIV DIA (IN)	BL DIA (IN)	FLOW RATE (LBIN/SEC)	DELT P (PSI)	(PSI)	(PA)			
SI UNITS	(PA)	(N)	(N-S/KG)	(M/S)	(M)	(M)	(M)	(M)	(M)	(M)	(M)	(M)	(KG/SEC)	(KG/SEC)	(KG/SEC)	(KG/SEC)			
3 -1	400.0	7	2.00	000	80	13.08	85.0	8558	.9230	1.0000	.9474	.9941	.9873						
	400.0	100	311.2	5410.0	2.85	12.50	.207	4.15	.0550	.0249	.0249	.0249	.32	69.4					
	2757901	445.	3052.1	1649.0	.0724	.3174	.0053	.1053	.140-02	.633-03	.633-03	.633-03	.1457	.6167-06					
3 -1	400.0	7	3.00	000	90	14.43	85.0	8408	.9082	1.0000	.9469	.9941	.9846						
	400.0	100	329.5	5193.7	4.00	11.90	.197	3.95	.0565	.0210	.0210	.0210	.30	89.4					
	2757901	445.	3231.1	1583.0	1016	.3023	.0050	.1003	.145-02	.533-03	.533-03	.533-03	.1377	.6167-06					
3 -1	400.0	7	4.00	000	80	14.50	85.0	8398	.9159	1.0000	.9374	.9941	.9846						
	400.0	100	316.9	4977.7	4.12	11.88	.197	3.94	.0602	.0191	.0191	.0191	.32	89.4					
	2757901	445.	3107.5	1517.2	1046	.3018	.0050	.1001	.153-02	.486-03	.486-03	.486-03	.1431	.6167-06					
3 -1	400.0	7	5.00	000	80	14.64	85.0	8449	.9119	1.0000	.9477	.9941	.9846						
	400.0	100	304.3	4726.2	4.12	11.81	.196	3.92	.0592	.0178	.0178	.0178	.32	89.4					
	2757901	445.	2984.5	1440.5	1046	.3000	.0050	.0996	.150-02	.453-03	.453-03	.453-03	.1490	.6167-06					
3 -1	400.0	24	2.00	000	80	8.00	85.0	8656	.9807	1.0000	.9075	.9941	.9846						
	100.0	100	314.5	563.1	5.25	25.51	.423	8.46	.0537	.0174	.0174	.0174	.32	31.6					
	689475	445.	3034.0	1735.3	1333	.6479	.0107	.2150	.136-02	.441-03	.441-03	.441-03	.1442	.2180-06					
3 -1	400.0	22	3.00	000	80	8.00	85.0	8012	.9442	1.0000	.8741	.9941	.9846						
	100.0	100	311.5	5247.1	5.67	24.72	.410	8.20	.0585	.0158	.0158	.0158	.32	31.6					
	689475	445.	3054.8	1614.5	1440	.6279	.0104	.2064	.149-02	.401-03	.401-03	.401-03	.1456	.2180-06					
3 -1	400.0	21	4.00	000	80	8.00	85.0	8076	.9428	1.0000	.8822	.9941	.9846						
	100.0	100	301.0	5023.1	5.31	24.49	.406	8.13	.0589	.0147	.0147	.0147	.32	31.6					
	689475	445.	2951.4	1531.1	1349	.6221	.0103	.2064	.150-02	.373-03	.373-03	.373-03	.1507	.2180-06					
3 -1	400.0	21	5.00	000	80	8.00	85.0	8255	.9507	1.0000	.8944	.9941	.9846						
	100.0	100	293.1	483.8	5.66	24.35	.404	8.08	.0593	.0136	.0136	.0136	.34	31.6					
	689475	445.	284.0	1473.7	1438	.6185	.0103	.2052	.151-02	.346-03	.346-03	.346-03	.1548	.2180-06					
3 -1	400.0	7	3.00	000	80	20.67	85.0	8542	.9066	1.0000	.9616	.9941	.9846						
	675.0	100	33.6	5219.4	3.75	9.10	.151	3.02	.0453	.0189	.0189	.0189	.30	132.4					
	4653957	445.	36.6	1590.0	0952	.2312	.0038	.0767	.115-02	.479-03	.479-03	.479-03	.1352	.9133-06					
3 -1	400.0	7	4.00	000	80	33.14	85.0	8693	.9291	1.0000	.9535	.9941	.9846						
	900.0	100	33.5	5102.0	4.00	7.85	.130	2.61	.0403	.0161	.0161	.0161	.30	164.3					
	6205276	445.	3240.8	1555.1	1016	.1994	.0033	.0662	.102-02	.409-03	.409-03	.409-03	.1373	.1133-07					

EFIN

229

RP-1 F = 445N (100 lbf) OX-REGEN-COLED

OF POOR QUALITY

DATE 101681										PAGE 3	
										BL EFF	BL EFF
FUEL FILM ARATIO	NEL	MR	7FILMCL	THTS	CRATIO	XISP	REXIT	KIN EFF	DIV EFF	FLDN RATE	DEL T P
CHAN PRESS	THRUST	ISP DEL	CSTAR	LPRIME	ATRDAT	(IN)	(IN)	(IN)	(IN)	(LBM/SEC)	(PSI)
ENGLISH	(PSIA)	(LBF)	(SEC)	(FT/SEC)	(IN)	(IN)	(IN)	(IN)	(IN)	(KG/SEC)	(PA)
SI UNITS	(PA)	(M)	(N-S/KG)	(M/S)	(M)	(M)	(M)	(M)	(M)	(KG/SEC)	(PA)
3 -1	400.0	22	2.00	0.00	80.	85.0	9320	9864	1.0000	.9606	.9941
	400.0	400.	338.9	5781.?	5.67	24.76	.411	.8.22	.0562	.0270	.1.18
	2757901.	1779	3323.6	1762.1	1.440	.6289	.0104	.2087	.148-02	.685-03	.5353
3 -1	400.0	20	3.00	0.00	80.	85.0	8824	9456	1.0000	.9496	.9941
	400.0	400.	345.8	5407.6	5.67	23.71	.393	.7.87	.0625	.0242	.1.16
	2757901.	1779	3390.9	1648.2	1.440	.6022	.0100	.1998	.159-02	.616-03	.5247
3 -1	400.0	20	4.00	0.00	80.	85.0	8827	9546	1.0000	.9411	.9941
	400.0	400.	333.1	5187.6	5.67	23.66	.392	.7.63	.0624	.0221	.1.20
	2757901.	1779	3267.1	1581.2	1.440	.6009	.0100	.1994	.159-02	.561-03	.5446
3 -1	400.0	20	5.00	0.00	80.	85.0	8861	9536	1.0000	.9450	.9941
	400.0	400.	319.2	4942.1	5.67	23.59	.391	.7.83	.0621	.0206	.1.25
	2757901.	1779.	3130.0	1506.3	1.440	.5992	.0099	.1988	.158-02	.523-03	.5685
3 -1	400.0	102	2.00	0.00	80.	85.0	9007	9921	1.0000	.9268	.9941
	100.0	400.	327.2	5759.3	7.79	50.30	.835	.16.69	.0500	.0165	.5894
	689475.	1779.	3209.0	1755.4	1.979	.2777	.0212	.4240	.127-02	.420-03	.5545
3 -1	400.0	96	3.00	0.00	80.	85.0	8395	9675	1.0000	.8869	.9941
	100.0	400.	326.4	5427.6	7.79	48.89	.811	.16.22	.0530	.0148	.1.23
	689475.	1779.	3200.8	1654.5	1.979	.2419	.0206	.4121	.135-02	.375-03	.5559
3 -1	400.0	95	4.00	0.00	80.	85.0	8445	9747	1.0000	.8856	.9941
	100.0	400.	314.7	5192.7	7.79	48.70	.808	.16.16	.0541	.0135	.1.27
	689475.	1779.	3066.3	1582.7	1.979	.2371	.0205	.4105	.137-02	.343-03	.5765
3 -1	400.0	94	5.00	0.00	80.	85.0	8530	9757	1.0000	.8938	.9941
	100.0	400.	302.8	4962.1	7.79	48.53	.805	.16.11	.0548	.0127	.1.32
	689475.	1779.	2969.8	1512.5	1.979	.2328	.0205	.4091	.139-02	.321-03	.5991

ORIGINAL PAGE IS
OF POOR QUALITY.

RP-1 F = 1775% (400 lbF) OA-REGEN-COOLED

EFIN

**ORIGINAL PAGE IS
OF POOR QUALITY**

10/16/81 13:46:20 LDMF 0427AA188		000427	2	400	ZBELL LNDZ (IN) (M)	ZISP RTHROAT (IN) (M)	ERE REXIT (IN) (M)	DATE 101681	PAGE 3	
FUEL FILM RATIO	MEL FFR	%FILMCL	TWTS	CRATTO LPRIME (IN) (M)	XIN	FUEL DIA (IN) (M)	FLW RATE (LBIN/SEC) (KG/SEC)	DIV EFF	SL EFF	
ENGLISH IPSIA)	CHAN PRESS THRT	ISP DEL (SEC)	CSTAR (FT/SEC) (M/S)	(PA)	(IN-S/RG) (M/S)			DEL P (PSI) (PA)		
3 -2	400.0	22 2.00	000	.80	8.00	85.0	.9204	.9790	1.0000	.9941
	1000.0	1000.	334.8	5740.5	4.85	24.87	.413	.825	.0618	.2.99
6894752	4448.	3283.6	1755.8	1232	.6316	.0105	.2096	.157-02	.917-03	1.3547
3 -1	400.0	20 3.00	000	.80	8.00	85.0	.8862	.9299	1.0000	.9941
	1000.0	1000.	348.9	5382.5	5.07	23.55	.391	.7.81	.0671	.2.87
6894752	4448	3421.4	1640.6	1288	.5981	.0099	.1985	.170-02	.816-03	1.3001
3 -1	400.0	19 4.00	000	.80	8.00	85.0	.9129	.9667	1.0000	.9941
	1000.0	1000.	347.5	5315.7	23.45	.089	.389	.7.78	.0720	.2.88
6894752	4448	3408.0	1620.2	1798	.5955	.0099	.1976	.163-02	.750-03	1.3052
3 -1	400.0	19 5.00	000	.80	8.00	85.0	.9069	.9629	1.0000	.9941
	1000.0	1000.	330.1	5046.4	23.44	.089	.389	.7.78	.0716	.2.87
6894752	4448	3237.1	1538.1	1798	.5954	.0099	.1976	.162-02	.703-03	1.3741
3 -1	400.0	59 2.00	000	.80	8.00	85.0	.9492	.9937	1.0000	.9941
	400.0	1000.	345.2	5824.5	7.00	.38.94	.646	.12.92	.0527	.0277
2757901	4448	3385.1	1775.3	1778	.9890	.0164	.3282	.134-02	.655-03	1.3141
3 -1	400.0	55 3.00	000	.80	8.00	85.0	.9029	.9639	1.0000	.9941
	400.0	1000.	353.8	5512.4	7.00	.37.42	.621	.12.42	.0551	.0228
2757901	4448	3469.4	1680.2	1778	.9504	.0159	.3154	.140-02	.580-03	1.2821
3 -1	400.0	54 4.00	000	.80	8.00	85.0	.9020	.9719	1.0000	.9944
	400.0	1000.	340.4	5282.1	7.00	.37.34	.619	.12.39	.0561	.0210
2757901	4448	3338.6	1610.0	1778	.9484	.0157	.3147	.142-02	.534-03	1.3324
3 -1	400.0	54 5.00	000	.80	8.00	85.0	.9034	.9711	1.0000	.9944
	400.0	1000.	365.4	5033.1	7.00	.37.28	.618	.12.37	.0568	.0196
2757901	4448	3191.4	1534.1	1778	.9469	.0157	.3142	.144-02	.498-03	1.3938
3 -1	400.0	257 2.00	000	.80	8.00	85.0	.9122	.9932	1.0000	.9941
	100.0	1000.	331.4	5777.2	9.61	79.15	.1.313	.26.27	.0462	.0164
689475	4448	3249.9	1760.9	2441	.2.0105	.0334	.6471	.117-02	.415-03	.3.07
3 -1	400.0	242 3.00	000	.80	8.00	85.0	.8564	.9749	1.0000	.9941
	100.0	1000.	333.0	5469.4	9.61	76.84	.1.275	.25.50	.0489	.0146
689475	4448	3265.2	1667.1	2441	.1.9516	.0324	.6476	.124-02	.370-03	.3.00
3 -1	400.0	241 4.00	000	.80	8.00	85.0	.8586	.9835	1.0000	.9941
	100.0	1000.	329.0	5239.9	9.61	76.72	.1.273	.25.46	.0499	.0133
689475	4448	3137.8	1597.1	2441	.1.9486	.0323	.6466	.127-02	.339-03	.3.13
3 -1	400.0	240 5.00	000	.80	8.00	85.0	.8651	.9842	1.0000	.9941
	100.0	1000.	307.1	5005.5	9.61	76.54	.1.270	.25.40	.0505	.0124
689475	4448	3011.8	1525.7	2441	.1.9440	.0323	.6451	.128-02	.316-03	.3.26

RP-1 F = 4448N (1000 lbF) OX-REGEN-COOLED

65IN

DATE	10/16/81	TIME	14:57:04	LOMF	0427AA100	000427	2	400					PAGE
FUEL FLOW RATIO	NEL	MFR	XFLNCL	TTS	CNTIO	ZBELL	XISP	ERE	FC EFF	XIN EFF	DIV EFF	DL EFF	3
CHAM PRESS	THRUST	ISP DEL	CSTAR	LPRIME	LN02	NTHROAT	REXIT	OX DIA	FUEL DIA	FLOW RATE	DELTA P	(PSI)	
ENGLISH	(PSIA)	(LBF)	(SEC)	(FT/SEC)	(IN)	(IN)	(IN)	(IN)	(IN)	(LB/SEC)	(PSI)	(PSI)	
SI UNITS	(PA)	(N)	(N-S/KG)	(M/S)	(M)	(M)	(M)	(M)	(M)	(KG/SEC)	(PA)	(PA)	
3 -1	400.0	8	1.00	.000	.30	34.80	85.0	.8522	.9804	1.0000	.8827	.9941	.9916
	1000.0	100.	258.8	4455.7	.017	7.87	.131	.2.61	.0371	.0270	.39	.177.8	
	6894752.	445.	2538.2	1358.1	.1059	.1998	.0053	.0663	.4355.03	.685-03	.1753	.1226.87	
3 -1	400.0	36	1.00	.300	.80	49.22	85.0	.8432	.9754	1.0000	.8793	.9941	.9931
	400.0	100.	253.5	4377.3	.412	12.46	.207	.4.13	.0100	.0157	.39	.78.4	
	2757901.	445.	2486.2	1334.2	.1046	.3164	.0052	.1050	.254-03	.398-03	.1769	.5445.06	
3 -1	400.0	22	1.00	.008	.80	8.00	85.0	.8343	.9737	1.0000	.8759	.9941	.9939
	100.0	100.	247.4	4283.5	.567	24.94	.414	.2.28	.0163	.0255	.40	.31.6	
	689475.	445.	2426.6	1305.6	.1440	.6336	.0105	.2102	.413-03	.647-03	.1633	.2130.06	
3 -1	400.0	24	2.00	.000	.80	8.00	85.0	.6352	.9563	1.0000	.8986	.9941	.9928
	100.0	100.	303.4	5551.3	.160	25.64	.425	.51	.0162	.0184	.53	.31.6	
	689475.	445.	2975.6	1692.0	.0466	.6513	.0198	.2161	.412-03	.467-03	.1495	.2130.06	

ORIGINAL PAGE IS
OF POOR QUALITY

F = 445N (100 lbf) MP-1-COOLED

EF1

**ORIGINAL PAGE IS
OF POOR QUALITY**

10/16/81 14:56:54 LOWF 0427AA168		009427		2 400				DATE 101681		PAGE 3	
FUEL FILM ARATIO	TEL MR	XFILMCL	TNTS	CRATIO	XISPL	ENE	FC EFF	RIN EFF	DIV EFF	SL EFF	
CHAN PRESS	ISP DEL	ISP DEL	CSTAR	LPRIME	RTHROAT	REXIT	ON DIA	FUEL DIA	FLOW RATE	DELT P	
(PSIA)	(SEC)	(SEC)	(FT/SEC)	(IN)	(IN)	(IN)	(IN)	(IN)	(LBH/SEC)	(PSIA)	
SI UNITS	(PA)	(N)	(M/S)	(M)	(M)	(M)	(M)	(M)	(KG/SEC)	(PA)	
3 -1	400.0	7 1.00	.000	.80	8.21	85.0	.8559	.9399	.8787	.9941	
1000.0	400.	259.9	4499.0	5.77	15.77	.262	5.23	.0364	.0575	1.54	
6894752.	1779.	2549.0	1371.3	.1466	.4007	.8066	.1330	.924-03	.146-02	.6980	
3 -1	400.0	7 2.00	.000	.80	8.43	85.0	.6604	.7134	.18800	.9941	
1000.0	400.	249.0	4197.9	.65	15.57	.258	5.17	.0429	.0474	1.61	
6894752.	1779.	2441.7	1279.5	.0166	.3954	.0066	.1312	.109-02	.121-02	.7287	
3 -1	400.0	22 1.00	.000	.80	8.00	85.0	.8473	.9808	.18000	.9941	
400.0	400.	254.8	4401.1	5.67	24.92	.413	8.27	.0247	.0386	1.57	
2757901.	1779.	2498.7	1341.5	.1439	.6329	.0105	.2180	.627-03	.981-03	.7121	
3 -1	400.0	22 2.00	.000	.80	8.00	85.0	.9111	.9787	.18000	.9941	
400.0	400.	331.3	5736.3	2.38	24.94	.414	8.28	.0250	.0283	1.21	
689475.	1779.	3249.2	1748.4	.0605	.6336	.0105	.2102	.635-03	.720-03	.5476	
3 -1	400.0	101 1.00	.000	.80	8.00	85.0	.8359	.9793	.18000	.9941	
1000.0	400.	267.9	4307.6	7.79	99.98	.829	16.58	.0152	.0236	1.61	
689475.	1779.	2451.3	1313.0	.1978	1.2695	.0211	.4121	.587-03	.599-03	.7318	
3 -1	400.0	101 2.00	.000	.80	8.00	85.0	.9085	.9966	.18000	.9941	
1000.0	400.	350.1	5785.6	4.24	50.20	.833	16.66	.0152	.0172	1.21	
689475.	1779.	3236.9	1763.4	.1076	1.2750	.0212	.4231	.387-03	.437-03	.5497	
3 -1	400.0	96 3.00	.000	.80	8.00	85.0	.8376	.9641	.18000	.9941	
1000.0	400.	325.7	5408.8	2.95	48.86	.811	16.21	.0167	.0154	1.23	
689475.	1779.	3194.5	1648.6	.0749	1.2410	.0206	.4118	.423-03	.391-03	.5570	
3 -1	400.0	95 4.00	.000	.80	8.00	85.0	.8454	.9761	.18000	.9941	
1000.0	400.	315.1	5206.5	2.93	48.71	.808	16.16	.0176	.0141	1.27	
689475.	1779.	3089.6	1585.1	.0745	1.2373	.0205	.4106	.447-03	.359-03	.5759	
3 -1	400.0	94 5.00	.000	.80	8.00	85.0	.8548	.9748	.18000	.9941	
1000.0	400.	303.5	4978.2	2.92	48.56	.806	16.11	.0184	.0133	1.32	
689475.	1779.	2975.9	1517.3	.0742	1.2335	.0205	.4093	.467-03	.337-03	.5979	

F = 1779N (400 1bf) RP-1-000ED

afin

ORIGINAL PAGE IS
OF POOR QUALITY

10/16/81 13:58:48 LOWF 0427AA160							008427 2 400 DATE 101681							PAGE 3											
FUEL FILM ARATIO	MEL	MR	XFILMCL	TWS	CSTAR	CRATIO	XBELL	XJSP	ERATE	FC EFF	KIN EFF	DIV EFF	BL EFF	CHAM PRESS	THRUST	CSTAR	LPRIME	THROAT	REXIT	OX DIA	FUEL DIA	FLOW RATE	DELT P		
ENGLISH	(PSIA)	(LBF)	(SEC)	(FT/SEC)	(IN)	(IN)	(IN)	(IN)	(IN)	(IN)	(IN)	(IN)	(IN)	SI UNITS	(PA)	(N-S/KG)	(M/S)	(M)	(M)	(MM)	(MM)	(MM)	(PSI)		
3 -1	400.0	23	1.00	.000	.80	8.00	85.0	.8467	.9920	1.0000	.8705	.9941	.9877	6894752.	1000.	257.1	4508.8	7.08	.417	8.33	.0502	3.89	177.8	.1226+0.7	
3 -1	400.0	62	1.00	.000	.80	8.00	85.0	.8440	.9854	1.0000	.8707	.9941	.9908	2757901.	1000.	253.8	4421.8	7.00	.417	8.33	.0363	3.94	89.4	.6167+0.6	
3 -1	400.0	60	2.00	.000	.80	8.00	85.0	.9365	.9921	1.0000	.9597	.9941	.9898	689475.	1000.	340.6	5815.0	3.02	.517	.650	.0235	2.34	89.4	.6167+0.6	
3 -1	400.0	258	1.00	.000	.80	8.00	85.0	.8361	.9848	1.0000	.8622	.9941	.9917	689475.	1000.	334.0	4331.9	9.61	1.315	26.29	.0233	4.03	31.6	.2180+0.6	
3 -1	400.0	256	2.00	.000	.80	8.00	85.0	.8354	.9848	1.0000	.8622	.9941	.9917	689475.	1000.	334.0	4331.9	9.61	1.315	26.29	.0233	4.03	31.6	.2180+0.6	
3 -1	400.0	100.	1.00	.000	.80	8.00	85.0	.9313	.9913	1.0000	.9355	.9941	.9893	689475.	1000.	334.0	4331.9	9.61	1.315	26.29	.0170	2.97	31.6	.2180+0.6	
3 -1	400.0	241	3.00	.000	.80	8.00	85.0	.8671	.9848	1.0000	.8966	.9941	.9892	689475.	1000.	337.1	3524.6	5.63	1.273	25.46	.0149	.0162	.0151	2.97	.2180+0.6
3 -1	400.0	241	4.00	.000	.80	8.00	85.0	.9314	.9914	1.0000	.9355	.9941	.9893	689475.	1000.	337.1	3524.6	5.63	1.273	25.46	.0149	.0162	.0151	2.97	.2180+0.6
3 -1	400.0	100.	4.00	.000	.80	8.00	85.0	.8671	.9848	1.0000	.8966	.9941	.9892	689475.	1000.	337.1	3524.6	5.63	1.273	25.46	.0149	.0162	.0151	2.97	.2180+0.6
3 -1	400.0	240	5.00	.000	.80	8.00	85.0	.8698	.9903	1.0000	.8947	.9941	.9887	689475.	1000.	308.9	5036.6	4.61	1.270	25.41	.0179	.0129	.324	31.6	.2180+0.6
3 -1	400.0	240	4.00	.000	.80	8.00	85.0	.8671	.9848	1.0000	.8966	.9941	.9892	689475.	1000.	308.9	5036.6	4.61	1.270	25.41	.0149	.0162	.0151	2.97	.2180+0.6

F = 4448N (1000 lbf) RP-1-COOLED

FIN

ORIGINAL PAGE
OF POOR QUALITY

10/20/81 15:46:43 LOWF 0427AA188 000427							DATE 10/20/81							PAGE 3	
FUEL FILM ARATIO	MFL	MFR	ZFL	FLNCL	TWS	CRRATIO	XBELL	XISP	ERE	KIN	EFF	DIV	EFF	BL	EFF
ENGISH	CHAR PRESS	THRUST	ISP DEL	CS7AR	LPMINC	LNOZ	THROAT	REXIT	OX DIA	FUEL DIA	FLOW RATE	DELTA P	(PSI)	(PSI)	(PSI)
SI UNITS	(PSIA)	(LBF)	(SEC)	(FT/SEC)	(IN)	(IN)	(IN)	(IN)	(IN)	(IN)	(IN/SEC)	(IN/SEC)	(IN)	(IN)	(IN)
(PA)	(Pa)	(m)	(m)	(m/s)	(m)	(m)	(m)	(m)	(m)	(m)	(m/s)	(m/s)	(Pa)	(Pa)	(Pa)
3 -1	400.0	22	2.00	.000	8.00	8.00	8.00	9.455	.9986	1.0000	.9943	.9878			
	1000.0	1086.	346.0	346.0	587.0	7.08	24.78	.411	8.22	.0627	2.91	177.8			
	6894752.	9498.	3373.1	3373.1	1790.9	.1798	.6294	.0104	.2088	.152-02	.917-03	1.5187	.1226-07		
3 -1	400.0	7	2.00	.000	16.34	.8	.8877	.9572	1.0000	.9463	.9943	.9875			
	500.0	100.	322.9	5617.1	3.41	11.18	.186	3.71	.0495	.0236	.31	105.7			
	3447376.	445.	3166.1	1712.1	.0866	.2841	.0847	.0943	.126-02	.599-03	.1405	.7298-06			
3 -1	400.0	7	2.00	.000	13.05	.8	.8749	.9459	1.0000	.9447	.9943	.9870			
	400.0	136.	318.1	553.8	3.17	12.51	.208	4.15	.0549	.0247	.31	89.4			
	2757901.	445.	3119.9	1689.8	.0805	.3178	.0053	.1055	.139-02	.628-03	.1426	.16167-06			
														DUAL REGEN COOLED	

#FIN

ORIGINAL PAGE IS
OF POOR QUALITY

$$F = 4451 \text{ (100 lbf) ON-REGEN HEATED FUEL}$$

ORIGINAL PAGE IS
OF POOR QUALITY

10/20/81 15:41:45 LOWF		0427AA168		000427		2		400		DATE 102881		PAGE	
FUEL	FUEL ARATIO	WEL	HR	XFILNCL	TWTS	CRA10	XSELL	XISP	ERF	FC EFF	KIN EFF	DIV EFF	BL EFF
CHAM PRESS	THRUST	ISP DEL	CSTAR	LPRATE	LNOZ	RTHROAT	RCXIT	OX DIA	FUEL DIA	FLOW RATE	DEL P	EPSI,	SPAD
(PSIA)	(LBF)	(SEC)	(SEC)	(IN)	(IN)	(IN)	(IN)	(IN)	(IN)	(LB/SEC)	(PSI)	(K6/SEC)	(PSI)
SI UNITS	SPAD	(IN)	(IN-SIGS)	(IN)	(IN)	(IN)	(IN)	(IN)	(IN)	(IN)	(IN)	(IN)	(IN)
3 -1	400.0	22	2.00	.000	.80	0.00	.9	.9467	.9986	1.0000	.9943	.9898	
	400.0	400.	344.3	344.3	5852.9	5.67	24.72	.410	.827	.0578	.0276	1.16	89.4
	2757901.	1779.	3376.2	1784.0	.1448	.6279	.0104	.2083	.147-02	.147-02	.700-03	.5270	.6167+06
3 -1	400.0	20	3.00	.000	.80	0.00	.8	.9081	.9694	1.0000	.9525	.9945	.9896
	400.0	400.	355.0	355.0	5544.0	5.67	23.66	.393	7.85	.0616	.0246	1.12	89.4
	2757901.	1779.	5489.5	1689.8	.1448	.6011	.0100	.1994	.157-02	.157-02	.626-03	.5099	.6167+06
3 -1	400.0	20	4.00	.000	.80	0.00	.8	.9142	.9874	1.0000	.9415	.9946	.9893
	400.0	400.	365.0	365.0	5365.9	5.67	23.64	.392	7.85	.0613	.0224	1.16	89.4
	2757901.	1779.	3585.5	1635.5	.1448	.6005	.0100	.1993	.156-02	.156-02	.568-03	.5259	.6167+06
3 -1	400.0	20	5.00	.000	.80	0.00	.8	.9127	.9844	1.0000	.9431	.9947	.9891
	400.0	400.	328.8	328.8	5102.0	5.67	23.62	.392	7.84	.0612	.0209	1.22	89.4
	2757901.	1779.	3224.8	1555.1	.1448	.5999	.0100	.1991	.155-02	.155-02	.531-03	.5519	.6167+06
3 -1	400.0	101	2.00	.000	.80	0.00	.8	.9123	.9990	1.0000	.9320	.9943	.9864
	100.0	400.	331.5	329.1	5792.1	7.79	50.15	.852	16.64	.0499	.0170	1.21	31.6
	689975.	1779.	3250.4	1767.6	.1979	1.2739	.0211	.4227	.127-02	.127-02	.432-03	.5474	.2180+06
3 -1	400.0	95	3.00	.000	.80	0.00	.8	.9588	.9841	1.0000	.8913	.9945	.9861
	100.0	400.	333.9	333.9	5520.8	7.79	48.75	.809	16.18	.0527	.0151	1.20	31.6
	689975.	1779.	3274.5	1682.7	.1979	1.2384	.0205	.4109	.134-02	.134-02	.384-03	.5434	.2180+06
3 -1	400.0	95	4.00	.000	.80	0.00	.8	.8589	.9929	1.0000	.8836	.9946	.9861
	100.0	400.	320.1	320.1	5289.6	7.79	48.74	.809	16.17	.0536	.0158	1.25	31.6
	689975.	1779.	3139.1	1612.3	.1979	1.2380	.0205	.4106	.136-02	.136-02	.351-03	.5668	.2180+06
3 -1	400.0	94	5.00	.000	.80	0.00	.8	.8655	.9916	1.0000	.8917	.9946	.9858
	100.0	400.	307.3	307.3	5042.9	7.79	48.57	.806	16.12	.0544	.0138	1.30	31.6
	689975.	1779.	3013.4	1537.1	.1979	1.2338	.0205	.4094	.138-02	.138-02	.329-03	.5905	.2180+06

F = 1779N (400 1bf) OX-REGEN HEATED FUEL

237

ORIGINAL PAGE IS
OF POOR QUALITY

三

卷之三

ORIGINAL PAGE IS
OF POOR QUALITY

10/28/81		15:41:32 LOWF		862/AA188		000427		2		400		DATE 10/28/81		PAGE 3	
FUEL FILM RATIO	MEL	MR	XFILMCL	TWTS	CRAFTO	ZBELL	XISP	ERE	FC EFF	KIN EFF	DIV EFF	BL EFF	BL RT	RTY P	
CMR PRESS	THRUST	ISP DEL	CSTAR	LPRIME	LNGZ	ATHROAT	OX DIA	FUEL DIA	OX DIA	FUEL DIA	FLOW RATE	RTY SEC	(PSI)	(PSI)	
ENGLISH	(PSIA)	(LBF)	(SEC)	(IN)	(IN)	(IN)	(IN)	(IN)	(IN)	(IN)	(LBM/SEC)	(Kg/SEC)	(PA)	(PA)	
SI UNITS	(Pa)	(N)	(m)	(m)	(m)	(m)	(m)	(m)	(m)	(m)	(kg/sec)	(kg/sec)	(Pa)	(Pa)	
3 -1	400.0	8	1.00	-800	+80	36.80	.9	.8521	.9809	1.0000	-8824	+9936	.9916		
	1600.0	100.	258.8	4458.4	4.17	7.87	.131	2.61	.8171	.9275	+3.59	177.8			
6894752.		445.	2537.7	1356.9	+1059	.1999	.0033	.06663	+435-0.5	.685-0.5	.1753	.1226-0.8			
3 -1	400.0	36	1.00	+000	+80	49.22	.8	+0453	.9742	1.0000	-8830	+9937	.9901		
	400.0	100.	254+2	4371.7	4.12	12.43	+286	4.13	.9100	.8157	+3.59	78.3			
2757901.		445.	2492.6	1332.5	+1046	.3158	.0052	+1048	+254-0.3	.396-0.3	.1785	.5401-0.8			
3 -1	400.0	22	1.00	+000	+80	8.00	.8	+8358	.9743	1.0000	-8753	+9937	.9860		
	100.0	100.	247.3	4285.9	5.67	24.96	+414	8.28	+0163	.0255	+4.0	31.6			
689475.		445.	2425.4	1306.4	+3440	.6359	.0105	+2103	+413-0.3	.647-0.3	.1834	.2180+0.8			
3 -1	400.0	23	2.00	+000	+80	8.00	.8	+8945	.9949	1.0000	-9257	+9943	.9807		
	100.0	100.	325.0	5775.6	4.25	25.27	+419	8.39	+0160	.0182	+3.1	31.6			
689475.		445.	3186.9	1760.4	+6419	.1079	.0107	+2130	+407-0.3	.461-0.3	.1396	.2180+0.8			

F = 445 (100 lbf) FUEL-REGEN-COOLED WITH LINER

卷之三

ORIGINAL PAGE IS
OF POOR QUALITY

10/28/81 15:45:58 LOWF 0427AA108										DATE 102391									
FUEL FLOW	ARATIO	NEL	MN	ZFILMCL	TWTS	CRAFTC	ZBELL	ZISP	ERF	FC EFF	RIN EFF	DIV EFF	BL EFF	FLOW RATE	DELT P				
ENGLISH	PSIA)	THRUST	LBS	ISP DEL	STAR	LPRIME	LNOZ	RTHROAT	REXIT	OX DIA	FUEL DIA	CIN)	CIN)	CLSN/SEC3	(PSI)				
SI UNITS	(PSI)	(LBFS)	(N)	(SEC)	(N)	(M)	(IN)	(IN)	(IN)	(MM)	(MM)	(MM)	(MM)	(K6/SEC3)	(PSI)				
3 -1	400.0	7	1.00	.000	.80	.21	.9	.8554	.9698	1.0000	.8787	.9935	.9907						
	1000.0	400.	259.8	449.6-7	5.77	15.78	.282	.924	.5-24	.0364	.0575	1.54	177.8						
	6894752.	1779.	2547.7	1371.2	.1466	.4008	.8866	.1330	.924-03	.146-82	.6984								
3 -1	400.0	7	2.00	.000	.80	.43	.8	.6021	.7107	1.0000	.9785	.9943	.9955						
	1000.0	400.	248.2	4182.0	.65	15.57	.258	.516	.0430	.0475	1.61	177.8							
	6894752.	1779.	2433.6	1274.7	.0166	.3954	.0066	.1312	.109-92	.121-92	.7311								
3 -1	400.0	22	1.00	.000	.80	.00	.8	.8468	.9802	1.0000	.8776	.9937	.9917						
	400.0	400.	254.6	4398.6	5.67	24.92	.413	.827	.0247	.0386	1.57	89.4							
	2757901.	1779.	2497.0	1340.7	.1439	.6329	.0195	.2100	.628-03	.981-03	.7116								
3 -1	400.0	22	2.00	.000	.80	.00	.8	.9415	.9771	1.0000	.9597	.9945	.9899						
	400.0	400.	342.4	5845.9	4.25	24.77	.411	.822	.0246	.0279	1.17	89.4							
	2757901.	1779.	3357.4	1781.2	.1079	.6291	.0104	.2086	.625-03	.708-03	.5300								
3 -1	400.0	101	1.00	.000	.80	.00	.8	.8340	.9787	1.0000	.8672	.9937	.9903						
	100.0	400.	247.4	4305.5	7.79	50.02	.830	.1660	.0152	.0236	1.62	31.6							
	689475.	1779.	2425.6	1312.3	.1978	1.2706	.0211	.4216	.387-03	.599-03	.7335								
3 -1	400.0	101	2.00	.000	.80	.00	.8	.9120	.9990	1.0000	.9317	.9945	.9864						
	100.0	400.	331.3	5799.1	5.84	50.16	.832	.1664	.0152	.0172	1.21	31.6							
	689475.	1779.	3249.4	1761.6	.1983	1.2741	.0211	.4228	.386-03	.436-03	.5476								
3 -1	400.0	95	3.00	.000	.80	.00	.8	.8576	.9833	1.0000	.6988	.9945	.9862						
	100.0	400.	335.4	5516.5	5.84	48.77	.809	.1618	.0166	.0153	1.20	31.6							
	689475.	1779.	3269.7	1681.4	.1483	1.2388	.0206	.4111	.421-03	.368-03	.5442								
3 -1	400.0	95	4.00	.000	.80	.00	.8	.8590	.9930	1.0000	.8936	.9946	.9861						
	100.0	400.	320.1	529.3	5.84	48.74	.809	.1617	.0175	.0140	1.25	31.6							
	689475.	1779.	3139.4	1612.5	.1483	1.2388	.0205	.4108	.443-03	.356-03	.5668								
3 -1	400.0	94	5.00	.000	.80	.00	.8	.8661	.9923	1.0000	.8917	.9946	.9858						
	100.0	400.	307.5	586.6	5.84	48.57	.806	.1612	.0185	.0132	1.30	31.6							
	689475.	1779.	3015.5	1538.2	.1483	1.2358	.0205	.4094	.464-03	.335-03	.5901								

FIN

F = 1779N (400 lbF) FUEL-REGEN-COULED WITH LINER

**ORIGINAL PAGE IS
OF POOR QUALITY**

PAGE 5									
DATE 10/20/01									
FUEL FILM AREA	MR	3FILMCL	TWTS	CARTRD	ZBELL	ERL	FC EFF	DIV EFF	BL EFF
CHAR PRESS	ISP DEL	CSTAR	LPRIME	REXIT	MIN DIA	ON DIA	FUEL DIA	FLOW RATE	DELT P
THRUST	(SEC)	(FT/SEC)	(IN)	(IN)	(IN)	(IN)	(IN)	(LB/SEC)	(PSI)
(LBF)	(SEC)	(IN-S/SEC)	(IN)	(IN)	(IN)	(IN)	(IN)	(LB/SEC)	(PSI)
SI UNITS	(N)	(N)	(N)	(N)	(MM)	(MM)	(MM)	(KG/SEC)	(PA)
3 -1	400.0	23	1.00	.000	8.00	.9	.8462	.9918	.9936
	1000.0	1000.	257.0	4507.9	7.08	25.11	-417	-8.33	-3.89
	6894752.	4448.	2520.3	1374.0	.1798	.6377	.0196	.2116	.1274-02
3 -1	400.0	62	1.00	.000	.80	.8	.8437	.9852	.9937
	400.0	1000.	253.7	4921.0	7.00	39.57	-657	15.13	.9908
	2757901.	4448.	2467.8	1347.5	.1778	1.0051	.0167	.3335	.994
3 -1	400.0	60	2.00	.000	.80	.8	.9369	.9924	.9957
	400.0	1000.	340.7	5816.5	3.12	39.17	-650	13.80	.9998
	689475.	4448.	3341.1	1772.9	.0792	.9948	.0165	.3301	.994
3 -1	400.0	258	1.00	.000	.80	.8	.8357	.9853	.9937
	100.0	1000.	247.9	4334.5	9.61	79.28	1.315	26.31	.9917
	689475.	4448.	2430.7	1321.1	.2441	2.0137	.0334	.6682	.9917
3 -1	400.0	256	2.00	.000	.80	.8	.9193	.9996	.9955
	100.0	1000.	334.0	5802.6	7.90	79.02	1.311	26.22	.9917
	689475.	4448.	3275.2	1768.6	.2007	2.0071	.0333	.6660	.9917
3 -1	400.0	241	3.00	.000	.80	.8	.8681	.9851	.9945
	100.0	1000.	337.5	5326.2	7.21	76.71	1.273	25.45	.9939
	689475.	4448.	3318.0	1684.4	.1831	1.9484	.0323	.6465	.9939
3 -1	400.0	241	4.00	.000	.80	.8	.8674	.9938	.9946
	100.0	1000.	323.2	5294.8	7.21	76.73	1.273	25.46	.9946
	689475.	4448.	3169.9	1613.0	.1831	1.9489	.0323	.6467	.9946
3 -1	400.0	240	5.00	.000	.80	.8	.8722	.9927	.9947
	100.0	1000.	309.7	5048.7	7.21	76.55	1.220	.455-03	.9947
	689475.	4448.	3036.7	1538.8	.1831	1.9444	.0323	.6452	.9947

F = 4448N (1000 lbf) FUEL-REGEN-COOLED WITH LINER

END

ORIGINAL PAGE IS
OF POOR QUALITY

10/21/01 11:30:54 LOWF 0427AA108										DATE 10/21/01		PAGE 3	
FUEL FILM RATIO	WEL	MR	TOTAL	LNB	21SP	ERE	FC EFF	KIN EFF	DIV EFF	BL EFF	DELTA FLOW RATE	DELTA P (PSI)	
CHAN PRESS	ISP DEL	CSTAR	ISI SEC	LPRINT	THROAT	REXIT	OX DIA	FUEL DIA	O2 DIA	1.0000	(LB/MIN SEC)	(PSI)	
ENGLISH	(PSIA)	(LBF)	(SEC)	(IN)	(IN)	(IN)	(IN)	(IN)	(IN)	1.0000	(LB/MIN SEC)	(PSI)	
SI UNITS	(PA)	(N)	(N-S/KG)	(M)	(M)	(M)	(MM)	(MM)	(MM)	1.0000	(KG/SEC)	(PA)	
1 -1	400.0	22	4.00	.000	.80	6.00	.9	.9764	.9958	.9978	.9945	.9879	
	1000.0	10C0.	466.7	7969.4	7.08	24.77	.911	8.22	.0306	.0519	.1214	.177.8	
	6894752.	4448.	4577.0	2429.1	.1798	.6292	.0104	.0288	.778-03	.132-02	.9719	.-1226+0	
1 -1	420.0	60	4.00	.000	.80	6.00	.8	.9795	.9988	.1.0000	.9945	.9885	
	400.0	1000.	468.1	7975.6	8.74	39.13	.649	12.98	.0220	.0429	.2.14	.69.4	
	2757901.	4448.	4550.7	2431.0	.2220	.9938	.0165	.3298	.558-03	.108-02	.9690	.-6167+0	
1 -1	406.0	252	4.00	.000	.80	6.00	.8	.9693	.9996	.1.0000	.9894	.9853	
	100.0	10C0.	463.0	7936.6	12.02	78.49	1.302	26.04	.0140	.0356	.2.16	.31.6	
	689475.	4448.	4540.7	2419.1	.3053	1.9936	.0031	.6615	.355-03	.905-03	.9796	.-2180+0	
1 -1	400.0	7	4.00	.000	.80	6.32	.8	.9729	.9927	.1.0000	.9988	.9945	
	400.0	400.	465.1	7944.3	5.73	15.67	.260	.520	.0344	.0597	.86	.177.8	
	2757901.	1779.	4560.7	2421.4	.1455	.3980	.0066	.1321	.874-03	.152-02	.3901	.-1226+0	
1 -1	400.0	22	4.00	.000	.80	6.00	.8	.9759	.9983	.1.0000	.9956	.9886	
	400.0	400.	466.4	7971.3	7.08	24.78	.411	8.22	.0230	.073	.86	.177.8	
	6894752.	1779.	4573.0	2429.7	.1798	.6295	.0104	.0289	.584-03	.128-02	.3890	.-1226+0	
1 -1	400.0	59	4.00	.000	.80	6.00	.8	.9639	.9995	.1.0000	.9879	.9945	
	160.0	400.	460.5	7936.2	9.74	49.78	.826	16.52	.0142	.0384	.87	.31.6	
	2757901.	1779.	4515.5	2419.0	.2474	1.2644	.0210	.4195	.360-03	.975-03	.3940	.-2180+0	
1 -1	400.0	7	4.00	.000	.80	6.00	.8	.9713	.9946	.1.0000	.9967	.9945	
	1000.0	100.	464.3	7959.6	4.17	7.85	.130	.260	.0172	.0307	.22	.177.8	
	6894752.	445.	4553.2	2425.1	.1059	.1994	.0033	.0662	.437-03	.780-03	.0977	.-1226+0	
1 -1	400.0	7	4.00	.000	.80	6.00	.8	.9662	.9967	.1.0000	.9932	.9814	
	400.0	150.	461.7	7955.9	5.15	12.94	.206	.413	.0225	.0460	.22	.89.4	
	2757901.	445.	4526.0	2425.7	.1306	.3161	.0052	.1049	.521-03	.117-02	.0982	.-6167+0	
1 -1	400.0	23	4.00	.000	.80	6.00	.8	.9533	.9995	.1.0000	.9852	.9945	
	100.	100.	455.9	7936.3	7.06	25.03	.415	.830	.0148	.0447	.22	.31.6	
	689475.	445.	4465.7	2419.0	.1798	.6357	.0105	.2109	.375-03	.975-03	.0996	.-2180+0	

LOX/LH_2 $MR = 4$ FUEL-COOLED

卷之三

**ORIGINAL IMAGE IS
OF POOR QUALITY**

WAX/LH₂ = 6 FUEL-EODELED

۲۱۰

ORIGINAL PAGE IS OF POOR QUALITY									
PAGE 3									
DATE 102181		DATE 102181		DATE 102181		DATE 102181		DATE 102181	
FUEL FILM RATIO	NEL	MR	ZFLMCL	TWS	CRAITI	XSP	KIN EFF	DIV EFF	BL EFF
CHAN PRESS	TEL	THRUST	TSP DEL	CSTAR	LNOZ	ATTHROAT	ON DIA	FUEL DIA	FLOW RATE
ENGLISH	(PSIA)	(LBFS)	(SEC)	LPRINT	(IN)	(IN)	(IN)	(IN)	DELT P
SI UNITS	(PA)	(M)	(M-S/MG)	(M/S)	(M)	(M)	(M)	(M)	(PSI)
1 -1	*00.0	19	*0.00	*80	8.00	*9	*9199	*9147	*9879
100.0	1000.	437.9	6662.7	7.08	23.39	*388	7.76	*0472	2.28
6H94752.	4448.	4294.2	2030.8	-1793	-5240	-0099	-1971	*120-02	1.0359
1 -1	*00.0	54	*0.00	*80	8.00	*8	*902	*9807	*9887
400.0	1000.	445.8	844.8	8.74	37.14	*616	12.32	*0250	2.24
2757901.	4448.	4372.3	2086.3	-2220	-9334	-0157	-3130	*943-03	1.0174
1 -1	*00.0	230	*0.00	*80	8.00	*8	*9246	*9938	*9865
400.0	1000.	435.3	9811.7	12.02	74.99	1.244	24.88	*0159	2.30
6H9475.	4448.	4268.8	2076.2	-3053	-1.9449	-0316	-6321	*044-03	1.0420
1 -1	*00.0	7	*0.00	*80	9.36	*8	*9022	*9253	*9890
400.0	460.	429.5	6524.4	5.73	14.78	*245	4.90	*0377	.93
6H94752.	1779.	4231.5	1958.6	-1455	-3754	-0062	-1246	*958-03	*150-02
1 -1	*00.0	19	*0.00	*80	8.00	*8	*9313	*9717	*9879
400.0	400.	431.4	6781.8	7.08	23.49	*390	7.80	*0268	.91
2757901.	1779.	4330.7	2067.1	-1798	-5967	-0099	-1980	*681-03	*109-02
1 -1	*00.0	91	*0.00	*80	8.00	*8	*9151	*9923	*9862
400.0	400.	430.8	6601.2	9.74	47.64	*790	15.81	*0161	.93
6H94752.	1779.	4224.4	2073.0	-2674	-1.2201	-0201	-4015	*409-03	*4121
1 -1	*00.0	7	*0.00	*80	37.24	*8	*9083	*9358	*9830
400.0	100.	432.4	6600.7	4.17	7.41	*123	2.96	*0265	*23
6H94752.	445.	4239.9	2011.7	-1054	-1.081	-0031	-0624	*478-03	*1049
1 -1	*00.0	7	*0.00	*80	14.72	*6	*9134	*9590	*9828
400.0	100.	433.1	6693.2	5.15	11.78	*196	*391	*0223	*23
2757901.	445.	4247.4	2040.1	-1368	-2693	-0050	-0993	*567-03	*1047
1 -1	*00.0	20	*0.00	*80	6.00	*8	*9007	*9897	*9757
400.0	100.	424.1	6763.1	7.98	23.98	*398	7.96	*0173	*24
6H9475.	445.	4158.6	2067.5	-1798	-6970	-0101	-2021	*439-03	*1070

LOX/LH₂ MR = 8 FUEL-CORED

EF1.

ORIGINAL PAGE IS
OF POOR QUALITY

DATE 102181										PAGE 3									
10/21/81	12:55:36	LWTF	0427AA188	000427	\$29	406				XISP	REXIT	DIY	BL	EFF	FC	EFF	KIN	EFF	DEL T P
FUEL FILM RATIO	MEL	MR	ZFLNCL	TWTS	XBELL	REXIT	DIY	EFF	ATMROAT	DX DIA	FLOW RATE								
CHAN PRESS	THRUST	ISP DEL	CSTAR	LNOZ	(IN)	(IN)	DX	DIA	(IN)	(IN)	(LBNS/SEC)								
ENGLISH	(LBF)	(SCC)	(FT/SEC)	LPRIME	(IN)	(IN)	(IN)	(IN)	(IN)	(IN)	(KG/SEC)								
SI UNITS	(PA)	(N-S/KG)	(M/S)	(IN-S/KG)	(IN)	(IN)	(IN)	(IN)	(IN)	(IN)	(KG/SEC)								
1 -1	.000-0	22	4.00	.000	.80	.00	.9	.9626	.9983	1.0000	.9826	.9945	.9867						
	.000-0	400-	496.9	8697.6	7.68	24.79	-411	.8-23	.00223	.0070	.0070	.081	.09-.4						
2757901-	1779.	4872.5	2590.1	.1798	.6297	.0104		.2090	.566-03		.178-02	.3652							
1 -1	.000-0	22	4.00	.000	.80	.00	.8	.9577	.9982	1.0000	.9779	.9945	.9866						
	.000-6	400-	508.4	8699.7	7.08	24.80	-411	.8-23	.00682	.0662	.0662	.079	.09-.4						
2757901-	1779.	4985.8	2651.7	.1798	.6299	.0105		.2090	.163-02		.168-02	.3569							
1 -1	.000-8	20	6.00	.000	.80	.00	.8	.9482	.9955	1.0000	.9701	.9996	.9873						
	.000-6	400-	4979.9	7714.4	7.08	24.04	.399	7.98	.0246	.0604	.0604	.083	.09-.4						
2757901-	1779.	4706.5	2351.3	.1798	.6105	.0101		.2026	.625-03		.154-02	.3702							
1 -1	.000-0	20	6.00	.000	.80	.00	.8	.9410	.9945	1.0000	.9639	.9946	.9873						
	.000-0	400-	489.3	7857.7	7.08	24.03	.399	7.97	.0733	.0599	.0599	.082	.09-.4						
2757901-	1779.	4798.1	2395.0	.1798	.6102	.0101		.2025	.186-02		.152-02	.3708							
1 -1	.000-0	19	8.00	.000	.80	.00	.8	.9267	.9731	1.0000	.9697	.9947	.9879						
	.000-0	400-	451.6	6942.5	7.08	23.51	.390	7.80	.0265	.0564	.0564	.089	.09-.4						
2757901-	1779.	4428.3	2316.1	.1798	.5971	.0099		.1981	.673-03		.143-02	.4018							
1 -1	.000-0	19	8.00	.000	.80	.00	.8	.9218	.9726	1.0000	.9652	.9947	.9878						
	.000-0	400-	459.9	7072.6	7.08	23.51	.390	7.80	.0790	.0558	.0558	.087	.09-.4						
2757901-	1779.	4510.0	2155.7	.1798	.5972	.0099		.1982	.201-02		.142-02	.3945							
1 -1	.000-0	23	2.00	.000	.80	.00	.8	.9784	1.0033	1.0000	.9939	.9943	.9864						
	.000-0	400-	505.5	9074.0	7.08	25.40	.421	8.43	.0197	.0339	.0339	.079	.09-.4						
2757901-	1779.	4957.1	2765.8	.1798	.6452	.0107		.2141	.501-03		.213-02	.3589							
1 -1	.000-0	23	2.00	.000	.60	.00	.8	.9772	1.0031	1.0000	.9930	.9943	.9862						
	.000-0	400-	518.1	9303.7	7.08	25.40	.421	8.43	.0586	.0829	.0829	.077	.09-.4						
2757901-	1779.	5061.0	2835.8	.1798	.6453	.0107		.2141	.149-02		.210-02	.3502							

2FIN

LOX/LH₂ HEATED M₂

ORIGINAL PAGE IS
OF POOR QUALITY

DATE 10/21/81										PAGE 3									
FUEL FILM RATIO	FUEL FILM RATIO	TEL	MR	XFLIMC:	TWS	CATIO	XBELL	ZISP	ERE	FC EFF	KIN EFF	DIV EFF	BL EFF	DELTA P					
CHAN PRESS	CHAN PRESS	ISP DEL	ISP DEL	LPRIME	LNOZ	THRCAT	FUELDIA	(IN)	(IN)	OX DIA	FUEL DIA	FLOW RATE	(LB/SEC)	(PSI)					
(PSIA)	(PSIA)	(SEC)	(SEC)	(IN)	(IN)	(IN)	(IN)	(IN)	(IN)	(IN)	(IN)	(KG/SEC)	(PA)						
SI UNITS	SI UNITS	(N)	(N)	(M)	(M)	(M)	(M)	(M)	(M)	(M)	(M)	(KG/SEC)	(PA)						
2 -1	400.0	26	3.50	.000	.80	8.00	.9	*9101	.9557	*0000	.9701	*9996	.9881						
	800.0	1000.	366.3	5734.6	5.78	26.52	*440	8.80	*0675	*0317	2.73	150.4							
5515601.	44448.	3592.0	1747.9	*1466.8	.6736	*0112	.2235	.171-02	.806-03	1.2384	*1037-07								
2 -1	400.0	26	3.50	.000	.80	8.00	.8	*9166	.9623	1.0000	*9703	*9946	*9880						
	800.0	1000.	368.9	5774.0	7.21	26.52	*440	8.80	*0671	*0316	2.71	150.4							
5515601.	44446.	3617.8	1759.9	*1331	.6735	.0112	.2235	.170-02	.803-03	1.2295	*1037-07								
2 -1	400.0	55	3.50	.000	.80	8.00	.8	*9336	.9868	1.0000	*9624	*9946	*9888						
	400.0	1000.	374.9	5869.2	8.76	37.50	*622	*12.44	*0571	*0245	2.67	89.4							
2757901.	44448.	3676.8	1788.9	*2210	.9526	.0158	.3161	.145-02	.623-03	1.2098	*1037-07								
2 -1	400.0	36	3.50	.000	.80	14.33	.8	*9207	.9753	1.0000	*9605	*9946	*9889						
	400.0	400.	400.	369.7	5801.0	4.80	23.75	*394	7.88	*0471	*0188	1.06	89.4						
2757901.	1779.	3626.0	1762.1	*1219	.6032	.0100	.2001	.120-02	.978-03	*4907	*4907	*6167-06							
2 -1	400.0	38	3.50	.000	.80	14.33	.8	*9240	.9794	1.0000	*9599	*9946	*9888						
	400.0	400.	400.	371.1	5825.5	5.70	23.75	*394	7.68	*0470	*0188	1.08	89.4						
2757901.	1779.	3639.2	1775.6	*1448	.6033	.0100	.2002	.119-02	.977-03	*477-03	*477-03	*6167-06							
2 -1	400.0	7	3.50	.000	.80	14.40	.8	*8855	*9442	1.0000	*9593	*9946	*9889						
	400.0	100.	100.	355.6	5615.6	2.85	11.91	*198	3.95	*0560	*0223	2.8	89.4						
2757901.	445.	3487.5	1711.6	*0724	.3026	.0050	.1004	.142-02	.567-03	*1275	*1275	*6167-06							
2 -1	400.0	7	3.50	.000	.80	14.39	.8	*9008	*9612	1.0000	*9584	*9946	*9887						
	400.0	100.	361.8	5716.9	5.20	11.92	*198	*3.95	*0555	*0221	*26	89.4							
2757901.	445.	3541.8	1742.5	*1321	.3027	.0050	.1004	.141-02	.563-03	*1254	*1254	*6167-06							

LOX/CH₄ MR = 3.5 OX-COOLED WITH AND WITHOUT LINERS

246

**ORIGINAL PAGE IS
OF POOR QUALITY**

PAGE 3																													
					PAGE 3																								
					DATE 10/21/81																								
FUEL FILM ARATIO NEL MR XFILMCL TUTS CRATI0 XISPL ERE DIV FC EFF KIN EFF BL EFF	CHAN PRESS THRUST ISP DEL CSTAR LPRIME LN02 RTHROAT EXIT INJ FUEL DIA RATE DELT P	LNO2 (IN)	XBELL (IN)	RTM02 RTHROAT EXIT INJ FUEL DIA RATE DELT P	XISPL ERE DIV FC EFF KIN EFF BL EFF	LN02 (IN)	XISPL ERE DIV FC EFF KIN EFF BL EFF	LN02 (IN)	XISPL ERE DIV FC EFF KIN EFF BL EFF																				
ENGLISH (PSIA) (LBF), (SEC) (N-S/KG) (PA)	(PSIA) (LBF), (SEC) (N-S/KG) (PA)	(IN)	(IN)	(IN)	RTM02 RTHROAT EXIT INJ FUEL DIA RATE DELT P	LN02 (IN)	RTM02 RTHROAT EXIT INJ FUEL DIA RATE DELT P	LN02 (IN)	RTM02 RTHROAT EXIT INJ FUEL DIA RATE DELT P																				
2 -1 400.0 25 4.00 .000 .80 8.00 .9 9087 .9532 1.0000 .9710 .9946 .9879	500.0 1000. 365.1 5579.5 6.68 26.20 .435 8.69 .0698 .0307 2.74 150.4	5515801. 4448. 3580.3 1700.6 .1697 .6655 .0110 .2208 .177-02 .781-03 1.2424 .1037-07	2 -1 400.0 25 4.00 .000 .80 8.00 .8 9116 .9564 1.0000 .9710 .9946 .9879	500.0 1000. 366.2 5598.2 7.44 26.21 .435 8.76 .0696 .0307 2.73 150.4	5515801. 4448. 3591.5 1706.3 .1890 .6656 .0110 .2209 .177-02 .779-03 1.2385 .1037-07	2 -1 400.0 54 4.00 .000 .80 8.00 .8 9237 .9789 1.0000 .9599 .9946 .9888	500.0 1000. 369.6 5678.5 8.70 37.15 .616 12.33 .0572 .0237 2.71 89.4	5515801. 4448. 3624.7 1730.8 .2210 .9437 .0157 .3131 .145-02 .601-03 1.2272 .6167-06	2 -1 400.0 231 4.00 .000 .80 8.00 .8 9014 .9864 1.0000 .9705 .9946 .9882	500.0 1000. 357.4 5626.4 12.00 75.22 1.248 24.96 .0473 .0151 2.80 31.6	689475. 4448. 3504.9 1714.9 .3048 1.9106 .0317 .6340 .120-02 .383-03 1.2691 .2180-06	2 -1 400.0 19 4.00 .000 .80 8.00 .8 9142 .9686 1.0000 .9602 .9946 .9889	500.0 1000. 365.5 5619.0 7.10 23.50 .390 7.80 .0666 .0254 1.09 89.4	2757901. 1779. 3587.3 1712.7 .1803 .5968 .0099 .1980 .169-02 .644-03 .4960 .6167-06	2 -1 400.0 91 4.00 .000 .80 8.00 .8 8919 .9858 1.0000 .9247 .9946 .9849	500.0 1000. 353.6 5623.1 9.70 47.81 .793 15.86 .0520 .0153 1.13 31.6	689475. 1779. 3468.1 1713.9 .2464 1.2144 .0201 .4030 .132-02 .388-03 .5130 .2180-06	2 -1 400.0 7 4.00 .000 .80 8.00 .8 8879 .9445 1.0000 .9612 .9946 .9850	500.0 1000. 355.3 5478.9 3.62 11.77 .195 3.91 .0568 .0212 .28 89.4	445. 3484.2 1670.0 .0919 .2990 .0050 .0992 .144-02 .539-03 .1277 .6167-06	2 -1 400.0 7 4.00 .000 .80 8.00 .8 8957 .9549 1.0000 .9589 .9946 .9848	500.0 1000. 358.4 5539.1 5.20 11.78 .196 3.91 .0566 .0211 .28 89.4	2757901. 445. 3514.7 1668.3 .1321 .2993 .0050 .0993 .144-02 .536-03 .1266 .6167-06	2 -1 400.0 21 4.00 .000 .80 8.00 .8 8760 .9828 1.0000 .9177 .9946 .9855	500.0 1000. 347.3 5606.1 5.5 24.08 .400 7.99 .0597 .0161 .29 31.6	689475. 445. 3406.2 1706.7 .1481 .6119 .0101 .2030 .152-02 .408-03 .1306 .2180-06	2 -1 400.0 21 4.00 .000 .80 8.00 .8 8760 .9828 1.0000 .9177 .9946 .9855	500.0 1000. 347.3 5606.1 7.10 24.08 .400 7.99 .0597 .0161 .29 31.6	689475. 445. 3406.2 1708.7 .1471 .6118 .0101 .2030 .152-02 .408-03 .1306 .2180-06

•FIN

**ORIGINAL PAGE IS
OF POOR QUALITY**

248

DATE 102181										PAGE 3			
FUEL	FILM	ARATIO	WEL	MR	TWTS	CRAFT	XBELL	XISP	ERE	FC EFF	KIN EFF	DIV EFF	BL EFF
CHAN	PRESS	THRUST	ISP DEL	CSTAR	LPRIME	RTHROAT	REXIT	OX DIA	FUEL DIA	FLOW RATE	DELT P	(LBW/SEC)	(PSI)
SI UNITS	(PSIA)	(LBF)	(SEC)	(IN)	(IN)	(IN)	(IN)	(IN)	(IN)	(IN)	(IN)	(Kg/SEC)	(PA)
2 -1	400.0	20	5.00	.000	.80	8.00	.9171	.9735	1.0000	.9612	.9947	.9864	
	1000.0	1000.	349.8	5433.0	7.10	23.63	.392	.784	.0731	.0307	.236	177.8	
6894752.	4448.	3430.2	1656.0	.1803	.6001	.0160	.1991	.166-02	.781-03	1.2968	-1226-07		
2 -1	400.0	55	5.00	.000	.80	8.00	.9332	.9945	1.0000	.9547	.9946	.9855	
	400.0	1000.	350.9	5490.5	6.70	37.49	.622	.1244	.0590	.0220	.285	89.4	
2757901.	4448.	3441.4	1673.5	.2210	.9523	.0158	.3160	.150-02	.558-03	1.2926	-6167-06		
2 -1	400.0	234	5.00	.000	.80	8.00	.9061	.9956	1.0000	.9265	.9946	.9884	
	100.0	1000.	339.0	5405.9	12.00	75.71	1.256	.2512	.0481	.0141	.295	31.6	
689475.	4448.	3324.2	1647.7	.3046	1.9230	.00319	.6381	.122-02	.357-03	1.3381	-2180-06		
2 -1	400.0	7	5.00	.000	.80	9.20	.8999	.9585	1.0000	.9638	.9947	.9889	
	1000.0	400.	343.2	5305.8	5.23	14.51	.247	.495	.0798	.0332	.117	177.8	
6894752.	1779.	3366.6	1617.2	.1328	.3786	.0063	.1256	.203-02	.842-03	.5286	-1226-07		
2 -1	400.0	7	5.00	.000	.80	9.19	.9027	.9537	1.0000	.9635	.9947	.9887	
	1000.0	400.	344.3	5323.4	5.70	14.91	.247	.495	.0796	.0331	.116	177.8	
6894752.	1779.	3376.2	1622.6	.1448	.3787	.0063	.1257	.202-02	.841-03	.5270	-1226-07		
2 -1	400.0	20	5.00	.000	.80	8.00	.9256	.9894	1.0000	.9516	.9946	.9888	
	400.0	400.	348.1	5462.3	7.10	23.75	.394	.788	.0636	.0231	.115	89.4	
2757901.	1779.	3413.5	1664.9	.1803	.6032	.0160	.2002	.162-02	.588-03	.5213	-6167-06		
2 -1	400.0	93	5.00	.000	.80	8.00	.8963	.9953	1.0000	.9200	.9946	.9852	
	100.0	400.	335.3	5404.6	9.70	48.14	.799	.1597	.0516	.0142	.119	31.6	
689475.	1779.	3286.2	1647.5	.2464	1.2227	.0203	.4057	.131-02	.360-03	.5411	-2180-06		
2 -1	400.0	7	5.00	.000	.80	8.00	.8977	.9524	1.0000	.9601	.9947	.9882	
	150.0	100.	342.4	5316.3	3.30	7.47	.129	.248	.0399	.0166	.29	177.8	
6894752.	445.	3357.6	1620.4	.0838	.1897	.0031	.0630	.101-02	.422-03	.1325	-1226-07		
2 -1	400.0	7	5.00	.000	.80	36.56	.8	.5039	.9605	1.0000	.9585	.9947	.9881
	100.0	100.	344.7	5363.6	4.20	7.48	.124	.248	.0398	.0165	.29	177.8	
6894752.	445.	3360.7	1634.2	.1067	.1899	.0032	.0630	.101-02	.420-03	.1316	-1226-07		
2 -1	400.0	7	5.00	.000	.80	14.40	.8	.9070	.9755	1.0000	.9501	.9946	.9850
	400.0	100.	341.1	5385.7	4.66	11.91	.198	.395	.0592	.0198	.29	89.4	
2757901.	445.	3364.7	1601.6	.1184	.3026	.0050	.1004	.150-02	.502-03	.1330	-6167-06		
2 -1	400.0	7	5.00	.000	.80	14.39	.8	.9084	.9781	1.0000	.9491	.9946	.9849
	100.0	100.	341.6	5400.0	5.20	11.92	.198	.395	.0591	.0197	.29	89.4	
2757901.	445.	3350.1	1645.9	.1321	.3027	.0050	.1004	.150-02	.501-03	.1328	-6167-06		

LOX/CH₄ MR = 5.0 OX-COOLED WITH AND WITHOUT LINERS

**ORIGINALITY AND
OF POOR QUALITY**

18/21/81 09:27:35 LOWF 0427AA4188										DATE 10/21/81										PAGE 1 4	
FUEL FILM RATIO	MEL	MR	X FILMCL	TWS	CRATIO	XISP	ERE	FC EFF	KIN EFF	DIV EFF	BL EFF	OX DIA	FUEL DIA	FLOW RATE	DEL T P	(PSI)	(PSI)	(PSI)	(PSI)		
CHAN PRESS	THRUST	ISP DEL	CSTAR	LPRINC	ATHRDAT	REXIT	(IN)	OX	OX	DIA	(IN)	FUEL	(LB/M SEC)	(IN)	DEL T P	(PSI)	(PSI)	(PSI)			
ENGLISH	4PSI)	6LBFS	(FT/SEC)	(SEC)	(IN)	(IN)	(IN)	DI	DI	DIA	(IN)	DIA	(IN)	(IN)	(IN)	(PSI)	(PSI)	(PSI)			
SJ UNITS	(PSI)	(IN)	(IN-S/KG)	(M/S)	(M)	(M)	(M)	(M)	(M)	(M)	(M)	(M)	(M)	(M)	(M)	(PSI)	(PSI)	(PSI)			
2 -1	400.0	21	5.00	.000	.80	8.00	.8	.8794	.9942	1.0000	.9102	.9946	.9790								
	100.0	100.	329.0	3398.6	6.95	24.29	.003	.006	.0627	.0627	.0151	.30	.31.6								
	689475.	445.	3226.2	1645.5	.1765	.6169	.0102	.2047	.159-02	.159-02	.383-03	.1379	.2180-06								
2 -1	400.0	21	5.00	.000	.80	8.00	.8	.8794	.9942	1.0000	.9102	.9946	.9790								
	100.0	100.	329.0	3398.6	7.10	24.29	.003	.006	.0627	.0627	.0151	.30	.31.6								
	689475.	445.	3226.2	1645.5	.1803	.6169	.0102	.2047	.159-02	.159-02	.383-03	.1379	.2180-06								

四

FUEL-REGEN-COOLED WITH AND WITHOUT LINERS

10/21/01 11:12:06 LOWF 04227AA188										DATE 10/21/01 PAGE 3	
FUEL FILM AREA	ID	MR	XFLMLCL	TNTS	CRATIO	ZISP	EAE	FC EFF	DIV EFF	BL EFF	DELTA P
CHAN PRES*	THRUST	ISP DEL	CSTAR	(SEC)	LPRIME	RTHROAT	REXIT	OK DIA	MIN DIA	FLOW RATE	(PSI)
ENGLISH	(LBFS)	(IN)	(IN-S/KG)	(IN/S)	(IN)	(IN)	(IN)	(IN)	(IN)	(LBW/SEC)	(KG/SEC)
SI UNITS	(PA)	(N)	(N-S/KG)	(N/S)	(IN)	(IN)	(IN)	(IN)	(IN)	(PA)	(PA)
2 -1	*000.0	23	2.00	.000	.80	8.00	.9	.9473	1.0130	.9500	.9858
	1000.0	1000.	532.6	5842.8	6.10	25.13	*417	.834	.0324	.0752	3.01
	6894752.	4448.	3261.6	1780.9	*1549	*6382	*0196	.2118	.823-03	*191-02	1.3638
2 -1	*000.0	23	2.00	.000	.80	8.00	.8	.9478	1.0121	1.0000	.9952
	1000.0	1000.	332.8	5838.1	7.10	25.11	*417	.833	*024	.0752	3.01
	6894752.	4448.	3263.3	1779.4	*1803	*6378	*0106	.2116	.823-03	*191-02	1.3633
2 -1	*000.0	61	2.00	.000	.80	8.00	.8	.9499	1.0045	1.0000	.9945
	400.0	1000.	333.5	5793.9	8.70	39.51	*655	13.11	*0236	.0660	.9882
	2757901.	4448.	3270.8	1766.0	*2213	1.0035	*0166	.3330	.5993-03	.168-02	3.00
											89.4
2 -1	*000.0	22	2.00	.000	.80	8.00	.8	.9498	1.0070	1.0000	.9955
	400.0	400.	333.5	5808.0	7.00	25.02	*415	.830	*0248	.0718	2.67
	2757901.	1779.	3270.4	1770.3	*1783	*6355	*0105	.2109	.631-03	*182-02	*5441
2 -1	*000.0	57	3.00	.000	.80	8.00	.8	.9519	.9948	1.0000	.9946
	400.0	1000.	374.6	6040.4	7.47	38.05	*631	12.63	*0244	.0718	2.67
	2757901.	4448.	3675.5	1841.1	*1897	*9666	*0160	.3207	.620-03	*146-02	1.2102
2 -1	*000.0	57	3.00	.000	.80	8.00	.8	.9535	.9959	1.0000	.9946
	400.0	1000.	375.9	6047.2	8.70	38.02	*631	12.62	*0244	.0718	2.67
	2757901.	4448.	3686.0	1843.2	*2210	*9657	*0160	.3205	.619-03	*146-02	1.2068
2 -1	*000.0	21	3.00	.000	.80	8.00	.8	.9313	.9862	1.0000	.9749
	400.0	400.	366.7	5987.9	9.53	24.23	*402	8.04	*0244	.0575	2.66
	2757901.	1779.	3596.2	1825.1	*151	*6153	*0107	.2042	.653-03	*154-02	1.2068
2 -1	*000.0	21	3.00	.000	.80	8.00	.8	.9430	.9922	1.0000	.9946
	400.0	400.	371.3	6024.7	7.10	24.15	*401	8.01	*0256	.0603	1.03
	2757901.	1779.	3641.1	1836.3	*1803	*6134	*0102	.2035	.649-03	*153-02	1.2067
2 -1	*000.0	93	3.00	.000	.80	8.00	.8	.9385	.9991	1.0000	.9946
	100.0	400.	366.6	5979.8	8.67	45.29	*801	16.03	*0158	.0518	1.09
	689475.	1779.	3614.5	1822.6	*2202	1.2267	-0204	.4070	*01-03	*132-02	1.2102
2 -1	*000.0	93	3.00	.000	.80	8.00	.8	.9383	.9991	1.0000	.9946
	100.0	400.	368.6	5979.8	9.70	48.29	*801	16.03	*0158	.0518	1.09
	689475.	1779.	3614.5	1822.6	*2464	1.2267	*0204	.4070	*01-03	*132-02	1.2102
2 -1	*000.0	35	3.50	.000	.80	8.00	.8	.9328	.9859	1.0000	.9946
	400.0	1000.	374.6	5866.0	6.97	37.50	*622	12.44	*0253	.0553	2.67
	2757901.	4448.	3673.7	1767.3	*1770	*9526	*0156	.3161	.643-03	*141-02	1.2108

ORIGINAL PAGE IS
OF POOR QUALITY

FUEL-REGEN-COOLED WITH AND WITHOUT LINERS

PAGE 4									
DATE 102181									
FUEL FILM AREA/IO	MR	%FILMCL	TUFS	CRAITQ	XISPL	ERE	FC EFF	KIN EFF	DIV EFF
CHAM PRESS THRUST	ISP DEL	CSTAR	LPRIME	RTHRDAT	REXIT	ON DIA	FUEL DIA	FLOW RATE	BL EFF
(PSIA)	(LBF)	(FT/SEC)	(IN)	(IN)	(IN)	(IN)	(IN)	(LBW/SEC)	DELT P
SJ UNITS	(IN)	(IN/S)	(M)	(M)	(M)	(M)	(M)	(KG/SEC)	(PSI)
2 -1	400.0	55	3.50	.000	.80	.00	.9367	.9902	.9946
	000.0	1000.	376.2	5689.5	8.70	37.51	-622	12.45	2.66
	2757901.	4448.	3689.1	1795.1	.2210	.9526	.0158	.3161	.0552
2 -1	400.0	20	3.50	.000	.80	.00	.9129	.9654	.9946
	000.0	400.	366.6	5742.0	1.23	23.73	.394	.787	1.09
	2757901.	1779.	3595.4	1750.2	.1074	.6016	.0100	.2000	.0268
2 -1	400.0	20	3.50	.000	.80	.00	.9239	.9792	.9946
	000.0	400.	371.6	5824.1	6.65	23.75	.394	.788	1.06
	2757901.	1779.	3638.5	1775.2	.1689	.6033	.0100	.2002	.0267
2 -1	400.0	92	3.50	.000	.80	.00	.9097	.9984	.9946
	000.0	400.	363.4	5846.4	8.17	48.07	.797	.95	1.10
	689475.	1779.	3564.0	1760.2	.2075	1.2209	.0203	.04051	.0163
2 -1	400.0	92	3.50	.000	.80	.00	.9097	.9984	.9946
	000.0	400.	363.4	5840.4	9.70	48.07	.797	.95	1.10
	689475.	1779.	3564.0	1760.2	.2464	1.2209	.0203	.04051	.0163

ORIGINAL PAGE IS
OF POOR QUALITY